AdS/CFT and strange metals

Universitá di Genova

Ph.D thesis

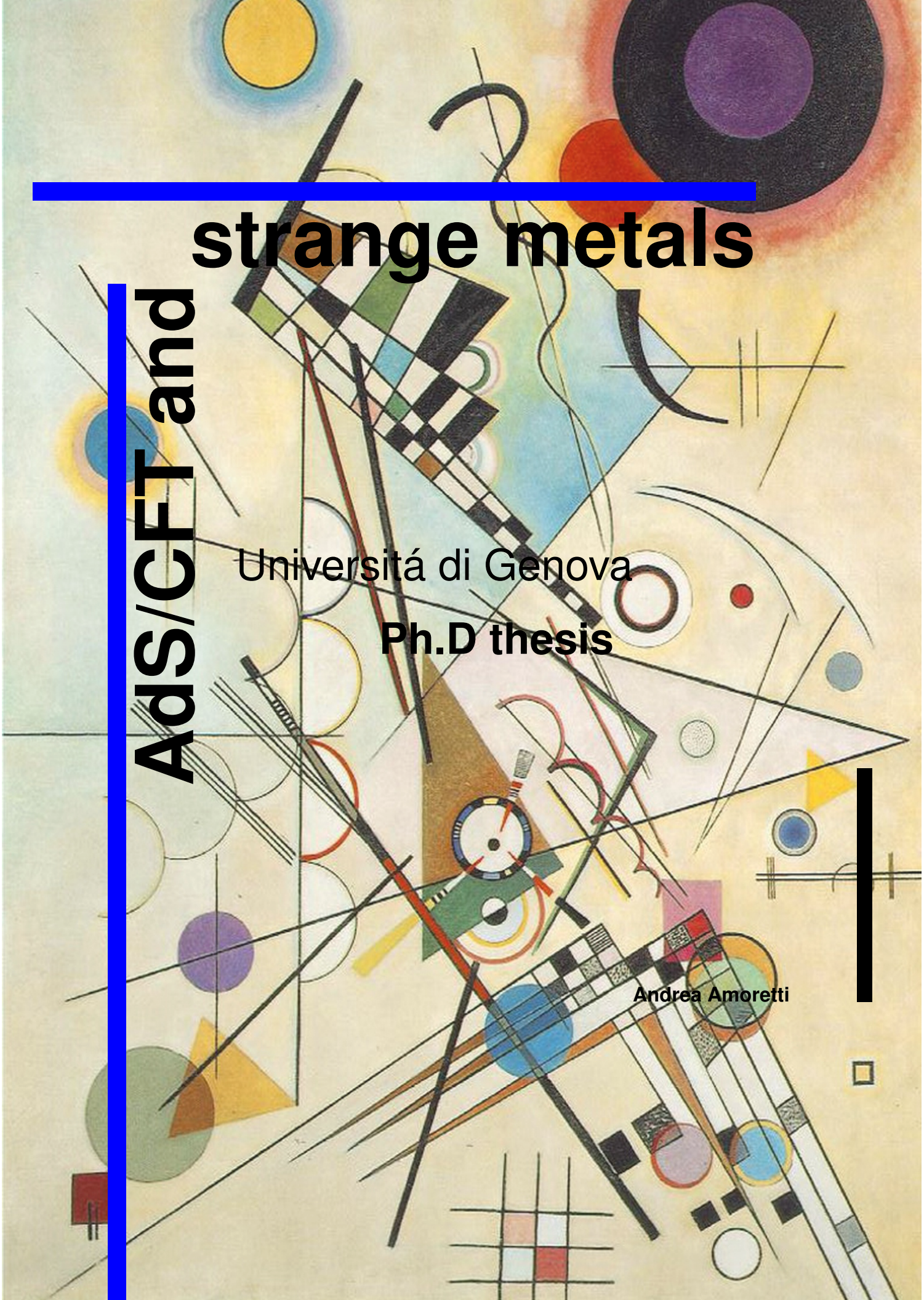

Andrea Amoretti

Contents

Preface

In the past century there have been very great progresses in understanding the world around us by means of the celebrated quantum field theory, an extremely powerful tool which allow us to understand a large amount of different physical phenomena, from elementary particle physics to condensed matter physics. Our ability to extract results from a quantum field theory mostly relies on perturbation theory. In this framework the physical observables are usually evaluated as an expansion in powers of the coupling constant, i.e. a dimensionless parameter, g, which measures the departure from a free field theory.

However, in the last decades the physical community has realised that nature can not be analysed always by means of perturbation theory. Some of the most known examples include quantum chromodynamics (QCD). The asymptotically-free nature of QCD makes perturbation theory reliable at high energy. On the other hand, at low energies, QCD becomes strongly coupled so that relevant phenomena such as confinement and chiral symmetry breaking are non-perturbative in nature. In the condensed matter framework the prototypical example is that of the high-T_c superconductors, where strong coupling causes the physical behaviour of these materials to abruptly deviate from the standard paradigm according to which we understand normal metals in nature, the Fermi liquid theory.

In this direction, in recent times a mathematical tools developed in string theory, the so called AdS/CFT correspondence (or gauge/gravity duality), has acquired a prominent role in understanding general properties of strongly coupled systems. The gauge/gravity duality provides the closest connection to date between string theory and the observable world. At the same time, it makes a rich playground for enhancing our theoretical understanding of strongly-interacting quantum systems, gravity, and ultimately string theory itself. Even though it was born out of string theory, in the past few years this duality has started a life of its own as an effective description of strongly-interacting quantum systems. Such an effective description forgets about the stringy origin of the duality and focuses on some of its properties that are believed to be universal to many other strongly-interacting systems with or without a stringy origin. Within this context, the duality has been used extensively to

describe phenomena similar to the ones encountered in QCD and in superconducting materials.

The aim of this thesis is to discuss how the AdS/CFT correspondence could help in getting some insight in the understanding of strongly coupled condensed matter systems. In particular, in this treatise the holographic correspondence is used to try to understand the peculiar properties of the high-T_c superconductors.

Since this is a line of research where techniques from very different fields of physics come together, in order for this treatise to be self-consistent and comprehensible a very huge introductory part is necessary. Consequently, the thesis is organised in three separate parts. The first two part are introductory while Part 3 contains the original result of the thesis.

In Part 1 the basic features of the high T_c superconductors are described. At first we will analyse the experimental properties of these peculiar materials, focussing in particular on the in-plane thermo-electric transport properties. At each step, the differences between the behaviour of the strange metals and the Fermi liquid prediction is remarked. In the last chapter we will focus on some theoretical attempts introduced in the past to explain the exotic behaviour of these materials, focussing in particular on the idea of the existence of a quantum critical point in their phase diagram.

In Part 2 the AdS/CFT correspondence is introduced. These Part is constructed in order to introduce the holographic correspondence as a series of computational rules, the so called holographic dictionary. The knowledge and the comprehension of the holographic dictionary is a necessary step in order to understand the discussion of Part 3.

Part 3 contains the original results of the thesis. In particular, the thermo-electric transport properties of a strongly coupled bi-dimensional plasma in presence of an extrinsic mechanism of momentum dissipation are deeply analysed using holography. The holographic results are compared with the phenomenology of the strange metals. In the last Chapter the conclusion of the thesis and the physical implications of these holographic toy models are discussed in details.

Part I
Condensed matter background

Chapter 1
Preamble: transport coefficients definition

In this manuscript we will analyse the thermo-electric transport properties of two-dimensional condensed matter systems. Then, in order to fix the notations in this brief preamble we will define the transport coefficients for the case at hand.

We will consider a two-dimensional system living in the plane $x-y$ and, in some cases, we will analyse also the effects due to an external magnetic field B applied in the direction perpendicular to the $x-y$ plane, z (see Figure 1).

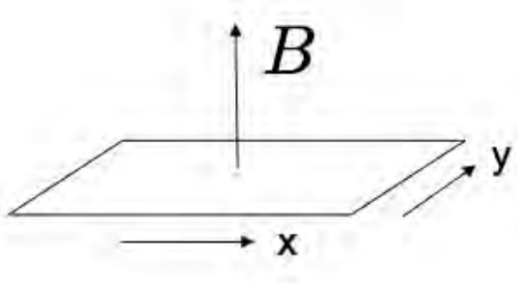

We are interested in the response of the electrical current J and the heat current Q to an applied electric field E and a temperature gradient ∇T. The electric field can be applied by allowing for a weak spatial dependence in the chemical potential μ (which is then, formally, the electrochemical potential) with $qE = \nabla\mu$ (where q is the charge of the excitations), while the temperature gradient describes a similar weak spatial dependence in T. The transport coefficients are defined by the relation

$$\begin{pmatrix} J \\ Q \end{pmatrix} = \begin{pmatrix} \hat{\sigma} & \hat{\alpha} \\ T\hat{\alpha} & \hat{\bar{\kappa}} \end{pmatrix} \begin{pmatrix} E \\ -\nabla T \end{pmatrix} . \tag{1.1}$$

In the presence of an external magnetic field B in the z-direction (see Figure 1) the transport coefficients $\hat{\sigma}$, $\hat{\alpha}$ and $\hat{\bar{\kappa}}$ are matrices, which, due to Onsager reciprocity, assume the following form:

$$\hat{\sigma} = \sigma_{xx}\hat{1} + \sigma_{xy}\hat{\varepsilon} \ , \tag{1.2}$$

where $\hat{1}$ is the identity, and $\hat{\varepsilon}$ is the antisymmetric tensor $\varepsilon_{ij} = -\varepsilon_{ji}$. σ_{xx} and σ_{xy} describe the longitudinal and Hall conductivity, respectively. The resistivity $\hat{\rho}$ is defined as the inverse of the conductivity matrix, namely $\hat{\rho} = \hat{\sigma}^{-1}$. An analogous form holds for the thermo-electric conductivity $\hat{\alpha}$, which determines the Seebeck coefficient S, namely:

$$S = \frac{\alpha_{xx}}{\sigma_{xx}} \ , \tag{1.3}$$

as well as for the matrix $\hat{\bar{\kappa}}$ which governs thermal transport in the absence of electric fields. The latter applies to samples connected to conducting leads, allowing for a stationary current flow. In contrast, the thermal conductivity, $\hat{\kappa}$, is defined as the heat current response to $-\nabla T$ in the absence of an electric current (electrically isolated boundaries). It is given by

$$\hat{\kappa} = \hat{\bar{\kappa}} - T\hat{\alpha}\cdot\hat{\sigma}^{-1}\cdot\hat{\alpha} \ . \tag{1.4}$$

Finally, the Nernst response is defined as the electric field induced by a thermal gradient in the absence of an electric current, and is given in linear response by the relation $E = -\hat{\theta}\nabla T$, with

$$\hat{\theta} = -\hat{\sigma}^{-1}\cdot\hat{\alpha} \ . \tag{1.5}$$

With these definitions at hand, we are now ready to start the analysis of the exotic and exciting properties of the cuprates superconductors, starting by understand how they differ from the Fermi Liquid theory, which is the theoretical framework according by which we comprehend the behaviour of most of metals and insulators existing in nature.

Chapter 2
Standard metals and the Fermi liquid

One of the milestones and great results of the 20$^{\text{th}}$ century is *Landau's Fermi liquid theory*, which underlines our present understanding of the majority of the known states of matter, like normal metals, semi-conductors, superconductors and superfluids. To better understand the differences between the predictions of this great theory and the behaviour of the cuprate superconductors, strange states of matter discovered since the early 80s, it is necessary to recall its basic properties in this Introduction referring the reader interested in the technical aspects to Appendix A or to standard condensed matter textbook (e. g. [1, 2]).

Let us start by recalling the basic properties of a system of free fermions in a box, where the Pauli exclusion principle controls everything. The ground state of this system is given by filling all the single-particle states inside a sphere (in case of rotational symmetry) in momentum space with radius k_F determined by the density of fermions, and with all the state outside the sphere empty. The boundary of this sphere is called the Fermi surface. The low-energy excitations of the system are given by either filling state slightly outside the Fermi surface or removing a fermion from a filled state slightly inside the Fermi surface, and are called particles and holes respectively. These excitations are gapless and have linear dispersion (for $k-k_F \ll k_F$):

$$\varepsilon(k) = \frac{k^2}{2m} - \mu = \frac{k_F}{2m}(k-k_F) \equiv v_F(k-k_F), \tag{2.1}$$

where m is the mass of the fermions, $\mu \equiv \frac{k_F^2}{2m}$ is the chemical potential, the quantity $v_F \equiv \frac{k_F}{m}$ is called the Fermi velocity and particles and holes are distinguished by the sign of $k-k_F$. Rephrasing the previous statements in a more formal language, the existence of these kind of excitations manifests itself as a pole in the complex frequency plane of the retarded Green' function $G_R(\omega,k)$ of the electron operator $\psi(\omega k)$:

$$G_R^0(\omega,k) \equiv \langle \psi(\omega,k)\psi(0,0)\rangle = \frac{1}{\omega - \varepsilon(k) + i0^+}, \tag{2.2}$$

which describes the causal response if we add an electron to the system. Fourier transforming the propagator (2.2) back in time we see that it describes, as it should,

the propagation of a free particle of energy $\varepsilon(k)$ (2.1):

$$G_R^0(t,k) = i\sqrt{2\pi}\theta(t)e^{-i\varepsilon(k)t}. \tag{2.3}$$

The situation becomes complicated when interactions are turned on, since the notion of single-particle state no longer makes sense. Even though one can expect that the qualitative picture of the non-interacting gas should remain valid if the interactions are weak, it is in principle not evident what should happen at strong coupling.

The basic assumption from which the phenomenological Landau theory starts is that the above qualitative picture for non-interacting Fermi gas in fact persist for a generic interacting fermionic system, also when the interactions between fermions are strong. Specifically, the basic Landau's starting assumptions are:

- The ground state of an interacting fermionic system is characterised by a Fermi surface in momentum space at $k = k_F$, defined as the locus of point in momentum space where $G_R^{-1}(0,k_F) = 0$.
- Despite the, possibly strong, interactions among fundamental fermions, the low energy excitations near the Fermi surface nevertheless behave like weakly interacting particles and holes, called collectively quasi-particles. They have the same charge as fundamental fermions and satisfy Fermi statistics. The dispersion of a quasi-particle resembles (2.1) in the free theory but with $m \to m^*$, where m^* can be considered as an effective mass of the quasi-particle and is in general different from the original fermion mass m, due to re normalization by many-body interactions.

Given these basic assumptions, one has to verify that the theory is stable, namely that, when the interactions between quasi-particles are switched on, the quasi-particles life-time is long enough such that an approximate particle picture still applies. Eventually, it can be proven that (see Appendix A) that, given a generic local interaction between quasi-particles, the decay rate of a quasi-particle obeys

$$\Gamma \sim \frac{\varepsilon^2}{\mu} \ll \varepsilon \ . \tag{2.4}$$

Thus, the despite potentially strong interactions, there is a region sufficiently near to the Fermi surface, where quasi-particles have long life-time and an approximate particle pictures still applies.

This implies that, near the Fermi surface, the retarded Green's function for the fermion operator should have the form:

$$G_R(\omega,k) = \frac{Z}{\omega - v_F(k-k_F) + \Sigma(\omega,k)} \ , \tag{2.5}$$

where $Z < 1$ is the quasi-particle weight, which can be interpreted as the overlap between the approximate one-particle state generated by acting with the electron operator on the vacuum, and $\Sigma(\omega,k)$ is called the free energy. Finally, according to (2.1), the free energy Σ has the property:

$$\Im\Sigma(\omega,k) = \frac{i\Gamma}{2} \sim i\omega^2 \ . \tag{2.6}$$

The concept of quasi-particle is extremely powerful, and makes it possible to develop a general low energy theory, independently of the precise microscopic details of the system.

Starting from the basic assumptions previously outlined, it is possible, introducing some phenomenological prescriptions, to derive the behaviour of the thermodynamical quantities like the specific heat C_V and the chemical potential μ, the entropy s and the thermo-electric transport coefficients (see Appendix A for more details).

Regarding the thermodynamical quantities, considering only the quasi-particle contribution we obtain:

$$C_V = T\left(\frac{\partial s}{\partial T}\right)_V = s = \frac{\pi^2}{3}N(0)k_B^2 T \ , \tag{2.7}$$

$$\mu(n,T) = \mu(n,0) - \frac{\pi^2}{4}k_B\left(\frac{1}{3} + \frac{n}{m^*}\frac{\partial m^*}{\partial n}\right)\frac{T^2}{T_F} \ . \tag{2.8}$$

where k_B is the Boltzmann constant, $N(0)$ is the density of carriers at the Fermi surface, n is the total density of quasi-particles and $T_F = k_F^2/(2m^*k_B)$ is the Fermi temperature.

Actually, when we have to compare the theoretical predictions with experiments, we have to keep in mind that the experimental results provide us not only the electronic contribution of the thermodynamical quantities (2.7), but the total contribution, which takes into account also the effect of lattice vibrations, i. e. *phonons*, and defects. Since, as we will see in the next Section, it is not always an easy task to extrapolate the electronic contribution from the experimental data, in this manuscript we will try, when it is possible, to specify how the external degrees of freedom like lattice vibrations and impurities modifies the properties of the electronic plasma. As an example, regarding the specific heat C_V, it is known [1] that the phonons contribution to this quantity can be expanded in series of odd powers of the temperature T, namely:

$$C_{ph} = B_{ph}T^3 + E_{ph}T^5 + \dots \ . \tag{2.9}$$

Then, the total specific heat in a normal metal should scale as:

$$C_V = \gamma T + C_{ph} \ . \tag{2.10}$$

As regards the thermo-electric transport coefficients (see Chapter 1 for their definition), the relevant quantities in experiments are the electric resistivity ρ, the thermal conductivity κ and the Seebeck coefficient S, which measure the voltage generated due to the presence of an applied external thermal gradient. Keeping into account the presence of phonons and defects, we find for these quantities the following behaviour:

where d is the number of spatial dimensions in the system. In deriving the previous temperature scalings we have taken into account four different kind of scattering processes: the electron-impurity scattering (subscript imp), the electron-electron scattering (subscript ee), the electron-phonon scattering (subscript e-ph) and the

	low T, $(T \ll T_D)$	high T, $(T \gg T_D)$
ρ	$A_{imp} + B_{e,e}T^2 + C_{e,ph}T^{d+2}$	$\mathscr{A}_{e,ph}T$
S	$DT + E_{phd}T^d$	$\mathscr{D}_{e,ph}T + \mathscr{F}_{phd}\frac{1}{T}$
κ	$H_{ee}\frac{1}{T} + L_{imp}T + G_{e,ph}T^{d-1}$	$\mathscr{H}_{e,ph}$

Table 2.1 Transport coefficients temperature dependence predicted by the Fermi liquid theory.

phonon-drag mechanism (subscript phd), namely the process according to which the heat transfer in the metal causes a flux of phonons which carries the electron with it. This mechanism is relevant only when one considers the Seebeck effect S and can be neglected in the analysis of the electric and thermal transport. In normal metals, the phonon-phonon scattering process is sub-dominant with respect to the previously outlined scattering mechanism and can be neglected in the analysis of the thermoelectric transport coefficients (see Appendix A).

We have divided the whole temperature range into two intervals separated by the Debye temperature T_D. The coefficients in front of the powers of the temperature T in Table 2, are constant which depends on the specific parameters of the metal under consideration. In the region $T \gg T_D$ the electron-phonon scattering mechanism largely dominates the transport. In the opposite regime, at very low T the scattering mechanisms are dominated by the effect of impurities. However, in the transition region between $T \sim 0$ and $T \sim T_D$, since the scattering rate of the electron-phonon processes decrease faster than that of electron-electron processes as the temperature is decreased, there may be a region in which the transport properties are dominated by the electron-electron interactions. In this region the resistivity of the Fermi liquid scales as T^2. The T^2 scaling of the resistivity is considered a standard evidence of the presence of the Fermi liquid in the experimental measurements (see Chapter 3).

Finally, let us make some comments about the celebrated Wiedemann-Franz law. This law states that in a Fermi liquid where only to elastic scattering processes occur, the ratio $\kappa/(\sigma T)$ is constant in temperature and assumes the value $L_0 = \frac{\pi^2}{3e^2}$. In the analysis of Table 2, the scattering processes considered are all elastic with the exception of the electron-phonon interaction, under which a fraction of the energy of the quasi-particles is transferred to the lattice. This is definitely true in the low-T region where, as one can see from the table, the Wiedemann-Franz law is not satisfied. However, in the high-T regime the fraction of energy transferred to the lattice is very small and also the electron-phonon scattering can be considered as elastic. In this region the Wiedemann-Franz law holds exactly.

Chapter 3
The Fermi liquid breakdown: high-T_c superconductivity

The Fermi liquid theory we have outlined in the previous Section has been tremendously successful in explaining *almost* all metallic states in nature. However, fortunately nature hides always great surprises. In fact the first big breakdown of the Fermi liquid came in the early 80s, with the discovery of the phenomenon of high-temperature superconductivity [3].

Whereas "ordinary" or metallic superconductors usually have transition temperatures T_c below 30 K (which is the maximum critical temperature predicted by BCS theory [4]), high-T_c superconductors have been observed with transition temperatures as high as 138 K.

Moreover, in these peculiar materials both the transport properties of the non-superconducting phase and the superconducting pairing mechanism differ significantly from whose predicted by the Fermi liquid and BCS theory (see [4] for a theoretical review on BCS).

Until 2008, only certain compounds of copper and oxygen (so-called "cuprates") were believed to have high-T_c superconductors properties, and the term high-temperature superconductor was used interchangeably with cuprate superconductor for compounds such as bismuth strontium calcium copper oxide (BSCCO) [6] yttrium barium copper oxide (YBCO) [7], lanthanum strontium copper oxide (LSCO) and the mercury barium calcium copper oxide ($HgBa_2Ca_2Cu_3O_x$) [8]. However, several iron-based compounds (the iron pnictides) are now known to be superconducting at high temperatures [9, 11, 10].

Although the theoretical effort in explaining the mechanisms which govern the physics of these materials has been remarkable, at present there is still no an accepted theory which describes the whole set of their peculiar properties.

This chapter is devoted to describe the experimental properties of these materials, focusing particularly on the way in which the normal phase transport properties differ from the Fermi liquid paradigm. [1]

[1] This is done in light of the holographic analysis of the normal phase transport properties which is the central part of the manuscript.

Since the iron pnictides superconductors have been discovered in very recent times we will focus basically on the cuprates, which are the best known materials from the experimental point of view.

To have in mind the experimental properties of these materials is extremely important. In fact in the lack of a solid theoretical model it is fundamental to face with the experimental data in order to try to develop a serious theoretical starting point.

3.1 Cuprates: crystalline structure and electronic properties

In this Section we briefly outline the basic crystalline structure of cuprate superconductors. This is far to be comprehensive. The main purpose of this brief introduction is to make the reader familiar with the microscopic composition of the most popular of these materials, focussing the attention of the common features of these large class of compound. In what follows, some standard concepts of Structure of matter, like tight binding and crystalline unite cells appear. We refer the reader not familiar with these concepts to standard condensed matter textbooks (see e. g. [5]).

All high-T_c superconductors share the following two elements: the CuO_2 planes that form single-layer or multilayer conducting blocks per unit cell, and the "charge reservoirs" in between the CuO_2 planes that are responsible for contributing either electrons or holes to the CuO_2 planes. The more layers of CuO_2 the higher T_c. This structure causes a large anisotropy in normal conducting and superconducting properties, since electrical currents are carried by holes or electrons induced in the oxygen sites of the CuO_2 sheets.

The first superconductor found with $T_c > 77$ K (liquid nitrogen boiling point) is yttrium barium copper oxide ($YBa_2Cu_3O_{6+\delta}$); the proportions of the three different metals in the $YBa_2Cu_3O_7$ superconductor are in the mole ratio of 1 to 2 to 3 for yttrium to barium to copper, respectively. Thus, this particular superconductor is often referred to as the 123 superconductor. The unit cell of $YBa_2Cu_3O_7$ (see Figure 3.1) consists of three pseudo-cubic elementary perovskite unit cells. Each perovskite unit cell contains a Y or Ba atom at the center: Ba in the bottom unit cell, Y in the middle one, and Ba in the top unit cell. Thus, Y and Ba are stacked in the sequence [Ba-Y-Ba] along the c-axis. All corner sites of the unit cell are occupied by Cu, which has two different coordinations, Cu(1) and Cu(2), with respect to oxygen. There are four possible crystallographic sites for oxygen: O(1), O(2), O(3) and O(4) [14]. The coordination polyhedra of Y and Ba with respect to oxygen are different. The tripling of the perovskite unit cell leads to nine oxygen atoms, whereas $YBa_2Cu_3O_7$ has seven oxygen atoms and, therefore, is referred to as an oxygen-deficient perovskite structure. The structure has a stacking of different layers: (CuO)(BaO)(CuO2)(Y)(CuO2)(BaO)(CuO). One of the key feature of the unit cell of $YBa_2Cu_3O_{6+\delta}$ (YBCO) is the presence of two layers of CuO_2. The role of the Y plane is to serve as a spacer between two CuO_2 planes. In YBCO, the Cu-O chains are known to play an important role for superconductivity. Tc is maximal near 92 K when $\delta \sim 0.85$ and the structure is orthorhombic. Superconductivity

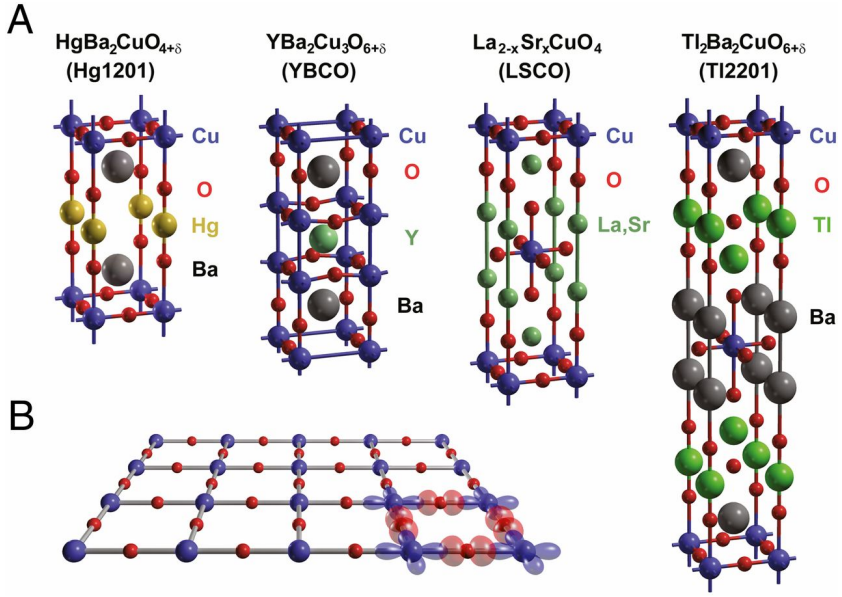

Fig. 3.1 Crystal structures of four hole-doped cuprates. (A) The unit cells (total number of atoms, individual versus pairs of CuO_2 sheets, c-axis dimensions, etc.). (B) The universal building block of the high-Tc cuprates is the CuO_2 sheet. The most important electronic orbitals, Cu $d_{x^2-y^2}$ and O p_σ, are shown. After [12].

disappears at $\delta \sim 0.4$, where the structural transformation of YBCO occurs from orthorhombic to tetragonal [15].

The crystal structures of Bi-, Tl-, Hg- and La-based high-T_c superconductors are very similar (see Figure 3.1) [16]. Like YBCO, the perovskite-type feature and the presence of CuO_2 layers also exist in these superconductors. However, unlike YBCO, Cu-O chains are not present in these superconductors. Moreover, contrary to the YBCO superconductor which, as previously said, has an orthorhombic structure, the other high-T_c superconductors have a tetragonal structure.

The cuprates previously discussed are all hole-doped, namely the "charge reservoirs" in between the CuO_2 contributes in adding holes to the CuO_2 planes. Although the majority of high-T_c superconductors are hole-doped compounds, there are a small number that can be doped with electrons (see [13] for a review on the topic). Along with the mostly commonly investigated compound $Nd_{2-x}Ce_xCuO_4$ (NCCO), most members of this material class have the chemical formula $RE_{2-x}M_xCuO_4$ where the lanthanide rare earth (RE) substitution is Pr, Nd, Sm or Eu and M is Ce or Th. These are single-layer compounds which, unlike their other brethren 214 hole-doped systems (for instance the T crystal structured $La_{2-x}Sr_xCuO_{4\pm\delta}$), have a T 0 crystal structure that is characterized by a lack of oxygen in the apical position (see Figure 3.2 left). [2]

[2] In what follow we will concentrate on the properties of the hole-doped cuprates.

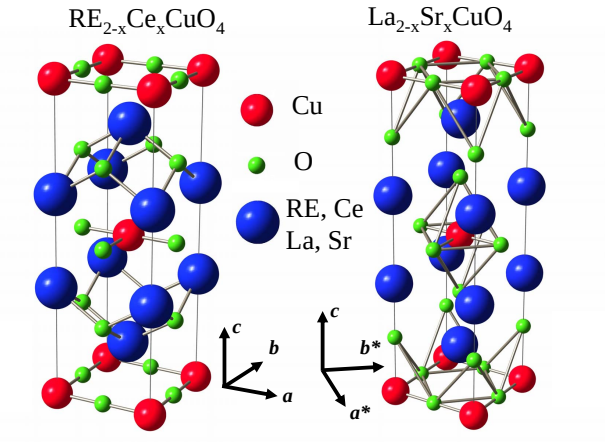

Fig. 3.2 A comparison of the crystal structures of the electron-doped cuprate $RE_{2x}Ce_xCuO_4$ and of its closest hole-doped counterpart $La_{2x}Sr_xCuO_4$. Here RE is one of a number of rare earth ions, including Nd, Pr, Sm, or Eu. One should note the different directions for the in-plane lattice parameters with respect to the Cu-O bonds. After [13].

As already mentioned, the common feature of all this compound is the presence of CuO_2 planes in their crystalline structure (hence the name cuprates). Then, even though no firm evidence has been provided, it is commonly believed that the superconductivity phenomenon and all the peculiar properties of these materials are due to the presence of these perovskite planes. The electronic structure of these perovskite planes is sketched in Figure 3.3. Its highest partially-filled band has predominantly $3d_{x^2-y^2}$ and $O_{2p_{x,y}}$ character. The resulting planar energy dispersion can be expressed in tight-binding representation as

$$\varepsilon(k) = \varepsilon_0 - 2t\,(\cos k_x + \cos k_y) + 4t'\,(\cos k_x \cos k_y) + 4t''\,(\cos 2k_x + \cos 2k_y)\ . \quad (3.1)$$

At half-filling, with only nearest-neighbour (t) hopping, a diamond-like Fermi surface is expected. Inclusion of next-nearest-neighbour (t) hopping leads to a more rounded topology. The ratio t'/t has been observed to be proportional to the critical temperature T_c in a large number of cuprates [18]. Low T_c cuprates like $La_{2x}Sr_xCuO_4$ and $Bi_2Sr_{2x}La_xCuO_6$ have a relatively low t'/t, whilst those with higher T_c values, such as $Bi_2Sr_2CaCu_2O_{8+\delta}$, $YBa_2Cu_3O_{6+\delta}$ and $Tl_2Ba_2CuO_{6+\delta}$, have much more rounded Fermi surface geometries characteristic of the higher t'/t values.

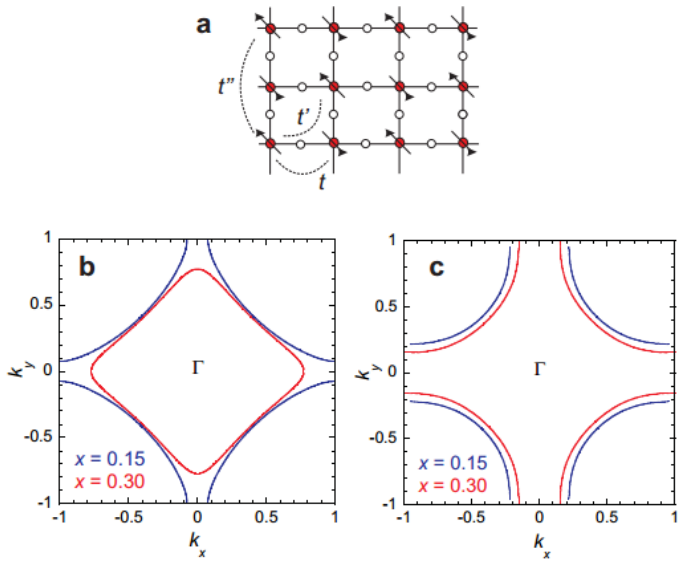

Fig. 3.3 **a**) Schematic figure of the CuO_2 plane showing the spin alignments of the Cu spins at half-filling within the basal lane and the three principal hopping parameters t, t' and t''. **b**) Schematic 2D projection of the Fermi surface in $La_{2x}Sr_xCuO_4$ for doping level p=0.15 (t'/t = 0.15) and 0.30 (t'/t = 0.12). **c**) Similar projections for $Tl_2Ba_2CuO_{6+\delta}$ for p = 0.15 (t'/t = 0.22) and 0.30 (t'/t = 0.22). In all cases, t''/t' = -0.5. After [17].

3.2 Cuprates: phase diagram

Since, as we have outlined in the previous Section, all the peculiar properties of the cuprates superconductors are believed to be caused by the presence of the perovkite planes, let us now analyse the in-plane phase diagram of these compounds. Basically, all the cuprates superconductors share the main features of the in-plane phase diagram. In this Section we will review schematically these properties, postponing a more precise characterization to the next Section, where the in-plane transport properties will be analysed.

The phase diagram of the cuprates is extremely reach and depends essentially on the temperature T and the doping concentration p (for hole-doped cuprates) or n (for electron-doped cuprates).

In Figure 3.4 the schematic phase diagram for both electron and hole-doped cuprate superconductor is plotted as a function of temperature and doping concentration. At zero doping, the electronic state of the parent compound is an anti-ferromagnetic Mott insulating state for both the n-type (electron-doped) and the p-type (hole-doped) cuprates. Strictly speaking however, the Hohenberg-Mermin-Wagner theorem (see e.g. [5]) asserts that an ideal two-dimensional (2D) magnetic system with isotropic anti-ferromagnetic Heisenberg couplings would remain magnetically disordered at finite temperature. The finding of long-range anti-

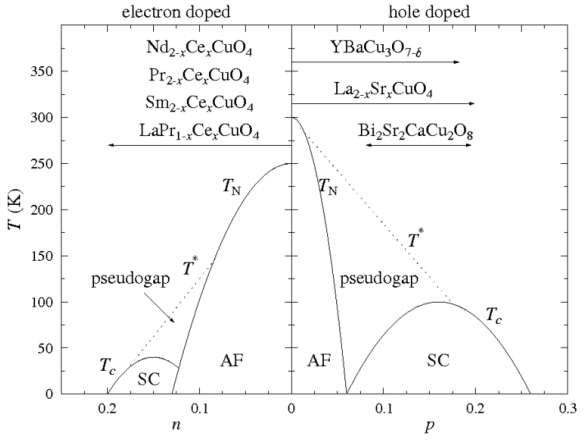

Fig. 3.4 Simplified doping dependent phase diagram of cuprate superconductors for both electron (n) and hole (p) doping. The phases shown are the anti-ferromagnetic (AF) phase close to zero doping, the superconducting phase (SC) around optimal doping, and the pseudo-gap phase. Doping ranges possible for some common compounds are also shown. After [19].

ferromagnetic ordering in real systems can be reconciled with theory by relaxing the strict 2D picture and incorporating three-dimensional (3D) anisotropic effects [20, 21, 22, 23].

As holes are introduced to the CuO_2 planes, the Néel temperature of the system decreases rapidly upon doping and the commensurate anti-ferromagnetic (AFM) long-range order disappears completely at around $p \sim 0.02$. Above this doping level, various types of spin fluctuations replace the original commensurate AFM order and continue to survive in the superconducting phase. In $La_{2-x}Sr_xCuO_4$ ($x = p$ for the one-layer systems), static incommensurate spin fluctuations develop beyond the Néel state and persist in the superconducting state, while in other compounds, such as $YBa_2Cu_3O_{6+\delta}$, commensurate magnetic resonance modes and significant dynamic spin fluctuations coexist with superconductivity in the under-doped and optimally doped region. When hole-doping is further increased, superconductivity sets in at $p \sim 0.05$ and lasts up to $p \sim 0.25$. Generally, the superconducting transition temperature T_c for copper-oxide superconductors has a parabolic dependence on the concentration of charge carriers p with a maximum at an optimal doping p_{opt} [24]. A universal formula for $T_c(p)$ can be proposed:

$$T_c(p) = T_{c,max}\left[1 - \beta(p - p_{opt})^2\right] \ , \tag{3.2}$$

where the parameters β and p_{opt} have the constant values, $\beta = 82.6$, p_{opt} =0.16 for a large number of compounds [25].

There is general consensus that the pairing symmetry of the superconducting order parameter of hole-doped cuprates is predominantly $d_{x^2-y^2}$-like in the under-doped and optimally doped region [26, 27]. In the heavily over-doped limit, on the

other hand, a significant s-wave component in addition to the $d_{x^2-y^2}$ component has been revealed [28]. In the normal state of the under-doped cuprates, various phenomena associated with a partially suppressed density of states around the Fermi level and an opening of the spectral gap in the spin and charge fluctuations have been observed [29]. This state is termed as the pseudo-gap phase.

Near the optimal doping, the pseudo-gap phase crosses over to an anomalous non-Fermi liquid region where the transport properties differ significantly from the Fermi liquid paradigm (see the following Section). As we further increase the doping to the over-doped range, some aspects of conventional Fermi liquid physics are eventually recovered.

Finally, let us make some comments on the phase-diagram of the electron doped cuprates. Even though, as we have noted previously, the low doping region is characterized by a Néel state as in the hole-doped compound, the phase diagram of the electron-doped cuprates is not simply the specular reflection of the hole-doped one (see Figure 3.4). Also about zero doping only an approximate symmetry exists between p- and n-type, as the anti-ferromagnetic phase is much more robust in the electron-doped material and persists to much higher doping levels (see Figure 3.4). Superconductivity occurs in a doping range that is almost five times narrower. In addition, these two ground states occur in much closer proximity to each other and may even coincide unlike in the hole-doped materials. Additionally, in contrast to many p-type cuprates, it is found that in doped compounds spin fluctuations remain commensurate. This asymmetry has tremendous consequences also in the transport properties. In what follows we will concentrate on the properties of the hole-doped cuprates referring to the literature for the electron-doped cuprates [13].

3.3 Cuprates: in-plane transport properties in the non-superconducting phase

We have noted in the previous sections that the typical order of magnitude of the critical temperature T_c of the superconducting phase transition is too high to be explained with the standard BCS theory. This is the first hint that the microscopic mechanisms that govern the behaviour of these materials must be different from that described for the Fermi Liquid in Chapter 2. In this Section, we will analyse carefully the transport properties in the non-superconducting phase, the so called strange metal phase. We will note that, even though the known thermodynamical properties in this phase are still Fermi liquid-like [54, 55, 56], the transport properties deviates significantly from the Fermi liquid prediction. Since it is commonly believed that a comprehension of the transport properties in the non-superconducting phase is mandatory in order to understand the pairing mechanism which generates superconductivity, from now on we will focus mainly on the strange properties of these phase.

In particular, also the basic assumption of the Fermi liquid theory, namely the existence of stable quasi-particles, has to be questioned in these materials. This can

be seen by the analysis of the spectral electric conductivity $\sigma_{xx}(\omega)$. In the standard Fermi liquid theory (see Appendix A), at low frequency this quantity has to follow a Drude-like behaviour, namely:

$$\sigma(\omega) \simeq \frac{N(0)e^2\tau}{m^*}\frac{1}{1-i\omega\tau}\,, \tag{3.3}$$

where τ quasi-particle life-time which in the Fermi liquid scales as $1/T^2$. As noted in 2 this temperature scaling ensure the stability of the quasi-particle near the Fermi surface and leads to the T^2 resistivity scaling which is characteristic of the Fermi liquid.

Optical conductivity data extending to temperatures up to and beyond 300 K have by now been collected on most cuprates (see [57, 58] for a review) and a generic and rather striking behaviour seems to be emerging. This is illustrated in Figure 3.5 where $\sigma_{xx}(\omega)$ data for under-doped $La_{1.9}Sr_{0.1}CuO_4$ are reproduced (without the phonon peaks).

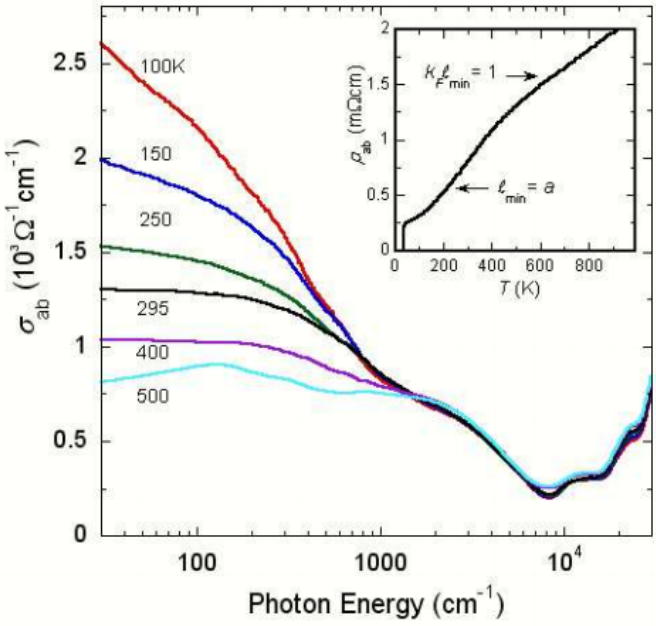

Fig. 3.5 Spectral conductivity $\sigma_{xx}(\omega)$ data for under-doped $La_{1.9}Sr_{0.1}CuO_4$ at various temperature T without the phonon peak. After [59].

At low T, $\sigma_{xx}(\omega)$ is dominated by a large Drude-like peak. As T increases, the low-frequency feature initially broadens and $\sigma(0)$ drops, thereby signalling an increase in the quasi-particle scattering rate plus in some cases, a redistribution of the

spectral weight. At a critical temperature T_{crit} ($\simeq$ 400 K for $La_{1.9}Sr_{0.1}CuO_4$) a subtle but fundamental change in the charge dynamics is heralded by the flattening out of $\sigma(\omega)$ in the low frequency limit at a corresponding value $\sigma_{crit}(0)$. Above T_{crit}, the plateau in $\sigma(\omega)$ evolves into a dip in the far infra-red limit, the low-frequency spectral weight being transferred to energies $\omega > W$ ($\simeq$ 1 eV).

The falloff of $\sigma_{xx}(\omega)$ in the Drude-like regime is significantly slower than is prescribed by the Drude formula (3.3). As discussed in detail in [60], it is impossible to fit the conductivity of the optimally doped cuprates with a simple Drude equation. If the scattering rate in the Drude equation is set at a low value to reproduce the shape of the low-frequency peak in $\sigma_{xx}(\omega)$, then the fit is completely wrong at higher frequencies. If the width of the Drude peak is chosen to be anomalously broad in accord with the behaviour of the conductivity at $\omega \simeq 600$ cm^{-1}, then the model yields the wrong magnitude of low ω behaviour and reveals strong disagreement with the DC conductivity.

The lack of a well defined Drude peak has led the physical community to think that the quasi-particle picture breaks down in these material (see Chapter 4 for more details). This fact is reflected in the other DC transport properties, which have a singular behaviour which strongly deviates from the Fermi Liquid picture, as we will illustrate in what follow.

3.3.1 Resistivity and Hall angle

In this Section we will review the basic known properties of the in-plane resistivity $\rho_{xx}(T)$ (see Chapter 1) and the Hall angle $\cot\theta_H$ defined as the ratio between the electric conductivity and the Hall conductivity, namely $\cot\theta_H \equiv \frac{\sigma_{xx}}{\sigma_{xy}}$.

Let us start from the resistivity. The temperature dependence of $\rho_{xx}(T)$ can be very carefully characterized in terms of the doping level, as sketched in Figure 3.6. In particular, as the reader will see by comparing the temperature dependence of $\rho_{xx}(T)$ with those described for the Fermi liquid in Table 2, the T^2 scaling, which is commonly considered as a distinguish feature of a Fermi liquid behaviour, is recovered only in specific regions of the phase diagram.

In particular, in Figure 3.6 the solid lines are the phase boundaries between the normal state and the superconducting or anti-ferromagnetic ground state, whilst the dashed lines indicate crossover in the $\rho_{xx}(T)$ behaviours which can not be uniquely associated with a fundamental change in the nature of the electronic states (no real phase transitions). The optimal doping level is indicated by the vertical dotted line corresponding to the pinnacle in the superconducting dome and the areas to the left (right) of this lines are the under-doped (over-doped) regions of the phase diagram respectively. In the under-doped regime, $\rho_{xx}(T)$ varies approximatively linear in temperature at high T, but as the temperature is lowered it deviates downward from linearity. This change of slope in $\rho(T)$ was initially interpreted as a "kink" in $\rho(T)$ at $T = T^*$ (marked on the Figure) [30, 31]. Plots of the derivative $d\rho/dT$ showed however that $\rho(T)$ in fact first deviates from linearity at a much higher T [32].

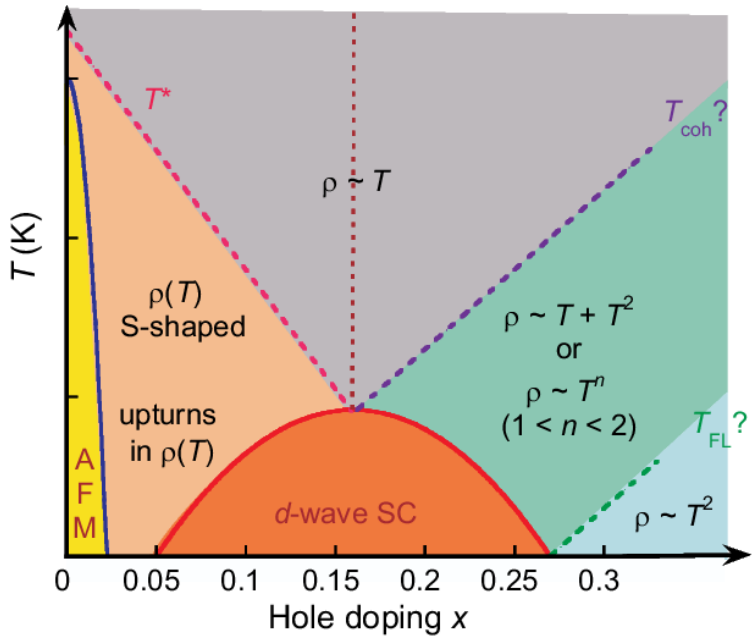

Fig. 3.6 Phase diagrams of the hole-doped cuprates. The different "phases" are mapped in terms of the different temperature behaviours of the in-plane resistivity. After [17].

Moreover, in the vicinity of T, there is no additional feature in $d\rho/dT$; the change of slope is a very gradual, continuous process with no clear evidence of a phase transition below T^*. In the more anisotropic cuprates such as LSCO [33] and Bi-2212 [34], it has proven difficult to distinguish between deviations from linearity due to genuine pseudo-gap effects and those due to para-conductivity fluctuations near T_c. The dashed line depicting T in Figure 3.6 reflects this ill-defined nature.

At sufficiently low temperatures, $\rho(T)$ of under-doped cuprates develops an upturn, suggestive of some form of (as yet unidentified) electronic localization. This upturn is characterized by a marked $\log(1/T)$ dependence [35]. The critical doping level p_{crit} at which these upturns occur differs amongst the various cuprate families [36, 37].

Optimally-doped cuprates are characterized by a T-linear resistivity that survives for all $T > T_c$. Despite the large variations in (optimal) T_c and in the crystallography of individual cuprate families, T-linear resistivity is a universal feature at optimal doping, confirming that it is intrinsic to the CuO_2 planes. Moreover, the value of ρ_{xx} at $T = 300$K normalized to a single CuO_2 plane is largely independent of the chemical composition of the charge transfer layers.

On the over-doped side, $\rho_{xx}(T)$ contains a significant supra-linear contribution that can be interpreted either as a sum of two components, one T-linear, the other quadratic, or a single power law T^n where n varies smoothly from 1 at optimal

doping to 2 at the superconducting transition boundary on the over-doped side [38, 39, 40]. At sufficiently high T however, $\rho(T)$ becomes T-linear once more. This crossover temperature [40] is marked in Figure 3.6 as a coherence temperature T_{coh}, in line with the suggestion from the ARPES community that the onset of T-linear resistivity coincides with the loss of the quasi-particles (coherence) peak in the energy dispersion curves [41].

The crossover to purely quadratic $\rho_{xx}(T)$, characteristic of a correlated Fermi liquid, is only observed beyond the superconducting dome. The dashed line marked T_{FL} represents this crossover to strictly T^2 resistivity. However, in this region the phenomenon of quantum oscillations [2], which is considered one of the fundamental evidence of a Fermi liquid behaviour, has never been measured.

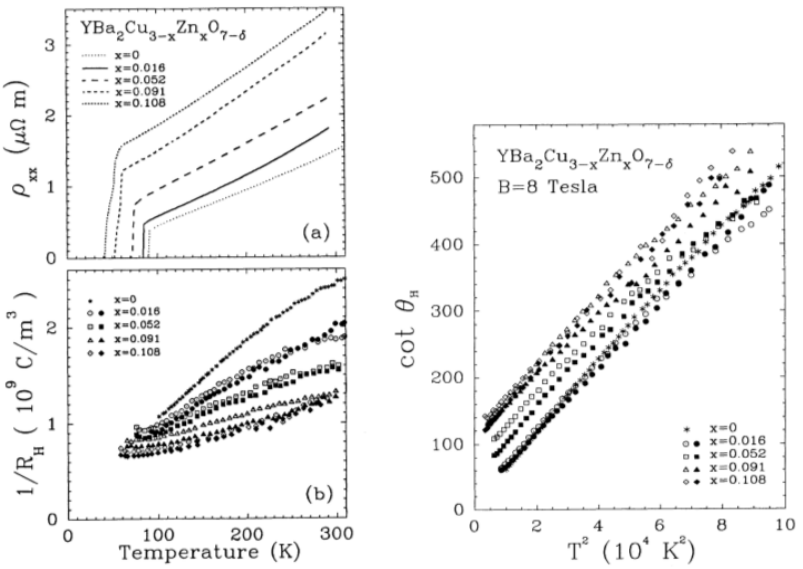

Fig. 3.7 Left: The temperature dependence of the in-plane YBCO resistivity of single-crystal doped with Zn. **Right:** Temperature dependence of the Hall angle $\cot\theta_H$ vs T^2 for a series of Zn-doped YBCO crystals. After [42].

In systems immersed in an external magnetic field, which is the common situation in measurements in cuprates, important physical quantities are the transverse transport coefficients (see Chapter 1).

In all hole-type cuprates near optimal doping, the Hall resistivity ρ_{xy}, which measure the transverse electrical response to an external applied voltage, displays a strong and complicated temperature dependence that persists to temperatures (T) as high as 500 K [42, 43, 44, 45]. An important clue to the origin of this anomaly was obtained by analysing the Hall angle $\cot\theta_H$ rather than ρ_{xy} or the Hall conductivity σ_{xy}. An investigation performed in [42] of how $\cot\theta_H$ varies with T and (concentration of Zn impurities c_{Zn}) in $YBa_2Cu_{3-x}Zn_xO_{7-\delta}$ revealed that the complicated

dependences of ρ_H on T and c_{Zn} simplify to the relationship

$$\cot\theta_H = \alpha T^2 + \beta c_{Zn} \ . \tag{3.4}$$

The Hall angle has been studied in La_2SrCuO_4 doped with 3d elements [43], as well as in the two-chain superconductor YBa_2CuO_4 [44]. These studies confirm that the $\cot\theta_H$ vs T relationship is valid (up to 500 K in some cases). In some cases, deviations from the T behaviour become significant in the under-doped or over-doped regimes [45].

Finally, whilst the T^2 dependence of $\cot\theta_H$ holds for a wide range of doping in most cuprates, it is not the case for the Bi-based cuprates Bi2212 and Bi2201. In these systems, the power exponent of $\cot\theta_H$ is closer to 1.75 than 2 [46].

3.3.2 Magneto-resistance and the Koheler's rule

According to Boltzmann transport theory (see Appendix A), the orbital transverse magneto-resistance of a metal $\Delta\rho/\rho$ is proportional to the cyclotron frequency $\omega_c = eB/m^*$ and to the quasi-particles life-time τ, namely

$$\Delta\rho/\rho \equiv \frac{\rho_{xx}(T,B) - \rho_{xx}(T,0)}{\rho(T,0)} \propto (\omega_c\tau) \propto (B\tau)^2 \ , \tag{3.5}$$

If the only effect of a change in temperature or of a change in the purity of the metal is to alter $\tau(k)$ to $\lambda\tau(k)$ where λ is not a function of the momentum k, then $\Delta\rho/\rho$ is unchanged if the magnetic field B is changed to B/λ. Thus the product $\Delta\rho\rho$ $(= \Delta\rho/\rho\rho_{xx}^2)$ is independent of τ and a plot of $\Delta\rho/\rho$ versus $(B/\rho)^2$ is expected to fall on a straight line with a slope that is independent of T (provided the carrier concentration remains constant).

This relation, known as Kohler's rule, is obeyed in a large number of standard metals, including those with two types of carriers, provided that changes in temperature or purity simply alter τ by the same factor. In HTC however, conventional Kohler's rule is strongly violated; instead of the data collapsing onto a single curve, there is a marked increase in the slope with decreasing temperature, as illustrated in the left panel of Figure 3.8 for $YBa_2Cu_3O_6.6$ [47].

Some progresses in the understanding of this violation were made in [47], where the authors studied the temperature behaviour for the Hall angle $\cot\theta_H$ and the orbital magneto-resistance $\Delta\rho/\rho$ for YBCO and LSCO at different doping levels. Specifically, they found the following temperature behaviour for the magneto-resistance:

$$\left(\frac{\Delta\rho}{\rho}\right)_{YBCO} \propto \frac{B^2}{T^4} \ , \qquad \left(\frac{\Delta\rho}{\rho}\right)_{LSCO} \propto \frac{B^2}{(A+CT^2)^2} \ , \tag{3.6}$$

where A and C are constants.

Moreover, for the Hall angle they found:

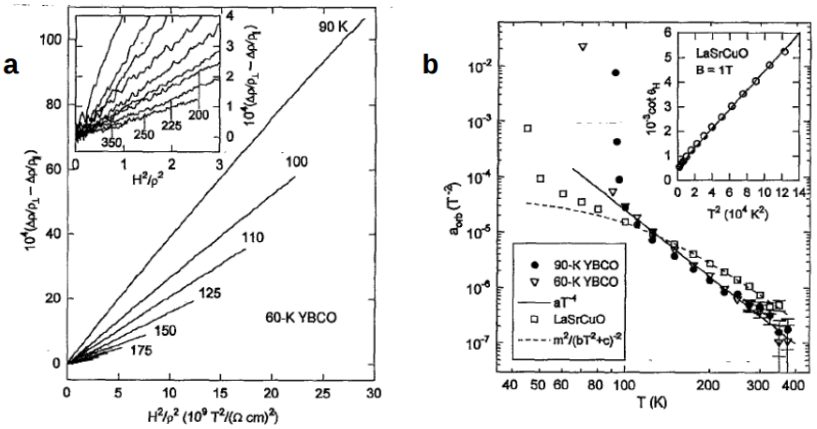

Fig. 3.8 a): Kohler plot for under-doped YBa2Cu3O6.6 at intermediate (main) and high (inset) temperatures . **b)** Temperature dependence of the orbital part of the magneto-resistance in $YBa_2Cu_3O_{6.6}$, optimally doped $YBa_2Cu_3O_7$ and $La_{1.85}Sr_{0.15}CuO_4$. The inset shows the inverse Hall angle $\cot\theta_H$ vs T^2 in optimally doped LSCO. Figures from [47].

$$\cot\theta_{H\,YBCO} \propto T^4 \,, \qquad \cot\theta_{H\,LSCO} \propto D + ET^2 \,, \tag{3.7}$$

where D and E are also constants. These behaviours allow them to introduce the following phenomenological modified Koheler's rule:

$$\frac{\Delta\rho}{\rho} \propto \tan^2\theta_H \,, \tag{3.8}$$

which seems to be satisfied (at least in the under-doped and optimally doped region of the phase diagram) as as one can see in Figure 3.8. Intriguingly, only in over-doped non-superconducting LSCO is conventional Kohler's scaling seemingly recovered [48].

As a final remark, we want to stress that in analysing the normal state orbital magneto-resistance, one must not overlook contributions to the orbital magneto-resistance from para-conductivity terms which can influence the in-plane magneto-transport over a wide temperature range in HTC due to their small superconducting coherence length and strong two-dimensionality (see e.g. [49] for a comprehensive review on the topic).

3.3.3 Thermal transport

The thermal transport properties, namely the thermo-electric (Seebeck) coefficient S and of the thermal conductivity matrix $\hat{\kappa}$ has been less studied than the electric transport properties previously described. This is firstly due to the difficulty of perform-

ing accurate measurements, and secondly, the problem of interpreting the ensuing results. Their interpretation is compounded of course by the additional contribution to $\hat{\kappa}$ from heat carrying phonons and the effect of the phonon drag mechanism on S (See also Appendix A). However, in recent time the developments of techniques for measurements at high magnetic field allowed the study of the Hall thermal properties. The latter are not substantially affected by phonons effects and can be used to get insight the electronic structure of the strange metals. In this brief Section we will review some of these results.

3.3.3.1 Seebeck coefficient

According to the simple Boltzmann picture (see Appendix A), the Seebeck coefficient S is governed both by the transport scattering rate (via its energy dependence) and the thermodynamic mass. Separating the effects of these two contributions can prove difficult and it is common practice to apply certain simplifying assumptions that may obscure some of the intrinsic physics especially in relation to the pseudogap. Whilst the interpretation of S may be difficult, its systematic behaviour in the strange metals has been well documented. In particular, a remarkable universal correlation was found early on between the room temperature value of S and the doping level [50]. This has been used subsequently to determine the doping concentration in a wide range of materials where determination of the hole concentration is ambiguous. Whilst this relation is not found to hold in $Bi_2\ Sr_{2-x}\ La_x\ CuO_{6+\delta}$ [51], its applicability to other HTC appears robust.

In under-doped cuprates, S has a large positive value and traces out a broad maximum whose peak temperature decreases with increasing doping. At optimal doping, $S(T)$ remains positive but has a negative linear slope, i.e.,

$$S_{OD}(T) = \beta - \alpha T \ . \tag{3.9}$$

As doping increases further, β continues to decrease whilst α remains relatively doping independent. Thus in the most over-doped samples, $S(T)$ is negative at all $T > T_c$.

3.3.3.2 Thermal conductivity and Lorentz ratio

The normal state in-plane thermal conductivity κ_{xx} of high-T_c superconductors is dominated by the phonon contribution. Typical estimates of the electronic contribution are of order 10-20 % of the total near $T = T_c$. Due to a lack of a solid theoretical model to compare it is almost impossible to subtract the phonon contribution and to analyse the pure electronic part; then the study of this quantity is not very helpful in understanding the electronic properties of the strange metals.

A more interesting quantity is the thermal Hall conductivity κ_{xy} which measure the transverse response to an applied longitudinal thermal gradient when the system

is immersed in an external magnetic field perpendicular to the plane. As all the transverse contribution, κ_{xy} is almost unaffected by phonons and allows to deduce some feature of the electronic structure of the strange metals.

The thermal Hall conductivity κ_{xy} was studied for the optimally doped YBCO in [52, 58]. In both the papers the authors found the following temperature dependence:

$$\kappa_{xy} \propto \frac{1}{T} , \tag{3.10}$$

and the two measurements agree also in the order of magnitude.

The two papers however disagree in the prediction of the Hall Lorentz ratio $L_{xy} \equiv \frac{\kappa_{xy}}{\sigma_{xy}T}$. This is an extremely interesting quantity since it has to be of the same order of magnitude of the Lorentz ration $L = \frac{\kappa_{xx}}{\sigma_{xx}T}$ and consequently it can provide an indirect measurement of the Wiedemann-Franz law which is an indicator of how much the system deviates from the Fermi liquid behaviour.

In [52] the authors found an Hall Lorentz ratio which varies approximatively linear in temperature and passes through several order of magnitude between 100 K and 300 K. On the over hand, the authors of [58] found a Hall Lorentz ratio approximatively constant in temperature and higher than the Fermi liquid prediction $L_0 = \frac{\pi^2 k_B^2}{3e^2}$. The discrepancy between the two results is not yet fully understood but it could be due to the fact that the authors of [52] measured the Hall conductivity σ_{xy} and the Hall thermal conductivity κ_{xy} in a different samples, while in [58] both σ_{xy} and κ_{xy} were measured in the same sample. However both the papers agrees in saying that the Wiedemann-Franz law seems to be strongly violated in these materials.

Chapter 4
Theoretical attempts

The experimental scenario described in the previous sections strongly suggest that the standard Fermi liquid paradigm is not valid for hight-T_c superconductors. Several attempts to explain the experimental observations within some modified Fermi liquid framework had always provided unsatisfactory results (see [17] for a detailed review on the topic).

Given this reliance on detail, other more exotic models, based on non-Fermi liquid physics, have gained prominence within the community; in this review we will concentrate on two model which provide inspiration also for the holographic treatment of Part 3. These are the two-lifetime picture of Anderson [61] and the Marginal Fermi liquid phenomenology of Varma and co-workers [62].

4.1 Anderson's model

In the two-lifetime approach, scattering processes involving momentum transfer perpendicular and parallel to the Fermi surface are governed by independent transport and Hall scattering rates $1/\tau_{tr}$ ($\propto T$) and $1/\tau_H (\propto T^2)$. In the usual Fermi liquid $\tau_{tr} = \tau_H$. To achieve different behaviours of the two scattering time, an effective Landau interaction between up and down spins is introduced (see [61] for more details). The effect of this interaction is not innocuous, and leads to separate Fermi velocities for charge- and spin-waves which, as a consequence, generate the unusual independence between τ_{tr} and τ_H.

Allowing τ_H to be independent of τ_{tr}, the inverse Hall angle can now be written as

$$\cot\theta_H = \frac{\sigma_{xx}}{\sigma_{xy}} \propto 1/\tau_H \ . \tag{4.1}$$

Thus the different behaviour of $\rho_{xx}(T)$ and $\cot\theta_H(T)$ reflects the different T dependencies of $1/\tau_{tr}$ and $1/\tau_H$.

Whilst the two lifetime model of Anderson has been successful in reproducing the experimental situation in optimally doped cuprates, it does not appear to be

consistent with ARPES results and is does not explain the evolution of the transport phenomena across the full cuprates phase diagram.

4.2 Phenomenological marginal Fermi liquid

The phenomenological marginal Fermi liquid developed by Varma and co-workers has acquired great relevance with mounting evidence for a Fermi surface accumulating from photoemission experiments.

In particular, we have learned in the previous sections that the correct theory has to keep into account for the existence of a Fermi surface but with no sharp defined quasi-particles. This gave support to the idea of a "marginal" Fermi liquid. Essentially, this is a theory that yields a Fermi surface in the weakest possible sense of the definition but otherwise does not make the same predictions as Fermi liquid theory.

To underline the differences between Fermi liquid theory and the marginal Fermi liquid let us recall briefly what we have outlined in Chapter 2 for the Fermi liquid.

In the presence of interactions the quasi-particles propagator acquires corrections due to the self-energy $\Sigma(\omega,k)$, namely:

$$G(\omega,k) = \frac{1}{\omega - \varepsilon_k - \Sigma(\omega,k)} \ , \tag{4.2}$$

where ε_k is the quasi-particle energy. The Fermi surface is defined as the locus in momentum space where $G^{-1}(0,k_F)$ vanishes (k_F is called the Fermi momentum). In the vicinity of the Fermi surface one can safely expand in series the denominator, obtaining:

$$G^{-1}(\omega,k) \simeq \omega \left(1 - \left.\frac{\partial \Re\Sigma}{\partial \omega}\right|_{\omega=0}\right) - [\varepsilon_k + \Re\Sigma(\omega,k)] - i\Im\Sigma(\omega,k) \ . \tag{4.3}$$

The quantity $z_k^{-1}(\omega) \equiv 1 - \frac{\partial \Re\Sigma}{\partial \omega}$ is called the quasi-particle residue and measure the amplitude of the jump in the quasi-particle distribution at the Fermi surface $k = k_F$, while $\Im\Sigma$ takes measures the decay rate of quasi-particles. In the standard Fermi liquid theory one finds:

$$\Re\Sigma \propto \omega \ , \qquad \Im\Sigma \propto \omega^2 \ . \tag{4.4}$$

Then, in the Fermi liquid theory the quasi-particle residue, which for free fermions is exactly equal to 1, assumes the following form

$$z_k(\omega = 0) = \frac{1}{1+\lambda} < 1 \ , \tag{4.5}$$

where λ measure the strength of the interactions. As we have proven in Appendix A, for $d \geq 2$ spatial dimensions, the quasi-particle residue does not vanish indepen-

dently of the strength of the interactions. This implies that the Fermi surface is well defined.

As we have previously said, we want to modify the Fermi liquid theory in order to still have a Fermi surface, but defined in a very weak sense. In order to do this, we phenomenologically modify the real part of the self-energy Σ as follow:

$$\Re\Sigma(\omega,k) \propto \omega \log\left|\frac{\omega}{\omega_c}\right| , \tag{4.6}$$

where ω_c is a high energy cut-off. Consequently, the quasi-particle residue is given by:

$$z_k(\omega) = \frac{1}{\log\left|\frac{\omega_c}{\omega}\right|} . \tag{4.7}$$

Now, in order to compute the quasi-particle residue on the Fermi surface we need to send ω to zero. In this limit we obtain $z_k \to 0$. Hence, the jump in the quasi-particle distribution tends to zero, but in a very weak way (i.e. logarithmically), and thus a Fermi surface just barely remains in the weakest sense. However, from the self-energy (4.6), all the other properties of the theory have a non-Fermi liquid like behaviour. This is one way to define the marginal Fermi liquid.

In order to completely characterize the phenomenology of the marginal Fermi liquid one has to find a consistent behaviour also for $\Im\Sigma$. To take into account the experimentally measured T-linear and ω-linear scattering rate τ_k, one has to guess:

$$\frac{1}{2\tau_k} = \Im\Sigma \propto x , \tag{4.8}$$

where $x = \max\{T, |\omega|\}$. Using the Drude result to roughly estimate the resistivity, namely $\rho_{xx} = (\omega_p \tau_k)^{-1}$ (where ω_p is the plasma frequency), the linear in temperature behaviour of the resistivity is recovered.

Having defined the basic ideas which yield the correct phenomenology we need to incorporate them in a consistent theory. Even though the attempt to construct a consistent microscopic theory with the marginal Fermi liquid phenomenology were numerous (see [68] for further details), a complete consistent way to microscopically reproduce the marginal Fermi liquid has not yet been discovered.

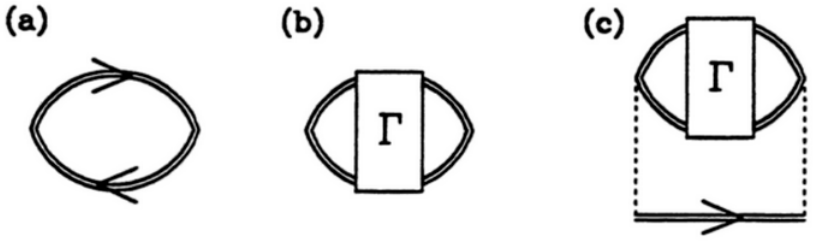

Fig. 4.1 Relevant diagrams for the self-energy computation in marginal Fermi liquid. After [68].

Rather to take the microscopic approach, another possibility is to assume a phenomenological model and should it work, then one would search for a microscopic description of the phenomenology after the fact. This was the approach followed by the authors of [62], where it was postulated that in the copper-oxide system there are charge and spin density fluctuations of the electrons which lead to a polarizability of the electron medium that would renormalize the electron propagator trough the self-energy. Such a polarizability is drawn in terms of the Feynmann diagrams in Figure 4.1. This is simply analogous to the electron-phonon interaction with the phonon line being replaced by the polarizability. Their proposal for the polarizability is as follows:

$$\Im P(\omega,k) = \begin{cases} -N(0)\frac{\omega}{T} , & for\ |\omega| < T , \\ -N(0) sign\omega & for\ |\omega| > T , \end{cases} \tag{4.9}$$

where $N(0)$ is the single particle density of states at the Fermi energy. The form of this polarizability is postulated to come from the vertex correction in the particle-hole susceptibility shown in Figure 4.1.

The self-energy that arises from applying the Feynmann rules to the diagrams in Figure 4.1 is given by:

$$\Sigma(\omega,k) \simeq g^2 N^2(0) \left(\omega \log \frac{x}{\omega_c} - i\frac{\pi}{2} x \right) , \tag{4.10}$$

which is consistent with that discussed previously and gives the correct phenomenology for the Fermi surface, the DC resistivity and also for the spectral conductivity (see [62] for further details on this quantity).

The basic marginal Fermi liquid assumption does not provide the correct behaviour for the magneto-transport. To get the correct prediction for the Hall angle and the magneto-resistance, the authors of [63] introduced anisotropy into their marginal Fermi liquid phenomenology via the elastic (impurity) scattering rate by assuming small angle scattering off impurities located away from the CuO_2 plane.

In other words, they phenomenologically modify the imaginary part of the self energy Σ as follows:

$$\Im\Sigma(T,k) = \Gamma_0(k) + \lambda T . \tag{4.11}$$

The anisotropic elastic part $\Gamma_0(k)$ has been ascribed to small-angle scattering from dopant impurities lying between the CuO_2 planes, an assumption supported by ARPES measurements [69]. Referring for the technical details to [63], with the phenomenological assumption (4.11) it is possible to reproduce the correct temperature behaviour for the Hall angle and the magneto-resistance.

Whilst this hypothesis seems consistent with certain ARPES measurements [64] and transport measurements [99], the legitimacy of the expansion in small scattering angle used in [65] has been subsequently challenged [66, 67]. In particular, it has been argued that the conditions that lead to a separation in lifetimes do not reproduce the violation of Kohlers rule [67]. Moreover, although the predictions of marginal Fermi liquid theory appear compatible with the empirical situation in op-

timally doped cuprates, their applicability to the rest of the cuprate phase diagram is less evident.

4.3 Quantum Criticality

Although a tremendous effort has been made to understand the strange metal better and beyond the phenomenology of the marginal Fermi liquid, only in one qualitative aspect has progress been made. In particular, in recent times the idea that the phenomenon of *Quantum Criticality* could be the responsible of the Fermi liquid break down in the strange metals has assumed growing importance. This is the critical universal behaviour that occurs in the vicinity of a *Quantum Phase transition* (see [71] for a review), which is a second order quantum phase transition. By definition, a quantum phase transition is a transition which occurs at zero temperature, as a result of varying some non-thermal control parameter, such as applied magnetic field or pressure. Since classically the entropy at zero temperature has to vanish, a quantum phase transition can not be caused by the competition between energy and entropy, like its finite-temperature counterpart. Rather, it is a result of competition between different terms in the Hamiltonian describing the system.

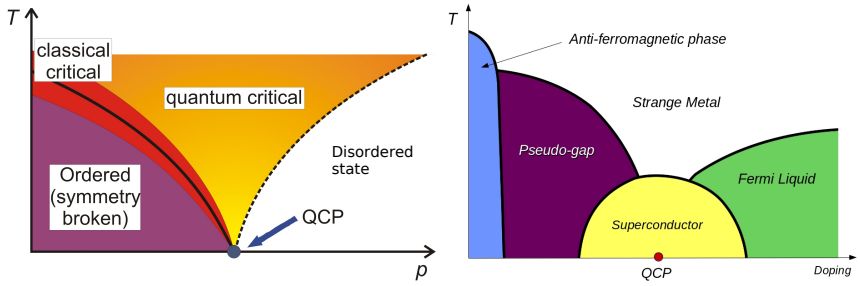

Fig. 4.2 Left: schematic typical phase diagram in the vicinity of a Quantum Critical point as a function of the temperature T and a generic tunable parameter p. **Right:** approximative phase diagram of the cuprates as a function of the temperature T and the doping.

Now, the relevant aspect is that, if this phase transition is second order, the absence of a scale at the critical point (due to the diverging correlation length) means that the quantum field theory describing this point must be a conformal field theory (See Part 2 for more details). The special aspect of a quantum critical theory compared to a classical critical theory is that one now raises the temperature in the conformal field theory, the conformal constraints resonate through in the finite temperature physics. A CFT at finite T is still very special in that all its dynamics are still controlled by the $T = 0$ conformal symmetry and in general the only aspect that changes is that all dimension-full quantities are now given in terms of the only present scale T. To get non-conformal (generic) behaviour one needs at least two

scales. This means that the phase diagram near a quantum critical point looks as in the left panel of Figure 4.3.

As one can see from the Figure, a common type of phase diagrams with a Quantum Critical point has a line of finite-temperature critical points where the transition temperature is depressed to zero by varying a coupling constant. Around this finite-temperature critical line, the system can be described by a classical field theory, even though the transition temperature may be very low. This is due to the fact that close to a critical point, the length scale above which the behaviour changes qualitatively is very large. Around any non-zero temperature critical point, therefore, one has $k_B T \geq \tilde{\omega}$ where $\tilde{\omega}$ is some typical energy scale above which the behaviour of the system changes (for example an energy gap). This reasoning clearly breaks down for a quantum phase transition, where the temperature is strictly zero. The behaviour at a Quantum Critical point is expected to be characterized by competition between low-lying states. This quantum critical behaviour is different from typical low energy behaviour, which can be understood in terms of quasi-particles on a ground state. This competition effect tends to break down away from the Quantum Critical point on the zero temperature line, as an energy gap forms and the system chooses a ground state. However, if the temperature is increased such that this gap may be overcome the interplay between the different energy levels again becomes the dominant behaviour. The finite temperature region of the phase diagram in which this quantum critical behaviour is important is called the quantum critical regime.

Comparing the typical Quantum Critical point phase diagram with those of the cuprates (right panel of Figure 4.3), it is very tempting to assume that the optimal doping region at $T = 0$ is associated with a quantum phase transition. Although the idea that the physics underlying the strange metal is a finite T conformal field theory, in detail it is not so simple. In particular scale-invariance is only observed in terms of energy-temperature scaling. In spatial directions one still notes a distinct Fermi surface with ARPES data and we have learned in the previous Section that the idea of the marginal Fermi liquid naturally takes into account this fact. This curious combination, scale-less in the "time-direction", but a distinct Fermi momentum in the spatial directions has been coined *local quantum criticality*.

It is important to note that the concept of local quantum criticality is naturally implemented in the marginal Fermi liquid picture. In fact, as it is evident from the Self energy (4.10) and from the polarizability (4.9), the spatial part of the susceptibility exhibits ordinary mean-field behaviour and the self-energy depends only on the frequency and exhibits non-trivial ω/T scaling. As we have previously explained, these are exactly the two basic ingredients to get local quantum criticality. For this reason the idea that the non-Fermi liquid behaviour of the strange metals is due to the influence of a quantum critical point is now predominant in the community.

However, at present, the existence of a Quantum Critical point in the phase diagram of the cuprates is still debated (see [70] for a review on the topic) and there are no measurements which strongly corroborate or confute this idea. This is, above all, due to the difficulty in performing measurements at very low temperature due to the presence of the superconducting dome.

Appendices

Appendix A
Basics of Fermi liquid theory

A.1 Quasi-particles and interactions

The basics assumptions, outlined in Chapter 2, above which the Fermi liquid theory is constructed, are equivalent to assume that there is a one-to-one correspondence between the state of the free Fermi gas and those of the interacting quasi-particles system, namely, if one takes a non interacting Fermi gas in a particular state and adiabatically turns on the interactions between particles, one obtains a state of the interacting system. Consequently, state in the interacting system may be classified by the distribution of particles $N_{p\sigma}$, (p is momentum and σ is spin), in the corresponding state of Free Fermi gas. $N_{p\sigma}$ is referred as the *quasi-particle distribution function* and quasi-particles obey the exclusion principle.

The distribution function $N_{p\sigma}$ of a general energy eigenstate is a highly discontinuous function of p. However, to describe the microscopic properties of the Fermi liquid is sufficient to consider the *mean quasi-particle distribution* $n_{p\sigma}$, that is the average of $N_{p\sigma}$ over a group of neighbouring single-particle states. In the microscopic state $n_{p\sigma}$ is a smooth function of p.

The energy of each state may be regarded as a functional $E\{N_{p'\sigma'}\}$ of the distribution function. If we add a quasi-particle to an unoccupied state $\{p,\sigma\}$, then the total energy of the system will increase by an amount $\varepsilon_{p\sigma}$ called the *quasi-particle energy* which is itself a functional of the distribution function. Without loss of generality, it is possible to assume that $\varepsilon_{p\sigma}$ is a smooth function of p and consequently the energy $E\{n_{p\sigma}\}$ is a functional of the mean quasi-particle distribution function $n_{p\sigma}$. Then, the quasi-particle energy is defined as the variation of the total energy per unit volume V with respect to $n_{p\sigma}$:

$$\delta E = \frac{1}{V}\sum_{p\sigma}\varepsilon_{p\sigma}\delta n_{p\sigma}\ . \tag{A.1}$$

The mean quasi-particle distribution $n_{p\sigma}$ can be determined via thermodynamic arguments. In fact, a macroscopic thermal state at equilibrium and at temperature T has to satisfy the relation:

$$\delta E = T\delta s + \mu\delta n \tag{A.2}$$

where δs is the variation of the entropy density, δn is the variation of the particle density, T is the temperature and μ is the chemical potential. Since quasi-particles are in one-to-one correspondence with the free Fermi gas, the entropy must have the same form, namely:

$$s = -\frac{k_B}{V}\sum_{p\sigma}\left[n_{p\sigma}\ln n_{p\sigma} + (1-n_{p\sigma})\ln(1-n_{p\sigma})\right] , \tag{A.3}$$

where k_B is the Boltzmann's constant. Moreover, since the total number of particles is conserved, the density n is given by:

$$n = \frac{1}{V}\sum_{p\sigma} n_{p\sigma} . \tag{A.4}$$

Now, substituting the variation of E (A.1), n and s with respect to $n_{p\sigma}$,

$$\delta s = -\frac{k_B}{V}\sum_{p\sigma}\delta n_{p\sigma}\ln\frac{n_{p,\sigma}}{1-n_{p\sigma}}, \qquad \delta n = \frac{1}{V}\sum_{p\sigma}\delta n_{p\sigma} , \tag{A.5}$$

in (A.2), and imposing that the relation have to be satisfied for every $\delta n_{p\sigma}$, we obtain:

$$n_{p\sigma} = \frac{1}{e^{(\varepsilon_{p\sigma}-\mu)/k_BT}+1} . \tag{A.6}$$

Namely, the quasi-particles obey the usual Fermi-Dirac distribution[1].

At $T = 0$ (A.6) takes the familiar form $\theta(\varepsilon_{p\sigma} - \mu)$ of a Fermi sea occupied up to a given momentum p_F, the Fermi momentum.

For small perturbation around the $T = 0$ equilibrium state, the quasi-particles distribution function varies only in the neighbourhood of the Fermi surface. Then, considering a state produced by adding a quasi-particle to the ground state, its energy measured relative to the ground state is given by:

$$\varepsilon^0_{p\sigma} = \varepsilon_{p\sigma}\{n^0_{p'\sigma'}\}, \tag{A.7}$$

where the superscript 0 denote the ground state. The velocity of the quasi-particle at the Fermi surface (the Fermi velocity) is given by:

$$v_F = \left(\frac{\partial\varepsilon^0_{p\sigma}}{\partial p}\right)_{p=p_F} . \tag{A.8}$$

The quasi-particle effective mass m^* is consequently defined by the relation:

[1] Note however that also $\varepsilon_{p\sigma}$ is a functional of $n_{p\sigma}$. Then the equation (A.6) is actually a quite complicated implicit functional equation for $n_{p\sigma}$.

$$v_F = \frac{p_F}{m^*}. \tag{A.9}$$

Note that m^* is in general different from the bare mass of an electron m.

In the neighbourhood of the Fermi surface the quasi-particle energy takes the form

$$\varepsilon^0_{p\sigma} = \mu + v_F(p - p_F)\ . \tag{A.10}$$

It is useful also to define the quasi-particles density at the Fermi surface, namely:

$$N(0) = \frac{1}{V}\sum_{p\sigma}\delta(\varepsilon^0_{p\sigma} - \mu) = -\frac{1}{V}\sum_{p\sigma}\frac{\partial}{\partial\varepsilon_{p\sigma}}n^0_{p\sigma} = \frac{\Omega_d m^* p_F^{d-1}}{\pi^{d-1}\hbar^d}\ , \tag{A.11}$$

where the last equivalence is obtained replacing the sum over p by an integral and taking $\varepsilon_{p\sigma}$ as the variable of integration and Ω_d is the solid angle in d spatial dimensions [2].

By now we have not considered the possibility of interactions between quasi-particles. Switching on interactions, the interaction energy of two quasi-particle is defined as the amount $f_{p\sigma,p'\sigma'}/V$ that the energy of one $(p\sigma)$ changes due to the presence of the other $(p'\sigma')$. Then, a variation of the distribution function produces a variation of $\varepsilon_{p\sigma}$ given by

$$\delta\varepsilon_{p\sigma} = \frac{1}{V}\sum_{p'\sigma'} f_{p\sigma,p'\sigma'}\delta n_{p'\sigma'}\ . \tag{A.12}$$

In other words, f is the second order variation of the energy E (A.1) with respect to $n_{p\sigma}$.

Consequently, in presence of interactions the variation of the energy due to a variation $\delta n_{p\sigma}$ from its ground state can be written as:

$$\delta E = \frac{1}{V}\sum_{p\sigma}\varepsilon^0_{p\sigma}\delta n_{p\sigma} + \frac{1}{2V^2}\sum_{p\sigma,p'\sigma'} f_{p\sigma,p'\sigma'}\delta n_{p\sigma}\delta n_{p'\sigma'}\ , \tag{A.13}$$

and the corresponding quasi-particle energy is:

$$\varepsilon_{p\sigma} = \varepsilon^0_{p\sigma} + \frac{1}{V}\sum_{p'\sigma'} f_{p\sigma,p'\sigma'}\delta n_{p'\sigma'}\ . \tag{A.14}$$

As it is evident, the presence of interactions between quasi-particles affects both the static properties of the Fermi liquid, like the effective mass m^*, both the transport properties, as we will discuss better in the following Sections.

[2] Remember that we are dealing with a $d+1$-dimensional Fermi liquid.

A.2 Thermodynamic properties

In this section we will review the low-temperature behaviour of the basic thermodynamical quantity of a Fermi liquid, namely the specific heat, the entropy and the chemical potential.

Quite generally, the low temperature behaviour of the specific heat of a Fermi liquid is linear in temperature, with a coefficient given in terms of the effective mass of the quasi-particles at the Fermi surface.

To see this, we calculate the variation of the quasi-particle entropy with respect to a variation of the temperature δT. Keeping into account (A.5) and (A.6), we obtain

$$\delta s = \frac{1}{TV}\sum_{p\sigma}(\varepsilon_{p\sigma}-\mu)\delta n_{p\sigma}\ . \tag{A.15}$$

Moreover, from (A.5) we obtain also the following relation:

$$\delta n_{p\sigma} = \frac{\partial n_{p\sigma}}{\partial \varepsilon_{p\sigma}}\left[-\frac{\varepsilon_{p\sigma}-\mu}{T}\delta T + \delta\varepsilon_{p\sigma} - \delta\mu\right]\ . \tag{A.16}$$

It is not difficult to prove that the leading low-T contribution to the previous formula is provided by the first term. Then, as long as we concern with the low-T behaviour, we can safely neglect $\delta\varepsilon_{p\sigma}-\delta\mu$ in (A.16). Finally, the variation of the entropy is:

$$\delta s = \frac{1}{V}\sum_{p\sigma}(\varepsilon_{p\sigma}-\mu)^2\frac{\partial n_{p\sigma}}{\partial\varepsilon_{p\sigma}}\frac{\delta T}{T^2} \tag{A.17}$$

Replacing the sum by an integral other the energies we have:

$$\delta s = -\sum_\sigma \int p^d \frac{dp}{d\varepsilon}\frac{\Omega_d}{(2\pi\hbar)^d}d\varepsilon\frac{\partial}{\partial\varepsilon}\left[\frac{1}{e^{(\varepsilon-\mu)/k_bT}+1}\right]\left(\frac{\varepsilon-\mu}{T}\right)^2\delta T \tag{A.18}$$

$$= -k_B^2 N(0)\int_{-\infty}^{\infty}dx\frac{\partial}{\partial x}\left(\frac{1}{e^x+1}\right)x^2\delta T\ . \tag{A.19}$$

Finally, we obtain the following expression for the entropy at low-T:

$$s = \frac{\pi^2}{3}N(0)k_B^2T\ . \tag{A.20}$$

Consequently, the specific heat at constant volume is:

$$C_V = T\left(\frac{\partial s}{\partial T}\right)_V = s \tag{A.21}$$

Considering the free energy $F = E - Ts$, the first temperature variation (at constant volume) is $-s\delta T$, so that at low temperature

$$F = E_0 - \frac{\pi^2}{3}N(0)k_B^2T^2\ , \tag{A.22}$$

where E_0 is the ground state energy density.

Finally, we calculate the first correction to the chemical potential by using the thermodynamic relation $\mu = -(\partial F/\partial n)_T$, obtaining:

$$\mu(n,T) = \mu(n,0) - \frac{\pi^2}{4} k_B \left(\frac{1}{3} + \frac{n}{m^*} \frac{\partial m^*}{\partial n} \right) \frac{T^2}{T_F} \,. \tag{A.23}$$

where $T_F = p_F^2/(2m^* k_B)$ is the Fermi temperature.

A.3 Quasi-particle life-time: the Fermi liquid stability

Until now we have assumed that, even in the case where interactions between quasi-particles are switched on, there is a region of the phase space sufficiently near to the Fermi surface in which the Fermi liquid is stable, namely, the quasi-particles have a sufficiently long life-time in order for the particle description to be consistent.

In this Section we will analyse this aspect in a more quantitative way, computing explicitly the quasi-particle life-time when interactions between quasi-particles are considered. To do this, we find quite instructive to take a different approach to what we have considered in the previous Sections, namely the renormalization group approach. We will do all the computations at $T = 0$; the $T \neq 0$ case is more technically involved but nothing changes in principle.

A.3.0.3 The renormalization group approach

In order to apply the renormalization group to the Fermi liquid we have to construct a low-energy effective theory for the quasi-particles and, once the low energy Lagrangian is defined, to determine a momentum cut-off and an associated scaling limit for the physical quantities of the theory. We know that quasi-particles are

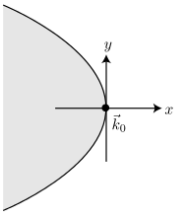

Fig. A.1 Arch of the Fermi surface near the point k_0.

gap-less fermionic excitations of the Fermi liquid around the Fermi surface. Then, in order to obtain a low energy effective field theory, we consider an arch in the

vicinity of an arbitrarily point k_0 on the Fermi surface [3] (see Figure A.1). We also consider d-dimensional fermionic fields $\psi_\sigma(k_x,k_y)$, where σ is the spin, k_x is the one-dimensional momentum orthogonal to the Fermi surface and k_y is the $d-1$-dimensional momentum orthogonal to k_x. The low energy effective field theory in the vicinity of k_0 is then given by a free fermion Lagrangian

$$S_0 = \int d\tau \int dk_x \int d^{d-1}k_y \psi^\dagger_\sigma \left(\frac{\partial}{\partial \tau} + \varepsilon(k_x,k_y) \right) \psi_\sigma \ , \tag{A.24}$$

where $\varepsilon(k_x,k_y)$ is the quasi-particle dispersion near k_0. Expanding this function for small k_x and k_y we obtain

$$S_0 = \int d\tau \int dk_x \int d^{d-1}k_y \psi^\dagger_\sigma \left(\frac{\partial}{\partial \tau} + v_F k_x + \frac{\kappa}{2} k_y^2 \right) \psi_\sigma \ , \tag{A.25}$$

where κ is the curvature of the Fermi surface in k_0. In this light, the Fermi surface in the vicinity of k_0 is defined as the locus of points where the quasi-particles have zero energy, namely

$$v_F k_x + \frac{\kappa}{2} k_y^2 = 0 \ . \tag{A.26}$$

The corrections due to the local curvature of the Fermi surface, as we will see explicitly in what follows, have relevant effects on the quasi-particle life-time.

The quantity $v_F k_x + \frac{\kappa}{2} k_y^2$ in (A.25) defines a natural momentum space cut-off, and associated scaling limit. Note that the momentum in the x direction scale as the square of the momentum in the y direction, and so we can choose the cut-off Λ so that $v_F^2 k_x^2 + \kappa^2 k_y^4 \ll \Lambda^4$ As we reduce Λ, the theory scales toward the single point k_0 on the Fermi surface, as we required above.

The renormalization group analysis can now be easily applied. Keeping the quantities v_F and κ fixed, the action (A.25) is invariant under the following rescaling of space-time:

$$k'_x = k_x e^{-2l}, \qquad k'_y = k_y e^{-l}, \qquad \tau' = \tau e^{-2l} \ , \tag{A.27}$$

where we have chosen the direction parallel to the Fermi surface as the ones defining the primary length-scale. The scalings above imply that the fermionic field has to scale in the following way:

$$\psi' = \psi e^{\frac{(d+1)l}{2}} \ . \tag{A.28}$$

Having determined the low energy theory and the fundamental scalings, we can now analyse the role of the interactions. The simplest contact interactions between quasi-particles has the form:

$$S_i = u_0 \int d\tau \int dk_x \int d^{d-1}k_y \psi^\dagger_\sigma \psi^\dagger_{\sigma'} \psi_{\sigma'} \psi_\sigma \tag{A.29}$$

Applying the renormalization group scaling (A.28) we obtain:

[3] It is possible to prove that the results is independent on the choice of k_0

$$u_0' = u_0 e^{(1-d)l} \ . \tag{A.30}$$

Namely, the interaction between the quasi-particle u_0 is irrelevant if $d > 1$. This strongly suggest that the Fermi liquid picture of non-interacting fermions is indeed renormalization group stable.

A.3.0.4 The quasi-particle life-time

To be more quantitative, let us compute the loop corrections to the free propagator,

$$G_T^0(\omega,k) = \frac{1}{\omega - \varepsilon(k_x,k_y) + i0^+}, \tag{A.31}$$

which occur due to the presence of the interaction (A.29). In this case, the propagator (A.31) is modified in the following way:

$$G_R(\omega,k) = \frac{Z}{\omega - \varepsilon(k_x,k_y) + \Sigma(\omega,k)}, \tag{A.32}$$

and, in order to compute the quasi-particle life-time, we are interested in computing the imaginary part of the fermion self-energy $\Sigma(\omega,k)$. To first order in u_0, the

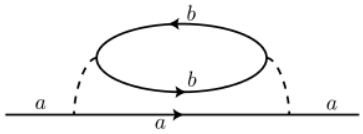

Fig. A.2 Relevant diagram for the u_0^2 correction to the free energy Σ.

fermion self energy is real, and only the quasi-particle residue Z is modified. In order to look at the possible instabilities of the quasi-particles, we have compute corrections at order u_0^2. The Feynman diagram contributing to the quasi-particle decay at order u_0^2 is indicated in Figure A.2, and it gives the following contribution to the self energy:

$$\Sigma(\varepsilon,k) = u_0^2 \int \frac{d^d q}{(2\pi)^d} \int \frac{d\omega}{2\pi} G_R^0(\varepsilon+\omega, k+q) \Pi(q,\omega), \tag{A.33}$$

where

$$\Pi(q,\omega) = \int \frac{d^d k}{(2\pi)^d} \int \frac{d\varepsilon}{2pi} G_R^0(\varepsilon+\omega, k+q) G_R^0(\varepsilon,k) \tag{A.34}$$

is the polarizability. Let us first compute explicitly this last quantity. We are only interested in terms that are singular in ω and q, and we can drop contribution from region of high momentum and frequency. In this case, it is legitimate to invert the

conventional order of integration and to first integrate over k_x. This procedure yields straightforwardly:

$$\Pi(\omega,q) = \frac{1}{v_F}\int \frac{d^{d-1}k_y}{(2\pi)^{d-1}}\int \frac{d\varepsilon}{2\pi}\frac{sign(\varepsilon+\omega)-sign(\varepsilon)}{\omega+iv_Fq_x+i\kappa q_y^2/2+i\kappa q_y\cdot k_y} \tag{A.35}$$

$$= \frac{|\omega|}{2\pi v_F}\int \frac{d^{d-1}k_y}{(2\pi)^{d-1}}\frac{1}{\omega+iv_Fq_x+i\kappa q_y^2/2+i\kappa q_y\cdot k_y} \tag{A.36}$$

$$= \frac{|\omega|}{2\pi v_F\kappa|q_y|}\int \frac{d^{d-2}k_y}{(2\pi)^{d-2}} \tag{A.37}$$

$$= \frac{|\omega|}{2\pi v_F\kappa|q_y|}\Lambda^{d-2}\,. \tag{A.38}$$

Now, inserting the last result in (A.35) in (A.33) and evaluating the integrals we obtain:

$$\Sigma(\omega,k) \quad = isign(\omega)\omega^2\tfrac{u_0^2}{4\pi v_F^2\kappa}\int\tfrac{d^{d-1}q_y}{(2\pi)^{d-1}}\tfrac{1}{|q_y|} \tag{A.39}$$

$$= isign(\omega)\omega^2\tfrac{u_0^2}{4\pi v_F^2\kappa}\Lambda^{d-2}\ ,\ for\ d>2\,. \tag{A.40}$$

In the important case of $d=2$, there is an infrared divergences in the integral for q_y in (A.39) which has to be regularized, yielding to a logarithmic correction to the result for $d>2$:

$$\Im\Sigma \sim u_0^2\omega^2\log\left(\frac{\Lambda}{u_0|\omega|}\right)\ ,\ for\ d=2\,. \tag{A.41}$$

Summarizing, up to logarithmic corrections, $\Im\Sigma\sim u_0^2\omega^2$ for $d\geq 2$. Thus the quasi-particle width vanishes as the square of the distance from the Fermi surface. Asymptotically close to the Fermi surface, the quasi-particle width is much smaller than the quasi-particle energy: this is sufficient to regard the quasi-particle as a sharp excitation, and confirm the validity of the basic Fermi liquid assumptions.

A.4 Thermo-electric transport

Having analysed the basic equilibrium properties of the Fermi Liquid, let us now focus on its response to small perturbations, such as an electric fields or a thermal gradient.

In the linear response framework, namely when the perturbations from the equilibrium are small, the thermo-electric transport properties in an isotropic system are controlled by three coefficients: the electric conductivity σ, the thermal conductivity (computed at null electric current) κ and the thermo-electric conductivity α. They relates the electric current j and the heat current q to the external electric field E and thermal gradient ∇T in the following way:

$$j = \sigma E - \alpha \nabla T \ , \tag{A.42}$$

$$q = \alpha T E - (\kappa + \frac{T\alpha^2}{\sigma}) \nabla T \ , \tag{A.43}$$

where the quantity $(\kappa + \frac{T\alpha^2}{\sigma})$ is usually called $\bar{\kappa}$ and is the thermal conductivity computed at null electric field.

In the next sections we will consider the Fermi liquid in non-equilibrium and inhomogeneous situations that differ little from the equilibrium state of the equilibrium state of the homogeneous liquid. In what follows, we will use a semi-classical description, specifying the quasi-particles distribution as a function of position and time, $n_{p\sigma}(t,r)$. The limit in this description resides in the uncertainty principle, which constraints to what extent the quasi-particles are localized in the position and momentum space.

More precisely, if the spatial inhomogeneity of the system occurs over a characteristic length λ, then the particles are localized in space only other a distance λ. At temperature T the distribution function varies in momentum space over a characteristic momentum $k_B T/v_F$. Then, the use of the distribution function does not require any localization of the quasi-particles in momentum space to less than $\Delta p = k_B T/v_F$. Thus, as long as $\lambda \gg \hbar v_F/k_B T$, the Heisemberg uncertainty principle causes no trouble. In what follow we will consider only this case.

A.4.1 The kinetic equation

With the assumptions outlined so far, the space and time dependence of the distribution function $n_{p\sigma}(t,r)$ is determined by the kinetic equation, which, in the absence of quasi-particle collisions, takes the form of the continuity equation for the distribution function in p and r space. Consequently, neglecting forces that rotate spin, the changes in the distribution function obey:

$$\frac{\partial n_{p\sigma}(t,r)}{\partial t} + \nabla_r \left[v_{p\sigma}(r,t) n_{p\sigma}(t,r) \right] + \nabla_p \left[f_{p\sigma}(r,t) n_{p\sigma}(t,r) \right] = I\left[n_{p'\sigma'} \right] \ . \tag{A.44}$$

In the previous formula $v_{p\sigma}$ is the quasi-particle velocity (dr/dt), $f_{p\sigma}$ is the time rate of change of the quasi-particle momentum (dp/dt) and $I\left[n_{p'\sigma'}\right]$ is the collision integral, which takes into account the possible presence of quasi-particle collisions, whose form we will discuss later.

The basic assumption of the quasi-particle kinetic theory is that the quasi-particle energy $\varepsilon_{p\sigma}(r,t)$ takes the role of the Hamiltonian, namely

$$v_{p\sigma}(r,t) = \nabla_p \varepsilon_{p\sigma}(r,t) \ , \tag{A.45}$$

$$f_{p\sigma}(r,t) = -\nabla_r \varepsilon_{p\sigma}(r,t) \ . \tag{A.46}$$

Substituting (A.45) in (A.44), we obtain the kinetic equation in its full glory:

$$\frac{\partial n_{p\sigma}(t,r)}{\partial t} + \nabla_p \varepsilon_{p\sigma}(r,t) \nabla_r n_{p\sigma}(t,r) - \nabla_r \varepsilon_{p\sigma}(r,t) \nabla_p n_{p\sigma}(t,r) = I\left[n_{p'\sigma'}\right] \ . \quad \text{(A.47)}$$

It is important to note that the Landau kinetic equation (A.47) is considerably richer than the usual Boltzmann equation used to describe weakly interacting gases. Specifically, there are two additional features included here. First, the quasi-particle velocity can depend on position and time, and this effect only arises in non-linear deviation from homogeneous equilibrium. Second, the force term $\nabla_r \varepsilon_{p\sigma}(r,t)$ includes effective field contributions due to the possibility interactions between quasi-particle which is hidden in $\varepsilon_{p\sigma}(r,t)$.

In all the cases we will discuss later, the distribution function differs by only a very small amount $\delta n_{p\sigma}$ from its value in uniform equilibrium $n^0_{p\sigma}$, namely:

$$n(r,p) = n^0_{p,\,\sigma}(\varepsilon_{p\sigma}) + \delta n_{p,\sigma}, \quad \text{(A.48)}$$

where we have defined $\delta n_{p,\sigma}$ such that the equilibrium distribution function n^0 is a function of the actual quasi-particle energy $\varepsilon_{p\sigma}$ and not of the equilibrium energy $\varepsilon^0_{p\sigma}$.

Then we will consider only the kinetic equation (A.47) linearised in $\delta n_{p\sigma}$, namely:

$$\frac{\partial\, \delta n_{p\sigma}}{\partial t} + \ v_{p\sigma} \cdot \nabla_r \delta n_{p\sigma} - \ v_{p\sigma} \cdot \nabla_r \varepsilon_{p\sigma} \frac{\partial n^0_{p\sigma}}{\partial \varepsilon_{p\sigma}} = I[\delta n_{p\sigma}] \ , \quad \text{(A.49)}$$

where $v_{p\sigma} \equiv \nabla_p \varepsilon_{p\sigma}$ is the quasi-particle velocity and $I[\delta n_{p\sigma}]$ is the linearised form of the collision integral, which we will discuss later.

The quantity $\nabla_r \varepsilon_{p\sigma}$ takes into account the effect of the external forces F applied to the system. For example, in presence of an external electric field E and a magnetic field B we will replace this quantity with:

$$-\nabla_r \varepsilon_{p\sigma} = F = -e\left(E + v_{p\sigma} \wedge B\right) \ . \quad \text{(A.50)}$$

Finally, Fourier transforming (A.49) in space and time, we obtain:

$$(\omega - q \cdot v_{p\sigma})\, \delta n_{p\sigma}(q,\omega) + F(q,\omega) \cdot v_{p\sigma} \frac{\partial n^0_{p\sigma}}{\partial \varepsilon_{p\sigma}} = iI[\delta n_{p\sigma}] \ . \quad \text{(A.51)}$$

A.4.2 Electric conductivity in a Galilean invariant Fermi liquid

In this Section we will compute the conductivity of a Galilean invariant Fermi liquid at zero temperature, namely we will consider a Fermi liquid in presence of an external electric field E and we will consider only the presence of collisions between quasi-particles which conserve the total momentum (we do not consider external collisions, $I[\delta n_{p\sigma}] = 0$). Our main goal is to prove that this kind of interactions do not contribute to the resistivity of a Fermi liquid.

To see this, let us consider the linearised kinetic equation (A.51) in presence of an external magnetic field, with $I[\delta n_{p\sigma}] = 0$ and at zero momentum $q = 0$, namely:

$$\omega \delta n_{p\sigma}(q,\omega) - ieE \cdot v_{p\sigma} \delta(\mu - \varepsilon_{p\sigma}) = 0 \ , \tag{A.52}$$

where we have used the relation $\frac{\partial n^0_{p\sigma}}{\partial \varepsilon_{p\sigma}} = -\delta(\mu - \varepsilon_{p\sigma})$ at $T = 0$.

Solving for $\delta n_{p\sigma}$ in (A.52) we obtain:

$$\delta n_{p\sigma}(q,\omega) = \frac{ieE \cdot v_{p\sigma} \delta(\mu - \varepsilon_{p\sigma})}{\omega} \ . \tag{A.53}$$

Now, in a Fermi liquid the total current density J may be expanded as a function of the deviation of the quasi-particle density from the equilibrium $\delta n_{p\sigma}$ in the following way:

$$eJ = e \sum_{p\sigma} \delta n_{p\sigma} j_{p\sigma} \ , \tag{A.54}$$

where $j_{p\sigma}$ is the current density of a quasi-particle ((p,σ).

In a Galilean invariant system, as a direct consequence of Galilean invariance, $j_p = p/m$, where m is the bare mass of the electron. Substituting this expression for $j_{p\sigma}$ in (A.54) and replacing the sum over p by an integral, it is easy to obtain:

$$\sigma(0,\omega) = \frac{iN(0)e^2}{m\omega} \ , \tag{A.55}$$

or, using the Kramers-Kronig relations:

$$\Re\sigma(0,\omega) = \frac{N(0)e^2}{m} \delta(\omega) \ . \tag{A.56}$$

As it is evident, if we consider only interactions between quasi-particles which conserve the total momentum, the Drude weight (the coefficient in front of the delta-function in (A.56)) depends only in the bare mass of the electron. In other worlds, this kind of interactions does not contribute to the resistivity.

In most of the qualitative arguments of the temperature scaling of the resistivity in a Fermi liquid, it is argued that the famous T^2 scaling is due to the scattering between quasi-particles. Actually this kind of interaction, as we have just proven, does not contribute by itself to the resistivity, and it is more precise to say that it is the combined action of the quasi-particle scattering and the Umklapp scattering which generates the T^2 scaling of the resistivity. This is not the case for the thermal conductivity, which is finite even if Umklapp scattering is not taken into account. We will clarify this aspect better in the following Sections.

A.4.3 Scattering mechanism in a metal

In the previous section we have considered the kinetic equations in the case that only interactions between quasi-particles are allowed. To be more realistic it is necessary to take into account the fact that in a metal several scattering mechanisms occur which dissipate momentum. In particular the most relevant interactions in a metal are those produced by interactions of quasi-particles with impurities and phonons. In this section we will analyze this kinds of scattering processes carefully using the kinetic equation (A.47).

In particular the linearised kinetic equation (A.49) in presence of an external static electric field E and a thermal gradient ∇T can be written as:

$$-eE \cdot v_{p\sigma} \frac{\partial n^0_{p\sigma}}{\partial \varepsilon_{p\sigma}} + v_{p\sigma} \cdot \nabla_r n^0_{p\sigma} = I[\delta n_{p\sigma}] \ . \tag{A.57}$$

In principle all the computation has to be done at fixed total number of quasi-particles ($N = const$). However, as we have computed in (A.23), the relative change in the chemical potential is actually very small, $(T/\mu)^2$. Thus, at the leading order in T/μ, all the physical effects can be calculated at $\mu = const$ instead that $N = const$. Consequently:

$$\nabla_r n^0_{p\sigma} = -\frac{\varepsilon_{p\sigma} - \mu}{T} \frac{\partial n^0_{p\sigma}}{\partial \varepsilon_{p\sigma}} \nabla_r T \ , \tag{A.58}$$

and the kinetic equation (A.57) may be written as:

$$-\left(eE + \frac{\varepsilon_{p\sigma} - \mu}{T} \nabla_r T \right) \cdot v_{p\sigma} \frac{\partial n^0_{p\sigma}}{\partial \varepsilon_{p\sigma}} = I[\delta n_{p\sigma}] \ , \tag{A.59}$$

where the collision integral $I[\delta n_{p\sigma}]$ has to be evaluated depending on the specific scattering mechanism.

Finally, the electric current j and the heat current q appearing in (A.54) assumes the following form:

$$j = -\frac{e}{V} \sum_{p\sigma} v_{p\sigma} \delta n_{p\sigma} \ , \qquad q = \frac{1}{V} \sum_{p\sigma} (\varepsilon_{p\sigma} - \mu) v_{p\sigma} \delta n_{p\sigma} \ . \tag{A.60}$$

A.4.3.1 Elastic scattering: impurities and the Wiedemann-Franz law

In a metal, the dominant scattering mechanism at low temperature is the scattering of quasi-particles by fixed impurities. One of the characteristic of this mechanism is that it is elastic. Because the atoms have large mass and are bounded in the lattice, the quasi-particle energy may be regarded as unchanged in the collision.

In this Section we first prove that the basic assumption of elastic scattering is by itself sufficient to give a simple relation between the electric and thermal conductivity in a Fermi liquid, the so called *Wiedemann-Franz law*. Secondly we will analyze

the temperature dependence of the transport coefficients due to the scattering of quasi-particles by impurities.

In order to derive the Wiedemann-Franz law, we first note that he elastic collision operator does not affect the dependence of the function $\delta n_{p\sigma}$ on the energy $\varepsilon_{p\sigma}$. This means that any factor $\delta n_{p\sigma}$, which depends only on the energy, can be taken outside the collision integral I. Consequently, under this assumption, the linearised collision integral $I[\delta n_{p\sigma}]$ can be written as:

$$I[\delta n_{p\sigma}] = \frac{\delta n_{p\sigma}}{\tau(p,T)} \,, \tag{A.61}$$

where $\tau(p,T)$ is a function those specific form has to be computed by explicitly evaluate the collision integral. Substituting (A.61) in (A.59), we obtain:

$$\delta n_{p\sigma} = -\tau(p,T)\left(eE + \frac{\varepsilon_{p\sigma}-\mu}{T}\nabla_r T\right)\cdot v_{p\sigma}\frac{\partial n^0_{p\sigma}}{\partial \varepsilon_{p\sigma}} \,. \tag{A.62}$$

Finally, substituting (A.62) in (A.60), and transforming the sum other p into an integral, the electric current j assumes the following form:

$$j = -e\sum_\sigma \int \frac{d^d p}{(2\pi\hbar)^d}\tau(p,T)\left(eE\cdot v_{p\sigma} + \frac{\varepsilon_{p\sigma}-\mu}{T}\nabla_r T\cdot v_{p\sigma}\right) v_{p\sigma}\frac{\partial n^0_{p\sigma}}{\partial \varepsilon_{p\sigma}} \,. \tag{A.63}$$

Comparing the previous equation with (A.42), the electric conductivity tensor is:

$$\sigma_{\mu\nu} = -e^2\sum_\sigma \int \frac{d^d p}{(2\pi\hbar)^d}\tau(p,T) v_{p\sigma,\mu} v_{p\sigma,\nu}\frac{\partial n^0_{p\sigma}}{\partial \varepsilon_{p\sigma}} \,. \tag{A.64}$$

In case of isotropic system $\sigma_{\mu\nu} = \sigma\delta_{\mu\nu}$, we can mediate other the space directions, obtaining

$$\sigma = -\frac{e^2}{3}\sum_\sigma \int \frac{d^d p}{(2\pi\hbar)^d}\tau(p,T) v^2_{p\sigma}\frac{\partial n^0_{p\sigma}}{\partial \varepsilon_{p\sigma}} \,. \tag{A.65}$$

The integral above can be simplified keeping into account the fact that, to the linear order in T/μ, $\frac{\partial n^0_{p\sigma}}{\partial \varepsilon_{p\sigma}} = -\delta(\varepsilon_{p\sigma}-\mu)$. Eventually, we obtain

$$\sigma = \frac{e^2}{3}\frac{N(0)}{\Omega_d} J(p_F) \,, \; \textit{where}\; J(p) = \sum_\sigma \int d\Omega_d \tau(p,\Omega,T) v^2_{p\sigma} \,. \tag{A.66}$$

As regards the thermo-electric conductivity α, comparing the second term in (A.63) with (A.60) we obtain:

$$\alpha = \tfrac{2e}{3T}\textstyle\sum_\sigma \int \frac{d^d p}{(2\pi\hbar)^d}(\varepsilon_{p\sigma}-\mu)\tau(p,T) v^2_{p\sigma}\frac{\partial n^0_{p\sigma}}{\partial \varepsilon_{p\sigma}} \tag{A.67}$$

$$= \tfrac{2e}{3T}\textstyle\int d\eta J(p)\eta\frac{\partial n^0_{p\sigma}}{\partial \eta} \,, \tag{A.68}$$

where $\eta = (\varepsilon_{p\sigma} - \mu)$ and we have mediated other the spatial directions. To evaluate the integral in (A.67) we note that the function $\frac{\partial n^0_{p\sigma}}{\partial \eta}$ goes to zero exponentially as $\eta \to \pm\infty$, and consequently we can safely extend the integration interval to $(-\infty, \infty)$. Moreover the function J is significantly different from zero only near the Fermi surface and then we can expand it as follows:

$$J(p,T) \sim J(p_F) + \eta \left.\frac{dJ(p)}{d\mu}\right|_{p=p_F} . \tag{A.69}$$

Stated this, we obtain:

$$\alpha = \frac{4e}{3T} \left.\frac{dJ(p)}{d\mu}\right|_{p=p_F} \int_0^\infty \eta^2 \frac{n^0_{p\sigma}}{\partial \eta} d\eta = -\frac{2e}{9} T \left.\frac{dJ(p)}{d\mu}\right|_{p=p_F} . \tag{A.70}$$

From the previous result we can derive the Mott low, which describes the behaviour of the Seebeck coefficient $s = \sigma/\alpha$ in a Fermi liquid where only elastic scattering phenomena are considered:

$$s = -\frac{2\Omega_d}{3N(0)e} T \left.\frac{d\log J(p)}{d\mu}\right|_{p=p_F} . \tag{A.71}$$

As regards the thermal conductivity, setting $E = 0$ and repeating the procedure outlined above for the heat current, we obtain:

$$q = -\frac{\pi^2}{9} \frac{N(0)}{\Omega_d} T J(p_F) \nabla_r T . \tag{A.72}$$

Finally, comparing (A.42) and (A.66) with (A.60) we obtain:

$$\kappa + \frac{T\alpha^2}{\sigma} = \frac{\pi^2 \sigma T}{3e^2} . \tag{A.73}$$

Actually, as we can argue from (A.70), the second term in the l.h.s. of (A.73) is of order T/μ and consequently we can neglect this term with respect to the r.h.s.. Considering (A.73) and (A.65), we eventually find this simple relation for the ratio $\frac{\kappa}{\sigma T}$:

$$\frac{\kappa}{\sigma T} = \frac{\pi^2}{3e^2} . \tag{A.74}$$

The previous formula is the celebrated Wiedemann-Franz law and is valid under the unique assumptions that all the scattering processes are elastic.

In order to determine the dependence on the temperature for the transport coefficients σ, α and κ in presence of scattering of quasi-particles by impurities separately, we have to analyze the specific form of the collision integral $I[n_{p\sigma}]$ for the case at hand. It assumes the following form:

$$I[n_{p\sigma}] = \\ N_{imp} \sum_{\sigma\,\sigma'} \int \frac{d^d p'}{(2\pi\hbar)^d} W(p,p') \left(n_{p',\sigma'}(1-n_{p\sigma}) - n_{p,\sigma}(1-n_{p'\sigma'}) \right) \delta(\varepsilon_{p\sigma} - \varepsilon_{p'\sigma'}) \,, \tag{A.75}$$

where N_{imp} is the density of impurities in the metal [4] and $W(p,p')$ is the scattering amplitude. The factors $(1-n_{p'\sigma'})$ and $(1-n_{p\sigma})$ take into account of the Pauli exclusion principle, namely a transition can take place only to an unoccupied state, while the factors $n_{p\sigma}$ and $n_{p'\sigma'}$ signify that the scattering can occur only from an occupied state. Linearising the collision integral in $\delta n_{p\sigma}$ we obtain:

$$I[\delta n_{p\sigma}] = N_{imp} \sum_{\sigma\,\sigma'} \int \frac{d^d p'}{(2\pi\hbar)^d} W(p,p') \left(\delta n_{p',\sigma'} - \delta n_{p,\sigma} \right) \delta(\varepsilon_{p\sigma} - \varepsilon_{p'\sigma'}) \,. \tag{A.76}$$

Moreover, due to the elastic hypothesis (A.76) becomes:

$$I[\delta n_{p\sigma}] = \delta n_{p,\sigma}) N_{imp} \sum_{\sigma\,\sigma'} \int \frac{d^d p'}{(2\pi\hbar)^d} W(p,p') \left(l(p') - l(p) \right) \delta(\varepsilon_{p\sigma} - \varepsilon_{p'\sigma'}) \,. \tag{A.77}$$

where $l(p)$ is a quantity which does not depend on the temperature. Consequently, since N_{imp} is temperature independent, the integral in (A.77) is independent on the temperature as the quantity $\tau(p)$ in the formulæ above.

Finally, we have found that, considering scattering of quasi-particles by fixed impurities, which are the dominant scattering phenomena in a metal at low temperature, the electric conductivity σ is constant in temperature, while the thermo-electric conductivity α and the thermal conductivity κ are both linear in T.

A.4.3.2 Electron-phonon scattering

In the previous Section we have derived the behaviour of the transport coefficients considering scattering mechanism due to the presence of a dilute density of impurities. Here we want to keep into account the effect of the presence of the lattice.

In real metal in fact, we can not assume the lattice to be perfect and the contributions due to lattice vibrations are in general relevant. As known (see [1] for more details), the lattice vibrations can be considered as fictitious spin-less particles, called phonons, obeying the Bose statistic. In formulæ, the equilibrium density of phonons N_p^0 is given by:

$$N_p^0 = \frac{1}{e^{\frac{\hbar\omega_p}{k_B T}} - 1} \,, \tag{A.78}$$

[4] We have assumed that the impurity atoms are randomly distributed and that the mean distance between them is much greater than the scattering amplitude, so that every event can be assumed as independent.

where ω_p is the phonons dispersion relations. At low momentum p, this is described by sound waves, namely

$$\omega_p = u_s p \tag{A.79}$$

where u_s is the sound velocity of phonos. The maximum physical significant value of p is associated to the boundary of the Broullion zone, which is roughly expressed in term of the lattice spacing a as $k_D \sim \pi/a$. The the maximum meaningful frequency for phonons, called the Debye frequency, is given by:

$$\omega_D \sim \frac{u_s \pi}{a} \ . \tag{A.80}$$

Since we are dealing with another type of particle involved in the transport mechanisms, one has to keep into account, in addition to the Boltzmann equation for quasi-particles (A.47), also the analogous equation for phonons:

$$\frac{\partial N_p}{\partial t} + u_k \cdot \nabla_r N_k = I_{ph,ph}[N_k] + I_{ph,e}[N_k] \ , \tag{A.81}$$

where $u_k \equiv \frac{\partial \omega_k}{\partial k}$. Note that it is necessary to add to the collision integral also the contribution due to the phonon-phonon interaction. This is because phonons do not conserve the total number of particle. Then the phonon-phonon interactions are not elastic and contribute to the collision integral I.

Stated this, let us now analyze how the interactions between phonons and quasi-particles affect the collision integral appearing in the quasi-particle kinetic equation (A.47) $I_{e,ph}[n_p]$, and that due to the phonons contribution in (A.81), $I_{ph,e}[n_p]$.

Regarding $I_{e,ph}[n_p]$, this is given by:

$$\begin{aligned} I_{e,ph}[n_p] = & \\ & \int \frac{d^d k}{(2\pi)^d} \delta\left(\varepsilon_p - \varepsilon_{p'} - \omega_k\right) w(p',k;p) \left[n_{p'}(1-n_p)N_k - n_p(1-n_{p'})(1+N_k)\right] \\ + & \int \frac{d^d k}{(2\pi)^d} \delta\left(\varepsilon_p - \varepsilon_{p'} + \omega_k\right) w(p';p,k) \left[n_{p'}(1-n_p)(1+N_k) - n_p(1-n_{p'})N_k\right] \ , \end{aligned} \tag{A.82}$$

where we have omitted the spin index since the interaction does not depend on the spin and we have performed the trivial summation over the two possible polarization state of the quasi-particle. The first term corresponds to processes with emission of a phonon having momentum k and by an electron having momentum p, and the reverse processes with absorption of a phonon k by an electron p' with return to p. The second term corresponds to processes with absorption of a phonon by an electron p and the reverse process of its emission by en electron p'. The delta function in the two integral ensures that the process conserves the total energy even though the energy of the quasi-particle is not conserved. Then, in general, this mechanism can not be considered as elastic with respect to the quasi-particles. Of course the collision integral vanishes identically if we replace both the quasi-particle density

n_p and the phonons density N_k with their equilibrium values n_p^0 and N_k^0. The two terms $w(p',k;p)$ and $w(p';p,k)$ are the probability weight corresponding to the two processes.

On the other hand, $I_{ph,e}[n_p]$ appearing in the kinetic equation for phonons (A.81) is the difference between the number of phonons k emitted by quasi-particles with any momenta p and the number absorbed by quasi-particles with any p':

$$I_{ph,e}[N_k] = 2\int \frac{d^d p}{(2\pi)^d}\delta\left(\varepsilon'_p - \varepsilon_p + \omega_k\right)\left[n_p(1-n_{p'})(1+N_k) - n_{p'}(1-n_p)N_k\right] , \tag{A.83}$$

where the factor 2 is due to the summation other the spin indices.

In order to solve the two coupled kinetic equations we need to linearise both the collision integrals (A.82) and (A.83) with respect to the fluctuations δn_p and δN_k, defined as:

$$n_p = n_p^0(\varepsilon) + \delta n_p , \tag{A.84}$$

$$N_k = N_k^0(\omega) + \delta N_k , \tag{A.85}$$

where, as above, $n_p^0(\varepsilon)$ and $N_k^0(\omega)$ are functions of the effective quasi-particle energy $\varepsilon_{p\sigma}$ and phonons energy ω_k respectively. Keeping in mind the form of the equilibrium distribution functions (A.6) and (A.78) we obtain:

$$\delta n_p = -\frac{\partial n_p^0}{\partial \varepsilon}\phi = \frac{n_p^0(1-n_p^0)}{T}\phi , \tag{A.86}$$

$$\delta N_k = -\frac{\partial N_k^0}{\partial \omega}\chi = \frac{N_k^0(1+N_k^0)}{T}\chi , \tag{A.87}$$

where ϕ and χ are unknown functions which measure the deviation from the equilibrium distributions. With this conventions the linearisation of the collision integrals (A.82) and (A.83) yields:

$$\begin{aligned} I_{e,ph}[\phi,\chi] = & \\ & -\int \tfrac{d^d k}{(2\pi)^d}\tfrac{\partial N_k^0}{\partial \omega} w(n_{p'}^0 - n_p^0)\big[(\phi_{p'} - \phi_p + \chi_k)\delta(\varepsilon_p - \varepsilon_{p'} - \omega_k) \\ & \qquad -(\phi_{p'} - \phi_p - \chi_{-k}) + \delta(\varepsilon_p - \varepsilon_{p'} + \omega_k)\big] , \end{aligned} \tag{A.88}$$

$$I_{ph,e}[\chi,\phi] = \frac{\partial N_k^0}{\partial \omega}\int \frac{d^d p'}{(2\pi)^d} w(n_{p'}^0 - n_p^0)\left[(\phi_{p'} - \phi_p + \chi_k)\delta(\varepsilon_p - \varepsilon_{p'} - \omega_k)\right] . \tag{A.89}$$

Unfortunately the previous integrals can not be treated analytically and the best one can do is to estimate their temperature behaviour. To proceed with a quantitative estimate, we need to evaluate the order of magnitude of the transition weight w. To do this, we note that the order of magnitude of the parameters of the electron spectrum in a metal can be expressed in terms of the lattice spacing a and the effective mass of the electrons m^* only; for example, the Fermi momentum $p_F \sim \hbar/a$, the speed $v_F \sim p_F/(m^* d)$ and the energy $E_F \sim v_F p_F \sim \hbar^2/(m^* d^2)$. The parameters of the phonons spectrum contain also the mass of the atoms of the lattice M. The density

of the substance $\rho_L \sim M$ and the speed of sound $u_s \sim \rho_L^{-1/2} \sim M^{-1/2}$. Consequently, we obtain for the speed of sound

$$u_s \sim v_F \sqrt{\frac{m^*}{M}}, \tag{A.90}$$

and the Debye temperature T_D associated to the Debye frequency ω_D is given by:

$$T_D \sim \hbar\omega_D \sim \frac{\hbar u_s}{d} \sim E_F \sqrt{\frac{m^*}{M}} \ . \tag{A.91}$$

As regards the transition probability w, as known (for more details see [1]), it proportional to the square of the electron-phonon scattering potential which is proportional to $M^{-1/4}$. Then making the dimensions right, we obtain:

$$w \sim T_D v_F a^2 \ . \tag{A.92}$$

The previous estimation is correct in case of optical phonons which has a dispersion relation which tends to a constant at low momentum. In case of emission or absorption of acoustic phonons we have to keep into account that the the dispersion relation is $\omega \sim u_s k$. Then the we need to add an extra factor k/k_D to the previous estimation, namely:

$$w \sim T_d v_F k a^3 \tag{A.93}$$

for acoustic phonons.

High-T behaviour ($T \gg T_D$)

At high temperatures, ($T \gg T_D$), phonons with all possible momenta are exited in the crystal, up to the maximum value which has the same order of the electron Fermi momentum: $k_{max} \sim p_F \sim 1/a$. By definition of the Debye temperature, the maximum phonon energy $\omega_{max} \sim T_D$, and consequently $\omega \ll T$ for all phonons. This allow us to treat the emission ad absorption of a phonon as an elastic scattering of a an electron and consequently, due to the discussion of the previous Section, to consider the Wiedemann-Franz law to hold. The scattering angle are not small, since the electrons and phonons momenta under these conditions are the same.

At high temperatures, when the phonon state occupation numbers are large, the establishment of equilibrium in each volume element of the phonon gas takes place very quickly. We can therefore regard the phonon distribution to be the equilibrium one when considering the electrical and thermal conductivity. This corresponds to take the function χ in (A.86) to be zero and to solve only the electron kinetic equation (A.47). As we will see, this approximation will be not valid in analysing the Seebeck coefficient where we need to take into account the effect of the phonon drag.

In order to analyze the temperature scalings of σ and κ, let us now analyze the temperature dependence of the collision integral $I_{e,ph}$. Because the phonon energy ω_k is small, we can expand the difference $n^0_{p'} - n^0_p$ in powers of ω_k:

$$n^0_{p'} - n^0_p \sim \omega_k \frac{\partial n^0_p}{\partial \varepsilon_p} \, . \tag{A.94}$$

We can than put $\omega_k = 0$ in the argument of the delta function, obtaining:

$$I_{e,ph}(\phi) = 2 \int \frac{d^d k}{(2\pi)^d} w \frac{\partial N^0_k}{\partial \omega_k} \frac{\partial n^0_p}{\partial \varepsilon_p} \delta(\varepsilon_{p'} - \varepsilon_p)(\phi_{p'} - \phi_p)\omega_p \, . \tag{A.95}$$

When $\omega_k \ll T$ the equilibrium phonon distribution function can be written as $N^0_k \sim T/\omega_k$. Moreover we have also $\frac{\partial n^0_p}{\partial \varepsilon_p} \sim -1/T$. Substituting these expressions in (A.95) and considering that the integral takes the major contribution from the region $k \sim k_{max}$ where $\omega_k \sim T_D$, we obtain:

$$I_{e,ph} \sim -w \frac{T}{T_D} \frac{k^{d-1}_{max}}{v^{d-2}_F} \frac{\phi_p}{T} \, . \tag{A.96}$$

Then considering the estimation for the scattering rate (A.92) and (A.93) and deriving the function ϕ_p from (A.86) at high temperatures, we obtain:

$$I_{e,ph} \sim -\phi_p \sim -T \delta n_p \, . \tag{A.97}$$

Putting this expression in the kinetic equation (A.47) and repeating the same steps of the previous Section for impurity scattering (remember that in this approximation the electron-phonon interaction is elastic as the scattering from fixed impurities) we finally obtain:

$$\sigma \sim \frac{N(0) e^2 \hbar}{m^* T} \, , \tag{A.98}$$

and applying the Wiedemann-Franz law:

$$\kappa \sim \frac{N(0) \hbar}{m^*} \, . \tag{A.99}$$

regarding the Seebeck coefficient α, as we have anticipated, the situation is more complicated. In fact, applying the Mott law (A.70), which is valid in general for elastic scattering mechanism, and considering the expression for the collision integral (A.97) we obtain:

$$\alpha^I \sim \frac{T}{e E_F} . \tag{A.100}$$

This contribution is extremely small due to the E_F factor at the denominator which comes from the logarithmic derivative in (A.70). This property may have the result

that a comparatively small addition to ϕ_p due to the non-equilibrium of the phonons yields a contribution to α which is comparable with (A.100).

In order to take into account the possible effect of the non-equilibrium of phonons let us suppose that the electron transport equation (A.47) in presence of an external thermal gradient can be expressed in the following form:

$$\frac{\partial n_p^0}{\partial T} v_p \cdot \nabla_r T = I_{e,ph}^{(1)}(\phi_p) + I_{e,ph}^{(2)}(\phi_p) \ , \tag{A.101}$$

and ϕ_p can be expressed as the sum of two contributions, $\phi_p = \phi_p^I + \phi_p^{II}$ where ϕ_p^I is the solution of (A.101) without $I_{e,ph}^2(\phi_p)$ and ϕ_p^{II} is the solution of the equilibrium equation for phonons

$$I_{e,ph}^{(1)}(\phi_p) + I_{e,ph}^{(2)}(\phi_p) = 0 \ . \tag{A.102}$$

repeating the previous steps for $I_{e,ph}^{(2)}(\phi_p)$ we find that this quantity is proportional to χ and then from (A.102) we obtain:

$$\frac{\phi^{II}}{\phi^I} \sim \frac{\chi}{\phi^I} \sim \frac{T_D}{T} \ll 1 \ , \tag{A.103}$$

namely ϕ^I is the major part of ϕ. However, unlike ϕ^I, ϕ^{II} is not zero when $\varepsilon_p = \mu$. Consequently, in the calculation the corresponding contribution to the current density is not cancelled, and the result is small only in the sense that ϕ^{II} is relatively small. This means that the additional contribution to the Seebeck coefficient due to the presence of ϕ^{II} is

$$\alpha^{II} \sim \alpha^I \frac{E_F}{T} \frac{T_D}{T} \sim \frac{T_D}{eT} \ . \tag{A.104}$$

The Seebeck coefficient is composed of two additive parts. These may be of the same order of magnitude but vary differently in temperature. The contribution α^{II} is commonly called phonon drag contribution and is due to the fact that the heat transfer in the crystal causes a flux of phonons which carries the electron with it.

Low-T behaviour ($T \ll T_D$)

At low temperature, $T \ll T_D$, the phonons distribution can not be regarded as the equilibrium one. Consequently, the electron-phonon interaction is not elastic in this case and one has to solve in a self consistent way both the kinetic equations for phonons and electrons.

In this spirit, it is important to note that, in this range of temperatures, the relaxation in the phonon system takes place mainly by phonon-electron and not by phonon-phonon collisions. To prove this statement let us first note that, at low T, and in the vicinity of the Fermi surface, $\omega \sim T$, $\varepsilon_{p\sigma} - \mu \sim T$ and therefore $N_0 \sim n_0 \sim 1$ and $\partial N_0 / \partial \omega \sim 1/T$. Moreover, the integration other $d^d p$ can be safely taken other a volume of a layer with thickness $\sim T/v_F$ along the Fermi surface. Since k/p is

small, the argument of the delta function can be expressed as:

$$\varepsilon_{p\sigma} - \varepsilon_{(p-k)\sigma} \simeq k \cdot \nabla_p \varepsilon_{p\sigma} - \omega \simeq v_F \cdot k - \omega \ . \tag{A.105}$$

The delta function is removed by integration over the direction of p for a given k, adding a factor $1/v_F k$ to the integrand. Finally, estimating the scattering weight w by means of (A.93), we obtain:

$$I_{ph,e}[\delta n_{p\sigma}] \sim -T\sqrt{\frac{m^*}{M}}\delta n_{p\sigma} \equiv \nu_{ph,e}\delta n_{p\sigma} \ , \tag{A.106}$$

where $\nu_{ph,e}$ is the phonon-electron collision frequency. It is known (see e.g. [2]) that the phonon-phonon collision frequency $\nu_{ph,ph}$ is given by:

$$\nu_{ph,ph} = T\sqrt{\frac{m^*}{M}}\left(\frac{T}{T_D}\right)^4 \ . \tag{A.107}$$

Then, due to the factor $\left(\frac{T}{T_D}\right)^4$ we have $\nu_{ph,ph} \ll \nu ph,e$ which proves the statement.

With the help of the observation above the behaviour of the relevant collision integrals which appear in the kinetic equation for phonons and electrons can be estimated using techniques similar to those illustrated in the previous Section. Referring to [1] for the technical details, we obtain the following temperature behaviours for the transport coefficients:

$$\sigma \sim C_{ph,e}T^{-(d+2)} \ , \tag{A.108}$$

$$S \sim DT + E_{phd}T^d \ , \tag{A.109}$$

$$\kappa \sim F_{ph,e}T^{d-1} \ , \tag{A.110}$$

where the coefficients in front of the temperature are model dependent constants.

References

1. L. P. Pitaevskii, E. M. Lifshitz, "Physical Kinetics: Volume 10 (Course of Theoretical Physics S)."
2. A. A. Abrikosov, "Introduction to the theory of normal metals."
3. J. G. Bednorz, K. A. Müller, "Possible high T_c superconductivity in the Ba-La-Cu-O system". Zeitschrift für Physik B 64 (2): 189-193 (1986).
4. M. Tinkham, "Introduction to Superconductivity: Second Edition (Dover Books on Physics) (Vol i)."
5. N. W. Ashcroft and A. Mermin "Solid state physics"
6. H. Maeda, Y. Tanaka, M. Fukutumi and T. Asano, "A New High-T_c Oxide Superconductor without a Rare Earth Element," Jpn. J. Appl. Phys. **27** (2) (1989), L209-L210.
7. M. K. Wu, J. R. Ashburn, C. J. Torng, P. H. Hor, R. L. Meng, L. Gao, Z. J. Huang, Y. Q. Wang, and C. W. Chu, "Superconductivity at 93 K in a New Mixed-Phase Y-Ba-Cu-O Compound System at Ambient Pressure," Phys. Rev. Lett. **58** (9) (1987), 908-910.
8. P. Dai, B. C. Chakoumakos, G. F. Sun, K. W. Wong, Y. Xin and D. F. Lu, "Synthesis and neutron powder diffraction study of the superconductor $HgBa_2Ca_2Cu_3O_{8+\delta}$ by Tl substitution," Physica C **243** (3-4) (1995), 201-206.
9. A. Leggett, "What DO we know about high-T_c?," Nat. Phys. **2** (3) (2006), 134.
10. C. Q. Choi, "Iron Exposed as High-Temperature Superconductor: Scientific American."
11. Z. Ren, G. C. Che, X. L. Dong, J. Yang Lu, Y. Wei, Wei, X. L. Shen, Li Zheng-Cai, Sun, Li-Ling, Zhou, Fang, Zhao, Zhong-Xian, "Superconductivity and phase diagram in iron-based arsenic-oxides $ReFeAsO_{1-}$ (Re = rare-earth metal) without fluorine doping," EPL **83**: 17002, (2008).
12. N. Barišić, Y. Li, G. Yu, X. Zhao, M. Dressel, A. Smontara, M. Greven, "Universal sheet resistance and revised phase diagram of the cuprate high-temperature superconductors," PNAS **110** (30), 12235-12240, (2013).
13. N. P. Armitage, P. Fournier, R. L. Greene, "Progress and perspectives on the electron-doped cuprates," Rev. Mod. Phys. **82**, 2421-2487, (2010).
14. R. Hazen, L. Finger, R. Angel,C. Prewitt, N. Ross, H. Mao, C. Hadidiacos, P. Hor, R. Meng, C. Chu. "Crystallographic description of phases in the Y-Ba-Cu-O superconductor," Phys. Rev. B **35** (13), 7238.
15. N. Khare, "Handbook of High-Temperature Superconductor Electronics." CRC Press. ISBN 0-8247-0823-7, (2006).
16. A. M. Hermann and J. V. Yakhmi, "Thallium-Based High-Temperature Superconductors."
17. N. E. Hussey, "Phenomenology of the normal state in-plane transport properties of high-T_c cuprates," J. Phys: Condens. Matter **20** (2008) 123201.
18. E. Pavarini, I. Dasgupta, T. Saha-Dasgupta, O. Jepsen and O. K. Andersen, Phys. Rev. Lett. 2001 **87** 047003.

19. C. Hartinger, "DFG FG 538 - Doping Dependence of Phase transitions and Ordering Phenomena in Cuprate Superconductors," Wmi.badw-muenchen.de. Retrieved 2009-10-29.
20. M. A. Kastner, R. J. Birgeneau, G. Shirane and Y. Endoh, Rev. Mod. Phys. **70**, 897 (1998).
21. T. Thio, T. R. Thurston, N. W. Preyer, P. J. Picone, M. A. Kastner, H. P. Jenssen, D. R. Gabbe, C. Y. Chen and R. J. Birgeneau, Phys. Rev. B **38**, 905 (1988).
22. T. Yildirim, A. B. Harris, O. Entin-Wohlman and A. Aharony, Phys. Rev. Lett. **72**, 3710 (1994).
23. H. Q. Ding, Phys. Rev. Lett. **68**, 1927 (1992).
24. M. R. Presland, J. L. Tallon, R. G. Buckley, R. S. Liu, N. E. Flower, Physica C **176**, 95 (1991).
25. J. L. Tallon, C. Bernhard, H. Shaked, R. L. Hitterman, J. D. Jorgensen, Phys. Rev. B **51**, 12911 (1995).
26. D. J. VanHarlingen, Rev. Mod. Phys. **67**, 515 (1995).
27. C. C. Tsuei and J. R. Kirtley, Rev. Mod. Phys. **72**, 969 (2000).
28. N. C. Yeh, C. T. Chen, G. Hammerl, J. Mannhart, A. Schmehl, C. W. Schneider, R. R. Schulz, S. Tajima, K. Yoshida, D. Garrigus, et. al., Phys. Rev. Lett. **87**, 087003 (2001).
29. T. Timusk and B. Statt, Rep. Prog. Phys. **62**, 61 (1999).
30. B. Bucher, P. Steiner, J. Karpinski, E. Kaldis and P. Wachter, Phys. Rev. Lett. **70**, 2012 (1993).
31. T. Ito, K. Takenaka and S. Uchida, Phys. Rev. Lett. **70**, 3995 (1993).
32. N. E. Hussey, K. Nozawa, H. Takagi, S. Adachi and K. Tanabe, Phys. Rev. B **56**, R11423 (1997).
33. T. Nakano, N. Momono, M. Oda and M. Ido, J. Phys. Soc. Japan **67**, 2622 (1998).
34. T. Watanabe, T. Fujii and A. Matsuda, Phys. Rev. Lett. **79**, 2113 (1997).
35. Y. Ando, G. S. Boebinger, A. Passner, T. Kimura and K. Kishio, Phys. Rev. Lett. **75**, 4662 (1997).
36. G. S. Boebinger et al. , Phys. Rev. Lett. **77**, 5417 (1995).
37. S. Ono, Y. Ando, T. Murayama, F. F. Balakirev, J. B. Betts and G. S. Boebinger, Phys. Rev. Lett. **85**, 638 (2000).
38. T. Manako, Y. Kubo and Y. Shimakawa, Phys. Rev. B **46**, 11019.
39. A. P. Mackenzie, S. R. Julian, D. C. Sinclair and C. T. Lin, Phys. Rev. B **53**, 5848 (2000).
40. S. H. Naqib, J. R. Cooper, J. L. Tallon and C. Panagopoulos, Physica **387**C, 365.
41. A. Kaminski, S. Rosenkranz, H. M. Fretwell, Z. Z. Li, H. Raffy, M. Randeria, M. R. Norman and J. C. Campuzano, Phys. Rev. Lett. **90**, 207003 (2003).
42. T. R. Chien, Z. Z. Wang, and N. P. Ong, Phys. Rev. Lett. **67**, 2088 (1991).
43. G. Xiao, P. Xiong, M. Z. Cieplak, Phys. Rev. B **46**, 8687 (1992).
44. B. Bucher, P. Steiner, J. Karpinski, E. Kaldis, and P. Wachter, Phys. Rev. Lett. **70**, 2012 (1993).
45. H. Y. Hwang, B. Batlogg, H. Takagi, H. L. Kao, J. Kwo, R. J. Cava, J. J. Krajewski, and W. F.vPeck Jr. , Phys. Rev. Lett. **72**, 2636 (1994).
46. Y. Ando and T. Murayama, Phys. Rev. B **60**, R6991 (1999).
47. J. M. Harris, Y. F. Yan,P. Matl, N. P. Ong, P. W. Anderson, T. Kimura and K. Kitazawa, Phys. Rev. Lett. **75**, 1391 (1995).
48. T. Kimura et al. , Phys. Rev. B **53**, 8733 (1996).
49. A. I. Larkin and A. A. Varlamov, The Physics of Superconductors: Vol. I Conventional and High-Tc Superconductors, (ed. K.-H. Bennemann and J. B. Ketterson) (Springer-Verlag, Tokyo), (2002).
50. S. D. Obertelli, J. R. Cooper and J. L. Tallon, Phys. Rev. B **46**, 14928 (1992).
51. Y. Ando, Y. Hanaki, S. Ono, T. Murayama, K. Segawa, N. Miyamoto and S. Komiya, Phys. Rev. B **61**, R14956 (2000).
52. Y. Zhang, N. P. Ong, Z. A. Xu, 1, K. Krishana, R. Gagnon and L. Taillefer, Phys. Rev. Lett. **84**, 10 (2000).
53. M. Matusiak, K. Rogacki1 and B. W. Veal, 2009 EPL **88** 47005.
54. J. W. Loram, K. A. Mirza, J. R. Cooper and W. Y. Liang, "Electronic Scpecific Heat of $YBa_2Cu_3O_{6+x}$ from 1.8 to 300 K," Phys. Rev. Lett. **71** (1993) 11.

55. J. W. Loram, K. A. Mirza, and P. A. Freeman, "Electronic Scpecific Heat of $YBa_2(Cu_{1-x}Zn_x)_3O_7$ from 1.6 to 300 K," Physica **171C** (1990) 243.
56. J. W. Loram, J. Luo, J. R. Cooper, W. Y. Liang and J. L. Tallon 'Evidence of pseudogap and condensate from the electronic specific heat," J. Phys. Chem. Sol. **62** (2001) 59-64.
57. N. E. Hussey, K. Takenaka, H. Takagi, Philosophical Magazine **84**, 2847-2864 (2004).
58. D. N. Basov and T. Timusk, Rev. Mod. Phys. **77**, (2005).
59. K. Takenaka, J. Nohara, R. Shiozaki and S. Sugai, Phys. Rev. B **68**, 134501 (2003).
60. J. Orenstein, G. A. Thomas, A. J. Millis, S. L. Cooper, D. Rapkine, T. Timusk, L. F. Schneemeyer and J. V. Waszczak, Phys. Rev. B **42**, 6342 (1990).
61. P. W. Anderson, Phys. Rev. Lett. **67**, 2092 (1991).
62. C. M. Varma, P. B. Littlewood,S. Schmitt-Rink, E. Abrahams and A. E, Ruckenstein, Phys. Rev. Lett. **63**, 1996 (1989).
63. C. M. Varma and E. Abrahams, Phys. Rev. Lett. **86**, 4652 (2001).
64. T. Valla, A. V. Fedorov, P. D. Johnson, Q. Li, G. D. Gu and N. Koshizuka, Phys. Rev. Lett. **85**, 828 (2000).
65. A. Narduzzo et al., arXiV:condmat0707.4601v1, (2007).
66. R. Hlubina, Phys. Rev. B **64**, 132508 (2000).
67. E. Carter and A. J. Schofield, Phys. Rev. B **66**, 241102.
68. A.Narlikar, Studies on high temperature superconductivity, Vol. 11.
69. T. Valla et al., Science **285**, 2110 (1999).
70. S. Sachdev, arXiv:0907.0008 [cond-mat.str-el].
71. S. Sachdev, "Quantum phase transitions".

Part II
Introduction to holography

Chapter 5
The gauge gravity duality

5.1 Review: Conformal Field Theory

In this Section we briefly review the basic concepts of Conformal Field Theories (CFTs) which are necessary to understand the AdS/CFT correspondence. This review is based on [17, 18]

5.1.1 The Conformal Group

A conformal transformation of the space-time coordinates is an invertible mapping $x \to x'$ which leaves the metric invariant up to a scaling factor:

$$g'_{\mu\nu}(x') = \Lambda(x) g_{\mu\nu}(x). \tag{5.1}$$

The set of conformal transformations forms a group, which has the Poincaré group as a subgroup, (we obtain Poincaré transformations for the special case $\Lambda(x) = 1$). The conformal transformations do not affect angles between arbitrary curves crossing each over at some point, and map circle in circle.

Let us now analyse infinitesimal conformal transformations. Under an infinitesimal coordinates transformation $x'_\mu = x_\mu + \varepsilon_\mu(x)$ the metric becomes:

$$g'_{\mu\nu} = g_{\mu\nu} - (\partial_\mu \varepsilon_\nu + \partial_\nu \varepsilon_\mu). \tag{5.2}$$

As it is evident from (5.1), in order for the previous transformation to be conformal ε_μ has to satisfy the following condition:

$$\partial_\mu \varepsilon_\nu + \partial_\nu \varepsilon_\mu = f(x) g_{\mu\nu}, \tag{5.3}$$

where $f(x)$ is a generic function whose specific form has to be determined. Considering the transformation as an infinitesimal deformation of the Minkowski metric

$\eta_{\mu\nu} = diag(-1,1,1...,1)$ in a d-dimensional space-time and by applying an extra derivative ∂_ρ to (5.3), permuting the indices and making a linear combination, we obtain:

$$2\partial_\mu\partial_\nu\varepsilon_\rho = \eta_{\mu\rho}\partial_\nu f + \eta_{\nu\rho}\partial_\mu f - \eta_{\mu\nu}\partial_\rho f. \tag{5.4}$$

It is not difficult to prove that (5.4) leads to the following equation for the function $f(x)$:

$$(d-1)\partial^2 f(x) = 0. \tag{5.5}$$

If $d = 1$ the previous equation is meaningless as it is evident from the fact that in one space-time dimension conformal transformations make not sense. The case $d = 2$ requires a more careful treatment and we shall briefly consider it at the end of the chapter.
Let us now restrict the attention to $d \geq 3$. In such a situation the solution of (5.5) is:

$$f(x) = A + B_\mu x^\mu, \qquad with\, A,\, B_\mu\, constants. \tag{5.6}$$

Substituting (5.6) in (5.4), we find that the general expression for ε_μ is:

$$\varepsilon_\mu = a_\mu + b_{\mu\nu}x^\nu + c_{\mu\nu\rho}x^\nu x^\rho,\ with\, c_{\mu\nu\rho} = c_{\mu\rho\nu}. \tag{5.7}$$

Since the equations (5.3) and (5.4) hold for every x, we may treat each power of x separately. It turns out that the constant term a_μ is unconstrained and corresponds to an infinitesimal translation. On the over hand, substituting the linear term in (5.4) we find the following constraint for $b_{\mu\nu}$:

$$b_{\mu\nu} + b_{\nu\mu} = \frac{2}{d} b^\lambda_\lambda \eta_{\mu\nu}, \tag{5.8}$$

which implies that $b_{\mu\nu}$ is a sum of an antisymmetric part and a pure trace:

$$b_{\mu\nu} = \alpha\eta_{\mu\nu} + m_{\mu\nu},\ with\, m_{\mu\nu} = -m_{\nu\mu}. \tag{5.9}$$

The pure trace term represents an infinitesimal scale transformation, while the antisymmetric part is an infinitesimal rotation.

In a similar way, substituting the quadratic term of (5.7) in (5.4), we obtain:

$$c_{\mu\nu\rho} = \eta_{\mu\rho}b_\nu + \eta_{\mu\nu}b_\rho - \eta_{\nu\rho}b_\mu,\ where\, b_\mu = \frac{1}{d}c^\sigma_{\sigma\mu}. \tag{5.10}$$

The infinitesimal transformation corresponding to the previous constraint is called the special conformal transformation (SCT),

$$x'_\mu = x_\mu + 2x_\nu b^\nu x_\mu - b_\mu x^2\ . \tag{5.11}$$

The corresponding finite transformations are:

$$translation \quad x'_\mu = x_\mu + a_\mu \tag{5.12}$$
$$dilatation \quad x'_\mu = \alpha x_\mu \tag{5.13}$$
$$rigid\ rotation\ x'_\mu = M^\mu_\nu x^\nu \tag{5.14}$$
$$SCT \qquad x'_\mu = \frac{x_\mu - b_\mu x^2}{1 - 2b_\nu x^\nu + b^2 x^2}. \tag{5.15}$$

The generators of the transformations (5.12) are:

$$translation \quad P_\mu = -i\partial_\mu \tag{5.16}$$
$$dilatation \quad D = -ix^\mu \partial_\mu \tag{5.17}$$
$$rigid\ rotation\ L_{\mu\nu} = i(x_\mu \partial_\nu - x_\nu \partial_\mu) \tag{5.18}$$
$$SCT \qquad K_\mu = -i(2x_\mu x^\nu \partial_\nu - x^2 \partial_\mu). \tag{5.19}$$

They satisfy the following algebra:

$$\begin{aligned}
\left[D, P_\mu\right] &= iP_\mu && (5.20)\\
\left[D, K_\mu\right] &= -iK_\mu && (5.21)\\
\left[K_\mu, P_\nu\right] &= 2i\left(\eta_{\mu\nu} D - L_{\mu\nu}\right) && (5.22)\\
\left[K_\rho, L_{\mu\nu}\right] &= i\left(\eta_{\rho\mu} K_\nu - \eta_{\rho\nu} K_\mu\right) && (5.23)\\
\left[P_\rho, L_{\mu\nu}\right] &= i\left(\eta_{\rho\mu} P_\nu - \eta_{\rho\nu} P_\mu\right) && (5.24)\\
\left[L_{\mu\nu}, L_{\rho\sigma}\right] &= i\left(\eta_{\nu\rho} L_{\mu\sigma} + \eta_{\mu\sigma} L_{\nu\rho} - \eta_{\mu\rho} L_{\nu\sigma} - \eta_{\nu\sigma} L_{\mu\rho}\right). && (5.25)
\end{aligned}$$

We can reorganise all generators in the following matrix:

$$J_{MN} = \begin{pmatrix} L_{\mu\nu} & \frac{K_\mu - P_\mu}{2} & -\frac{K_\mu + P_\mu}{2} \\ -\frac{K_\mu - P_\mu}{2} & 0 & D \\ \frac{K_\mu + P_\mu}{2} & -D & 0 \end{pmatrix} \ with\ M,\ N = 1, ..., d+2, \tag{5.26}$$

and check that the antisymmetric matrix J_{MN} is a rotation in a $d+2$-dimensional space-time with signature $(2,d)$:

$$[J_{MN}, J_{RS}] = i\left(\eta_{NR} J_{MS} + \eta_{MS} J_{NR} - \eta_{MR} J_{NS} - \eta_{NS} J_{MR}\right). \tag{5.27}$$

This prove the isomorphism between the conformal group in d dimensions (for $d \geq 3$) and the group $SO(2,d)$, with $\frac{1}{2}(d+2)(d+1)$ generators.

Let us now briefly consider the case $d = 2$. In this case there are more solution than that listed above. In order to prove this statement, it is useful to introduce the complex variable

$$z = x_1 + ix_2, \ \ \bar{z} = x_1 - ix_2, \qquad ds^2 = dz d\bar{z}. \tag{5.28}$$

It is easy to see that the transformation $z \to f(z), \ \ \bar{z} \to f(\bar{z})$, with f an analytic function, corresponds to a conformal rescaling of the metric: $g'_{\mu\nu} = |f(z)|^2 g_{\mu\nu}$.

Consequently, in addition to the solutions (5.12) we find also solutions corresponding to the infinitesimal transformations $\delta z \sim z^n$, $n > 2$, which are new conformal transformations existing only in two space-time dimensions. This implies that the conformal "group" is the infinite dimensional group of all the analytic functions. It is due to the infinite dimensionality of this group that CFTs in two dimensions are more constrained that CFTs in higher dimensions.
However there is a subtlety in the previous argument. We have proven in the first part of the chapter that the conformal group in $d \geq 3$ is finite dimensional while the previous reasoning tells us that in two dimensions the same "group" is infinite dimensional. Actually we have put the word group between "..." since our argument is purely local and we have not used yet the fact that conformal transformations must be defined everywhere and invertible. In $d \geq 3$ these requirements are automatically satisfied. In $d = 2$ we have to distinguish between global conformal transformation which satisfy this request and local conformal transformation which are not everywhere well defined. The set of global conformal transformations form the so called proper conformal group. It turns out that the complete set of such mappings is

$$f(z) = \frac{az+b}{cz+d}, \, with \, ad-dc = 1, \tag{5.29}$$

which is the $SL(2,\mathbf{C})$ group. It is known that this group is isomorphic to $SO(3,1)$. Thus, as far as the proper conformal group is considered, there are no differences between $d = 2$ and $d > 2$.

5.1.2 Field Theory and Conformal Invariance

Having explained what a conformal transformation is, let us now discuss the implications of conformal invariance on a quantum field theory.

At the classical level, a field theory is conformal invariant if its action is invariant under conformal transformations. On the hover hand, it is important to observe that conformal invariance at the classical level generally does not imply conformal invariance at the quantum level. A quantum field theory necessitates of a regularization prescription in order to make sense, and this introduces a scale in the theory which, in general, breaks conformal invariance except in the fixed point of the renormalization group.
In fact, quantum field theory is, in most general terms, the study of the Renormalization Group (RG) flows, i.e. how the theory evolves from the ultraviolet (UV) to the infra-red (IR) regimes. One can ask which IR phases are possible. In principle, there are three possibilities:

- A theory with a mass gap, as the non-abelian Yang-Mills theory in $d = 4$ space-time dimensions.
- A theory with massless particles in the IR, as the QED.

- A scale invariant (SI) theory with a continuous spectrum, as the $\lambda\phi^4$ scalar theory.

It is the last class of theories which is commonly called Conformal Field Theory (CFT).

5.1.2.1 Conformal invariance at the classical level

Let us first analyse the consequences of conformal invariance in a field theory at the classical level.
The first thing to clarify is how classical fields transform under conformal transformation. Let T_g be a matrix representation of a conformal transformation parametrized by ω_g such that the multicomponent field $\Phi(x)$ transforms as

$$\Phi'(x') = (1 - \omega_g T_g)\Phi(x). \tag{5.30}$$

The generator T_g must be added to the space-time part of the transformation (5.20) in order to obtain the full generator of the symmetry. Then, to obtain the full form of these generators, we use a standard trick in field theory, i.e. we establish the action of these generators at the origin $x = 0$ and we subsequently translate the generator at an arbitrary point in space time using the well known Hausdorf formula. As an example, in order to applying this method to the angular momentum, we introduce the spin matrix representation $S_{\mu\nu}$ to define the action of the angular momentum on the field $\Phi(0)$:

$$L_{\mu\nu}\Phi(0) = S_{\mu\nu}\Phi(0). \tag{5.31}$$

Then we apply the Hausdorf formula to translate the previous expression to a non-zero x:

$$e^{ix^\rho P_\rho} L_{\mu\nu} e^{-ix^\rho P_\rho} = S_{\mu\nu} - x_\mu P_\nu + x_\nu P_\mu. \tag{5.32}$$

This allow us to write the action of the generators on the fields as follows:

$$P_\mu \Phi(x) = -i\partial_\mu \Phi(x) \tag{5.33}$$

$$L_{\mu\nu}\Phi(x) = i(x_\mu \partial_\nu - x_\nu \partial_\mu)\Phi(x) + S_{\mu\nu}\Phi(x). \tag{5.34}$$

We can extend the previous argument to the full conformal group. The subgroup that leaves the origin $x = 0$ is generated by rotations, dilatations and special conformal transformations. Consequently, defining $S_{\mu\nu}$, $\tilde{\Delta}$ and κ_μ as the eigenvalues of the generators $L_{\mu\nu}$, D and K_μ at the origin respectively, the conformal algebra (5.20) implies that these generators must satisfy the following commutation relations:

$$\left[\tilde{\Delta}, S_{\mu\nu}\right] = 0 \tag{5.35}$$
$$\left[\tilde{\Delta}, \kappa_\mu\right] = -i\kappa_\mu \tag{5.36}$$
$$\left[\kappa_\mu, \kappa_\nu\right] = 0 \tag{5.37}$$
$$\left[\kappa_\rho, S_{\mu\nu}\right] = i\left(\eta_{\rho\mu}\kappa_\nu - \eta_{\rho\nu}\kappa_\mu\right) \tag{5.38}$$
$$\left[S_{\mu\nu}, S_{\rho\sigma}\right] = i\left(\eta_{\nu\rho}S_{\mu\sigma} + \eta_{\mu\sigma}S_{\nu\rho} - \eta_{\mu\rho}S_{\nu\sigma} - \eta_{\nu\sigma}S_{\mu\rho}\right). \tag{5.39}$$

The previous algebra allow us to use the Hausdorf formula in the same way as we have just done for the angular momentum and to determine the full action of the generators K_μ and D on the field $\Phi(x)$:

$$D\Phi(x) = \left(-ix^\nu\partial_\nu + \tilde{\Delta}\right)\Phi(x) \tag{5.40}$$
$$K_\mu\Phi(x) = \left(\kappa_\mu + 2x_\mu\tilde{\Delta} - x^\nu S_{\mu\nu} - 2ix_\mu x^\nu\partial_\nu + ix^2\partial_\mu\right)\Phi(x). \tag{5.41}$$

If we demand that $\Phi(x)$ belongs from an irreducible representation of the Lorentz group, then, by Shur's lemma, any matrix that commutes with all generators $S_{\mu\nu}$ must be a multiple of the identity. Consequently, the matrix $\tilde{\Delta}$ is a multiple of the identity and the algebra (5.35) forces all the matrices κ_μ to vanish. $\tilde{\Delta}$ is then a simple number, manifestly equal to $-i\Delta$, where Δ is the scaling dimension of the field Φ. In principle we are now able to find the finite conformal transformation for the field $\Phi(x)$. In the case of a scalar field ϕ ($S_{\mu\nu} = 0$) the result is:

$$\phi'(x') = \Lambda(x)^{\frac{\Delta}{2}}\phi(x), \tag{5.42}$$

where $\Lambda(x)$ is the conformal scaling factor defined in (5.1). A field which transforms as in (5.42) is called a primary field. [1] If the field $\Phi(x)$ belongs from an irreducible representation R of the Lorentz group with non-zero spin, its transformation rule should depend on the rotation matrix M^μ_ν defined in (5.12). Consequently, its transformation is:

$$\Phi'(x') = \Lambda(x)^{\frac{\Delta}{2}} R\left[M^\mu_\nu\right]\Phi(x), \tag{5.43}$$

where $R\left[M^\mu_\nu\right]$ is a representation matrix acting on the indices of $\Phi(x)$.

The stress-energy Tensor and conformal invariance

It is a well know theorem by Polyakov [20] that, at the classical level, a field theory which is local, invariant under rotations a translations and posses the scale transformation symmetry is invariant under the whole conformal group.
The proof runs as follows: locality implies that, under an infinitesimal transformation $x'_\mu = x_\mu + \varepsilon_\mu(x)$ the action S of the theory changes as follows:

[1] Note that the requirement that ϕ belongs from an irreducible representation of the Lorentz group is necessary for the definition of primary field.

$$\delta S = \int d^d x T^{\mu\nu} \partial_\mu \varepsilon_\nu, \tag{5.44}$$

where $T_{\mu\nu}$ is the stress-energy tensor of the theory. In other words, locality implies the existence of a privileged tensor $T_{\mu\nu}$ which is the conjugate variables of the metric $g_{\mu\nu}$.
Invariance under rotations implies that $T_{\mu\nu}$ is a symmetric tensor while translational invariance means that $\partial_\mu T^{\mu\nu} = 0$.
Finally, invariance under scale transformations implies that $T_{\mu\nu}$ is traceless: $T^\mu_\mu = 0$.
Stated this, if the infinitesimal transformation under consideration is a conformal transformation, it is evident from the definition (5.3) that:

$$\delta S = \frac{1}{d} \int d^d x T^\mu_\mu \partial_\rho \varepsilon^\rho = 0, \tag{5.45}$$

which prove the statement.
The converse is in general not true, i.e. conformal invariance does not implies in general the tracelessness of $T_{\mu\nu}$ since $\partial_\rho \varepsilon^\rho$ is not an arbitrary function.
However, it is possible to prove, (for more details see [17]), that under very general conditions also the converse is true. Then, in the large majority of field theory at the classical level, conformal invariance is a consequence of scale invariance and Poincaré invariance.

5.1.2.2 Conformal invariance at the quantum level

Let us now analyse the consequence of conformal invariance at the quantum level (i. e. on a regularized theory at the fixed point of the RG flow) on the two and three-point functions. At first we restrict our analysis on primary scalar fields.

Consider the two-point function

$$\langle \phi_1(x_1)\phi_2(x_2)\rangle = \frac{1}{Z} \int D\Phi \phi_1(x_1)\phi_2(x_2) e^{-iS[\Phi]}, \tag{5.46}$$

where ϕ_1 and ϕ_2 are two primary scalar fields not necessarily distinct, Φ denotes the set of all functionally independent field of the theory and $S[\Phi]$ is the conformally invariant action.
The assumed conformal invariance of the action and of the functional integration measure leads to the following transformation of the correlation function, according to (5.42):

$$\langle \phi_1(x_1)\phi_2(x_2)\rangle = \Lambda(x_1)^{\frac{\Delta_1}{d}} \Lambda(x_2)^{\frac{\Delta_1}{d}} \langle \phi_1(x_1')\phi_2(x_2')\rangle \tag{5.47}$$

If we consider only scale transformation $x \to \lambda x$, the previous equation becomes:

$$\langle \phi_1(x_1)\phi_2(x_2)\rangle = \lambda^{\Delta_1+\Delta_2} \langle \phi_1(\lambda x_1)\phi_2(\lambda x_2)\rangle. \tag{5.48}$$

Rotational and translational invariance requires that

$$\langle \phi_1(x_1)\phi_2(x_2)\rangle = f(|x_1 - x_2|), \tag{5.49}$$

where $f(x)$ is a scale invariant function by virtue of (5.48). Consequently

$$\langle \phi_1(x_1)\phi_2(x_2)\rangle = \frac{C_{12}}{|x_1 - x_2|^{\Delta_1+\Delta_2}} \tag{5.50}$$

where C_{12} is a constant coefficient. Finally if we impose the invariance under SCT ($\Lambda(x) = (1 - 2b_\mu x^\mu + b^2x^2)^{-d}$), we obtain the following constraint:

$$\frac{C_{12}}{|x_1 - x_2|^{\Delta_1+\Delta_2}} = \frac{C_{12}}{\gamma_1^{\Delta_1}\gamma_2^{\Delta_2}} \frac{(\gamma_1\gamma_2)^{\frac{\Delta_1+\Delta_2}{2}}}{|x_1 - x_2|^{\Delta_1+\Delta_2}}, \tag{5.51}$$

with $\gamma_i = (1 - 2b_\mu x_i^\mu + b^2x_i^2)$. This constraint is identically satisfied if $\Delta_1 = \Delta_2$. Finally, we find that the two primary fields are correlated only if they have the same scaling dimension:

$$\langle \phi_1(x_1)\phi_2(x_2)\rangle = \begin{cases} \frac{C_{12}}{|x_1 - x_2|^{2\Delta_1}}, & if\ \Delta_1 = \Delta_2 \\ 0 & if\ \Delta_1 \neq \Delta_2 \end{cases} \tag{5.52}$$

A similar analysis, performed on the three-points function of scalar primary fields, yields:

$$\langle \phi_1(x_1)\phi_2(x_2)\phi_3(x_3)\rangle = \frac{C_{123}}{x_{12}^{\Delta_1+\Delta_2-\Delta_3} x_{23}^{\Delta_2+\Delta_3-\Delta_1} x_{13}^{\Delta_3+\Delta_1-\Delta_2}}, \tag{5.53}$$

where $x_{ij} = |x_i - x_j|$ and C_{123} is an undetermined constant.
As regards the n-points Green's functions with $n \geq 4$ conformal invariance does not determines the form of the correlators as in the case $n \leq 3$. This is due to the fact that with four (or more) point it is possible to construct conformal invariants, the so called anharmonic ratios. The n-points functions may have an arbitrary dependence on these ratios.

Conformal invariance constrains also the form of two and three-points correlators of higher spin primary fields. For details on this topic see [18, 19].

Conformal Ward Identities

In this section we will analyse the Ward Identities associated to conformal symmetry.
Let us consider the following infinitesimal symmetry transformation on the field:

$$\delta\Phi(x') = -i\omega_a T_a \Phi(x), \tag{5.54}$$

where T_a are the infinitesimal generators of the transformation and ω_a are the infinitesimal parameter associated to the symmetry. Let j^a_μ be the conserved current associated to the symmetry (5.54). The Ward identity corresponding to the transformation (5.54) is:

$$\partial_\mu \langle j^{a\,\mu}(x)\Phi(x_1)...\Phi(x_n)\rangle = -i\sum_{i=1}^{n}\delta(x-x_i)\langle\Phi(x_i)...T_a\Phi(x_i)...\Phi(x_n)\rangle. \quad (5.55)$$

As regards translational invariance, the generator associated to this symmetry is $P_\mu = -i\partial_\mu$. Consequently, the associated Ward Identity is:

$$\partial_\mu\langle T^\mu_\nu X\rangle = -\sum_i \delta(x-x_i)\partial^i_\nu\langle X\rangle, \quad (5.56)$$

where, from now on X stands for the collection of fields $\Phi(x_1)...\Phi(x_n)$.
Let us now consider the Lorentz transformation. The associated current has the following form:

$$J^{\mu\nu\rho} = T^{\mu\nu}x^\rho - T^{\mu\rho}x^\nu. \quad (5.57)$$

The infinitesimal generator of the symmetry is given by (5.20), namely

$$T_a = -i(x_\nu\partial_\rho - x_\rho\partial_\nu) + S_{\nu\rho}\ . \quad (5.58)$$

Substituting these quantities in (5.55), and considering the Ward Identity (5.56), we obtain

$$\langle(T^{\mu\nu}-T^{\nu\mu})X\rangle = -i\sum_i \delta(x-x_i)S^{\mu\nu}_i\langle X\rangle\ , \quad (5.59)$$

which is the Ward identity associated to Lorentz symmetry.

Equation (5.59) means that the energy-momentum tensor is symmetric in the Green's function except correction given by contact points in the correlators.
Finally, as regard dilatation invariance, the associated current may be written as

$$j^\mu_D = T^{\mu\nu}x_\nu\ , \quad (5.60)$$

while the infinitesimal generator is given by (5.20), $D = -ix^\nu\partial_\nu - i\Delta$, for a field of scaling dimension Δ. Consequently the Ward Identity associated to this symmetry is

$$\langle T^\mu_\mu X\rangle = -\sum_i \delta(x-x_i)\Delta_i\langle X\rangle, \quad (5.61)$$

where we have used (5.56).
Equations (5.56), (5.59) and (5.61) are the Ward Identities associated with conformal invariance.

5.1.3 Unitarity bounds

To conclude this brief review on CFTs we observe how the unitarity constraint imposes bounds on the scaling dimensions of the primary fields (for more details see Appendix C).

As we have outlined in the previous Sections, each representation of the conformal group contains several fields with different scaling dimensions. However, as known, a general field theory should not admit states with negative norm, i.e. the theory should be unitary. A conformal field theory satisfies this request only under particular conditions depending on the fields and the space-time dimensions d. In particular for primary fields of integer angular momentum l it is possible to find:

$$\Delta_{min}(l) = l + d - 2, \text{ for } l = 1,2,3... \tag{5.62}$$

$$\Delta_{min}(l = 0) = \tfrac{d}{2} - 1 \tag{5.63}$$

The previous relations are commonly known as unitarity bounds. Similar bounds can be derived for antisymmetric tensor and fermionic representation of the Lorentz group.

5.2 Review: anti-de Sitter spaces

In this Section we shall review the basic aspects of the anti-de Sitter (AdS) space-time. The the review is based on [1, 2, 3, 4].

5.2.1 AdS as a maximally symmetric solution of Einstein's equations

AdS_{d+1} is the maximally symmetric metric space in $d+1$ dimension with positive curvature, where maximally symmetric means that it admits the maximum number of independent killing vectors, namely $\frac{(d+1)(d+2)}{2}$.

It is possible to prove that a maximally symmetric $d+1$-dimensional metric space is homogeneous and isotropic and that the curvature tensor can be expressed as a function of the metric as follows:

$$R_{\lambda\rho\sigma\nu} = \frac{\mathscr{R}}{(d+1)d}(g_{\nu\rho}g_{\lambda\sigma} - g_{\rho\sigma}g_{\lambda\nu}), \tag{5.64}$$

where $\mathscr{R}$ is the Ricci scalar. Moreover, due to the homogeneity and isotropy of the space, at every point X, the Bianchi identity assumes the following form:

$$\left(\frac{1}{d+1}-\frac{1}{2}\right)\partial_\rho \mathscr{R} = 0, \tag{5.65}$$

which means that for $d > 1$ the Ricci scalar $\mathscr{R}$ is constant, namely

$$\mathscr{R} = const \equiv d(d+1)K\ , \tag{5.66}$$

where K is called the curvature constant. Consequently, taking into account (8.32), the Ricci tensor and the curvature tensor may be written in the following form:

$$R_{\mu\nu} = dKg_{\mu\nu} \tag{5.67}$$

$$R_{\lambda\rho\sigma\nu} = K(g_{\sigma\rho}g_{\lambda\nu} - g_{\nu\rho}g_{\lambda\sigma}). \tag{5.68}$$

A metric space in which the Ricci tensor and the curvature tensor can be expressed in the form (8.34) is called space of constant curvature.

It is possible to prove that, given the curvature constant K, the dimensionality $d+1$ of the space and the number of positive and negative eigenvalues of the metric tensor, there exists an unique non-equivalent maximally symmetric metric space.

Since now, we have described only geometric properties of maximally symmetric metric space. Let us now analyse under which conditions these particular metric spaces are solutions of the Einstein's equations. A maximally symmetric space-time is a solution of the Einstein's equation in $d+1$ dimension with cosmological constant Λ:

$$R_{\mu\nu} - \frac{g_{\mu\nu}}{2}\mathscr{R} = -\frac{\Lambda}{2}g_{\mu\nu}, \tag{5.69}$$

Taking the trace of the previous equation and keeping in mind that $\mathscr{R} = d(d+1)K$, we obtain:

$$\mathscr{R} = \frac{d+1}{d-1}\Lambda = -d(d+1)K, \tag{5.70}$$

which implies that

$$R_{\lambda\rho\sigma\nu} = -\frac{\Lambda}{d(d-1)}(g_{\sigma\rho}g_{\lambda\nu} - g_{\nu\rho}g_{\lambda\sigma}). \tag{5.71}$$

The $\Lambda = 0$ solution is the Minkowsky space-time [2], for $\Lambda > 0$ the solution is called de Sitter (dS_{d+1}) space-time, while, for $\Lambda < 0$ we have the AdS_{d+1} space-time.

Eventually, AdS_{d+1} is the unique maximally symmetric solution of the Einstein's equation in $d+1$ dimensions with negative cosmological constant Λ.

[2] In particular every flat solution of the Einstein's equation is maximally symmetric.

5.2.2 Hyper-surface embedding and geometric properties

The geometrical properties of AdS_{d+1} are better understood by embedding it in a higher dimensional flat space-time with line element

$$ds^2 = -dx_0^2 - dx_{d+1}^2 + dx_1^2 + ... + dx_d^2. \tag{5.72}$$

The AdS_{d+1} space can be represented as an hyperboloid in this flat $d+2$-dimensional space-time, described by the equation

$$x_0^2 + x_{d+1}^2 - x_1^2 - ... - x_d^2 = L^2, \tag{5.73}$$

where L is a constant parameter called the AdS radius. From (5.73), it is evident that AdS_{d+1} has the topology of $S^1 \times R^d$.
Equation (5.73) can be solved by introducing the parametrisation

$$x_0 = L\sqrt{1+\tfrac{r^2}{L^2}}\cos\tau, \tag{5.74}$$

$$x_{d+1} = L\sqrt{1+\tfrac{r^2}{L^2}}\sin\tau, \tag{5.75}$$

$$x_i = \sinh r\theta_i, \qquad \textstyle\sum_{i=1}^{d}\theta_i^2 = 1. \tag{5.76}$$

where $\rho \in (0,\infty]$ and $\tau \in (0,2\pi]$ [3]. Substituting (5.74) in (5.72) we find that the induced metric on the hyperboloid (5.73) is:

$$ds^2 = L^2\left(-\left(1+\frac{r^2}{L^2}\right)d\tau^2 + \frac{dr^2}{\left(1+\frac{r^2}{L^2}\right)} + \rho^2 d\Omega_{(d-1)}^2\right), \tag{5.77}$$

where $d\Omega_{(d-1)}^2$ is the line element on a $d-1$-dimensional sphere. The curvature tensor associated with the metric (5.77) is:

$$R_{\lambda\rho\sigma\nu} = \frac{1}{L^2}(g_{\nu\rho}g_{\lambda\sigma} - g_{\rho\sigma}g_{\lambda\nu}), \tag{5.78}$$

which coincides with the AdS_{d+1} one if

$$\frac{1}{L^2} = -\frac{\Lambda}{d(d-1)}\ . \tag{5.79}$$

Moreover the group of isometries of the metric (5.77) is the same group under which the hyperboloid (5.73) is invariant, namely $SO(2,d)$ which has $\frac{(d+1)(d+2)}{2}$ generators, which is exactly the maximum number of linearly independent Killing vectors admissible in a $d+1$-dimensional space.

[3] Note that the time is 2π-periodic. As we will see in the next section this fact implies that geodesic are also 2π-periodic.

The parametrisation (5.74) is called the global parametrisation of AdS_{d+1} and it covers the hyperboloid (5.73) exactly once. Another parametrization which shall be useful is the so called Poincaré parametrization:

$$x_0 = \frac{1}{2u}\left(1+u^2\left(L^2-t^2+\sum_{i=1}^{d-1}x_i^2\right)\right), \tag{5.80}$$

$$x_i = Lux_i, \qquad i,1,...,d-1, \tag{5.81}$$

$$x_d = \frac{1}{2u}\left(1-u^2\left(L^2-t^2+\sum_{i=1}^{d-1}x_i^2\right)\right), \tag{5.82}$$

$$x_{d+1} = Lut, \qquad u\in(0,\infty) \tag{5.83}$$

which yields

$$ds^2 = L^2\left(u^2\eta^{\mu\nu}dx_\mu dx_\nu + \frac{du^2}{u^2}\right), \tag{5.84}$$

where $\eta^{\mu\nu}$ is the diagonal flat metric with Minkoskian signature $(1,d-1)$. This parametrization cover only half of the hyperboloid and has a Killing horizon at $u=0$ where $g_{tt}=0$. In this parametrization the subgroup (of $SO(2,d)$) $ISO(1,d-2)$, which represents the Poincaré invariance on the hyperplane $(t,\ x_i)$, and $SO(1,1)$, which represents the scale transformation under which the AdS metric is invariant

$$(t,\ x_i,\ u)\to(at,\ ax_i,\ a^{-1}u), \qquad a>0, \tag{5.85}$$

are manifest.
Another useful parametrization is obtained by the previous with the change of coordinates $z=\frac{1}{u}$, which yields

$$ds^2 = \frac{L^2}{z^2}\left(dz^2+\eta^{\mu\nu}dx_\mu dx_\nu\right). \tag{5.86}$$

5.2.3 Geodesic motion in AdS_{d+1}

We have seen in the previous Section that in the global parametrization (5.77) the time coordinate τ is periodic. This fact has consequences on causality in the motion of massive particles in AdS which has to be analysed carefully.

Because of the negative (attractive) cosmological constant Λ, the motion of massive particles in AdS_{d+1} is in a certain sense confined. In order to clarify this point and to better understand the conformal structure of the space (as we will see in the next section) it is useful to analyse the geodesic equation:

$$\frac{d^2x^\mu}{d\tau^2}+\Gamma^\mu_{\nu\lambda}\frac{dx^\nu}{d\tau}\frac{dx^\lambda}{d\tau}=0, \tag{5.87}$$

where τ is the proper time of the particle. To simplify the computation, we will study only the radial motion of a massive and massless particle in the global coordinate system (5.77). In this case the quadri-velocity has only two components:

$$u^t \equiv \dot{t}(\tau), \tag{5.88}$$

$$u^r \equiv \dot{r}(\tau), \tag{5.89}$$

where the dot stands for the total derivative with respect to the proper time τ. Substituting these two components of u in the geodesic equation (5.87) we obtain two ordinary differential equation for t and r:

$$\ddot{t} + 2\dot{t}\dot{r}\frac{r}{r^2+L^2} = 0 \tag{5.90}$$

$$\ddot{r} + \dot{t}^2\frac{r}{L^2}\left(1+\frac{r^2}{L^2}\right) - \dot{r}^2\frac{r}{r^2+L^2} = 0, \tag{5.91}$$

which are valid both for massive and for massless particles.

Massive particles

In the case of massive particles we can normalize the velocity u as follows:

$$u_a u^a = -1. \tag{5.92}$$

The condition (5.92) allow us to simplify the equations (5.90) and (5.91). In particular, it permits to derive a differential equation for $r(\tau)$ alone:

$$\ddot{r} + \frac{r}{L^2} = 0. \tag{5.93}$$

Consequently, the general solution of the differential equations (5.90) and (5.91) is:

$$r(\tau) = r_0 \cos\left(\tfrac{\tau-\tau_0}{L}\right), \tag{5.94}$$

$$t(\tau) = t_0 + L\arctan\left[\frac{1}{\sqrt{1+\frac{r_0^2}{L^2}}}\tan\left(\tfrac{\tau-\tau_0}{L}\right),\right] \tag{5.95}$$

where r_0 ant τ_0 are arbitrary parameters to be determined by the initial conditions. First of all, we note that the motion is periodic and bounded in r. This implies that no massive particles can escape to infinity.

The problem of the periodicity of massive geodesic could appear as a problem of causality of the space but in reality, it has a simple solution. In fact, one has to keep in mind that, as the global parametrisation (5.77) shows, AdS is not simply connected, but has the topology of $S^1 \times R^d$. Consequently, we can unwrap the circle S^1 (to obtain its covering R^1) obtaining the universal covering of Anti-de Sitter space, which does not contain any closed time-like lines. This space has the topology of R^{d+1}.

We shall in future mean by Anti-de Sitter space this universal covering space.

Massless particles

For massless particles the velocity u must be normalized as follows:

$$u_a u^a = 0. \tag{5.96}$$

As a consequence, the equation for $r(\tau)$ (5.90) becomes:

$$\ddot{r} = 0. \tag{5.97}$$

The general solution of the differential equations (5.90) and (5.91) is:

$$r(\tau) = a(\tau - \tau_0), \tag{5.98}$$

$$t(\tau) = t_0 + L \arctan\left(\tfrac{r(\tau)}{L}\right), \tag{5.99}$$

where a and t_0 are arbitrary parameters to be determined by the initial conditions. We see that null geodesic can reach $r \to \infty$ at finite proper time $\tau \to \infty$ which however corresponds to finite coordinate time interval, $t - t_0 = \frac{\pi L}{2}$.

5.2.4 Carter-Penrose diagram and conformal boundary

In the previous Section we have seen that light-like geodesic can reach $r = \infty$ in finite coordinate time $t < \infty$. The hyper-surface $r = \infty$ is called the *conformal boundary* of *AdS*. In order to understand the property of the boundary, let us try to sketch the Carter-Penrose diagram for *AdS* space-time. The basic philosophy of the Carter-Penrose diagram is to map a non-compact metric space in a compact one which is related to the previous by a Weyl rescaling. The basic idea of this procedure is that if two metrics differ by a Weyl rescaling, the null geodesic trace the same space-time points. For AdS_{d+1} space-time in global coordinates (5.77), we can make the following change of coordinates:

$$r = L \tan\theta, \tag{5.100}$$

$$t = L\tau, \tag{5.101}$$

$$\tau \in (-\infty, \infty), \qquad \theta \in \left[0, \tfrac{\pi}{2}\right), \tag{5.102}$$

which maps the coordinate r in a finite interval. With the parametrization (5.100), the metric becomes:

$$ds^2 = \frac{L^2}{\cos^2\theta}\left[-d\tau^2 + d\theta^2 + \sin^2\theta d\Omega_{d-1}^2\right]. \tag{5.103}$$

Making a Weyl rescaling with factor $\frac{\cos^2\theta}{L^2}$ we obtain the metric

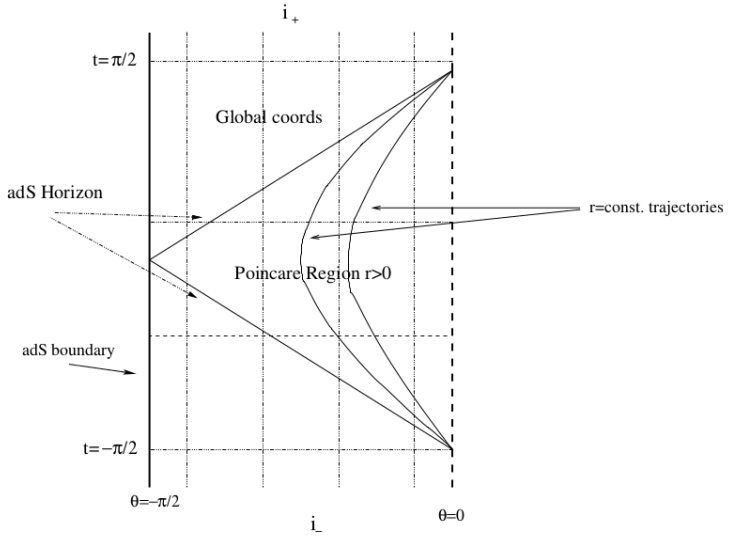

Fig. 5.1 Carter-Penrose diagram of the AdS_{d+1} space-time.

$$ds^2 = -d\tau^2 + d\theta^2 + \sin^2\theta d\Omega_{d-1}^2, \tag{5.104}$$

which describe half of the Einstein static cylinder [4]. The conformal boundary of AdS_{d+1} is defined to be the hyper-surface $\theta = \frac{\pi}{2}$. It has the topology of $R \times S^{d-1}$. On the other hand, it is not possible to find a transformation which map the proper time τ into a finite interval.[5] Consequently the time-like infinity points i^+ and i^- can not be smoothly included in the Carter-Penrose diagram (see Figure 5.1). As a consequence, there exist no Couchy surface whatever in the space. While one can find families of space-like surfaces (such as the surfaces $t = const$) which cover the space completely, each surface being a complete cross-section of the space-time, one can find null geodesics which never intersect any given surface in the family. This is due to the fact that, as illustrated in the previous Section, only null geodesic can reach the conformal boundary. This means that AdS is not globally hyperbolic: Cauchy data on arbitrary space-like surface X, determines the evolution of the system only in a region bounded by a null hyper-surface (called a Cauchy horizon). Physics on AdS depends also on the boundary conditions imposed at the boundary.

---

[4] This implies that AdS_{d+1} is conformally flat. Remember that for conformally flat metric spaces the Weyl tensor defined as

$$C_{abcd} \equiv R_{abcd} - \left(a_{a[c}R_{d]b} - a_{a[c}F_{d]a}\right) + \frac{1}{3}\mathscr{R}g_{a[c}g_{d]b} \tag{5.105}$$

identically vanishes.

[5] By the way, I did not find a formal proof of this statement, even though this assertion is present in almost every gravity textbook.

5.3 Motivating the duality

Having reviewed the basics aspect of both the Conformal Field Theories and the anti-de Sitter spaces we are now ready to understand the basic statement of the duality. In this Section we try to motivate the gauge/gravity correspondence using simple intuitive idea referring to [11] for the original string framework in which Maldacena firstly obtains the conjecture [11].

It is common folklore to intuitive express the duality using the following phrase:

$d+1$-dimensional classical gravity theories on AdS_{d+1} vacuum are equivalent to the large N (degrees of freedom per site) limit of strongly coupled d-dimensional CFTs in flat space.

There are three issues which we have to clarify in order to understand the previous statement, namely:

- Why conformal field theories?
- How can we match the degrees of freedom of a $d+1$-dimensional theory with that of a d-dimensional one?
- Why the dual CFTs are strongly coupled and in the large N limit?

The answer to the first question is very simple if one has in mind the basic properties of CFTs and AdS spaces. In fact, we have explained in the previous Section that the isometry group $SO(2,d)$ of AdS_{d+1} is exactly the symmetry group of a d dimensional CFT. Then, if there is some region of AdS in which a quantum field theory lives it is natural to assume that it has to be invariant under the same symmetry of AdS_{d+1}.

To get intuition on the second issue we need the help of the holographic principle [12]. This principle states that a theory of gravity in $d+1$ space time dimensions, in a local region of space has a number of degrees of freedom which scales like that of a quantum field theory in the boundary of that region.

To understand this basic principle we need to use the celebrated Bekenstain-Hawking area law [13, 14] for the entropy of a black hole. According to [13, 14], in fact, black holes are thermodynamical object and have an entropy which is proportional to the area A of their horizon, namely (see also Appendix B):

$$S_{BH} = \frac{A}{4G_{d+1}}, \tag{5.106}$$

where G_{d+1} is the Newton's constant in Planck units. Now, since we are considering a black hole, its entropy has to be the maximal entropy of anything else in the same volume. Consequently, every region of space has a maximum entropy scaling with the area of the boundary and not with the enclosed volume, as one may think. This is much smaller than the entropy of a local quantum field theory in the same space, which would have a number of states $N \sim e^V$, and the maximum entropy $S \sim \log N$ would have been proportional to the volume V . The maximum entropy in a region of space can instead be related to the number of degrees of freedom N_d of a local quantum field theory living in fewer dimensions

$$S = \frac{A}{4G_{d+1}} = N_d. \tag{5.107}$$

The AdS/CFT correspondence is a particular realization of this principle where the gravity theory lives in an AdS_{d+1} vacuum, and its degrees of freedom are encoded on the conformal boundary, which contains all the space. [6] To clarify this point, let us compute the area of the conformal boundary of AdS_{d+1}. Using the metric (5.86) embedded in a hyper-surface of constant radius z and time t we obtain:

$$A = \int_{z\to 0} d^{d-1}x\sqrt{g_{d-1}} = \int_{z\to 0} d^{d-1}x\frac{L^{d-1}}{z^{d-1}}\ , \tag{5.108}$$

where g_{d-1} is the determinant of the embedded metric, and we have taken the limit $z \to 0$ since this is the locus where the conformal boundary is located, as we have explained in the previous Section.

The integral (5.108) suffers from divergences coming both from the $z \to 0$ limit and from the $d^{d-1}x$ integration, and need to be regularized. In order to do this, we will perform the integral (5.108) up to a small value $z = R$ and we enclose the space in a closed space volume V_{d-1}, namely:

$$A = \frac{L^{d-1}}{R^{d-1}}V_{d-1}\ . \tag{5.109}$$

Finally, in accordance to (5.107) the maximum entropy in the bulk of AdS_{d+1} is

$$\frac{A}{4G_{d+1}} \sim \frac{L^{d-1}}{R^{d-1}}\frac{V_{d-1}}{4G_{d+1}}\ . \tag{5.110}$$

The dual quantum field theory in d dimensions is also UV and IR divergent and needs to be regularized in the same way, by introducing a box of volume V_{d-1} , and a short distance cut-off a. To get intuition on what a should be on the gravity side, we note that from, the Quantum field theory point of view, a is an arbitrary small UV cut-off. We need to construct, on the gravity side, a quantity with the dimension of a length which has to be arbitrary small. But, in the previous steps we have set a small cut-off R to the radial AdS coordinate z which has the dimension of an energy. Consequently, a natural candidate is $a \sim RL^2$. [7] The total number of degrees of freedom N_d of a quantum field theory in d dimensions is given by the number of spatial cells $V_{d-1}/a^{d-1} \sim V_{d1}/(L^{2d-2}R^{d-1})$ times the number of degrees of freedom per lattice site N. As an example, a quantum field theory with matrix fields ϕ_{ab} in the adjoint representation of the symmetry group $U(N)$ has a number of degrees of freedom per point equal to N^2. Thus

[6] It is worth noting that, even though the common language could generate misunderstandings, the dual field theory is not living on the conformal boundary of AdS.

[7] This identification will be made clear when we will solve the third issue, identifying the radial coordinate z with the renormalization group scale.

$$N_d \sim \frac{V_{d-1}N^2}{L^{2d-2}R^{d-1}} \ . \tag{5.111}$$

Finally, we have estimated the relation between the bulk gravitational degrees of freedom and whose of the dual CFT and, using the holographic principle we have understood why the CFT live in one less dimension. However, the estimation (5.111) allow us also to understand the first part of the third issue, namely why the number of degrees of freedom per site in the dual CFT has to be large. This is related to the fact that we are considering classical gravity. In order to do this it is necessary that the typical excitation length of the gravity theory is much larger than the Planck's length l_p. Considering AdS, its typical length scale is given by its radius L, then, keeping in mind that the gravitational Newton's constant is proportional to the Planck's length, $G_{d+1} \sim l_p^{d-1}$, and using the relations (5.107) and (5.108), we obtain:

$$\frac{L^{d-1}}{G_{d+1}} \sim \frac{L^{d-1}}{l_p^{d-1}} \sim N^2 \gg 1 \ , \tag{5.112}$$

which proves the assertion.

We need now only to understand the last part of the third issue, namely why the CFT is strongly coupled. This is related to the problem of giving physical interpretation of the extra radial gravitational coordinate z at the dual level. In the previous paragraphs of this Section we have identified the cut-off R of this coordinates with the UV cut-off of the dual quantum field theory. Then we can already argue that the radial coordinate has to be related to the renormalization group flow in some way.

To understand better this point, let us come back to a d-dimensional quantum field theory. A possible way to describe such a theory is to organize the physics in terms of lengths or energy scales. If one is interested in the properties of the theory at a large length scale $r \gg a$, where a is the spacing of the lattice degrees of freedom or a possible cut-off of the theory, instead of using the bare theory defined at a microscopic scale a, it is more convenient to integrate-out short distance degrees of freedom and obtain an effective field theory at a scale r. One can proceed further and define an effective field theory at a scale $r' \gg r$. This procedure defines a renormalization group flow and gives rise to a continuous family of effective theories in d-dimensional Minkowski space-time labelled by the RG scale r. A remarkable fact is that the RG equations are local in $u = 1/r$ interpreted as an energy scale. This means that we dont need to know the behaviour of the physics deeply in the UV or in the IR to understand how things are changing in u. At this point we can visualize this continuous family of effective theories as a single theory in $d+1$-dimensions with the RG scale r becoming a spatial coordinate.

It is tempting to identify this extra scale dimension with the radial dimension on the gravity side. In order to understand how this is possible, let us recall that the AdS_{d+1} metric can be cast in the following form:

$$ds^2 = \frac{r^2}{L^2}\eta_{\mu\nu}dx^\mu dx^\nu + \frac{L^2}{r^2}dr^2 \ , \tag{5.113}$$

where the conformal boundary is now located at $r \to \infty$. This parametrization makes clear that the AdS_{d+1} geometry can be viewed as a family of copies of Minkowski spaces parametrized by the radial coordinate r, whose size is seen to shrink when

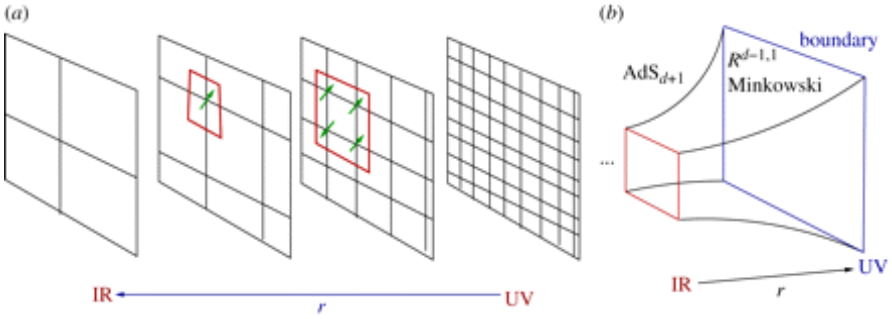

Fig. 5.2 Connection between the radial coordinates in AdS and the renormalization group flow in the dual quantum field theory. Figure from [21].

r decreases from the conformal boundary $r \to \infty$ to the AdS horizon at $r \to 0$. This clarify the UV/IR connection between gravity and the dual field theory and explain why the field theory living on the boundary is strongly coupled. In fact, from the view point of the gravity theory, physics near the conformal boundary $r \to \infty$ is the large volume physics, i.e. IR physics. Near the horizon $r = 0$ is instead the short distance UV physics. In contrast, from the view point of the quantum field theory, physics at large r corresponds to short distance UV physics and vice versa (see Figure 5.2).

5.4 The GKPW rule and its consequences

In the previous Section we have given arguments to justify, at least at the conceptual level, the duality between a strongly coupled conformal field theory in the large N limit and a classical gravitational theory in one more space-time dimension. Since the gravitational theory is classical in principle, using the duality we can compute easily observables in the strongly coupled CFT.

To do this, however, we need a prescription to relate observables in the gravitational theory to observables in the dual strongly coupled field theory. In particular, we have learned in Section 5.1 that the fundamental objects of CFTs are the primary fields. Then in order to compute observables in the CFT we need a prescription to relate the fields in the gravity sector to the primary fields of the CFT.

Let us consider a conformal field theory Lagrangian $\mathscr{L}_{CFT}$. It can be perturbed by adding arbitrary functions, namely sources $h^A(x)$ of local operators $\mathscr{O}_A(x)$:

$$\mathscr{L}_{CFT} \to \mathscr{L}_{CFT} + \sum_A h^A(x)\mathscr{O}_A(x) \ , \tag{5.114}$$

This is a UV perturbation because it is a perturbation of the bare Lagrangian by local operators. According to the general connection between the radial AdS coordinate and the renormalization group it corresponds to a perturbation near the boundary $r \to \infty$ in AdS space. Thus the perturbation by a source $h(x)$ of the CFT will be encoded in the boundary condition on the bulk fields.

Take now the source and extend it to the bulk side $h(x) \to h(x_\mu, r)$ with the extra coordinate r being the radial dimension of AdS_{d+1} (see the metric (5.113)). Fields in the boundary will be denoted with coordinates x, and bulk fields will be dependent on the coordinates (x_μ, r). Suppose $h(x_\mu, r)$ to be the solution of the equations of motion in the bulk with boundary condition

$$\lim_{r\to\infty} h(x_\mu, r) = h(x), \tag{5.115}$$

and another suitable boundary condition at the horizon to fix $h(x_\mu, r)$ uniquely [8]. As a result we have a one to one map between bulk fields and boundary fields [22, 23]. In fact, to each local operator $\mathscr{O}(x)$ corresponds a source $h(x)$, which is the boundary value in AdS of a bulk field $h(x_\mu, z)$ [9].

In order to deduce which field should be related to a given operator, symmetries come in help, because there is no completely general recipe. As a rule of the thumb, since internal symmetry of field in the gravitational sector are preserved in the dual field theory, in general, we can say that the spin of the bulk fields correspond to the spin of the dual operators in the boundary field theory.

To make a quantitative example, let us analyse how a very fundamental quantity of a quantum field theory, the stress-energy tensor $T_{\mu\nu}$, is encoded in the dual gravitational sector using the previous prescription. In particular, the source of $T_{\mu\nu}$ should be a tensor $g_{\mu\nu}$. To have a gauge invariant coupling

$$\int d^d x T_{\mu\nu}(x) g^{\mu\nu}(x) \ , \tag{5.116}$$

$g_{\mu\nu}(x)$ should be the boundary value of a gauge field corresponding to the local translational invariance. The field we are talking about is of course the metric tensor $g_{ab}(x_\mu, r)$ with boundary value

$$\lim_{R\to\infty} g_{ab}(x_\mu, r)\big|_{r=R} = g_{\mu\nu}(x) \ . \tag{5.117}$$

The right-hand side of the previous equation is to be intended as the embedding of the bulk metric on the hyper-surface $r = const$.

The previous example allow us to make an important observation. In fact, we have just explained that the metric tensor $g_{\mu\nu}$, which encodes local diffeomorphisms

[8] As noted in Section 5.2 AdS_{d+1} is not globally hyperbolic and one has to provide boundary conditions both at the horizon and at the boundary to find a solution.

[9] This statement will be clarified better when we will take as an example the scalar field i AdS.

invariance in the gravitational bulk, sources the stress-energy tensor $T_{\mu\nu}$ of the dual field theory, which is a global conserved current ($\partial_\mu T^{\mu\nu} = 0$) due to the global translational and rotational invariance of the dual field theory. In this sense we can affirm that, on the gravity side, the global symmetries arise as large gauge transformations, namely there is a correspondence between global symmetries in the gauge theory and gauge symmetries in the dual gravity theory. This correspondence will become more clear when we will treat the Maxwell field in AdS in Section 5.6.2

This connection between field and operators allow us to express the duality as an equality between partition function.

Namely, the proposal of Gubser, Klebanov, Polyakov and witten (GKPW) [22, 23], which, as everything in this framework is still a conjecture, affirms that the partition function of the CFT $Z_{CFT}[\{h(x)\}]$ is equal to the partition function of the dual gravitational theory $Z_{AdS}[\{h(x_\mu, z)\}]$:

$$Z_{CFT}[\{h(x)\}] = Z_{AdS}[\{h(x_\mu, r)\}] \,, \tag{5.118}$$

where $\{h(x)\}$ is the collection of all the sources associated to each local operator in the field theory side, and $\{h(x_\mu, r)\}$ is the collection of the bulk fields. However, as we have outlined in the previous Section, we do not have a very useful idea of what is the right hand side of this equation, except in the large N limits where this gravity theory becomes classical. In these limits we can do the path integral by a saddle point approximation, and the statement of the duality (5.118) becomes

$$Z_{CFT}[\{h(x)\}] = e^{iS_{on-shell}[\{h(x_\mu, r)\}]} \,, \tag{5.119}$$

where $S_{on-shell}[\{h(x_\mu, r)\}]$ is the classical gravitational action computed on-shell.

Finally, we are able to formulate the first operative rule of the AdS/CFT correspondence, namely:

Rule 1: *The gauge/gravity duality is a duality between partition functions which relate the partition function of a CFT in d dimension to the on-shell action of a gravitational theory in AdS_{d+1}, namely:*

$$Z_{CFT}[\{h(x)\}] \leftrightarrow e^{iS_{on-shell}[\{h(x_\mu, r)\}]} \,.$$

The operators of the CFT are related to the fields in the bulk according to the following prescription:

$$\textit{field in } AdS_{d+1} \leftrightarrow \textit{local operators of } CFT_d$$
$$\textit{spin of the gravitational fields} \leftrightarrow \textit{spin of the local CFT operators.}$$

The sources for the operators are encoded in the boundary behaviour of the fields in the gravitational side.

5.4.1 Holographic renormalization and the prescription for the correlators

In the previous Section we have expressed the AdS/CFT conjecture as an correspondence between partition functions (5.119), according to the proposal of [22, 23]. However, the equality (5.119) is not well defined since both the r.h.s. and the l.h.s suffer from divergences and need to be carefully renormalized.

In this Section we will outline the steps necessary to define a proper renormalized on-shell gravitational action $S^{(ren)}_{on-shell}$, which is necessary to consider the correspondence (5.119) as a computational device to compute correlators in the dual field theory. The renormalization procedure is known with the name of holographic renormalization (for a review see [24]). Here we want only to outline the basic steps of the procedure and discuss its physical relevance without entering in technicalities which will be carefully treated in the next Section where we will apply the prescription of the gauge/gravity duality to compute the correlators dual to a massive scalar field in AdS.

Schematically, the holographic renormalization procedure consists in the following steps:

1. **Fix the boundary conditions and find a solution of the equations of motion:** the first step needed is to provide suitable boundary condition both for the horizon and the boundary and to solve the gravitational equation of motion. The boundary condition has to be chosen carefully both at the horizon and at the conformal boundary since they determines the physical relevance of the solution. We will be more clear about these issues when we will describe the holographic scalar field in the next Section.
2. **Compute the on-shell action and isolate the divergent part:** the on-shell action in AdS_{d+1} typically suffers of divergences due to the divergence of the boundary volume (limit at infinity of the radial coordinates r). In order to compute the on-shell action and isolate the divergent part we need to put an UV cut-off at $r = R$ and compute the action using the solution of the equations of motion previously obtained. Typically, the action computed in this way splits into two parts:

$$S_{on-shell}(\phi_i, R) = S^{(reg)}(\phi_i, R) + S^{(div)}(\phi_i, R) \ , \tag{5.120}$$

   where ϕ_i is the collection of fields involved in the gravitational theory, $S^{(reg)}$ is part of the on-shell action regular in the $R \to \infty$ limit while $S^{(div)}$ is the divergent one.
3. **Find appropriate counterterms:** once the divergent terms have been recognized the last step is to find the proper counterterms $S^{(c.t.)}(\phi_i(x,R);R)$ which cancel the divergences. In order for the gravitational theory to be consistent $S^{(c.t.)}(\phi_i(x,R);R)$ has to respect the following properties:

   - It has to be a local function of the fields of the gravitational theory evaluated at $r = R$ and of the induced metric γ_{ij} on the manifold $r = R$.

- It has to preserve the boundary value problem previously defined, namely it must not modify the boundary condition at the conformal boundary previously setted (this point will become more clear in the next Section, when we will discuss the scalar field as an example).

Having done the previous steps, the renormalized on-shell action is defined as follows:

$$S^{(ren)}_{on-shell} = \lim_{R\to\infty} \left(S_{on-shell}(\phi_i, R) + S^{(c.t.)}(\phi_i(x,R);R) \right) . \tag{5.121}$$

At this point, keeping in mind the field operator correspondence outlined in the previous section, we can give the prescription to compute the correlators of the dual CFT from the renormalized on-shell gravitational action.

Rule 2: *Once one has obtained the on-shell renormalized action $S^{(ren)}$ as a function of the boundary value of the gravitational fields $\phi_i(x)$, (which act as sources for local operators in the dual field theory), the correlators of the boundary CFT are given by the following relation:*

$$\langle \mathcal{O}_i(x_1)\mathcal{O}_j(x_2)...\mathcal{O}_l(x_n)\rangle = \frac{\delta^n S^{(ren)}(h_i(x))}{\delta\phi_i(x1)\delta\phi_j(x_2)...\delta\phi_l(x_n)} .$$

5.5 An example: scalar field in AdS_{d+1}

Having established the basic rules of the AdS/CFT correspondence, let us now analyse deep further how it works.

As outlined in the previous sections, we will deal with a dual theory in the large N limit, since only in this limit we can consider a classical gravitational theory in the bulk. The main goal of this Section is to prove that the two point correlation function of a scalar operator computed from a gravity theory using the GKPW rule matches the Conformal Field theory result obtained in Section 5.1.

Our starting point is to consider the action of a scalar massive field ϕ of mass m in a fixed AdS_{d+1} background. For simplicity, we will work in the probe limit, i.e. we will assume that the scalar field does not back-react on the space-time, which is considered as non-dynamical. The corresponding action is:

$$S_s = -\frac{1}{2\kappa^2_{d+1}} \int d^d x \sqrt{|g|} \left(g^{\mu\nu}\partial_\mu\phi\partial_\nu\phi + m^2\phi^2 \right) , \tag{5.122}$$

where κ_{d+1} is the gravitational constant in $d+1$ dimensions and we consider the AdS_{d+1} metric $g_{\mu\nu}$ in the the Poincarè form as in (5.86), namely:

$$ds^2 = \frac{L^2}{z^2}\left(dz^2 + \eta^{\mu\nu}dx_\mu dx_\nu\right). \tag{5.123}$$

The metric (5.123) is expressed in terms of the AdS radius L, and the conformal boundary is located at $z = 0$. Regarding the metric $\eta_{\mu\nu}$ this is the flat metric in d dimensions, but we take for the moment the freedom of not specifying the signature. This is due to the fact that the appropriate choice of the boundary conditions depends on the signature of $\eta_{\mu\nu}$ (Euclidean or Minkowski). Specifically, in the Euclidean case the interior of AdS $z \to \infty$ is the center point of the space and requiring the regularity of the solution is enough to specify the solution of the equations of motion in the whole space. On the other hand, in the case of Minkowski signature, $z \to \infty$ is actually a killing horizon and suitable boundary conditions for the scalar field have to be chosen in order to ensure the causality of the solution. This point will be clarified in what follows.

Having defined the gravitational model at hand, in order to compute the on-shell action we need to find a suitable solution for the scalar field ϕ. The equation of motion associated to the action (5.122) is:

$$z^{d+1}\partial_z\left(\frac{1}{z^{d-1}}\partial_z\phi\right) + z^{d+1}\partial_\mu\left(\frac{1}{z^{d-1}}\eta^{\mu\nu}\partial_\nu\phi\right) = m^2L^2\phi \tag{5.124}$$

As it is evident from the metric (5.123), the space is homogeneous in the $x_\mu = (t,x)$ hyper-plane, then it is convenient to Fourier transform ϕ in this plane, namely:

$$\phi(z,x_\mu) = \int \frac{d\omega}{2\pi}\frac{d^{d-1}k}{(2\pi)^{d-1}}e^{-i\eta^{\mu\nu}k_\mu x_\nu}\tilde{\phi}(z,\omega,k_\mu)\,, \tag{5.125}$$

where $k_\mu = (\omega,k)$.

Considering the previous mode decomposition, the equation (5.124) becomes:

$$z^{d+1}\partial_z\left(\frac{1}{z^{d-1}}\partial_z\tilde{\phi}\right) + z^2k^2\tilde{\phi} - m^2L^2\tilde{\phi} = 0\,. \tag{5.126}$$

In order to find a solution of the previous differential equation we need to specify appropriate boundary conditions for the scalar field ϕ. Since, as we have explained in Section 5.2, AdS is not globally hyperbolic, we need to specify boundary conditions both at the conformal boundary $z = 0$ and in the interior of AdS $z \to \infty$. As we have anticipated the boundary conditions at $z \to \infty$ depend on the signature of the metric $\eta_{\mu\nu}$ and they will be discussed in detail later in the text.

At first, let us concentrate on the condition at the conformal boundary which is, in both case, a regular point of the space. The equation (5.126) is a second order differential equation of the Fuchsian type [25], which has $z = 0$ has a singular point. Then, the Frobenius method [25] can be applied to find the two independent solutions near the point $z = 0$. This basically consist in expanding the field ϕ near $z = 0$ and solve the equation term by term in the series expansion. The condition due to the leading term in the expansion is called the indicial equation and provides the

two independent solutions for ϕ near $z=0$. Then, substituting the ansatz $\phi \sim z^{\alpha}$ in (5.126) and solving the equation at the leading order we find the following indicial equation for α:

$$\alpha(\alpha-d) = m^2L^2 \,, \tag{5.127}$$

which has two solutions of the following type:

$$\alpha_{\pm} = \frac{d}{2} \pm \sqrt{\frac{d}{4}+m^2L^2} \,. \tag{5.128}$$

Note that $\alpha_{\pm}$ respects the identity $\alpha_+ + \alpha_- = d$, then, Fourier transforming back to real space, the solution for $\tilde{\phi}$ near $z=0$ can be expressed as:

$$\phi \simeq C_1(x_\mu) z^{\alpha_-} + C_2(x_\mu) z^{d-\alpha_-} \,. \tag{5.129}$$

At this point some comments are in order. At first, note that $\alpha_{\pm}$ are real numbers provided that $m^2L^2 \geq -\frac{d}{4}$. This is the so called Breitenlohner-Freedman (BF) bound [26]; it was prove in [26] that once the mass of the scalar m violates this bound, the solution becomes unstable. This tells us that also negative values of the mass squared are allowed provided that they are not "too negative".

Secondly, we need to keep into account that, since we are dealing with a field theory on a curved space time, in order for the solution to be regularly quantized it has to be normalizable with respect to the inner product defined as follows [30]:

$$(\phi_1,\phi_2) = i\int \left(\phi_2^* \overleftrightarrow{\partial_\mu} \phi_1\right) n^\mu d\Sigma \tag{5.130}$$

where $d\Sigma$ is a volume element in a given space-like hyper-surface and n_μ is the unit time-like vector normal to this hyper-surface. It can be proven that this inner product is independent on the choice of n_μ which consequently can be safely taken to be proportional to ∂_t. Then, considering the theory enclosed in a finite space volume V, and keeping $\phi \sim C(t,x)z^{\alpha}$ we find that the condition

$$\alpha \geq \frac{d+2}{2} \tag{5.131}$$

ensures the normalizability of the solution.

Stated this, there are three possibilities:

- when $m^2L^2 \geq -\frac{d}{4}+1$ the first term in (5.129) is always non-normalizable and encodes the leading behaviour of the solution as $z \to 0$.
- in the finite interval $-\frac{d}{4} < m^2L^2 < -\frac{d}{4}+1$ both of the terms in (5.129) are normalizable.
- if m^2 saturates the BF bound, namely $m^2 = -\frac{d}{4}$, there are still two normalizable solutions but, since the indicial equation (5.127) has two coincident solutions, according to the Frobenius theorem the asymptotic behaviour of $\tilde{\phi}$ has to be modified as follows:

$$\phi \simeq C_1(x_\mu) z^{\frac{d}{2}} \ln z + C_2(x_\mu) z^{\frac{d}{2}} \ . \tag{5.132}$$

At this point we have not jet specified the boundary conditions for the scalar field. According to the basic GKPW rule, the asymptotic behaviour of the field at the conformal boundary $z = 0$ coincides with the source for the field in the dual field theory. Then, it is tempting to fix the leading term in the asymptotic expansion (5.129) to be the source J_ϕ in the dual conformal field theory. Actually, as we will see in what follow, the allowed boundary conditions do not reduce only to this simple case, and they depend on the value of the m^2 [27, 28].

As we have noted previously, there are three different cases:

1. $m^2 L^2 \geq -\frac{d}{4} + 1$.
   In this case, since the leading behaviour of the expansion (5.129) is non-normalizable, we need to fix $C_1(x_\mu)$ to be non-dynamical in order for the theory to be consistent. Namely it is necessary to set $C_1(x_\mu)$ as the source for the scalar operator in the dual field theory:
   $$C_1(x_\mu) = J_\phi^{C_1}(x_\mu) \ . \tag{5.133}$$
   Consequently, the coefficient $C_2(x_\mu)$ has to be determined from the equation of motion (5.124) and the initial condition in the interior of AdS $z \to \infty$ which, for the moment, we take to be given by specifying fixed values for ϕ:
   $$\lim_{z\to\infty} \phi(z, x_\mu) = \phi_+(x_\mu) \ . \tag{5.134}$$
   A valid action has to be stationary on the solution and, in order to apply the GKPW rule to compute correlators, has also to be finite. The action (5.122) does not meet any of these requirements. It is fact simple to verify that the the action (5.122), considering the asymptotic behaviour near $z = 0$ (5.129) and the boundary conditions (5.133) and (5.134), diverges on-shell. Moreover, considering the variation of (5.122) we obtain:
   $$\delta S_s = \int d^{d+1}x \sqrt{|g|} \left(\nabla^2 \phi - m^2 L^2 \phi\right) \delta\phi - \int_{z=\varepsilon} d^d x \sqrt{|h|} \frac{1}{\sqrt{|g^{tt}|}} \partial_z \phi \, \delta\phi \ , \tag{5.135}$$
   where $h_{\mu\nu}$ is the induced metric on the manifold $z = \varepsilon$. The first term vanishes on-shell due to the equation of motion (5.124). On the other hand, keeping into account the asymptotic expansion (5.129), the second term becomes:
   $$\begin{aligned} \int_{z=\varepsilon} d^d x \sqrt{|h|} \frac{1}{\sqrt{|g^{tt}|}} \partial_z \phi \, \delta\phi = \\ - \int d^d x \left(z^{\alpha_- - \alpha_+} \alpha_- C_1 \delta C_1 + \alpha_- C_1 \delta C_2 + \alpha_+ C_2 \delta C_1 \right) + \mathscr{O}(\varepsilon) \ , \end{aligned} \tag{5.136}$$
   where we have neglected terms which vanish in the $\varepsilon \to 0$ limit.
   Due to the boundary condition (5.133), the terms proportional to δC_1 vanish on-shell since C_1 is non-dynamical. However this is not the case for the terms

proportional to δC_2. Then, the action is not stationary on-shell and we are dealing with an ill defined variational problem. In order to solve both these issues, it is necessary to add to the action (5.122) the following boundary term:

$$S^{C_1}_{c.t.} = \int_{z=\varepsilon} d^d x \sqrt{|h|}\phi^2 \ . \tag{5.137}$$

It is easy to verify that $S^{C_1}_{ren} = S_s + S_{c.t.}$ is finite once compute on-shell, while its variations yields:

$$\delta S^{C_1}_{ren} = \delta S_s + \delta S^{C_1}_{\text{c.t.}} = \int d^{d+1}x \sqrt{|g|}\left(\nabla^2\phi - m^2L^2\phi\right)\delta\phi + (\alpha_+ - \alpha_-)\int_{z=\varepsilon} d^d x C_2 \delta C_1 \ , \tag{5.138}$$

which vanishes on-shell due to the boundary condition (5.133).
Now, having a well defined on-shell action, we can apply the GKPW prescription to compute the expectation value $\langle \mathscr{O}^{C_1}_\phi \rangle$, namely:

$$\langle \mathscr{O}^{C_1}_\phi(x)\rangle = \left.\frac{\delta S^{C_1}_{ren}}{\delta J^{C_1}_\phi(x)}\right|_{J_\phi=0} = (\alpha_+ - \alpha_-)C_2(x) \ . \tag{5.139}$$

Regarding the two point function, we need the second order variation of the renormalized action, namely:

$$\langle \mathscr{O}^{C_1}_\phi(x)\mathscr{O}^{C_1}_\phi(0)\rangle = \left.\frac{\delta S^{C_1}_{ren}}{\delta J^{C_1}_\phi(x)\delta J^{C_1}_\phi(0)}\right|_{J_\phi=0} = (\alpha_+ - \alpha_-)\frac{\delta C_2(x)}{\delta C_1(0)} \ . \tag{5.140}$$

Now, since the equations of motion are linear in the field ϕ, C_2 can be only a linear function of the source C_1. Eventually, exploiting linearity, we obtain:

$$\langle \mathscr{O}^{C_1}_\phi(x)\mathscr{O}^{C_1}_\phi(0)\rangle = (\alpha_+ - \alpha_-)\frac{C_2(x)}{C_1(0)} \ . \tag{5.141}$$

2. $-\frac{d}{4} < m^2L^2 < -\frac{d}{4}+1$.
As we have previously explained, in this case both the terms in (5.129) are normalizable. It is of course possible to take C_1 as the source for the dual operator and to obtain the same result of the previous case, but there is also the possibility of choosing C_2 as the source, namely:

$$C_2(x) = J^{C_2}_\phi(x) \ . \tag{5.142}$$

This is commonly referred to choose a different quantization for the theory [28]. In this case, in order to have a finite stationary on-shell action we need to add a different set of boundary terms:

$$S^{C_2}_{ren} = S_s + \frac{1}{2}\alpha_- \int_{z=\varepsilon} d^d x \sqrt{|h|} + \int_{z=\varepsilon} d^d x \sqrt{|h|} \frac{1}{\sqrt{|g^{tt}|}} \partial_z \phi \phi \ . \tag{5.143}$$

Evaluating the previous action on the asymptotic expansion (5.129), we obtain

$$S^{C_2}_{ren} = S^{C_1}_{ren} - (\alpha_+ - \alpha_-) \int_{z=\varepsilon} d^d x C_1 C_2 \ , \tag{5.144}$$

namely, the two quantizations are related by a Legendre transformation [27]. Varying $S^{C_2}_{ren}$ we obtain:

$$\delta S^{C_2}_{ren} = \int d^{d+1}x \sqrt{|g|} \left(\nabla^2 \phi - m^2 L^2 \phi\right) \delta\phi - \int_{z=\varepsilon} d^d x C_1 \delta C_2 \ , \tag{5.145}$$

which vanishes on-shell if one consider the boundary condition (5.142). Then, repeating the same steps of point 1, we obtain:

$$\begin{aligned} \langle \mathscr{O}^{C_2}_\phi(x) \rangle &= \left. \frac{\delta S^{C_2}_{ren}}{\delta J^{C_2}_\phi(x)} \right|_{J^{C_2}_\phi = 0} = -(\alpha_+ - \alpha_-) C_1(x) \ , \\ \langle \mathscr{O}^{C_2}_\phi(x) \mathscr{O}^{C_2}_\phi(0) \rangle &= \left. \frac{\delta S^{C_2}_{ren}}{\delta J^{C_2}_\phi(x) \delta J^{C_2}_\phi(0)} \right|_{J^{C_2}_\phi = 0} = -(\alpha_+ - \alpha_-) \frac{C_1(x)}{C_2(0)} \ . \end{aligned} \tag{5.146}$$

As a final comment we note that, as illustrated in [28] more general boundary condition, where the source is a ultralocal function of C_1 or C_2 (depending on the quantization), can be considered. Since this issue is beyond the scope of this review, we refer to [28] for further details.

3. $m^2 = -\frac{d}{4}$.
   In this case there are still two normalizable solutions and booth the quantization can be defined repeating the steps of point 1 and 2. However, due to the logarithmic term which appears in (5.132) it is necessary to add the proper counterterms in order to have a finite on-shell action. Since this is only a technical issue and does not introduce any conceptual novelty, we refer to [28] for further details.

At this point we have provided a prescription to compute the expectation value and the two point functions of the operator dual to the scalar field in a fixed AdS background, once one has chosen a quantization for the theory, namely once one has decided how to define the sources which couples to the dual scalar operator. In order to be more quantitative and to compare the holographic result with the CFT result of Section 5.1 we need to solve the differential equation (5.124), providing a form for C_1 and C_2. In solving the equation one has to face the problem of fixing the boundary condition in the interior of AdS, which, as anticipated, depends on the signature of the metric $\eta_{\mu\nu}$. We will discuss separately the Euclidean signature case, which corresponds to compute the correlators in the imaginary time, and the Minkowski case, which correspond to compute the correlator in the real time. In what follows we will consider only the quantization in which C_1 is identified as the

source, which is valid for every value of the mass m. As we will see later, the alternative quantization modifies only the scaling dimension of the dual scalar operator but does not introduce any conceptual novelty.

Euclidean signature: correlators in the imaginary time

In the Euclidean signature case, namely when $k^2 = \omega^2 + k^2 > 0$ in (5.124), the equation (5.124) has the following solution:

$$\begin{aligned} &\tilde{\phi}(z,k) = a_K \left((L^2 z)^{\frac{d+1}{2}}\right) K_\nu \left(k\frac{z}{L^2}\right) + a_I \left((L^2 z)^{\frac{d+1}{2}}\right) I_\nu \left(k\frac{z}{L^2}\right) , \\ &\nu = \sqrt{\frac{d^2}{4} + m^2 L^2} , \end{aligned} \tag{5.147}$$

where a_k and a_I are undetermined constants, $k = \sqrt{\omega^2 + k^2}$ and I_ν and K_ν are the Bessel functions of the second kind.

Since in this case the interior of AdS $z \to \infty$ is a regular point, we need to impose the regularity of the solution at this point. The asymptotic behaviour of the Bessel functions at $z \to \infty$ is:

$$\begin{aligned} &\lim_{z\to\infty} I_\nu(z) = \infty , \\ &\lim_{z\to\infty} K_\nu(z) = 0 . \end{aligned} \tag{5.148}$$

Then in order for the solution to be regular we need to impose $a_I = 0$. Eventually, the solution is uniquely determined except a normalization constant a_K which is irrelevant in the computation of the correlators since they are given by ratio of the leading and the subleading term of $\tilde{\phi}$, as evident in (5.140).

Having a solution for the scalar field, we can apply the prescription (5.141) to compute the two point function. In the momentum space this reads:

$$\langle \mathcal{O}_\phi^{C_1}(k) \mathcal{O}_\phi^{C_1}(k') \rangle = (2\pi)^d \delta^d(k+k') \left(\alpha_+ - \alpha_-\right) \frac{\tilde{C}_2(k)}{\tilde{C}_1(k')} \tag{5.149}$$

where $\tilde{C}_{1,2}$ are the Fourier transform of $C_{1,2}$.

The expansion near $z = 0$ of the Bessel function $K_\nu \left(k\frac{z}{L^2}\right)$ is:

$$K_\nu \left(k\frac{z}{L^2}\right) \simeq \left(\frac{kz}{2L^2}\right)^{-\nu} \frac{\Gamma(\nu)}{2} + \left(\frac{kz}{2L^2}\right)^{\nu} \frac{\Gamma(-\nu)}{2} + \dots . \tag{5.150}$$

From the previous expression, and considering the explicit form of ν , the correlator is easily obtained:

$$\langle \mathcal{O}_\phi^{C_1}(k) \mathcal{O}_\phi^{C_1}(k') \rangle = (2\pi)^d \delta^d(k+k') 2\nu \frac{\Gamma(-\nu)}{\Gamma(\nu)} \left(\frac{k}{2}\right)^{-2\alpha_-} . \tag{5.151}$$

Then coming back to real time ($\omega \to i\omega$) and Fourier transforming, we obtain:

$$\langle \mathscr{O}_\phi^{C_1}(x)\mathscr{O}_\phi^{C_1}(0)\rangle = \frac{2\nu\Gamma(\Delta)}{\pi^{\frac{d}{2}}\Gamma(\nu)}\frac{1}{|x|^{2\alpha_+}} \ . \tag{5.152}$$

Comparing the holographic result with the standard conformal field theory result of Section 5.1 we see that, except an unconventional normalization [10], they agree if we identify α_+ with the scaling dimension of the operator $\mathscr{O}^{C_1}$, namely:

$$\Delta = \alpha_+ \ . \tag{5.153}$$

Note that the normalizability condition (5.131) on the behaviour of ϕ automatically implies that:

$$\Delta \geq \frac{d-2}{2} \ , \tag{5.154}$$

which is exactly the unitarity bound for the scalar operator discussed in Section 5.1.

As a final comment, note that if we had considered the alternative quantization, the scaling dimension of the dual scalar operator would be α_- which is always above the unitarity bound in the region where the solution is stable.

We are now ready to introduce the third computational rule of the AdS/CFT correspondence:

Rule 3: *The scaling dimension of the operator in the dual field theory is setted by the mass of the field in the gravitational bulk.*
Regarding the the scalar field, which is dual to a scalar operator, we have:

$$\Delta_\pm = \frac{d}{2} \pm \sqrt{\frac{d}{4} + m^2L^2} \ . \tag{5.155}$$

Considering a generic massive p-form of mass m in the bulk, we can find a similar relation:

$$\Delta_{p,\pm} = \frac{1}{2}\left(d \pm \sqrt{d^2 - 4dp + 4L^2m^2 + 4p^2}\right) \ . \tag{5.156}$$

In the massless case and for $p = 1$, the positive root is $d-1$ which is the usual dimension of a conserved current.

[10] The normalization of this propagator is unconventional but is natural in AdS/CFT. For two point correlation functions it plays no further role, but dealing with multi-point correlation functions, the normalisation relative to lower-point ones does matter. This normalisation depends sensitively on the regularisation procedure. For the choice which is natural in the bulk (placing the boundary at $z = \varepsilon$ first, taking the limit $\varepsilon \to 0$ at the very end) are one is guaranteed that all relative normalisation factors are correct

Minkowski signature: correlators in real time

Let us now analyze the Minkowski signature case [29]. As previously anticipated, in this case the interior of AdS is a killing horizon. Moreover, in this case $k^2 = -\omega^2 + k^2$ is not positive definite and we have to distinguish between the time-like and the space-like case. In the space-like case $k^2 > 0$, and nothing changes with respect to the Euclidean case. On the other hand, in the time-like case $k^2 < 0$, and the solution of the equation (5.124) is expressed in terms of the Henkel functions:

$$\tilde{\phi} = a_+ \left(\frac{z}{L^2}\right)^{\frac{d}{2}} H_\nu^{(1)}\left(\frac{\sqrt{\omega^2 - k^2}z}{L^2}\right) + a_- \left(\frac{z}{L^2}\right)^{\frac{d}{2}} H_\nu^{(2)}\left(\frac{\sqrt{\omega^2 - k^2}z}{L^2}\right) . \quad (5.157)$$

Expanding the previous solution in the interior of AdS, we obtain:

$$\tilde{\phi} \simeq a_+ e^{-i\frac{\sqrt{\omega^2-k^2}z}{L^2}} + a_- e^{i\frac{\sqrt{\omega^2-k^2}z}{L^2}} \ \ at\ z \to \infty . \quad (5.158)$$

Unlike the previous case, we can not impose a regularity condition. Instead we are dealing with truly fluctuating fields. We have two choices: the first one is to impose in-falling boundary conditions with $a_+ = 0$. Note that combined with the standard $e^{i\omega t}$ this describes a wave-front moving to the interior at large z for positive ω. The other choice is to impose out-going boundary conditions with $a_- = 0$ for positive ω. Let us analyze which are the consequences of both these choices on the correlators. At the computational level, they can be computed in the same way as in the Euclidean signature expanding the Henkel functions near $z = 0$, obtaining:

$$\langle \mathscr{O}^{C_1}(-k)\mathscr{O}^{C_1}(k)\rangle = \begin{cases} 2\nu \frac{\Gamma(-\nu)}{\Gamma(\nu)} \left(\frac{k}{2}\right)^{-2\alpha_-} & k^2 > 0 \\ 2\nu e^{i\pi\nu sgn(\omega)} \frac{\Gamma(-\nu)}{\Gamma(\nu)} \left(\frac{ik}{2}\right)^{-2\alpha_-} & k^2 < 0\ ,\ in \\ -2\nu e^{-i\pi\nu sgn(\omega)} \frac{\Gamma(-\nu)}{\Gamma(\nu)} \left(\frac{ik}{2}\right)^{-2\alpha_-} & k^2 < 0\ ,\ out \end{cases} \quad (5.159)$$

Then Fourier transforming, we obtain:

$$\langle \mathscr{O}^{C_1}(x)\mathscr{O}^{C_1}(0)\rangle = \begin{cases} \frac{2\nu\Gamma(\Delta)}{\pi^{\frac{d}{2}}\Gamma(\nu)} \frac{1}{|x|^{2\alpha_+}} & k^2 > 0 \\ i\theta(x_0) \frac{2\nu\Gamma(\Delta)}{\pi^{\frac{d}{2}}\Gamma(\nu)} \frac{1}{|x|^{2\alpha_+}} & k^2 < 0\ ,\ in \\ -i\theta(-x_0) \frac{2\nu\Gamma(\Delta)}{\pi^{\frac{d}{2}}\Gamma(\nu)} \frac{1}{|x|^{2\alpha_+}} & k^2 < 0\ ,\ out \end{cases} \quad (5.160)$$

Then, as it is evident from the previous expression, the ingoing wave boundary condition corresponds to compute the retarded correlators, while the outgoing wave boundary condition corresponds to compute the advanced correlator. This is actually a general rule in AdS/CFT [29].

Rule 4: *Considering Minkowski signature, it is important to keep into account the causal structure of the correlators. Specifically imposing ingoing wave boundary*

conditions for the field at the horizon corresponds to compute the retarded correlators in the dual field theory, while imposing out-going wave boundary condition corresponds to compute the advanced correlators in the dual field theory.

Finally we note that also the holographic three point function agrees with the CFT result but in order to compute this correlator we have to use the Witten diagrams technique [27]. Since this is beyond the scope of this review we refer to [27] for further details.

5.6 Thermal AdS/CFT

In the previous chapters we have discussed the properties of zero temperature CFTs and we have outlined how they are related to the gravitational field theory in asymptotically AdS space via the gauge/gravity correspondence. Having in mind the possible application of the holographic technique to the study of strongly correlated condensed matter systems it is a necessary step to understand how the temperature can be introduced in the holographic approach.

In order to do this, let us first analyze how the temperature is commonly introduced in standard quantum field theory (for a review on the topic see for example [32]). In order to understand the fundamental properties of a finite temperature quantum field theory we will analyze the system in the canonical ensemble. Generalization of the following statements to the grand canonical ensemble are only a matter of technicality.

Consider now a dynamical system characterized by a Hamiltonian H. The equilibrium state of the system of volume V is described by the canonical density operator

$$\rho = e^{-\beta H} \,, \tag{5.161}$$

where $\beta \equiv \frac{1}{k_B T}$. Recall that in the zero temperature quantum field theory, the expectation value of a given operator A is

$$\langle A \rangle_0 = \sum_n \langle n|A|n\rangle \,, \tag{5.162}$$

where $|n\rangle$ is a complete set of orthonormal states. However, in a heat bath, the operator expectation value should be calculated as the ensemble average with a Boltzmann weight factor, namely:

$$\langle A \rangle_\beta = \frac{1}{Tr\rho} \sum_n \langle n|A|n\rangle e^{-\beta H} = \frac{Tr(\rho A)}{Tr\rho} \,. \tag{5.163}$$

Let us now consider the two point correlation function of a generic operator ϕ immersed in the heat-bath. Using the previous relation we find:

$$\begin{aligned}\langle\phi(t,x)\phi(0,y)\rangle_\beta =&\frac{1}{Tr\rho}Tr\left[e^{-\beta H}\phi(t,x)\phi(0,y)\right]\\ =&\frac{1}{Tr\rho}Tr\left[\phi(t,x)e^{-\beta H}e^{\beta H}\phi(0,y)e^{-\beta H}\right]\\ =&\frac{1}{Tr\rho}Tr\left[\phi(t,x)e^{-\beta H}e^{i(-i\beta H)}\phi(0,y)e^{-i(-i\beta H)}\right]\\ =&\frac{1}{Tr\rho}Tr\left[e^{-\beta H}\phi(-i\beta,y)\phi(t,x)\right]\\ =&\langle\phi(-i\beta,y)\phi(t,x)\rangle_\beta\ .\end{aligned} \tag{5.164}$$

We see that imaginary temperature plays the role as a time variable. If we define the imaginary time variable $\tau = it$, then the relation above can be rewritten as

$$\langle\phi(\tau,x)\phi(0,y)\rangle_\beta = \langle\phi(\beta,y)\phi(\tau,x)\rangle_\beta\ . \tag{5.165}$$

This is called the Kubo-Martin-Schwinger relation. It basically means that studying a quantum field theory at finite temperature is equivalent to the study of the same field theory in the imaginary time where, for the time component we need to take periodic (or anti-periodic) boundary condition,

$$\phi(0,x) = \pm\phi(\beta,x), \tag{5.166}$$

depending on whatever the fields under consideration are bosonic or fermionic, respectively.

Since holography is an equivalence between partition function it is convenient for our purposes to rephrase the previous statement in the partition function language. By noting that

$$e^{-\beta H} = e^{-i\int_0^{-i\beta}Hdt} = e^{-\int_0^\beta Hd\tau}\ , \tag{5.167}$$

we may think at $e^{-\beta H}$ ad an evolution operator in the imaginary time. Then, by repeating the usual steps which lead to the path integral partition function, we obtain:

$$Z = \int\mathscr{D}\phi\langle\phi|e^{-\beta H}|\phi\rangle = \int\mathscr{D}\phi e^{-\int_0^\beta d\tau\mathscr{L}(\tau,\phi)}\ , \tag{5.168}$$

where $\mathscr{L}$ is the Lagrangian density of the theory under consideration and the paths $\phi(\tau,x)$ have to satisfy the periodic (or anti-periodic) boundary conditions (5.166).

As a final comment about standard finite temperature quantum field theory, let us recall some basic properties of the Euclidean and Minkowski correlators which will be useful in what follows. In the Euclidean formalism, due to the periodicity in the imaginary time, it is convenient to express the field as a Fourier series:

$$\phi(\tau,x) = \sum_n\tilde{\phi}(\omega_n,x)e^{i\omega_n\tau}\ , \tag{5.169}$$

where the frequencies ω_n are called Matsubara frequencies [33], and assume the following form:

$$\begin{aligned} \omega_n &= \frac{2\pi n}{\beta} \qquad for\, bosonic\, fields\,, \\ \omega_n &= \frac{2\pi(n+1)}{\beta} \qquad for\, fermionc\, fields\,, \end{aligned} \tag{5.170}$$

for n integer. Then, the Euclidean propagator G_E in momentum space is defined only for integer values of the frequency ω which corresponds to the Matsubara frequencies previously defined and it assumes the following form:

$$G_E(\omega_n,k) = \int d\tau d^d x e^{i\omega_n t + ik\cdot x} \langle T_E \mathscr{O}(\tau,x)\mathscr{O}(0)\rangle\,, \tag{5.171}$$

where $\mathscr{O}$ is a generic operator of the field theory and T_E is the Euclidean time ordering operator. On the other hand, in the real time case, due to the causal structure of Minkowski space-time, one has to deal with different propagators, namely the advanced propagator G^A, the retarded propagator G^R, and the Feynmann propagator G^F defined as:

$$\begin{aligned} G^A(k_\mu &= i\int d^d x e^{-ik_\mu x^\mu}\,\theta(-t)\langle\mathscr{O}(x_\mu)\mathscr{O}(0)\rangle\,, \\ G^R(k_\mu &= -i\int d^d x e^{-ik_\mu x^\mu}\,\theta(t)\langle\mathscr{O}(x_\mu)\mathscr{O}(0)\rangle\,, \\ G^F(k_\mu) &= -i\int d^d x e^{-ik_\mu x^\mu}\,\langle T\,\mathscr{O}(x_\mu)\mathscr{O}(0)\rangle\,. \end{aligned} \tag{5.172}$$

They are, of course, defined for continuous values of ω and k and, at finite temperature T, they are related as follows:

$$G^F(k_\mu) = \Re G^F(k_\mu) + i\coth\frac{\omega}{2T}\Im G^R(k_\mu)\,. \tag{5.173}$$

The Euclidean and Minkowski propagators are closely related. The retarded propagator $G^R(k_\mu)$, as a function of ω, can be analytically continued to the whole upper half plane and, moreover, at complex values of ω equal to $i\omega_n$, reduces to the Euclidean propagator, while the advanced propagator, analytically continued to the lower half plane, is equal to the Matsubara propagator at the points $\omega = -i\omega_n$, namely:

$$G^R(i\omega_n,k) = -G^E(\omega_n,k)\,, \qquad G^A(-i\omega_n,k) = G^E(-\omega_n,k)\,. \tag{5.174}$$

5.6.1 Introducing temperature in holography

We have now to face the problem of how we can introduce the concept of temperature in the holographic framework previously discussed. Specifically we need a way to introduce the concept of temperature in gravity.

As a first comment, it is important to note that in the situations discussed in the previous chapters we were dealing with exact scale invariance, since we were analysing conformal field theory at zero temperature. One has to expect that the introduction of a finite temperature adds a scale in the system and consequently breaks scale invariance. Since scale invariance is recovered at energies well above the characteristic scale of the deformation, we expect that the gravitational space-time should also recover scaling invariance as we go to the conformal boundary, which, as we have explained, corresponds to the UV sector of the dual field theory. In other words we need a gravitational space-time which takes into account the notion of temperature but recover scale invariance in the conformal boundary, namely we need a space-time which has to be asymptotically AdS.

In this light, the fact illustrated in the previous Section that black holes are actually thermal states comes in help. Let us then analyze the most simple asymptotically AdS black hole solution known, the AdS-Shrwarzshild black hole, in order to understand in which sense the temperature of the black hole is related with the notion of temperature in the dual field theory. In this Section we want to discuss this black hole solution in the framework of the holographic techniques discussed in the previous chapters, mainly focussing on the properties of the dual field theory described by this gravitational state. The construction of the solution and its stability is discussed in Appendix B, to which we refer for more details.

Let us then consider the Einstein- Hilbert action (in Minkowski signature):

$$S=\frac{1}{2\kappa_{d+1}^2}\int d^{d+1}x\sqrt{-g}\left(R+\frac{d(d-1)}{L^2}\right)+\frac{1}{2\kappa_{d+1}^2}\int_{\partial M}d^dx\sqrt{-\gamma}\left(2K+\frac{2(d-1)}{L^2}\right). \tag{5.175}$$

In the previous expression, the specific value of the cosmological constant $\Lambda=\frac{d(d-1)}{L^2}$ is required to have an asymptotically AdS solution. We have also added two boundary terms on the manifold $\partial M=\{z=0\}$, expressed in terms of the induced metric on this manifold $\gamma_{\mu\nu}$, and the trace of the extrinsic curvature $K=\gamma^{\mu\nu}\nabla_\mu n_\nu$, where n^μ is an outward pointing normal vector to the boundary $z=0$. These boundary terms are necessary in order to have a well defined variational problem and a finite on-shell action in the same spirit as what has been explained in details for the scalar field in the previous Section (see, for example, Appendix E of [31] for more details).

There is a very simple black hole solution associated to the previous action, namely:

$$ds^2=\frac{L^2}{z^2}\left(-f(z)dt^2+\frac{dz^2}{f(z)}+dx_idx^i\right),\qquad f(z)=1-\frac{z^d}{z_h^d}. \tag{5.176}$$

At $z=z_h$, g_{tt} vanishes, and it can be proven that this is a real horizon (see Appendix B). In order to make contact with the notion of temperature in the dual field theory, let us analyze the previous metric in the imaginary time coordinate, $\tau=it$. Since the properties of the black hole are encoded in the near horizon geometry, let us also expand the metric near $z=z_h$:

$$ds_E^2 \simeq -\frac{L^2 d}{z_h^3}(z-z_h)d\tau^2 - \frac{dz^2}{\frac{L^2 d}{z_h^3}(z-z_h)} + \frac{L^2}{z_h^2}dx_i dx^i \,. \tag{5.177}$$

It is now convenient to perform the following re-parametrization:

$$\rho = 2\sqrt{\frac{z-z_h}{\frac{L^2 d}{z_h^3}}}\,, \qquad t_E = \frac{1}{2}\frac{L^2 d}{z_h^3}\tau\,, \tag{5.178}$$

under which the metric (5.177) becomes:

$$ds^2 \simeq \rho^2 dt_E^2 + d\rho^2 + \frac{L^2}{z_h^2}dx_i dx^i \,. \tag{5.179}$$

The important region to analyse is the plane spanned by ρ and the imaginary time t_E. This is just the metric of a plane in polar coordinates with τ acting as the compact angular direction. Upon approaching the horizon $\rho \to 0$ one sees that the pre-factor of dt_E^2 is vanishing: this means that the Euclidean time direction shrinks to a point. However, since the horizon is not a special point, we should not allow this point to be singular. Smoothness at the horizon can be achieved by insisting that $\rho = 0$ is the center of a Euclidean polar coordinates system, and this implies that t_E is periodic with period

$$\beta = 4\pi\sqrt{\frac{g'_{zz}(z_h)}{g_t t'(z_h)}} = \frac{4\pi z_h}{d}\,. \tag{5.180}$$

But we have learned in the previous Section that, at the level of the dual field theory, studying the theory in the imaginary time with a periodic time coordinate of period β is equivalent to study the field theory at finite temperature $T = \frac{1}{\beta}$. Since the gravitational time coordinate is inherited by the dual field theory we can affirm that that β in expression (5.180) is exactly the inverse of the temperature in the dual field theory.

We care then ready to list the fifth computational holographic rule: **Rule 5:** *Strongly coupled quantum field theories at finite temperature are dual to black hole solutions on the gravitational side. The temperature of the black hole is exactly the temperature of the dual field theory.*

5.6.1.1 Thermodynamics

Having understood how to introduce thermal states in holography we want to make some comments on the thermodynamics of the simple thermal state illustrated in the previous Section, namely the dual of the AdS-Shwarzshild black hole.

In order to obtain the thermodynamics of the dual system we need the partition function and consequently the on-shell action. In the previous Section we have outlined that the action (5.175) has the correct counterterms which ensure its finiteness

once computed on the solution (5.176) (once rotated to imaginary time). Then to compute the on-shell action is only a matter of computation. We recall, however, that the correct procedure to obtain a finite on-shell action is to evaluate the action (5.175) on the solution (5.176) but limiting the radial coordinate z to the interval $[\varepsilon, z_h]$ and to perform the $\varepsilon \to 0$ limit only at the end of the computation. Moreover we recall that the on-shell action is also divergent due to integration over the space coordinates and we need to enclose the system in a finite volume V in order to obtain a finite result. Keeping this in mind, the Euclidean on-shell action S_E and the partition function Z are given by:

$$S_E = -\frac{V(4\pi)^d L^{d-1}}{2\kappa_{d+1}^2 d^d} T^{d-1} , \qquad Z = e^{-S_E} , \tag{5.181}$$

where we have used the relation (5.180) to express T as a function of z_h. The relevant thermodynamical quantities are now easily achieved. The pressure p is given by:

$$p = T\frac{\partial \log Z}{\partial V} = \frac{(4\pi)^d L^{d-1}}{2\kappa_{d+1}^2 d^d} T^d \equiv -F , \tag{5.182}$$

where F is the free energy. The entropy s is given by:

$$s = T\frac{\partial \log Z}{\partial T} = \frac{V(4\pi)^d L^{d-1}(d-1)}{2\kappa_{d+1}^2 d^d} T^{d-1} . \tag{5.183}$$

It is easy to prove that the previous result is consistent with the area law (see Appendix B) which relates the entropy of the black hole with the area of the horizon $A(z_h)$ as follows:

$$s_{bh} = \frac{2\pi A(z_h)}{\kappa_{d+1}^2} = \frac{V(4\pi)^d L^{d-1}(d-1)}{2\kappa_{d+1}^2 d^d} T^{d-1} . \tag{5.184}$$

Finally the energy ε can be derived from the thermodynamic relation $\varepsilon = -p + Ts$, obtaining:

$$\varepsilon = (d-1)\frac{(4\pi)^d L^{d-1}}{2\kappa_{d+1}^2 d^d} T^d , \tag{5.185}$$

which is exactly the energy of the AdS-Shwarzshild black hole derived in Appendix B.

In conclusion, the dual field theory inherit the thermodynamics from the black hole state in the gravity side.

5.6.2 Holography at finite charge density

A common additional structure that arises in condensed matter systems is a $U(1)$ symmetry. This could be, for instance, the electromagnetic $U(1)$ symmetry. In this section we will consider the gravitational dual of theories with a global $U(1)$ symmetry. The electromagnetic U(1) symmetry in nature is of course gauged (local). However, there are at least two reasons why photons can be correctly neglected in many condensed matter processes. Firstly the electromagnetic coupling is observed to be small. Secondly, the electromagnetic interaction is screened in a charged medium. This come in help in the holographic framework where typically the gauge field is non dynamical at the boundary [34].

So what is the dual to a global $U(1)$ symmetry in field theory? We can take our cue from the symmetries that we have already discussed in previous sections. Another global symmetry that the field theory possesses (in a fixed Minkowski background metric, say) is $SO(d-1)$ rotational invariance. In the bulk this symmetry symmetry also appears, but it is gauged. Namely, it is part of the diffeomorphism invariance of general relativity: we can act on our AdS space-time with a local $SO(d-1)$ rotation and we simply obtain AdS again in a different coordinate system. This observation suggests the general correspondence:

Rule 6: *Gauged symmetries in the gravitational theory corresponds to global symmetries in the dual field theory.*

To describe the physics of the global $U(1)$ symmetry we should therefore add a Maxwell field to our bulk space-time. The minimal bulk action is thus Einstein-Maxwell theory:

$$S_{E-M} = \frac{1}{2\kappa_{d+1}^2}\int d^{d+1}x\sqrt{-g}\left(\mathscr{R}+\frac{d(d-1)}{L^2}\right) - \frac{1}{4q^2}\int d^{d+1}x\sqrt{-g}F_{ab}F^{ab} + \frac{1}{2\kappa_{d+1}^2}\int_{\partial M} d^dx\sqrt{-\gamma}\left(2K+\frac{2(d-1)}{L^2}\right), \quad (5.186)$$

where $F \equiv \partial_{[a}A_{b]}$ is the field strength of the gauge field A_μ, q is a coupling constant which takes into account the strength of the back-reaction of the gauge field on the gravity sector, and we have added, as in the previous Section, the boundary terms necessary to have a finite on-shell action and a well defined variational problem. Actually these boundary terms are the correct ones only for $d > 2$. For $d = 2$ the asymptotically AdS solution of the Einstein Maxwell theory has some technical peculiarities and requires a separate treatment. We do not discuss this case in this review.

The Einstein's equation of motion is:

$$R_{ab} - \frac{1}{2}g_{ab}\mathscr{R} - \frac{d(d-1)}{2L^2}g_{ag} = -\frac{\kappa_{d+1}^2}{2q^2}T_{ab}, \quad (5.187)$$

where T_{ab} is the stress-energy tensor

$$T_{ab} = \frac{1}{4} g_{ab} F_{cd} F^{cd} - F_{ac} F_b^{\ c}. \tag{5.188}$$

The equations of motion for F_{ab} are:

$$\nabla_a F^{ab} = 0, \tag{5.189}$$

where ∇_a is the usual covariant derivative.

Before finding a particular solution of the previous set of equations, let us clarify what we need to obtain in the holographic framework. Our main purpose is to study a strongly coupled field theory at finite density and finite temperature. Regarding the finite temperature we have learned in the previous Section that this is achieved by studying a black hole solution of the gravitational theory. Concerning the finite density issue, we have just learned that the gauge field in the gravitational side sources a current density J_a in the dual field theory. If we want a finite density ρ we need to switch on the gauge field in the bulk so that the time component of J_a, $\langle J_t \rangle = \rho$, has a non-zero expectation value. But, according to the standard holographic dictionary, the value of the field at the conformal boundary acts as the sources for the dual operator. Putting all together, and keeping in mind that at the dual level the source of the charge density ρ is the chemical potential μ, in order to find the gravitational dual of a finite charge density system we need to impose: [11]

$$\lim_{z \to 0} A_t = \mu \ . \tag{5.190}$$

This is the first basic condition. The second one is that we want to recover scale invariance at energy scales much greater than the chemical potential μ, namely we want the space-time to be asymptotically AdS.

We are now ready to find the gravity dual of a field theory at finite density and temperature. We consider the following ansatz for the metric g_{ab} and the gauge field A_a:

$$A = A_t(z) dt \ , \tag{5.191}$$

$$ds^2 = \frac{L^2}{z^2} \left[-g(z) dt^2 + h_{ij}(x_l) dx^i dx^j + \frac{dz^2}{g(z)} \right] \ , \tag{5.192}$$

where h is the horizon metric and $i = 1, ..., d-1$.
The solution of the equations (5.187) and (5.189) with the ansatz (5.191) and (5.192), imposing the flatness of the horizon, the asymptotically AdS-ness and the boundary condition (5.190), is the following

[11] To work instead in the canonical ensemble, fixed charge density ρ, we should add a boundary term to the Euclidean action so that $\Delta S_E = \frac{1}{q^2} \int_{\partial M} d^d x \sqrt{\gamma} \frac{1}{\sqrt{g^{rr}}} F_{zb} A^b$. This term changes the variational problem so that one must keep the field strength F_{rb} fixed at the boundary rather than the potential A_a. It can be seen to imply the standard thermodynamic relation $F = \omega + \mu Q$. Here $Q = \rho V$ is the total charge.

$$g(r) = 1 - \left(1 + \frac{d-2}{d-1}\frac{\bar{\gamma}^2\mu^2}{L^2}\right)\left(\frac{z}{z_h}\right)^d + \frac{d-2}{d-1}\frac{\bar{\gamma}^2\mu^2}{L^2}\left(\frac{z}{z_h}\right)^{2(d-1)}, \tag{5.193}$$

$$A_t = \mu\left(1 - \left(\frac{z}{z_h}\right)^{d-2}\right), \tag{5.194}$$

where z_h is an outer planar horizon and $\bar{\gamma} \equiv \frac{\kappa_{d+1}}{q}$. It is important to note that in order to completely determine the profile of the gauge field we need to provide also a condition at the horizon which, in this case, is that it should be vanishing, $A_t(z_h) = 0$. It can be retained by requiring the norm of the vector field $g^{tt}\sqrt{-g}A_tA_t$ to be finite at the horizon.

Actually, in the case at hand, where the gauge field is not coupled to matter, the constant in (5.194) can be rescaled by means of a gauge transformation. Imposing that $A_t(z_h) = 0$ is then a gauge choice. According to the holographic dictionary, it is only in this gauge that μ in (5.194) plays actually the role of the chemical potential [16].

Moreover we note that we have indicated with z_h the *outer* horizon, but this solution presents also an *inner* horizon hidden by z_h. The two horizons coincide in the limit of zero temperature. In this case the black hole is said to be extremal.

The derivation of the thermodynamical quantities associated to this black hole solution proceeds analogously as what has been done for the zero density case in the previous section. In particular, the black hole temperature is given by:

$$T = -\frac{g'(z_h)}{4\pi} = \frac{1}{4\pi z_h}\left(d - \frac{(d-2)^2 z_h^2\mu^2\bar{\gamma}^2}{(d-1)L^2}\right). \tag{5.195}$$

Since we are working in the grand canonical ensemble (μ fixed) the referring potential is the Landau potential Ω which can be derived from the partition function $Z = e^{-S^E_{E-M}}$ as follows:

$$\Omega = -T\log Z = -\frac{L^{d-1}V}{2\kappa^2_{d+1}z_h^d}\left(1 + \frac{(d-2)z_h^2\mu^2\bar{\gamma}^2}{(d-1)L^2}\right) = \mathscr{F}\left(\frac{T}{\mu}\right)VT^d \tag{5.196}$$

where the function $\mathscr{F}$ is easily obtained by solving (5.195) for z_h. This function is a non-trivial output from AdS/CFT. At low temperatures we have $\Omega \simeq a\mu^d + b\mu^{d-1}T + c\mu^{d-2}T^2 + \ldots$. In particular, the leading non-trivial temperature dependence of the thermodynamic potential is linear, as is the leading low temperature dependence of the heat capacity $c = T\frac{\partial S}{\partial T}$. At high temperatures one finds $\Omega \simeq \mu^{2(d-1)}/T^{d-2} + \ldots$.

The transport properties and their relations with thermodynamics for these solution will be treated carefully in Part 3.

5.7 Summa: the Holographic Dictionary

In the previous Sections we have illustrated the basic technical tools necessary to implement the AdS/CFT correspondence at the computational level. All the prescriptions outlined above can be collected in a table which constitutes an a sort of dictionary with all the basic ingredients necessary to use the gauge/gravity duality. This goes under the name of *holographic dictionary*.

Boundary: field theory	**Bulk: gravity**
partition function	partition function
scalar operator/order parameter $\mathcal{O}_b$	scalar field ϕ
source of the operator	boundary value of the field (leading coefficient of the non-normalizable solution)
VEV of the operator	boundary value of radial momentum of the field (leading coefficient of the normalizable solution; subleading to the non-normalizable solution)
conformal dimension of the operator	mass of the field
spin/charge of the operator	spin/charge of the field
energy momentum tensor T^{ab}	metric field g_{ab}
global internal symmetry current J^a	Maxwell field A_a
Fermionic operator $\mathcal{O}_f$	Dirac field ψ
two-point correlation function	ratio of non-normalizable to normalizable solution evaluated at the boundary
higher-point correlation functions	Witten diagram computation
RG flow	evolution in the radial AdS direction
global space-time symmetry	local isometry
internal global symmetry	local gauge symmetry
finite temperature	black hole Hawking temperature or radius of compact Euclidean time circle
chemical potential/charge density	boundary value of the electrostatic potential A_t
free energy	on-shell value of the action
entropy	area of the black hole horizon
phase transition	instability of black holes

Appendices

Appendix B
Asymptotically AdS space-time: AdS black holes

In this Appendix we will describe the main properties of the black holes whose metric are asymptotically Anti-de Sitter. In particular we will focus our attention on the Schwarzshild-Anti-de Sitter black hole and its charged version, the Reissner-Nordström-Anti-de Sitter black hole. These two kind of asymptotically Anti-de Sitter black holes will be extremely important in the formulation of thermal AdS/CFT correspondence, as outlined in the main text.

The main properties of these space-times is that they should look like Anti-de Sitter space-time "far-away" from any mass concentration or black hole that may be present.
Before analysing in detail the main features of these black holes, let us define the asymptotically AdS space time.
Definition: a d-dimensional metric space $(\mathscr{M}, g_{ab})$ is said to be asymptotically Anti-de Sitter if there exist a manifold $\bar{\mathscr{M}}$ with boundary $\mathscr{I}$, equipped with a metric $\bar{g}_{ab}$ and a diffeomorphism from $\mathscr{M}$ onto $\bar{\mathscr{M}} - \mathscr{I}$ of $\bar{\mathscr{M}}$ and the interior of $\bar{\mathscr{M}}$ such that:

- there exists a function Ω on $\bar{\mathscr{M}}$ for which $\bar{g}_{ab} = \Omega^2 g_{ab}$ on $\mathscr{M}$
- $\mathscr{I}$ has the topology of S^{d-2}, Ω vanishes on $\mathscr{I}$ but $\nabla_a \Omega$ normal vector on $\mathscr{I}$ is nowhere vanishing in $\mathscr{I}$
- on $\mathscr{M}$, g_{ab} satisfies the Einstein's equation
- the Weyl tensor of $\bar{g}_{ab}$ is such that $\Omega^{d-4} C_{abcd}$ is smooth on $\mathscr{M}$ and vanishes on $\mathscr{I}$.

The first condition ensures that the new metric $\bar{g}_{ab}$ is conformally related to the physical metric g_{ab}; the second instead requires that the topology of the boundary is the one suggested by the geometry of anti-de Sitter space-time, and that the boundary itself is attached at infinity with respect to the physical metric. The requirement on the normal of $\mathscr{I}$ implies that Ω is a good radial coordinate in a neighbourhood of $\mathscr{I}$ in the barred space-time. Third condition is a restriction to the asymptotic behaviour of matter fields which ensures that the fluxes of some conserved quantities across $\mathscr{I}$ are well-defined. We also expect that the limit of $\Omega^{4-d} C_{abcd}$ on the

conformal boundary vanishes since as a property of the Weyl tensor, $C_{abcd} = 0$ in Anti-de Sitter space-time.

B.1 *AdS*-Schwarzshild black hole

We now attempt to construct a static $d+1$-dimensional solution of the Einstein's equation with negative cosmological constant Λ which admits a black hole interpretation.
Let us start with the most general ansatz for a static, isotropic and spherically symmetric metric:

$$ds^2 = -f(r)dt^2 + f^{-1}(r)dr^2 + r^2 h_{ij}(x)dx^i dx^j, \tag{B.1}$$

where the coordinates are labelled as $x_\mu = (t, r, x_i),\ (i, 1, ..., d-1)$. The metric h_{ij} is a function of the coordinates x_i only, and is the horizon metric.[1] The non-vanishing component of the Ricci tensor associated with the metric B.1 are:

$$R_{tt} = \tfrac{1}{2} f f' + \tfrac{1}{2r}(d-1) f f', \tag{B.2}$$

$$R_{rr} = -\tfrac{1}{2}\tfrac{f''}{f} - \tfrac{1}{2r}(d-1)\tfrac{f'}{f}, \tag{B.3}$$

$$R_{ij} = R_{ij}(h) - h_{ij}\left[(d-3)f + rf'\right], \tag{B.4}$$

where $R_{ij}(h)$ is the Ricci tensor derived from the horizon metric h only, and the primes denote the derivative with respect to the radial coordinate r. Let us now take the following ansatz for f:

$$f(r) = \kappa - \frac{M}{r^{d-2}} + \frac{r^2}{L^2}, \tag{B.5}$$

where κ and M are two yet undetermined parameter and L is an arbitrary parameter with dimension of a length[2]. With this form for f, one can easily see that the space-time is an Einstein space with negative cosmological constant, namely

$$R_{\mu\nu} = -\frac{d}{l^2} g_{\mu\nu} \tag{B.6}$$

provided the horizon is an Einstein space-time of the form:

$$R_{ij}(h) = (d-2)\kappa h_{ij}. \tag{B.7}$$

It is important to observe here that we have obtained a solution to Einstein's equation with a negative cosmological constant for any value of κ, provided the horizon is

[1] We will explain later, when we outline the black hole interpretation of the solution, why this is actually the horizon metric.

[2] This is related to the *AdS* radius previously defined, as we will see.

itself Einstein. However, the horizon may be an Einstein space with positive, zero, or negative curvature. This opens up the possibility to construct black hole solutions in which the topology of the horizon is non-spherical.
We have now to prove that the solution we have found is actually asymptotically Anti-de Sitter in the sense we have explained in the previous section. In order to do this, let us analyse the non vanishing components of the curvature tensor:

$$R_{trtr} = \tfrac{1}{2}f'', \qquad R_{titj} = \tfrac{r}{2}ff'h_{ij}, \qquad R_{rirj} = -\tfrac{rf'}{2f}h_{ij} \tag{B.8}$$

$$R_{ijkl} = r^2 R_{ijkl}(h) - r^2 f\left[h_{ik}h_{jl} - h_{il}h_{jk}\right], \tag{B.9}$$

where $R_{ijkl}(h)$ is the curvature tensor constructed from the horizon metric h_{ij}. It is apparent from the previous equations that the $M = 0$ solution is locally isometric to Anti-de Sitter ($R_{\mu\nu\rho\sigma} = -\frac{1}{L^2}\left(g_{\mu\rho}g_{\nu\sigma} - g_{\mu\sigma}g_{\nu\rho}\right)$), provided that the horizon is itself a constant curvature space with curvature constant κ, ($R_{\mu\nu\rho\sigma} = \kappa\left(g_{\mu\rho}g_{\nu\sigma} - g_{\mu\sigma}g_{\nu\rho}\right)$).
Thus, imposing the extra requirement that the $M = 0$ solution be a constant curvature space-time, forces the horizon to be a constant curvature space, and not simply Einstein. However, once again there is no restriction on the sign of κ. Although the $M = 0$ space-time is locally isometric to Anti-de Sitter space, its topology depends on the value of κ, and hence on the topology of the horizon. In particular, we have the three possibilities, namely elliptic horizons ($\kappa = 1$), flat horizons ($\kappa = 0$), and hyperbolic horizons ($\kappa = -1$). We note from B.5 that the dominant behaviour of the metric at infinity is determined by the cosmological constant term, for any value of M. Since the $M = 0$ solution is locally isometric to anti-de Sitter space, we have a class of black hole solutions which are asymptotically locally Anti-de Sitter, for all values of M.

Black hole interpretation

We have constructed a solution of the Einstein's equation which is asymptotically Anti-de Sitter. We have now to prove that the horizon of this solution, namely the surface $f(r) = 0$, is actually a black hole horizon. In order to do this we have to prove that $f(r)$ has a simple positive root r_+, such that $f(r) > 0$ for all $r > r_+$. Under these conditions, in fact, the surface $r = r_+$ has an horizon interpretation.
To see this, consider a particle with four momentum $P = (-E, p)$. A static observer at infinity has four velocity $U = \frac{k_\mu}{\sqrt{-k^2}}$, where $k = -\partial_t$. The energy measured by the local observer is

$$E = -g_{\mu\nu}U^\mu P^\nu = \frac{E_\infty}{\sqrt{-g_{tt}}}. \tag{B.10}$$

So E is red-shifted by a factor $\sqrt{-g_{tt}}$ from E_∞. Consequently, from the point of view of an observer at infinity (whose proper time corresponds to the coordinate t), due to the positivity of $f(r)$ for $r > r_+$ and the fact that $f(r_+) = 0$, the surface $r = r_+$ is a surface of infinite red-shift.

For $\kappa = \pm 1$ it is not a simple task to prove that there exists a positive root r_+ of $f(r)$ that satisfies the conditions illustrated above for arbitrary dimension d, and we refer to [3, 5, 6, 9] for more detail.
On the other hand, for $\kappa = 0$, which is the most relevant case in AdS/CFT correspondence, it is apparent that $f(r)$ has a positive solution for

$$r_+ = (ML^2)^{\frac{1}{d}}, \tag{B.11}$$

and $f(r)$ is positive for $r > r_+$. Thus, for $\kappa = 0$ we have black hole solution with toroidal topology.

B.1.1 Thermodynamical quantities

We want now to calculate the thermodynamical quantities associated with our black hole solution. The arguments illustrated below are valid for every black hole solution which has an acceptable horizon located at r_+. The parameter M is specified in terms of r_+ as follows:

$$M = r_+^{d-2}\left(\kappa + \frac{r_+^2}{L^2}\right). \tag{B.12}$$

Before calculating the thermodynamical quantities associated with the black hole solution, we have to show how a black hole is a thermal state. In other words we have to compute the partition function $\mathscr{Z}$ associated to the black hole.
In quantum field theory, the amplitude for a field to propagate from an initial field configuration to a final field configuration is given by the weighed sum over all field configurations, where the weights are determined by the action of the field: $\mathscr{Z} = \int D\phi\, e^{iS[\phi]}$. One needs to be careful about the convergence associated with the oscillatory integral. To circumvent this issue, it is useful to perform a Wick rotation $t \to i\tau$, thereby rotating the contour of integration of time by $\frac{\pi}{2}$ counter-clockwise. The Wick rotated path integral becomes $\mathscr{Z}_E = \int \mathscr{D}\phi\, e^{-S_E[\phi]}$, which converges. If one wants to define a thermal state of the quantum field theory, it is necessary to restrict the imaginary time τ to a finite interval and to impose periodic boundary condition. The period of the imaginary time is identified with the inverse of the temperature $\beta = \frac{1}{T}$.
In curved space-time, the path integral is generalized to sum over variations in geometry as well as fields. If we consider only variation of the metric, the Euclidean partition function is $\mathscr{Z}_E = \int \mathscr{D}g e^{-I_E[g]}$, where $I_E[g]$ is the usual Wick rotated Einstein-Hilbert action with cosmological constant Λ:

$$I_E = -\frac{1}{16\pi G_{d+1}}\int d^{d+1}x\sqrt{g_E}\,(\mathscr{R} - 2\Lambda). \tag{B.13}$$

Because we are dealing with manifolds with boundary, we also need to consider the Hawking-Gibbons boundary term, though, as we will see, it is not relevant for our

discussion.

In the case of the black hole, the requirement for the Euclidean metric to have no conical singularity at the horizon $r = r_+$, fixes the period of the imaginary time τ and consequently the temperature T which must be identified with the temperature of the black hole. In this sense the black holes have to be considered as thermal states.
Let us consider the AdS-Shwarzshild solution we have constructed in the previous section. The euclidean metric g_E is:

$$ds_E^2 = f(r)d\tau^2 + f^{-1}(r)dr^2 + r^2 h_{ij}(x_i)dx^2 dx^j, \tag{B.14}$$

where we recall that $f(r) = \left(\kappa - \frac{M}{r^{d-2}} + \frac{r^2}{L^2}\right)$ and $f(r_+) = 0$. The near horizon behaviour of g_E is:

$$\left(ds_E^2\right)_{r\approx r_+} = f'(r_+)(r-r_+)d\tau^2 + \frac{dr^2}{f'(r_+)(r-r_+)} + r_+^2 h_{ij}(x_i)dx^2 dx^j. \tag{B.15}$$

Defining new coordinates

$$\rho = 2\sqrt{\frac{r-r_+}{|f'(r_+)|}}, \qquad t_E = \frac{1}{2}\left|f'(r_+)\right|\tau, \tag{B.16}$$

we finally find the near horizon geometry

$$\left(ds_E^2\right)_{r\approx r_+} = \rho^2 dt_E^2 + d\rho^2 + r_+^2 h_{ij}(x_i)dx^2 dx^j. \tag{B.17}$$

This metric has the topology of the horizon described by the metric h times an euclidean plane in polar coordinates $(\rho,\, t_E)$. There is a deficit angle which leads to a conical singularity in $\rho = 0$ unless t_E is 2π-periodic. The corresponding period in the euclidean time coordinate τ is:

$$\beta = \frac{4\pi}{f'(r_+)}. \tag{B.18}$$

As we have outlined above, this period has to be identified with the inverse of the black hole temperature T. Consequently, remembering the expression of the parameter M in terms of the horizon radius r_+ B.12, we find:

$$\beta = \frac{1}{T} = \frac{4\pi L^2 r_+}{dr_+^2 + (d-2)\kappa L^2}. \tag{B.19}$$

It is worth highlighting some of the features of these black holes which depend on the value of κ [3]. For $\kappa = 1$, it has been shown in [6] that the inverse temperature B.19

[3] These properties are extremely important in the computation of the thermodynamical quantities, as we will see in what follows

has a maximum value. Hence, the black hole solutions only exist for temperatures greater than a certain minimum value. On the other hand, for the case of $\kappa = 0$ and $\kappa = -1$, it is easy to check from B.19 that there is no such minimum temperature; hence, the $\kappa = 0$ and $\kappa = -1$ black holes exist for all temperatures. However, one does notice that for $\kappa = -1$, the requirement of positivity of temperature enforces an inequality on the value of r_+ , namely that $r_+ > r_{\text{crit}}$, where

$$r_{\text{crit}} = \left(\frac{d-2}{d}\right)^{\frac{1}{2}} L, \tag{B.20}$$

which corresponds to a critical mass

$$M_{\text{crit}} = -\frac{2}{d}\left(\frac{d-2}{d}\right)^{\frac{d-2}{2}} L^{d-2}. \tag{B.21}$$

The next step toward the computation of the thermodynamical quantities is the calculation of the on-shell action associated to the black hole. The Euclidean action B.13 is proportional to the space-time volume, namely

$$I_E = \frac{d}{16\pi G_{d+1} L^2} \int d^{d+1}x \sqrt{g_E}, \tag{B.22}$$

where we have substituted the value of the cosmological constant $\Lambda = -\frac{d(d-1)}{2L^2}$. Since the integral B.22 diverges we have to regularise it in order to compute the action. The standard way to regularize gravitational actions is to compare them with a convenient background, which is, in a sense, the thermal background of our black hole solution [10]. The choice of a suitable background depends on the particular value of κ. For $\kappa = -1$, since, as we have said, the black hole solution exist only for temperature greater than a certain minimum value, the background solution can be taken to be Anti-de Sitter space with arbitrary Euclidean time period. For $\kappa = 0$, since the black hole solution exists for every temperature, a suitable background solution is the space B.1 with $M = 0$. Finally for $\kappa = -1$ due to the positivity condition on the temperature, the background metric is the metric B.1 with $M = M_{\text{crit}}$ given by B.21. As regards the Gibbons-Hawking boundary term, we can forget about it since it cancels in the subtraction of the background action from the black hole one.
We have now to evaluate the difference between the on-shell action of the black hole and of the background. Since the two integrals diverge by themselves, we put a cut-off at $r = K$ and we evaluate the difference in the limit $K \to \infty$:

$$I_E^f = \lim_{K\to\infty} \frac{d}{8\pi G_{d+1} L^2} \left(\int_0^\beta dt \int_{r_+}^K r^{d-1} dr \int_{M_h} \sqrt{h} - \int_0^{\beta_0} dt \int_0^K r^{d-1} dr \int_{M_h} \sqrt{h} \right), \tag{B.23}$$

where M_h is the manifold with metric h, β is given by B.19, β_0 is the period of the background metric [4]. The condition that the black hole metric and the background metric must match at $r = K$ allow to express β_0 in terms of β. In particular, in order for the two metric to match, the Euclidean period at $r = K$ must be the same, namely

$$\beta_0 \sqrt{\kappa - \frac{M_{\text{crit}}}{K^{d-2}} + \frac{K^2}{L^2}} = \beta \sqrt{\kappa - \frac{M}{K^{d-2}} + \frac{K^2}{L^2}}. \tag{B.24}$$

Evaluating the integral B.23 with the condition B.24 yields:

$$I_E^f = \frac{Vol(M_h)}{16\pi G_{d+1} L^2} \beta \left[-r_+^d + \kappa L^2 r_+^{d-2} - L^2 M_{\text{crit}} \right]. \tag{B.25}$$

The thermodynamical quantities are now easily computed. The energy and the entropy per unite volume are given by:

$$\frac{E}{Vol(M_h)} = \frac{1}{Vol(M_h)} \frac{\partial I_E^f}{\partial \beta} = \frac{1}{16\pi G_{d+1}} (M - M_{\text{crit}}), \tag{B.26}$$

$$\frac{S}{Vol(M_h)} = \frac{1}{Vol(M_h)} \left(\beta E - I_E^f \right) = \frac{1}{16\pi G_{d+1}} r_+^{d-1}. \tag{B.27}$$

Finally we note that the specific heat of the $\kappa = 0$ and $\kappa = 1$ solutions is positive. For $\kappa = 0$, we find:

$$\frac{C}{Vol(M_h)} = \frac{1}{Vol(M_h)} \frac{\partial E}{\partial T} = \frac{1}{4\pi G_{d+1}} r_+^{(d-1)}, \tag{B.28}$$

while for $\kappa = -1$, we have

$$\frac{C}{Vol(M_h)} = \frac{1}{4\pi G_{d+1}} r_+^{(d-1)} \left[\frac{d r_+^2 - (d-2)L^2}{d r_+^2 + (d-2)L^2} \right]. \tag{B.29}$$

In the latter case, we see that the specific heat is positive provided $r_+ > r_{\text{crit}}$. We contrast this with the case $\kappa = 1$, where for temperatures greater than a minimum value there are two black holes, the smaller of which has negative specific heat, the larger having positive specific heat [6].

[4] Note that in the background action the integration in the radial coordinate stars from $r = 0$ also for the space-time with $M = M_{\text{crit}}$ since this space-time has no black hole interpretation. Consequently the period β_0 of the background space-time is arbitrary regardless the sign of κ.

Appendix C
Radial quantization and unitarity bounds

In this brief Appendix we shall illustrate the radial quantization and how, with this tool, it is possible to impose constraints on the conformal dimension of the fields in a unitary theory, the so called unitarity bounds.

C.1 The radial quantization

In quantum field theory, in order to construct an Hilbert space we have to chose a foliation of space-time. Each leaf of the foliation becomes endowed with its own Hilbert space.
We create in and out states $|\psi_{in}\rangle$ and $\langle\psi_{out}|$ by inserting operator respectively in the past or in the future of a given surface. The overlap of in and out states living on the same surface is equal to the correlation function $\langle\psi_{out}|\psi_{in}\rangle$. On the other hand, if the two states belong to different foliation there must be a unitary operator U which connect the two states, and the same correlation function is equal to $\langle\psi_{out}|U|\psi_{in}\rangle$.
Usually, in order to chose a proper foliation, it is convenient to look at the symmetry of the theory. For example, in a Poincaré invariant theory it is convenient to foliate the space by surface of constant time.
On the other hand, in a CFT it is convenient to chose foliations by S^{d-1} spheres of various radii: this is called the *radial quantization*. We will assume that the spheres are centred in $x = 0$, even though quantizing with respect to any other point should give the same correlators.
The evolution generator, in this case, is given by the dilatation operator D, and it shall play the role of the Hamiltonian:

$$U = e^{iD\tau}, \tag{C.1}$$

where $\tau = \log r$.The states living on a sphere are classified by their scaling dimension Δ and by their $SO(d)$ spin l

$$D|\Delta,\, l\rangle = i\Delta|\Delta,\, l\rangle \tag{C.2}$$

$$L_{\mu\nu}|\Delta,\, l\rangle_a = S^b_{\mu\nu\, a}|\Delta,\, l\rangle_b, \tag{C.3}$$

since, as it is evident from the conformal algebra 5.20, the only generator which commutes with D is the angular momentum L. The spin matrix S is different from zero only in the case of non-zero spin operators.

State-operator correspondence

In radial quantization we create states on the sphere by insert operator inside the sphere. Consequently, the vacuum state $|0\rangle$ corresponds to inserting nothing. The dilatation eigenvalue, which corresponds to the energy of this state, is zero.
If we insert an operator with scaling dimension Δ at the origin $\mathcal{O}_\Delta(x=0)$, the corresponding state $|\Delta\rangle = \mathcal{O}_\Delta(x=0)|0\rangle$ has energy equal to Δ. In fact,

$$D|\Delta\rangle = D\mathcal{O}_\Delta(x=0)|0\rangle = [D, \mathcal{O}_\Delta(x=0)]|0\rangle = i\Delta|\Delta\rangle, \tag{C.4}$$

where we have used the commutation relation 5.20.
Finally the state generated by the insertion of an operator at non-zero x, $\mathcal{O}_\Delta(x)$, is not an eigenstate of D. This fact is evident:

$$|\Psi\rangle = \mathcal{O}_\Delta(x)|0\rangle = e^{iPx}\mathcal{O}_\Delta(0)e^{-iPx}|0\rangle \tag{C.5}$$

$$= e^{iPx}|\Delta\rangle = \textstyle\sum_{n=0}^{\infty} \frac{(iPx)^n}{n!}|\Delta\rangle \tag{C.6}$$

Moreover it is easy to see that the operator P_μ and K_μ acts as the creation and annihilation operators in radial quantization. This is evident from the fact that, as we have said in the previous section, they satisfy the following commutation relations:

$$[D, P_\mu] = iP_\mu \tag{C.7}$$

$$[D, K_\mu] = -iK_\mu. \tag{C.8}$$

In other words, each time the momentum operator P_μ acts on $|\Delta\rangle$ a state with energy $\Delta + 1$ is generated, while the operator K_μ lowers the dimension by 1.
This algebraic construction of state with definite energy allow us to make clearer the definition of local primary operator. In fact if we did not have a primary, then we could keep lowering dimensions. Assuming that dimensions are bounded from below (as they are in unitary theories, see below), eventually we must hit zero, and this will give us a primary.
Let us go back to the states generated by inserting a primary operator at the origin. We saw that these states have scaling dimension Δ and are annihilated by K_μ. We can go backwards as well: given a state such that its scaling dimension is Δ which is

annihilated by K_μ , we can construct a local primary operators. [1] Indeed, to construct an operator we must define its correlation functions with other operators. And it is easy to see that a good definition could be:

$$\langle \phi_1(x_1)\phi_2(x_2)...\mathscr{O}_\Delta(0)\rangle = \langle 0|\phi_1(x_1)\phi_2(x_2)...|\Delta\rangle. \tag{C.9}$$

The last thing we have to do is to define the conjugation operator in radial quantization. A hint in this direction is given by the fact that the operator K_μ and P_μ are conjugate by applying the inversion operator $\mathscr{R}$ twice

$$K_\mu = \mathscr{R}P_\mu\mathscr{R}. \tag{C.10}$$

Since we have previously identified these operators as the creation and annihilation operators of the radial quantized theory, it is natural to try to define the conjugation operator as the inversion, so that

$$K_\mu = P_\mu^\dagger. \tag{C.11}$$

Consequently, given a state $|\psi\rangle = \phi(x)|0\rangle$, we define its conjugate $\langle\psi|$ by:

$$\langle\psi| = \langle 0|[\phi(x)]^\dagger, \text{ with } [\phi(x)]^\dagger = r^{-2\Delta_\phi}\phi(\mathscr{R}x) = \mathscr{R}[\phi(x)]. \tag{C.12}$$

This definition has the property that, as we will see, in a unitary theory the correlation function are $\mathscr{R}$-reflection positive.

Two point functions in radial quantization

Let us now outline how to compute correlation functions in radial quantization. For simplicity, we shall restrict our analysis to the scalar-scalar two point function.
Since $\phi(x_1)|0\rangle = e^{iPx_1}|\Delta_\phi\rangle$ and keeping into account our definition of the conjugate state in radial quantization C.12, we obtain:

$$\langle 0|\phi(x_1)\phi(x_2)|0\rangle = r_2^{-2\Delta_\phi}\langle\Delta_\phi|e^{-iK\mathscr{R}x_2}e^{iPx_1}|\Delta_\phi\rangle. \tag{C.13}$$

Expanding in series both the exponential inside the mean value and $r_2^{-2\Delta_\phi}$, and multiplying and dividing by $r_1^{\Delta_\phi}$ we obtain the following expansion for the two point function:

$$\langle 0|\phi(x_1)\phi(x_2)|0\rangle = \frac{1}{r_1^{\Delta_\phi}r_2^{\Delta_\phi}}\sum_N \langle N,\underline{n}_2|N,\underline{n}_1\rangle\left(\frac{r_1}{r_2}\right)^{\Delta_\phi+n}, \tag{C.14}$$

[1] This is called state-operator correspondence: states are in one-to-one correspondence with local operators.

where $|N,\underline{n}_1\rangle = \frac{1}{N!}(P_\mu \underline{n}^\mu)^N |\Delta_\phi\rangle$, and we have taken into account the fact that the expectation value of product of operator involving different power of K_μ and P_μ vanishes since states with different energies are orthogonal to each over.
Then, the coefficients of the expansion of the correlator in radial quantization are certain matrix elements which could be computed using only the conformal algebra. It is possible to see that the expansion agrees with the series expansion of the exact two-point function in radial coordinates.

C.2 Unitarity bounds

Finally, we are now able outline how to obtain unitarity bounds for the scaling dimensions of primary operators with the help of radial quantization.
By unitarity bounds we mean that the dimension of a symmetric traceless primary field must be above a certain minimal value which depends on the spin l of such field:

$$\Delta_{min}(l) = l + d - 2, \text{ for } l = 1,2,3... \tag{C.15}$$

$$\Delta_{min}(l=0) = \tfrac{d}{2} - 1 \tag{C.16}$$

Similar bounds can be derived for antisymmetric tensor and fermionic representation of the Lorentz group.
In order to prove the bounds 9.16, let us consider the matrix element

$$\langle \Delta, l | K_\nu P_\mu | \Delta, l \rangle. \tag{C.17}$$

This value has only positive eigenvalue in a unitary theory. In fact, suppose than there is a negative eigenvalue $\lambda < 0$ with ξ_μ the corresponding eigenvector. Then consider the state $|\psi\rangle = \xi_\mu P_\mu |l\rangle$. With $\lambda < 0$ this state has negative norm and consequently violates the unitarity of the theory:

$$\langle \psi | \psi \rangle = \xi^\dagger A \xi = \lambda \xi^\dagger \xi < 0. \tag{C.18}$$

Now, using the fact that $[K_\mu, P_\nu] \sim i(D\delta_{\mu\nu} - M_{\mu\nu})$, we obtain that the eigenvalue of A get two contribution: one is proportional to Δ, while the second will be the eigenstates of the hermitian matrix

$$B_{\nu\{s\},\{t\}\mu} = \langle \{s\} | i M_{\mu\nu} | \{t\} \rangle, \tag{C.19}$$

where $\{s\}$ and $\{t\}$ are the spin index.
The condition that $\lambda_A \geq 0$ is equivalent to:

$$\Delta \geq \lambda_{\max}(B), \tag{C.20}$$

where $\lambda_{\max}(B)$ is the maximum eigenvalue of B. It turns out (form more details see [18]) that

$$\lambda_{\max}(B) = D - 2 + l, \text{ for } l \geq 1, \tag{C.21}$$

and this prove the first of the unitarity bound 9.16.
In principle we can consider matrix element involving more Ks and Ps and get stronger bounds. This is indeed the case for $l = 0$ at level 2, where, imposing the positivity of

$$A_{\mu\nu,\,\rho\sigma} = \langle \Delta | K_\mu K_\nu P_\rho P_\sigma | \Delta \rangle, \tag{C.22}$$

we obtain $\Delta(l = 0) \geq \frac{D}{2} - 1$ which is the second of the bounds 9.16.
However, it is possible to prove that the constraints we have shown above are necessary and sufficient to have unitarity at all level. In other words higher levels than 1 are not needed for $l \geq 1$, and higher levels than 2 are not needed for $l = 0$.

References

1. S. Weinberg, Gravitation and Cosmology, 1972.
2. S. W. Hawking and G. F. R. Ellis, Cambridge University Press, Cambridge, 1973
3. D. Birmingham, Class. Quant. Grav. **16** (1999) 1197 [hep-th/9808032].
4. C. Charmousis, Anti de Sitter black holes.
5. R. B. Mann, Class. Quant. Grav. **14** (1997) L109 [gr-qc/9607071].
6. S. W. Hawking and D. N. Page, Commun. Math. Phys. **87** (1983) 577.
7. D. R. Brill, J. Louko and P. Peldan, Phys. Rev. D **56** (1997) 3600 [gr-qc/9705012].
8. L. Vanzo, Phys. Rev. D **56** (1997) 6475 [gr-qc/9705004].
9. S. Aminneborg, I. Bengtsson, S. Holst and P. Peldan, Class. Quant. Grav. **13** (1996) 2707 [gr-qc/9604005].
10. G. W. Gibbons and S. W. Hawking, Phys. Rev. D **15** (1977) 2752.
11. J. M. Maldacena, Int. J. Theor. Phys. **38** (1999) 1113 [Adv. Theor. Math. Phys. **2** (1998) 231] [hep-th/9711200].
12. L. Susskind and J. Lindesay, Hackensack, USA: World Scientific (2005) 183 p
13. J. D. Bekenstein, Phys. Rev. D **7** (1973) 2333.
14. S. W. Hawking, Nature **248** (1974) 30.
15. L. Susskind and E. Witten, hep-th/9805114.
16. G. T. Horowitz, Introduction to holographic superconductors.
17. P. Di Francesco, P. Mathieu and D. Senechal, New York, USA: Springer (1997) 890 p
18. S. Rychkov, "EPFL Lectures on Conformal Field Theory in $D \geq 3$ Dimensions,"
19. A. Bzowski, P. McFadden and K. Skenderis, arXiv:1304.7760 [hep-th].
20. A. M. Polyakov, JETP Lett. **12** (1970) 381 [Pisma Zh. Eksp. Teor. Fiz. **12** (1970) 538].
21. J. McGreevy, Adv. High Energy Phys. **2010** (2010) 723105 [arXiv:0909.0518 [hep-th]].
22. S. S. Gubser, I. R. Klebanov and A. M. Polyakov, Phys. Lett. B **428** (1998) 105 [hep-th/9802109].
23. E. Witten, Adv. Theor. Math. Phys. **2** (1998) 253 [hep-th/9802150].
24. K. Skenderis, Class. Quant. Grav. **19** (2002) 5849 [hep-th/0209067].
25. E. A. Coddington, N. Levinson, New York: McGraw-Hill (1955).
26. P. Breitenlohner and D. Z. Freedman, Annals Phys. **144** (1982) 249.
27. L. Susskind and E. Witten, hep-th/9805114.
28. D. Marolf and S. F. Ross, JHEP **0611** (2006) 085 [hep-th/0606113].
29. D. T. Son and A. O. Starinets, JHEP **0209** (2002) 042 [hep-th/0205051].
30. R. M. Wald, "Quantum field theory in curved space-time,"
31. R. M. Wald, Chicago, Usa: Univ. Pr. (1984) 491p
32. J. Zinn-Justin, hep-ph/0005272.
33. T. Matsubara, Prog. Theor. Phys. **14** (1955) 351.
34. K. Kannike, G. Htsi, L. Pizza, A. Racioppi, M. Raidal, A. Salvio and A. Strumia, arXiv:1502.01334 [astro-ph.CO].

Part III
Thermo-electric transport in AdS/CFT

Chapter 6
Preamble: linear response theory

In this preamble we want to review some standard concepts of linear response theory which will be useful in what follows. In particular we want to relate the thermoelectric transport coefficients to the correlations function of the associated conserved currents. The formulæ we will derive are commonly known under the name of Kubo formulæ.

The master formula for the whole of linear response theory comes from first-order time-dependent perturbation theory in quantum mechanics. For a system with a time-independent Hamiltonian H and a collection of operator $A_a(t,x)$ in the Heisemberg picture defined with respect to the Hamiltonian H, we imagine to add a time-dependent contribution $\delta H(t)$ to the Hamiltonian. Then the change in the expectation values for $A_a(t,x)$ are:

$$\delta\langle A_a(t,x)\rangle = -i\int_{-\infty}^{t} dt' \langle \left[A_a^t,x), \delta H(t')\right] \rangle \ , \tag{6.1}$$

to first order in δH. Usually the time-dependent part of the Hamiltonian δH is constructed by switching on an external sources $\lambda_a(t,x)$ for each operator $A_a(t,x)$, namely:

$$\delta H(t) = -\int d^d x\, A_a(t,x)\lambda_a(t,x) \ , \tag{6.2}$$

where the index a is summed. Specifically we want to switch on the perturbation adiabatically at $t \to -\infty$ and to switch it off at $t = 0$. To do this, we will consider the following form for the sources:

$$\lambda_a(t,x) = e^{\varepsilon t}\lambda_a(x)\theta(-t) \ , \tag{6.3}$$

where ε is an arbitrary small parameter. Using the expression (6.3), we can express equation (6.1) in the following way:

$$\delta\langle A_a(t,x)\rangle = i\int_{-\infty}^{t} dt' e^{\varepsilon t'}\theta(t-t')\int d^d x' \lambda_b(x')\langle\left[A_a(t,x),A_b(t',x')\right]\rangle \quad (6.4)$$

$$= i\int_{-\infty}^{0} dt' e^{\varepsilon t'}\theta(t-t')\int d^d x' \lambda_b(x')\left[A_a(t,x),A_b(t',x')\right]\rangle \quad (6.5)$$

$$= -\int_{-\infty}^{0} dt' e^{\varepsilon t'}\int d^d x' \lambda_b(x') G^R_{ab}(t-t',x-x') \ , \quad (6.6)$$

where we have used the definition of the retarded Green's function

$$G^R_{ab}(t-t',x-x') \equiv -i\theta(t-t')\langle\left[A_a(t,x),A_b(t',x')\right]\rangle \ . \quad (6.7)$$

Then, Fourier transforming along the spatial directions and Laplace transforming along the temporal direction, we obtain:

$$\delta\langle A_a(z,k)\rangle = -\lambda^0_b(k)\int\frac{d\omega}{2\pi}\frac{G^R_{ab}(\omega,k)}{(i\omega+\varepsilon)(i(\omega-z)+\varepsilon)} \ . \quad (6.8)$$

In order to evaluate the $d\omega$ integral in (6.8), we have to keep in mind that $G^R_{ab}(tk)$ is non-zero only for $t>0$, hence $G^R_{ab}(\omega k)$ is an analytic function in the upper half-plane of complex ω. Consequently we close the contour of the integration in the upper-half plane, where G^R_{ab} is analytic. There are two poles inside the contour, at $\omega = i\varepsilon$ and $\omega = z+i\varepsilon$, thus

$$\delta\langle A_a(z,k)\rangle = -\lambda^0_b(k)\frac{G^R_{ab}(z,k)-G^R_{ab}(0,k)}{iz} \ , \quad (6.9)$$

where the argument of G^R is understood to be slightly above the real axis. Then sending to zero the regulator ε and evaluating the $k\to 0$ limit, we find the well known Kubo formulæ:

$$\delta\langle A_a(z,0)\rangle = \lim_{k\to 0} -\lambda^0_b(k)\frac{G^R_{ab}(\omega,k)-G^R_{ab}(0,k)}{i\omega} \ . \quad (6.10)$$

If we are specifically interested in the response of the system to a temperature gradient $\partial_i T$ and an electric field E_i, then the change in the Hamiltonian can be written in the flowing form [1]:

$$\delta H = -\int d^d x \left(T^{0j}-\mu J^j\right)\frac{\partial_j T}{T} + J^j\frac{E_j}{T} \ , \quad (6.11)$$

where $T^{\mu\nu}$ is the stress energy tensor associated to the system, μ is the chemical potential and J^j is the charge density current. The last expression makes clear that the heat current Q^j can be expressed as $Q^j = T^{0j}-\mu J^j$.

Moreover, as we have already stressed in the previous chapters, the electric conductivity σ, the thermo-electric conductivity α and the thermal conductivity $\bar{\kappa}$ are related to the charge density and heat current in the following way:

$$\begin{pmatrix} J \\ Q \end{pmatrix} = \begin{pmatrix} \sigma & \alpha T \\ \alpha T & \bar{\kappa} T \end{pmatrix} \begin{pmatrix} E \\ -\nabla T/T \end{pmatrix} . \tag{6.12}$$

Finally, putting all together, we obtain the following expressions for the spectral transport coefficients:

$$\begin{aligned} \sigma(\omega) &= \lim_{k\to 0} \frac{G^R_{JJ}(\omega,k) - G^R_{JJ}(0,k)}{i\omega} , \\ \alpha(\omega) &= \lim_{k\to 0} \frac{G^R_{JQ}(\omega,k) - G^R_{JQ}(0,k)}{i\omega T} , \\ \bar{\kappa}(\omega) &= \lim_{k\to 0} \frac{G^R_{QQ}(\omega,k) - G^R_{QQ}(0,k)}{i\omega T} . \end{aligned} \tag{6.13}$$

Chapter 7
The simple Raissner-Nordström case

In the previous chapters we have learned that the 4-dimensional Einstein-Hilbert-Maxwell model on a Reissner-Nordström *AdS* black hole is the most simple holographic dual of a three-dimensional strongly coupled system with a non-zero charge density.

In this chapter we will review the thermo-electric transport properties of this simple model in order to prepare the ground for the introduction of momentum dissipation mechanism in holography, which will be discussed in later chapters.

7.1 Bulk solution

As explained in the previous Part, the simplest 4-dimensional gravitational model admitting asymptotically *AdS* charged black hole solutions, namely an Einstein-Hilbert-Maxwell theory, corresponds to the action

$$S_{\rm RN} = \int d^4x\sqrt{-g}\left[\frac{1}{2\kappa_4^2}\left(R-\frac{\Lambda}{L^2}\right)-\frac{1}{4q^2}F_{\mu\nu}F^{\mu\nu}\right]+\frac{1}{2\kappa_4^2}\int_{z=z_{UV}} d^3x\,\sqrt{-g_b}\,2K\,, \tag{7.1}$$

where we have already included the Gibbons-Hawking boundary term, which is expressed in terms of the induced metric $(g_b)_{\mu\nu}$ and the extrinsic curvature K on the surface at $z = z_{UV}$. Actually z_{UV} represents a UV cut-off that will be sent to zero in the final step of the holographic renormalization procedure. As it is well known (see for example [31]) the Gibbons-Hawking term is necessary in order to have a well-defined bulk variational problem. In the action (7.1) $\Lambda = -6$ is the dimensionless cosmological constant measured in units of the AdS_4 radius L; κ_4 and q are respectively the gravitational and Maxwell coupling constants and their dimension is $[\kappa_4] = 1$ and $[q] = 0$.

From the action (7.1) we get the Einstein and Maxwell equations

$$\begin{aligned} &R_{\mu\nu} - \frac{g_{\mu\nu}}{2}\left(R - \frac{\Lambda}{L^2}\right) = \gamma^2\left(F_{\mu\rho}F_{\nu}^{\ \rho} - \frac{g_{\mu\nu}}{4}F_{\rho\sigma}F^{\rho\sigma}\right) , \\ &\partial_\mu\left(\sqrt{-g}F^{\mu\nu}\right) = 0 , \end{aligned} \tag{7.2}$$

where we have introduced the ratio of the gravitational and Maxwell couplings, namely $\gamma \equiv \frac{\kappa_4}{q}$. Being the equations of motion (7.2) insensitive to an overall rescaling of the action (7.1), they depend only on γ and not on the individual couplings. It is worth noticing that for the simple model at hand γ could be rescaled away by means of a field redefinition[1].

As already derived, the model admits the following black-brane solution:

$$ds^2 = \frac{L^2}{z^2}\left[-f(z)dt^2 + dx^2 + dy^2 + \frac{1}{f(z)}dz^2\right] , \qquad A = \phi(z)dt , \tag{7.3}$$

$$f(z) = 1 - \left(1 + \frac{z_h^2\gamma^2\mu^2}{2L^2}\right)\left(\frac{z}{z_h}\right)^3 + \frac{z_h^2\gamma^2\mu^2}{2L^2}\left(\frac{z}{z_h}\right)^4 , \tag{7.4}$$

$$\phi(z) = \mu - q^2\rho z = \mu\left(1 - \frac{z}{z_h}\right) . \tag{7.5}$$

where z is the radial coordinate running from z_{UV} at the UV radial shell to z_h at the black hole horizon. Of course, in the limit of vanishing cut-off, the radial UV shell is identified with the conformal boundary of the asymptotic AdS geometry.

We recall that the coefficients of the leading and subleading near-boundary terms of the bulk gauge vector are respectively mapped to the dual chemical potential μ and charge density $\rho \equiv \mu/(q^2 z_h)$ of the corresponding global current in the boundary theory. Eventually, the black hole temperature (which coincides with that of the boundary theory) and the other thermodynamical quantities, such as the energy density $\mathscr{E}$, the entropy density $\mathscr{S}$ and the pressure P, can be derived in the standard holographic way (see Chapter 5.6.2). Finally, one obtains

$$\begin{aligned} &T = -\frac{1}{4\pi}f'(z)\Big|_{z=z_h} = -\frac{\gamma^2\mu^2 z_h}{8\pi L^2} + \frac{3}{4\pi z_h} , \\ &\mathscr{E} = 2P = \frac{L^2}{z_h^3\kappa_4^2}\left(1 + \frac{z_h^2\mu^2\gamma^2}{2L^2}\right) \qquad \mathscr{S} = \frac{2\pi L^2}{\kappa_4^2 z_h^2} . \end{aligned} \tag{7.6}$$

To get some physical insight we note that for $T = 0$ the black hole has a non-zero horizon radius $z_h^* = \sqrt{6}\frac{L}{\gamma\mu}$. Consequently the horizon area is non-zero and the system has non-vanishing ground state energy. Regarding the temperature dependence of the entropy density, at low T we have

$$\mathscr{S} \simeq const + BT \qquad for\ T \ll \mu , \tag{7.7}$$

where B is a constant. This implies that the specific heat $C_v = T\partial\mathscr{S}/\partial T$ is linear in temperature. In the opposite regime ($T \gg \mu$) the system approaches the simple

[1] Nevertheless this is not a general feature (e.g. it is not true for the holographic superconductor) and we prefer to keep γ explicit.

Shwarzshild conformal configuration, and the specific heat goes like T^2 as expected for a three-dimensional CFT at finite temperature.

To conclude this section it is relevant to pinpoint an interesting properties of the near horizon geometry of the Reissner-Nordström black brane. We have learned in the previous Part that the radial coordinates encodes the renormalization group flow of the dual field theory. Consequently studying the near horizon properties of the black branes is equivalent to analyse the IR features of the dual field theory. To do this, we set $T = 0$ and we expand the metric (7.3) near the horizon z_h^*, obtaining:

$$ds^2 = \frac{L}{\zeta^2}\left(-dt^2 + d\zeta^2\right) + \frac{L^2}{z_h^{*\,2}}\left(dx^2 + dy^2\right) \,, \tag{7.8}$$

where we have defined the radial quantity ζ in the following way:

$$\zeta = \frac{\sqrt{6}}{z_h^*}\left(1 - \frac{z}{z_h^*}\right) \,. \tag{7.9}$$

We started out this story with the "central dogma" of holography, that the isometries in the bulk code for the global space-time and scaling symmetries in the boundary field theory. We therefore just have to inspect the scaling isometry of the metric (7.8):

$$t \to \lambda t \,, \qquad \zeta \to \lambda \zeta, \qquad x \to x \,, \tag{7.10}$$

Comparing this with the scaling isometry of the pure AdS_{d+1} geometry (z is the radial direction),

$$t \to \lambda t \,, \qquad \zeta \to \lambda \zeta, \qquad x \to \lambda x \,, \tag{7.11}$$

we directly infer that we are dealing with a (quasi) local quantum critical state in the boundary field theory: in spatial directions there is no sense of scale invariance, while the dynamics of the fields is scale invariant merely in temporal regards! Such an emergence scale invariance seems to be ubiquitous in the strange metals, according to a variety of experimental properties in various laboratory systems. It is just fascinating that the most primitive gravitational set up for a finite density system (the Reinssner-Nordström black hole) gives rise to this very peculiar behaviour. Both the zero temperature entropy and this local quantum criticality are phenomena which are alien in any known bosonic field theory.

7.2 Fluctuations

Having analysed the basic physical properties of the background solutions, we want now to compute the relevant correlators for computing the thermo-electric transport coefficients. As it is evident from (6.13), in order to evaluate the spectral thermo-electric transport coefficient we need to compute the retarded Green's functions both at zero momentum $G^R(\omega, 0)$ and at zero frequency $G^R(0, k)$. In this section we will

derive in detail $G^R(\omega,0)$ and we will analyse in the following section in which case the counter-terms $G^R(0,k)$ are relevant in defining the transport coefficients.

We consider vector fluctuations on the homogeneous and isotropic background specified by (7.3), (7.4) and (7.5). Without spoiling the generality of the treatment, the fluctuating fields that we study are the gauge field fluctuations along the x spatial direction, namely a_x, and the vector mode of the metric, h_{tx}; these are the relevant fluctuations in order to analyse the thermo-electric transport (see below). We further assume harmonic temporal dependence and isotropic spatial dependence (null momentum) for the fluctuations.

The fluctuation dynamics is governed by the Einstein and Maxwell equations (7.2) which assume the following explicit form

$$a_x'' + \tfrac{f'}{f} a_x' + \tfrac{\omega^2}{f^2} a_x = -\tfrac{z^2\phi'}{fL^2}\left(h_{tx}' + \tfrac{2}{z} h_{tx}\right) , \tag{7.12}$$

$$h_{tx}' + \tfrac{2}{z} h_{tx} + 2\gamma^2 \phi' a_x = 0 , \tag{7.13}$$

where all the fields are functions of the z variable alone and the primes denote derivatives with respect to z. Despite the dynamics for the fluctuations a_x and h_{tx} is coupled, combining (7.12) and (7.13) we obtain an equation where only a_x and derivatives thereof appear,

$$a_x''(z) + \frac{f'(z)}{f(z)} a_x'(z) + \left[\frac{\omega^2}{f(z)^2} - 2\gamma^2 \, \frac{z^2\phi'(z)^2}{f(z)L^2}\right] a_x(z) = 0 . \tag{7.14}$$

To actually solve the differential problem governing the fluctuation dynamics, we need to specify appropriate boundary conditions at the horizon; we consider in-falling boundary conditions which are those needed to compute retarded correlators of the dual theory [2]. From (7.14) we have that the gauge field fluctuations can be analysed and solved without considering the metric fluctuations which are later determined by means of (7.13) upon substituting the solution for a_x. Therefore we have to impose the in-falling boundary conditions at the horizon on the gauge field alone,

$$a_x^{(\mathrm{IR})} = (z_h - z)^{-\frac{i\omega}{4\pi T}} \left(b_0 + \mathscr{O}(z_h - z)\right) . \tag{7.15}$$

Since the equation (7.14) is homogeneous, we can rescale the parameter b_0 to 1, as a consequence a_x and h_{tx} are completely determined in terms of the frequency ω and the background quantities.

7.2.1 Renormalization of the fluctuation action

In order to compute the correlators to be plugged into the Kubo formulæ for the transport coefficients, we need to consider the on-shell bulk action expanded at the second order in the fluctuations. The gauge/gravity prescription identifies the boundary value of the bulk fluctuation fields with the dual sources. The correlators of inter-

est are then obtained taking appropriate functional derivatives of the on-shell action with respect to these sources. This entire procedure represents the gauge/gravity version of the standard field theory paradigm to derive correlation functions.

In general the bulk on-shell action for the fluctuating field is divergent and needs to be properly renormalized. As explained in the previous Part, the holographic renormalization procedure consists in considering a regularized action to be integrated up to a near-boundary radial cut-off; then, appropriate boundary counter-terms are considered and eventually the limit of zero cut-off defines the renormalized action. The boundary counter-terms make the on-shell action finite once the UV cut-off goes to zero. They must respect the symmetries of the boundary theory and provide a well-defined bulk variational problem. As mentioned before, in (7.1) we have already added the Gibbons-Hawking boundary terms to the bulk action; this provides a well-defined bulk variational problem for the fields. Then (see for instance [3]) the only well-behaved boundary term needed in order to render the on-shell action finite is

$$S_{\text{c.t.}} = \frac{1}{2\kappa_4^2} \int_{z=z_{UV}} d^3x \, \sqrt{-g_b} \, \frac{4}{L} \, . \tag{7.16}$$

Eventually, the limit of vanishing cut-off is considered and (as we are interested in the linear response or, said otherwise, to two-point correlators) only the quadratic part of the action in the fluctuating field is retained. The renormalized quadratic action is defined as

$$S^{(2)}_{\text{ren}} = \lim_{z_{UV}\to 0} S_{\text{RN}} + S_{\text{c.t.}} \Big|_{\mathscr{O}(a_x, h_{tx})^2} \, . \tag{7.17}$$

Once we have obtained a finite on-shell action, it is perfectly legitimate to ask ourselves whether finite counter-terms could also be added. Such finite counter-terms would lead to ambiguities in the definition of the renormalized action. We state once more that the counter-terms have to respect all the symmetries of the boundary theory[2], the power counting and the definition of the bulk variational problem. This latter characteristic amounts to avoid introducing boundary terms containing radial derivatives. The former symmetry requirements impede us to consider terms as $a_i a^i$ which would brake the boundary gauge symmetry. The power-counting criterion instead forbids us to consider $F_{ij}F^{ij}$ which is allowed by the symmetries but would force us to introduce new dimensionful parameters. We further notice that a Chern-Simons term is always trivial on our background solutions as a consequence of spatial rotational invariance. Such arguments exhaust all the possibilities as far as the gauge field is concerned. Turning our attention to the metric, we are allowed to consider two kinds of terms: a boundary cosmological constant

[2] As a general feature, the correlators satisfy Ward identities related to the symmetries of the model. In a generating functional framework, such identities (as the correlators themselves) are obtained by appropriate functional derivatives of the generating functional itself and of the expectation values of the various quantities in the theory. Counter-terms (either finite or not) in the QFT action which respect the symmetries of the original theory affect both the Ward identities and the correlators in a consistent way.

and a term proportional to the boundary Ricci scalar. The first actually appeared in (7.16); the latter is null as the manifold transverse to the radial coordinate z is flat Minkowski space-time upon which we are considering homogeneous configurations in the space coordinates (i.e. null momentum).

From an asymptotic study of the equations of motion we have that the boundary expansions of the fields a_x and h_{tx} are

$$a_x(z) = a_x^{(0)} + a_x^{(1)} \frac{z}{L} + \dots , \qquad h_{tx}(z) = \frac{L^2}{z^2} h_{tx}^{(0)} + h_{tx}^{(1)} \frac{z}{L} + \dots , \tag{7.18}$$

and consequently the renormalized quadratic on-shell action for the model at hand is given by

$$\begin{aligned} S_{\text{ren}}^{(2)} = \int d^3x \Big[& \frac{1}{2q^2 L} a_x^{(0)}(-\omega) a_x^{(1)}(\omega) \\ & - \frac{1}{2\kappa_4^2} \frac{3}{L} h_{tx}^{(0)}(-\omega) h_{tx}^{(1)}(\omega) - \frac{\mathscr{E}}{4} h_{tx}^{(0)}(-\omega) h_{tx}^{(0)}(\omega) \Big] + (\omega \leftrightarrow -\omega) , \end{aligned} \tag{7.19}$$

where we have Fourier transformed with respect to the time coordinate.

7.3 Correlators and transport coefficients

We are now ready to compute the relevant correlators to define the thermo-electric transport coefficients. As it is evident from (6.13) we need to identify the sources for the charge density current J and for the heat density current Q. As explained in the previous Part, the sources for J is simply the leading term of the gauge field at the boundary, namely $a_x^{(0)}$. Regarding the heat current, it is a composite operator involving the tx-component of stress energy tensor T^{tx}. Since we know that the sources for the stress energy tensor are encoded in the leading terms of the metric fluctuations $h_{\mu\nu}^{(0)}$, we obtain:

$$J_Q = h_{tx}^{(0)} - \mu a_x^{(0)} . \tag{7.20}$$

From (7.20) we have the following relations among the corresponding functional derivatives

$$\frac{\delta}{\delta J_x} = \frac{\delta}{\delta a_x^{(0)}} , \tag{7.21}$$

$$\frac{\delta}{\delta J_Q} = \frac{\delta}{\delta h_{tx}^{(0)}} - \mu \frac{\delta}{\delta a_x^{(0)}} , \tag{7.22}$$

where the partial derivatives with respect to the sources $a_x^{(0)}$ and $h_{tx}^{(0)}$ are to be taken keeping to zero the source upon which one does not differentiate. We underline that

the sources $a_x^{(0)}$ and $h_{tx}^{(0)}$ are, in principle, independent quantities. Stated this, in order to compute the explicit expressions of correlators in terms of the background quantities and the near-boundary fluctuations, we start taking double functional derivatives of the on-shell renormalized and quadratic action (7.19). Namely,

$$\frac{\delta^2 S}{(\delta J_x)^2} = \frac{1}{q^2 L}\frac{\delta a_x^{(1)}}{\delta a_x^{(0)}} , \tag{7.23}$$

$$\frac{\delta^2 S}{\delta J_Q \delta J_x} = \frac{\delta^2 S}{\delta J_x \delta J_Q} = -\frac{3}{2L\kappa_4^2}\frac{\delta h_{tx}^{(1)}}{\delta a_x^{(0)}} - \mu\frac{1}{q^2 L}\frac{\delta a_x^{(1)}}{\delta a_x^{(0)}} , \tag{7.24}$$

and

$$\frac{\delta^2 S}{(\delta J_Q)^2} = -\frac{3}{\kappa_4^2 L}\frac{\delta h_{tx}^{(1)}}{\delta h_{tx}^{(0)}} - \mathscr{E} - \frac{\mu}{q^2 L}\frac{\delta a_x^{(1)}}{\delta h_{tx}^{(0)}} + \frac{3\mu}{\kappa_4^2 L}\frac{\delta h_{tx}^{(1)}}{\delta a_x^{(0)}} + \frac{\mu^2}{q^2 L}\frac{\delta a_x^{(1)}}{\delta a_x^{(0)}} . \tag{7.25}$$

To proceed, we observe that the equation for the fluctuations of the gauge field is independent of h_{tx} and that, because of equation (7.13), $h_{tx}^{(1)}$ is completely determined in terms of $a_x^{(0)}$ and the parameters of the background,

$$h_{tx}^{(1)} = \frac{2}{3}\gamma^2 q^2 \rho L a_x^{(0)} ; \tag{7.26}$$

hence we have

$$\frac{\delta a_x^{(1)}}{\delta h_{tx}^{(0)}} = \frac{\delta h_{tx}^{(1)}}{\delta h_{tx}^{(0)}} = 0 \qquad \text{and} \qquad \frac{\delta h_{tx}^{(1)}}{\delta a_x^{(0)}} = \frac{2}{3}\gamma^2 q^2 \rho L . \tag{7.27}$$

Eventually, the correlators assumes the following form:

$$G^R_{J_x J_x}(\omega,0) = \frac{1}{q^2 L}\frac{\delta a_x^{(1)}}{\delta a_x^{(0)}} , \qquad \frac{1}{T}G^R_{J_x J_Q}(\omega,0) = -\frac{1}{T}\rho - \frac{\mu}{T}G^R_{J_x J_x}(\omega,0) , \tag{7.28}$$

and

$$\frac{1}{T}G^R_{J_Q J_Q}(\omega,0) = \frac{1}{T}\left(-\mathscr{E} + 2\mu\rho\right) + \frac{\mu^2}{T}G^R_{J_x J_x}(\omega,0) . \tag{7.29}$$

In order to evaluate the Kubo formlæ(6.13) we need also to compute the retarded green's functions at non-vanishing momentum, namely $G^R(0,k)$. In principle this can be done exactly in the same way as explained in the zero momentum case, switching on the momentum and setting to zero the frequency ω. Actually, with an analytical computation illustrated in [4], one can prove that:

$$\begin{aligned} G^R_{J_x J_x}(0,k) &= \mathscr{O}(k^2) , \\ G^R_{J_x J_Q}(0,k) &= \mathscr{O}(k^2) , \\ G^R_{J_Q J_Q}(0,k) &= -P + \mathscr{O}(k^2) , \end{aligned} \tag{7.30}$$

where P is the pressure, defined in (7.6). Consequently, in the zero momentum limit only $G^R_{J_Q J_Q}(0,k)$ contributes to the transport coefficient with a non-trivial counterterm.

Finally, using (6.13), the thermo-electric transport coefficients assume the following form:

$$\begin{aligned}\sigma(\omega) &= -\frac{i}{q^2 L\omega}\frac{\delta a_x^{(1)}}{\delta a_x^{(0)}}\,,\\ \alpha &= \frac{i}{T\omega}\rho - \frac{\mu}{T}\sigma(\omega)\,,\\ \bar{\kappa}(\omega) &= \frac{i}{\omega T}(\mathscr{E}+P-2\mu\rho)+\frac{\mu^2}{T}\sigma(\omega)\end{aligned} \tag{7.31}$$

7.4 Physical properties of transport coefficients

To conclude this chapter we want to analyse some physical properties of the transport coefficients previously derived. As it is evident from (7.31), the spectral behaviour of the transport coefficients is completely determined once the thermodynamical quantities and the electric conductivity $\sigma(\omega)$ is known. The real and imaginary part of $\sigma(\omega)$ are plotted in Figure 7.1 for different values of the ratio T/μ. As one can see from the Figure, the imaginary part of the electric conductivity has a pole in $\omega = 0$. Using the Kramers-Kronig relations,

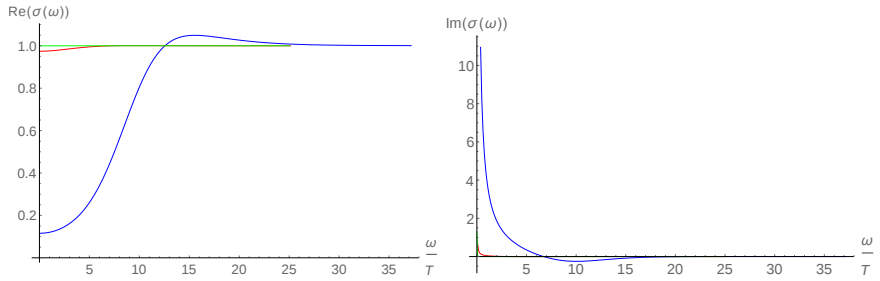

Fig. 7.1 Real (left) and imaginary (right) part of the electric conductivity $\sigma(\omega)$ for different values of the ratio T/μ, ($T/\mu = 0.1$ (blue), $T/\mu = 1$ (green) and $T/\mu = 10$ (red).

$$\Re\sigma(\omega) = \frac{1}{\pi}\mathscr{P}\int_{-\infty}^{\infty}\frac{\Im\sigma(\omega')}{\omega'-\omega}d\omega'\,,\qquad \Im\sigma(\omega) = -\frac{1}{\pi}\mathscr{P}\int_{-\infty}^{\infty}\frac{\Re\sigma(\omega')}{\omega'-\omega}d\omega'\,, \tag{7.32}$$

this pole is related to the existence of a delta function in the real part of the conductivity. This is perfectly consistent with hydrodynamics [2], since the conservation of momentum implies that the DC conductivity diverges. Actually, an analytical

computation performed in [4] shows that the residue of $\sigma(\omega)$ at $\omega = 0$ behaves as follows:

$$\Re\sigma(\omega) = \frac{\rho}{\mathscr{E}+P}\delta(\omega) + \dots \,. \tag{7.33}$$

The previous expression is consistent with the numerical computation shown in Figure 7.1, where once the ration T/μ is lowered (or equivalently the chemical potential μ is increased), a depletions zone develops near $\omega = 0$. Using the relations (7.32) it is evident that the spectral weight is transferred in the pole at $\omega = 0$ (7.33), since the charge density ρ is proportional to the chemical potential μ. At high frequency $\omega \gg \mu$ the conductivity approaches a constant values $1/q^2$ consistent with the conformal prediction.

In the neutral case ($\mu = 0$) the delta function int he electric conductivity disappear. In this case explicit form of $\sigma(\omega)$ can be computed exactly [5], leading to

$$\tilde{\sigma}(\omega) = \frac{1}{q^2} \,. \tag{7.34}$$

Then in the purely conformal case the electric conductivity is constant both in temperature and in frequency as it should. Regarding the other transport coefficients, the thermo-electric conductivity α vanishes as it is the case for a neutral plasma, while the thermal conductivity is a pure delta functions whose residue is proportional to the entropy, namely:

$$\tilde{\bar{\kappa}} = \mathscr{S}\delta(\omega) \,. \tag{7.35}$$

Chapter 8
Momentum dissipation in holography

8.1 Adding a mass to the graviton to break momentum conservation

In this Section, after discussing the basic properties of the massive gravity model which we consider, we will explain how to compute the thermo-electric transport coefficients for this system.

8.1.0.1 The massive gravity model

The idea underlying the application of massive gravity in holography consists in breaking the diffeomorphism invariance in the bulk by introducing a mass term for the graviton in such a way that one has momentum dissipation in the boundary dual field theory. Actually, several ways to give a mass to the graviton had been studied, but, following [6], we work here with the formulation of the massive gravity presented for the first time in [7]. The action of the model is:

$$\begin{aligned} S = \int d^4x\,\sqrt{-g}\left[\frac{1}{2\kappa_4^2}\left(R+\frac{6}{L^2}+\beta\left([\mathscr{K}]^2-[\mathscr{K}^2]\right)\right)-\frac{1}{4q^2}F_{\mu\nu}F^{\mu\nu}\right] \\ +\frac{1}{2\kappa_4^2}\int_{z=z_{UV}} d^3x\,\sqrt{-g_b}\,2K\,, \end{aligned} \tag{8.1}$$

where β is an arbitrary parameter having the dimension of a mass squared and the small square brackets denote a trace operation. Notice that the action (8.1) contains already the Gibbons-Hawking term necessary to have a well-defined bulk variational problem. The matrix $(\mathscr{K}^2)^{\mu}_{\ \nu}$ is defined in terms of the dynamical metric $g_{\mu\nu}$ and a fiducial fixed metric $f_{\mu\nu}$ in the following way[1]

[1] Within this formulation of massive gravity, it is possible to consider also a linear term in the trace of $\mathscr{K}$; namely an $\alpha[\mathscr{K}]$ term in the Lagrangian density where α is a numerical coefficient. However in this paper we always consider the case $\alpha = 0$. The reason for doing so is twofold: first

$$(\mathscr{K}^2)^\mu_{\ \nu} \equiv g^{\mu\rho} f_{\rho\nu} \ , \qquad \mathscr{K} \equiv \left(\sqrt{\mathscr{K}^2}\right)^\mu_{\ \nu} . \tag{8.2}$$

Along the lines of [6], we consider the following form for $f_{\mu\nu}$:

$$f_{\mu\nu} = \text{diag}(0,0,1,1) \ . \tag{8.3}$$

Considering this particular form for the fiducial metric means that the action is still invariant under diffeomorphism in the (z,t) plane, but not in the (x,y) plane. At the dual level this implies that the theory has conserved energy but no conserved momentum.

8.1.0.2 Background and thermodynamic

The equations of motion descending from the action (8.1) are:

$$\begin{aligned} &R_{\mu\nu} - \frac{R}{2} g_{\mu\nu} + \frac{\Lambda}{2L^2} g_{\mu\nu} + X_{\mu\nu} = \gamma^2 T_{\mu\nu} \ , \\ &\partial_\mu \left(\sqrt{-g} F^{\mu\nu}\right) = 0 \ , \end{aligned} \tag{8.4}$$

where $\gamma \equiv \frac{\kappa_4}{q}$ and

$$\begin{aligned} T_{\mu\nu} &= F_{\mu\rho} F_\nu^{\ \rho} - \frac{g_{\mu\nu}}{4} F_{\rho\sigma} F^{\rho\sigma} \ , \\ X_{\mu\nu} &= -\beta \left(\mathscr{K}^2_{\mu\nu} - [\mathscr{K}] \mathscr{K}_{\mu\nu} + \frac{g_{\mu\nu}}{2} \left([\mathscr{K}]^2 - [\mathscr{K}^2] \right) \right) \ . \end{aligned} \tag{8.5}$$

We want to study the system in the presence of a chemical potential, we then consider the same background ansatz as in (7.3). In the massive case the black-brane solution is:

$$\begin{aligned} \phi(z) &= \mu - q^2 \rho z = \mu \left(1 - \frac{z}{z_h}\right) \ , \qquad \rho \equiv \frac{\mu}{q^2 z_h} \ , \\ f(z) &= \frac{\gamma^2 \mu^2 z^4}{2L^2 z_h^2} - \frac{\gamma^2 \mu^2 z^3}{2L^2 z_h} - \frac{z^3}{z_h^3} - \frac{\beta z^3}{z_h} + \beta z^2 + 1 \ . \end{aligned} \tag{8.6}$$

In the limit $\beta \to 0$ the emblackening factor $f(z)$ reduces to that corresponding to the standard Reissner-Nordström solution. The black hole temperature is computed in the usual way leading to

$$T = -\frac{f'(z_h)}{4\pi} = -\frac{\gamma^2 \mu^2 z_h}{8\pi L^2} + \frac{\beta z_h}{4\pi} + \frac{3}{4\pi z_h} \ . \tag{8.7}$$

---

a rigorous proof of the absence of ghosts in the model exists only in this $\alpha = 0$ case [6]; secondly, as noted in [8], with $\alpha \neq 0$ logarithmic terms appear in the near-boundary expansion of the bulk fields. The latter fact introduces non-standard divergences in the on-shell $2+1$-dimensional action.

The full set of thermodynamical quantities were derived in [12]. For the sake of later need, we report here the explicit expressions for the entropy density $\mathscr{S}$, the energy density $\mathscr{E}$ and the pressure P,

$$\mathscr{S} = \frac{2\pi}{\kappa_4^2}\frac{L^2}{z_h^2}\,, \quad \mathscr{E} = \frac{L^2}{z_h^3\kappa_4^2} + \frac{L^2\beta}{z_h\kappa_4^2} + \frac{\mu^2}{2q^2 z_h}\,, \quad P = \frac{L^2}{2\kappa_4^2 z_h^3} - \frac{\beta L^2}{2\kappa_4^2 z_h} + \frac{\mu^2}{4q^2 z_h}\,. \tag{8.8}$$

Notice that the dual theory of a massive gravity has in general $\mathscr{E} \neq 2P$. The equation of state $\mathscr{E} = 2P$ is expected for a $2+1$ dimensional conformal theory but, as it happens with the conservation laws of the stress-energy tensor, the massive gravity set-up introduces modifications that are proportional to the mass parameter β.

Scales and scalings

As we have just noted observing the thermodynamic quantities, the massive parameter β introduces a new scale in the model. This new scale affects the scaling symmetries of the bulk fields. In fact, if we rescale the radial coordinate z as $z \to az$, we find that the other quantities of the model must scale as

$$(t,x,y) \to a(t,x,y)\,, \qquad \beta \to \frac{\beta}{a^2}\,, \qquad \mu \to \frac{\mu}{a}\,, \qquad z_h \to a z_h \tag{8.9}$$

in order for this scaling to be a symmetry of the action. In particular, if we consider the scale invariant temperature $\tilde{T} \equiv T/\mu$ we find from (8.7) that this is a function of the scale invariant quantities β/μ^2 and μz_h:

$$\tilde{T} \equiv \frac{T}{\mu} = F\left(\frac{\beta}{\mu^2}, z_h\mu\right)\,. \tag{8.10}$$

Moving the temperature while keeping fixed both the chemical potential μ and the mass parameter β (which, as we will see, is related to the momentum dissipation rate in the dual field theory) corresponds to varying the horizon radius z_h.

Finally, we note that, as in the massless case, the constant γ can be rescaled away from the action (8.1) by means of a redefinition of the gauge field. In fact the system is invariant under the scaling

$$\gamma \to a\gamma\,, \qquad \mu \to \mu/a\,, \tag{8.11}$$

namely the same scaling symmetry found in the Reissner-Nordström AdS black hole. This scaling affects in particular the transport coefficients and consequently to compute the transport coefficients at different values of γ is equivalent to compute the same quantities at the corresponding rescaled values of the chemical potential.

8.1.1 Massive gravity and momentum dissipation

In the previous Section we have analysed the basic properties of the background black-brane solution in the presence of a mass term for the graviton. We need now to understand how a mass potential for the graviton is related to momentum dissipation in the dual strongly coupled field theory.

The basic idea illustrated in [6] is that the massive gravity potential breaks the diffeomorphism invariance in the bulk. Since we have learned in the previous part that diffeomorphism invariance in the bulk is related to the conservation of the stress-energy tensor in the dual field theory, a gravitational theory with a mass potential would correspond to a dual theory where

$$\partial_\mu T^{\mu\nu} \neq 0 \,. \tag{8.12}$$

Specifically, since considering the fiducial metric (8.3) corresponds to breaks the diffeomorphism invariance along the x and y directions one would expect that the model we are considering corresponds to a theory in which momentum is not conserved in some way.

A more precise statement was provided in [8] where, by analysing the poles of the correlation functions in the hydrodynamic limit (namely at sufficiently low momentum dissipation rate τ^{-1}, where momentum is an almost conserved quantity), it was discussed that massive gravity is the dual gravitational realization of a system in which the conservation law for the stress-energy tensor is modified as follows:

$$\partial_t T^{tt} = 0, \qquad \partial_t T^{ti} = -\tau^{-1} T^{ti} \,, \tag{8.13}$$

where τ^{-1} is the momentum dissipation rate. At order $\mathscr{O}(\beta)$ the scattering rate is expressed in terms of the thermodyanamical quantities (7.6) and of the graviton mass β in the following way [2]:

$$\tau^{-1} = -\frac{\mathscr{S}\beta}{2\pi(\mathscr{E}+P)} \,. \tag{8.14}$$

A further evidence of the analogy between massive gravity and momentum dissipation was provided in [10], where it was proven that the holographic lattices [11] gives an effective mass term for the graviton.

As a final comment it is important to note that the explicit form of the scattering rate (8.14) constrains the possible values of the mass parameter β. In particular, since τ^{-1} has to be positive, β must assume negative values. Th situation is more involved once one considers non linear massive potential, as discussed in [13].

Eventually, we have argued that the massive gravity model which we have analysed in the previous sections provides an interesting effective gravitational theory useful to study the effects of momentum dissipation in an holographic strongly cou-

[2] For a more precise definition of the momentum dissipation rate see [29].

pled dual field theory. In the next sections we will focus on the thermo-electric transport properties of the system.

8.1.2 Fluctuations and transport in the massive case

We are now ready to compute the correlators and consequently to define the thermo-electric transport coefficient analogously to what has been done for the massless case in the previous chapter. Firstly we will focus our attention to the retarded Green's function at zero momentum $G^R(\omega,0)$. As noted before, in order to properly define the transport coefficients we need to compute also the correlation function in the opposite limit, namely $G^R(0,k)$. We will comment at the end of the section about the importance of these counter-terms in the definition of the transport coefficients.

8.1.2.1 Linearised equations and asymptotic expansions

In order to obtain the correlation functions $G^R(\omega,0)$, we need to expand the action (8.1) at the second order in the fluctuation fields analogously to what has been don in the massless case. However, as opposed to the massless case, here the equations for h_{tx} and h_{zx} are independent and then we have to turn on both the fluctuations to be consistent. Hence we consider the following set of fluctuations

$$\begin{aligned} &A \to A + e^{-i\omega t}\, a_x(z)\, dt \ , \\ &ds^2 \to ds^2 + 2e^{-i\omega t}\, h_{zx}(z)\, dz\, dx + 2e^{-i\omega t}\, h_{tx}(z)\, dt\, dx \ . \end{aligned} \tag{8.15}$$

Expanding the equations of motion (8.4) to the linear order in the fluctuations (8.15) we obtain:

$$\begin{aligned} &h'_{tx} + \frac{2}{z} h_{tx} + i\omega h_{zx} + 2\gamma^2 \phi' a_x + 2\beta \, \frac{if}{\omega} h_{zx} = 0 \ , \\ &\frac{d}{dz}\left[h'_{tx} + i\omega h_{zx} + \frac{2}{z} h_{tx} + 2\gamma^2 \phi' a_x \right] + 2\beta \, \frac{h_{tx}}{f} = 0 \ , \\ &\frac{d}{dz}\left(f a'_x \right) + \frac{\omega^2}{f} a_x + \frac{\phi' z^2}{L^2} \left(h'_{tx} + \frac{2}{z} h_{tx} + i\omega h_{zx} \right) = 0 \ . \end{aligned} \tag{8.16}$$

There are no derivatives of h_{zx} in the first equation of motion which therefore can be algebraically solved to obtain h_{zx}. We then substitute the solution inside the second equation. Finally we are left with two coupled equations for a_x and h_{tx}:

$$\begin{aligned} &\frac{d}{dz}\left[f a'_x \right] + \frac{2\phi' z}{L^2} \, \frac{-\gamma^2 \phi' \omega^2 z a_x + \beta f \left(z h'_{tx} + 2 h_{tx} \right)}{2\beta f + \omega^2} + \frac{\omega^2}{f} a_x = 0 \ , \\ &\frac{d}{dz}\left[\frac{f}{z} \, \frac{2\gamma^2 \phi' z a_x + z h'_{tx} + 2 h_{tx}}{2\beta f + \omega^2} \right] + \frac{1}{f} h_{tx} = 0 \ . \end{aligned} \tag{8.17}$$

In the $\beta \to 0$ limit the first equation in (8.17) reduces to (7.14) obtained in standard massless gravity. This, however, cannot be simply interpreted as the fact that the fluctuation dynamics in the limit $\beta \to 0$ coincides with that arising in the massless gravity on the Reissner-Nordström black hole. Indeed, the second equation in (8.17) shows that the limits $\beta \to 0$ and $\omega \to 0$ do not commute. Since we are interested in computing DC observables we always consider the $\omega \to 0$ first.

IR expansion

As usual, in order to compute the retarded correlators, we have to numerically solve the equations (8.17) imposing the in-going wave boundary conditions at the horizon $z = z_h$, namely

$$\begin{aligned} h_{tx}^{(\mathrm{IR})} &= (z_h - z)^{-\frac{i\omega}{4\pi T}} (a_0 + \mathscr{O}(z_h - z)), \\ a_x^{(\mathrm{IR})} &= (z_h - z)^{-\frac{i\omega}{4\pi T}} (b_0 + \mathscr{O}(z_h - z)). \end{aligned} \tag{8.18}$$

It is important to note that, unlike the case of fluctuations on pure Reissner-Nordström black hole, it is impossible to combine the two equations (8.17) in a unique equation for a_x. The dynamics of electric and thermal fluctuations is consequently more intimately mixed. From the bulk standpoint, it is possible to rescale to 1 only one of the two coefficients a_0 and b_0. Said otherwise, the physics of the model is sensitive to the ratio $\eta = a_0/b_0$. In the computations aimed at getting the transport coefficients, in order to isolate the purely electric response of the system, we have to tune the coefficient η so that the thermal source vanishes. Symmetrically, to compute the pure thermal contribution, we must fix η so that the electric field source is zero.

UV expansion

Near the boundary $z = 0$ the expansion of the fluctuations in powers of z is:

$$\begin{aligned} h_{tx}^{\mathrm{UV}}(\omega, z) &= \frac{L^2}{z^2} \left[h_{tx}^{(0)}(\omega) + \frac{1}{2}(2\beta + \omega^2) \frac{z^2}{L^2} h_{tx}^{(0)}(\omega) + \frac{z^3}{L^3} h_{tx}^{(1)}(\omega) + \mathscr{O}\left(\frac{z^4}{L^4}\right) \right] , \\ a_x^{\mathrm{UV}}(\omega, z) &= a_x^{(0)}(\omega) + \frac{z}{L} a_x^{(1)}(\omega) + \mathscr{O}\left(\frac{z^2}{L^2}\right) . \end{aligned} \tag{8.19}$$

The coefficients of the higher orders in the z expansions can be determined in terms of the background parameters and the integration constants $h_{tx}^{(0)}, h_{tx}^{(1)}, a_x^{(0)}, a_x^{(1)}$. Since we are concerned with solutions of a system of second-order differential equations,

these integration constants remain arbitrary in the UV analysis. As usual, once one imposes the above-mentioned IR boundary conditions at the horizon they are determined and can be read from the full bulk solution. According to the standard holographic dictionary, we interpret $h_{tx}^{(0)}$ and $a_x^{(0)}$ as the sources of the dual operators whose vacuum expectation values are given by $h_{tx}^{(1)}$ and $a_x^{(1)}$.

8.1.2.2 On-shell action and renormalization

The action (8.1) diverges if evaluated on-shell at the quadratic order in the fluctuations. The counter-term which is necessary to make the quadratic action finite is, as in the massless case,

$$S_{\text{c.t.}}^{(\text{div})} = \frac{1}{2\kappa_4^2}\int_{z=z_{UV}} d^3x\,\sqrt{-g_b}\,\frac{4}{L}\,. \tag{8.20}$$

Finally, as usual, the total on-shell action reduces to a purely boundary term. Fourier transforming the fields and substituting h_{zx} by means of the second equation in (8.16) we obtain

$$\begin{aligned} S_{\text{tot}} &= S + S_{\text{c.t.}}^{(\text{div})} \\ &= \lim_{z_{UV}\to 0} V\int\frac{d\omega}{2\pi}\Big[\frac{\mu z^2\left(\beta f+\omega^2\right)}{L^2q^2z_h\left(2\beta f+\omega^2\right)}a_x h_{tx} + \frac{\beta z^2 f}{2\kappa_4^2L^2\left(2\beta f+\omega^2\right)}h_{tx}h'_{tx} \\ &\quad - \frac{f}{2q^2}a_x a'_x + \frac{z}{2\kappa_4^2L^2\sqrt{f}}h_{tx}h_{tx}\Big]_{z=z_{UV}} + (\omega\leftrightarrow-\omega)\,, \end{aligned} \tag{8.21}$$

where the prime denote the derivative with respect to the radial variable z, the arguments of the first and second fluctuation in each pair are respectively $(-\omega,z)$ and (ω,z) and V represents the volume of the spatial manifold.

The boundary action (8.21) evaluated on the boundary expansions (8.19) allows us to compute the correlators and consequently the transport coefficients as we will explain below.

8.1.2.3 Definition of the correlators at zero momentum

The computation of $G^R(\omega,0)$ is analogous to that illustrated for the massless case, but with two important differences. The first one is that, since we are dealing with two coupled differential equations, relations (7.27) are not valid and we have to keep into account that:

$$\frac{\delta a_x^{(1)}}{\delta h_{tx}^{(0)}} \neq 0\,, \qquad \text{and} \qquad \frac{\delta h_{tx}^{(1)}}{\delta h_{tx}^{(0)}} \neq 0\,. \tag{8.22}$$

The second is that, on the computational level, in the massive case the IR parameter $\eta = a_0/b_0$ coming from the boundary conditions at the horizon (8.18) has a physical

relevance and cannot be simply rescaled to 1. Indeed we have to tune η depending on which source we need to set to zero in performing the functional derivatives. We resort to a numerical shooting method to the purpose of finding the value of η corresponding to the desired UV source set-up.

Eventually, differentiating with respect to the sources following what has been done for the massless case in the previous chapter,we obtain:

$$G^R_{JJ}(\omega,0) = \frac{1}{q^2 L}\frac{\delta a_x^{(1)}}{\delta a_x^{(0)}}\bigg|_{h_{tx}^{(0)}=0}\,, \tag{8.23}$$

$$G^R_{QQ}(\omega,0) = 2\Big[-1\frac{\mathscr{E}}{2} - \frac{3\beta}{2\kappa_4^2 L(2\beta+\omega^2)}\,\frac{\delta h_{tx}^{(1)}}{\delta h_{tx}^{(0)}}\bigg|_{a_x^{(0)}=0} - \frac{\mu}{2q^2 L}\,\frac{\delta a_x^{(1)}}{\delta h_{tx}^{(0)}}\bigg|_{a_x^{(0)}=0} + \frac{\mu^2}{z_h q^2}\frac{\beta+\omega^2}{2\beta+\omega^2} + \frac{3\mu\beta}{2\kappa_4^2 L(2\beta+\omega^2)}\,\frac{\delta h_{tx}^{(1)}}{\delta a_x^{(0)}}\bigg|_{h_{tx}^{(0)}=0} + \frac{\mu^2}{2q^2 L}\,\frac{\delta a_x^{(1)}}{\delta a_x^{(0)}}\bigg|_{h_{tx}^{(0)}=0}\Big]\,, \tag{8.24}$$

$$G^R_{JQ}(\omega,0) = \frac{1}{2q^2 L}\,\frac{\delta a_x^{(1)}}{\delta h_{tx}^{(0)}}\bigg|_{a_x^{(0)}=0} - \frac{\mu}{z_h q^2}\frac{\beta+\omega^2}{2\beta+\omega^2} - \frac{3\beta}{2\kappa_4^2 L(2\beta+\omega^2)}\,\frac{\delta h_{tx}^{(1)}}{\delta a_x^{(0)}}\bigg|_{h_{tx}^{(0)}=0} - \frac{\mu}{q^2 L}\,\frac{\delta a_x^{(1)}}{\delta a_x^{(0)}}\bigg|_{h_{tx}^{(0)}=0}\,. \tag{8.25}$$

8.1.3 Counter-terms and transport coefficients definition

In order to define the transport coefficient as in (6.13) we need also to evaluate the retarded Green's function at non-zero momentum, namely $G^R(0,k)$. The computation proceeds analogously to what has been done in the previous section for $G^R(\omega,0)$ except that in this case it is necessary to switch on also the fluctuation h_{xy} which couples to the other fluctuations through the non-zero momentum along the x direction. A numerical computation leads to:

$$\begin{aligned} G^R_{JJ}(0,k) &= \mathscr{O}(k^2)\,,\\ G^R_{JQ}(0,k) &= \mathscr{O}(k^2)\,,\\ G^R_{QQ}(0,k) &= \frac{\mathscr{E}}{2} + \mathscr{O}(k^2)\,. \end{aligned} \tag{8.26}$$

Consequently, the counter-terms play an important role only in defining the thermal conductivity. Actually, it is important to note that the counter-term in the thermal conductivity is exactly those which removes an non-physical pole at $\omega = 0$ which

would have no explanation in a plasma where momentum is not conserved such as those described by massive gravity.

Finally the thermo-electric transport coefficients $\sigma(\omega)$, $\alpha(\omega)$ and $\bar{\kappa}(\omega)$ assumes the following form:

$$\begin{aligned}\sigma(\omega) &= \frac{1}{i\omega} G^R_{JJ}(\omega,0)\ ,\\ \alpha(\omega) &= \frac{1}{i\omega T} G^R_{JQ}(\omega,0)\ ,\\ \bar{\kappa}(\omega) &= \frac{1}{i\omega T}\left(G^R_{QQ}(\omega,0) - \frac{\mathscr{E}}{2}\right)\end{aligned} \tag{8.27}$$

where the quantities $G^R_{IJ}(\omega,0)$ are defined in (8.23)-(8.25).

8.2 Spectral properties of transport coefficients

Having furnished a prescription for numerically compute the transport coefficient in holographic massive gravity let us now discuss briefly their spectral properties.

The real and imaginary part of the electric conductivity $\sigma(\omega)$ are plotted in Figure 8.1 for different values of the scale invariant ratio T/μ. As it is evident from the Figure, at high T/μ a smooth Drude peak develops in the low frequency region of the spectrum while the imaginary part of the conductivity goes to zero indicating the absence of a delta function at $\omega = 0$, as expected.

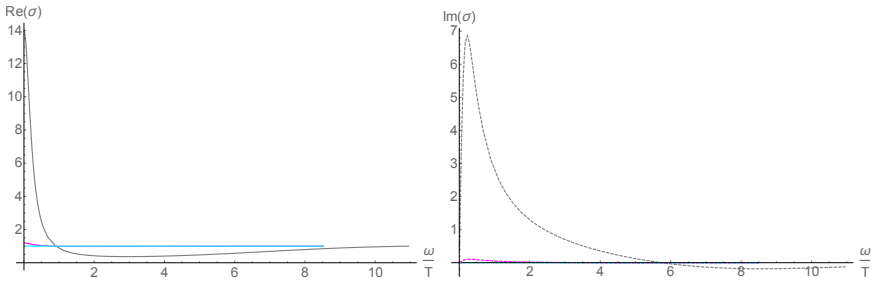

Fig. 8.1 Real (left) and imaginary (right) part of the electric conductivity $\sigma(\omega)$ for $\beta = -0.1$ and different values of the ratio T/μ, ($T/\mu = 0.1$ (grey), $T/\mu = 1$ (purple) and $T/\mu = 10$ (light blue).

At high frequency the conductivity approaches a constant values in agreement with the conformal prediction. In this region in fact $\omega \gg T, \mu, |\beta|$ and the model comes back to the conformal regime.

Once the ratio T/μ is lowered a depletion region develops in the low frequency region and the lack of spectral weight is transferred in the Drude-like peak which

becomes narrower and higher eventually transforming into a delta function in the limit $T/\mu \to 0$.

A similar qualitative behaviour can be seen, as expected in the thermal conductivity $\bar{\kappa}(\omega)$, plotted in Figure 8.2. We note in particular that the imaginary part of $\bar{\kappa}(\omega)$ goes to zero, as expected. This is due to the fundamental presence of the counterterm $G^R_{QQ}(0,k)$ in the Kubo formulæ (6.13).

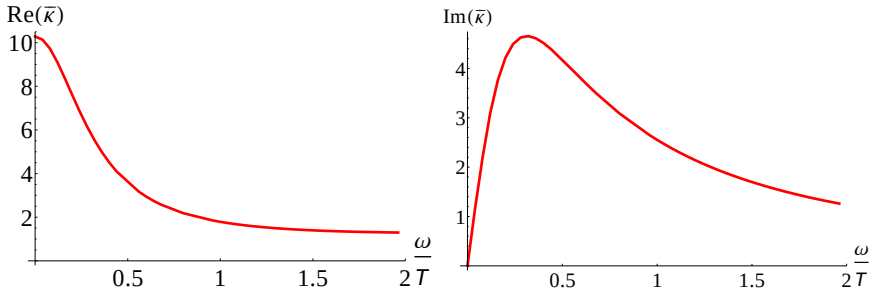

Fig. 8.2 Real (left) and imaginary (right) part of the thermal conductivity $ka\bar{p}pa(\omega)$ for $T/\mu = 1$ and $\beta = -0.1$.

8.3 DC transport coefficients

Having analysed the basic spectral properties of the transport coefficients, we can now move to the analysis of the DC transport properties. To do this we will follow the method developed in [15] to compute analytically the DC thermo-electric response. This approach is based on the analysis of quantities which do not evolve from the IR to the UV. In other words, it relies on a "membrane paradigm" [16] for massive gravity bulk models.

8.3.1 The electric conductivity and the Seebeck coefficient

Due to the isotropy of the system we are allowed to consider just perturbations in the x direction without loss of generality. Then the static electric conductivity σ_{DC} and the Peltier coefficient Π_{DC} are defined in terms of the electric field E_x, the charge density current J_x and the heat flow Q_x in the following way

$$\sigma_{DC} \equiv \left.\frac{J_x}{E_x}\right|_{\nabla_x T=0}, \qquad \Pi_{DC} \equiv \left.\frac{Q_x}{E_x}\right|_{\nabla_x T=0}. \tag{8.28}$$

The definitions (8.28) imply that, in order to compute σ_{DC} and s_{DC}, we must consider non-zero electric field and vanishing thermal gradient.

Inspired by [15], we turn on the following fluctuating components

$$a_x(t,z) = -E\,t + \tilde{a}_x(z)\ , \tag{8.29}$$

$$h_{tx}(t,z) = \tilde{h}_{tx}(z)\ , \tag{8.30}$$

$$h_{zx}(t,z) = \tilde{h}_{zx}(z)\ , \tag{8.31}$$

where the temporal dependence of the 4-potential a_μ corresponds to a constant electric field E along x and with h we denote fluctuations of the metric components.

The set of coupled linearised equations of motion for the fluctuating fields are

$$\tilde{h}''_{tx}(z) + \frac{2}{z}\,\tilde{h}'_{tx}(z) + 2\left(\frac{\beta}{f(z)} - \frac{1}{z^2}\right)\tilde{h}_{tx}(z) - \frac{2\gamma^2\mu}{z_h}\,\tilde{a}'_x(z) = 0\ , \tag{8.32}$$

$$\frac{E\,z^2\mu\,\gamma^2}{z_h f(z)} + \left(\frac{z^4\mu^2\gamma^2}{2z_h^2L^2} - z f'(z) + 3f(z) - 3\right)\tilde{h}_{zx}(z) = 0\ , \tag{8.33}$$

$$\tilde{a}''_x(z) + \frac{f'(z)}{f(z)}\tilde{a}'_x(z) - \frac{z^2\mu}{L^2 z_h f(z)}\tilde{h}'_{tx}(z) - \frac{2z\mu}{L^2 z_h f(z)}\tilde{h}_{tx}(z) = 0\ . \tag{8.34}$$

Note that equation (8.33) for $\tilde{h}_{zx}$ can be solved algebraically and, recalling the explicit expression of the emblackening factor $f(z)$ given in (8.75), the solution can be expressed as follows

$$\tilde{h}_{zx}(z) = -\frac{E\gamma^2\mu}{z_h\beta f(z)}\ . \tag{8.35}$$

In order to completely determine the solution of the remaining two equations (8.32) and (8.34), we have to provide suitable boundary conditions for the fluctuation fields $h_{tx}(t,z)$ and $a_x(t,z)$ at the conformal boundary $z=0$ and at the horizon $z=z_h$. At the horizon we require the regularity of the fluctuations; this requirement can be easily fulfilled by switching to the Eddington-Finkelstein time coordinate

$$v = t - \frac{1}{4\pi T}\log\left(\frac{z_h - z}{L}\right)\ , \tag{8.36}$$

leaving untouched all the other coordinates. From the IR regularity requirement for all the metric components in the new coordinate system we derive the behaviour of $\tilde{h}_{tx}$ at the horizon, namely

$$\tilde{h}_{tx}(z) = -\frac{E\gamma^2\mu}{z_h\beta} + \mathcal{O}(z - z_h)\ . \tag{8.37}$$

An analogous regularity requirement at the horizon applied to the gauge field yields

$$\tilde{a}_x(z) = \frac{E}{4\pi T}\log\left(\frac{z_h - z}{L}\right) + \mathcal{O}(z - z_h)\ . \tag{8.38}$$

As we will explain better in what follows, considering the conformal boundary located at $z = 0$, we have to furnish boundary conditions in such a way that the dual system has an external electric field and vanishing thermal gradient. Given the ansatz (8.86), the small-z leading behaviour of the fluctuating field $a(t,z)$ corresponds to a constant electric field E. According to the standard holographic dictionary, the coefficient of the subleading fall-off in z of the field $a(t,z)$ corresponds to the charge density current J_x; namely $\tilde{a}_x \sim J_x z$ at small z. Regarding the metric fluctuation $\tilde{h}_{tx}$, from equation (8.32) it is easy to see that it has two independent behaviours in the near-boundary region, i.e. z and z^{-2}. The holographic dictionary prescribes that imposing that there are no sources associated to thermal gradients corresponds to setting to zero the coefficient of the leading z^{-2} term. All in all, the set of boundary conditions that we have just illustrated determines the solution of the differential equations (8.32) and (8.34) completely.

In order to compute the DC transport coefficients it is fundamental to note that there are two linear combinations of the fluctuations which are independent of the coordinate z and are respectively related to the charge density current and the heat current. The first conserved current is

$$\bar{J}^{\mu} = -\frac{\sqrt{-g}}{q^2} F^{z\mu} \ , \tag{8.39}$$

with $\mu = t,x,y$. Given the ansatz (8.86), the only non-zero component of the Maxwell equation $\sqrt{-g}\nabla_M F^{MN} = \partial_z(\sqrt{-g}F^{zx}) = 0$ states that $\bar{J}^x$ is independent of the radial coordinate z and it assumes the following explicit form in terms of the fluctuating fields

$$\bar{J}^x = -\frac{\sqrt{-g}}{q^2} F^{zx} = \frac{z^2\mu}{L^2 q^2 z_h}\tilde{h}_{tx}(z) - \frac{f(z)}{q^2}\tilde{a}'_x(z) \ . \tag{8.40}$$

Relying on the "radial conservation" we can compute $\bar{J}^x$ both at the horizon $z = z_h$ and at the boundary $z = 0$ knowing that the two results must correspond. Computing it at $z = 0$ and recalling the above-mentioned UV behaviours, it is possible to see that this quantity is actually the charge density current J^x of the dual field theory. Then, evaluating (8.40) at $z = z_h$ we find:

$$J^x = \left(\frac{1}{q^2} - \frac{\gamma^2\mu^2}{L^2 q^2 \beta}\right) E \ . \tag{8.41}$$

The electric conductivity σ_{DC} is now easily computed by means of (8.28),

$$\sigma_{DC} = \frac{J^x}{E} = \frac{1}{q^2} - \frac{\gamma^2\mu^2}{L^2 q^2 \beta} \ , \tag{8.42}$$

which corresponds exactly with the analytical expression found in [12].

The second conserved quantity, which is related to the heat current, is subtler to identify. Indeed, as noted in [15], it is associated to the existence of the Killing vector $k = \partial_t$ and it assumes the following form:

$$\bar{Q} = \frac{\sqrt{-g}}{\kappa_4^2}\nabla^z k^x - \phi J^x = \left(\frac{\phi\ \tilde{a}_x'}{q^2} + \frac{\tilde{h}_{tx}'}{2\kappa_4^2} + \frac{\tilde{h}_{tx}}{\kappa_4^2 z}\right) f + \left(-\frac{f'}{2\kappa_4^2} - \frac{\mu z^2 \phi}{L^2 q^2 z_h}\right)\tilde{h}_{tx}\ , \tag{8.43}$$

where in the second passage we gave an explicit expression of $\bar{Q}$ in terms of the fluctuation fields. Evaluating $\bar{Q}$ on the equations of motion (8.32) and (8.34) and keeping into account the particular form of the background quantities f and ϕ (8.75), one has that $\partial_z \bar{Q} = 0$. Namely $\bar{Q}$ is radially conserved.

Having obtained a radially conserved quantity, in order to repeat the same steps done previously for the electric conductivity, we have to prove that $\bar{Q}$ coincides, if evaluated on the boundary, with the heat current in the x direction $Q^x = T^{tx} - \mu J^x$ of the dual field theory. Actually, in this case, the proof of this statement is straightforward. In fact, J^x is constant along the radial direction and $\phi(0) = \mu$, and consequently the term ϕJ^x reduces to μJ^x when evaluated at the conformal boundary. Moreover, it is not difficult to see that $\frac{\sqrt{-g}}{\kappa_4^2}\nabla^z k^x$ coincides with the linearised tx component of the stress-energy tensor of the dual field theory[3] evaluated at the conformal boundary $z = 0$, namely

$$T^{tx} = \frac{L^5}{\kappa_4^2 z^5}\left(-K^{tx} + K g_b^{tx} + \frac{2}{L} g_b^{tx}\right) = \frac{\tilde{h}_{tx}'}{2\kappa_4^2\sqrt{f}} - \frac{\tilde{h}_{tx}}{\kappa_4^2 z\sqrt{f}} + \frac{2\tilde{h}_{tx}}{\kappa_4^2 z f}\ . \tag{8.44}$$

Finally, having associated the quantity $\bar{Q}$ with the heat flow, the Peltier coefficient is straightforwardly obtained evaluating $\bar{Q}$ at the horizon $z = z_h$ and relying on the IR behaviour of the fluctuating fields. We obtain

$$\Pi_{DC} = \frac{\bar{Q}}{E} = -\frac{2\pi\mu}{\beta q^2 z_h}\left(-\frac{\gamma^2\mu^2 z_h}{8\pi L^2} + \frac{3}{4\pi z_h} + \frac{\beta z_h}{4\pi}\right)\ . \tag{8.45}$$

The expressions for the DC electrical conductivity (8.5.2.1) and the Peltier coefficient (9.52) obtained here with an analytical computation along the lines described by [15] coincide with those found in [35] using numerical methods. Note that the term inside the parenthesis of equation (9.52) coincides exactly with the temperature (8.8). Consequently, by Onsager reciprocity (see later), one has $\alpha_{DC} = \frac{\Pi_{DC}}{T}$, finding exactly formula (1.4) of [35], which was satisfied by numerical data.

8.3.2 Thermal conductivity and Onsager reciprocity

The thermal conductivity $\bar{\kappa}_{DC}$ is defined as

[3] To have an explicit expression of the stress-energy tensor we refer for instance to [19]

$$\bar{\kappa}_{DC} \equiv \left.\frac{Q_x}{-\nabla_x T}\right|_{E_x=0} . \tag{8.46}$$

Symmetrically to what we have done in the previous Section, to compute this quantity we must consider a thermal gradient at vanishing electric field. To this end, we rely on the elegant method described in [15]; we consider the following set of fluctuations

$$a_x(t,z) = \alpha_2\,\phi(z)\,t + \tilde{a}_x(z) , \tag{8.47}$$

$$h_{tx}(t,z) = -\alpha_2\,\frac{L^2}{z^2}\,f(z)\,t + \tilde{h}_{tx}(z) , \tag{8.48}$$

$$h_{zx}(t,z) = \tilde{h}_{zx}(z) . \tag{8.49}$$

As we will explain at the end of the section α_2 is the source for the thermal gradient along the x direction, $\nabla_x T/T$. Namely, we will have to derive the heat current with respect to α_2 in order to compute the thermal conductivity.

Considering the ansatz (8.47), (8.48) and (8.49), one finds that the equations of motion for $\tilde{h}_{tx}$ and $\tilde{a}_x$ are the same as those given in Section 8.3.1, namely (8.32) and (8.34). The equation for $\tilde{h}_{zx}$ looks slightly different but is still algebraically solvable; its solution being

$$\tilde{h}_{zx}(z) = -\frac{L^2\alpha_2\left\{2L^2q^2\left[3z\left(\beta z_h^2+1\right)-2\beta z_h^3\right]-\kappa_4^2\mu^2 z z_h^2\right\}}{2\beta z(z-z_h)\left\{\kappa_4^2\mu^2 z^3 z_h - 2L^2q^2\left[z^2\left(\beta z_h^2+1\right)+z z_h+z_h^2\right]\right\}} . \tag{8.50}$$

As regards the boundary conditions, the regularity of the fluctuations at the horizon, in this case, implies that

$$\tilde{h}_{tx}(z) = -\frac{\alpha_2\left(2L^2q^2\left(\beta z_h^2+3\right)-\kappa_4^2\mu^2 z_h^2\right)}{4\beta z_h^3 q^2} + \frac{\alpha_2 L^2 f(z)}{2\pi T z^2}\log\left(\frac{z_h-z}{L}\right) + \mathscr{O}(z-z_h) , \tag{8.51}$$

and

$$\tilde{a}_x = \mathscr{O}(z-z_h) . \tag{8.52}$$

Moreover, at the boundary $z=0$ we require that $\tilde{h}_{tx}$ is proportional to z and, as before, we have $\tilde{a}_x = J_x z + ...$, where the ellipsis indicates higher power of z.

Importantly, since the equations of motion for $\tilde{h}_{tx}$ and $\tilde{a}_x$ are the same as in the case studied in the previous Section, the quantities $\bar{J}^x$ (8.40) and $\bar{Q}$ (8.43) are still independent of z. Enforcing the near-boundary conditions discussed previously, we have that also in this case $\bar{J}^x$ corresponds to the x component of the dual charge density current. However, the relation between $\bar{Q}$ and the heat current Q^x is in this case more subtle than before. Indeed the tx component of the holographic stress-energy tensor evaluated on the ansatz (8.47), (8.48) and (8.49) for the fluctuations assumes the following form

$$T^{tx} = t\left(-\frac{\alpha_2 L^2 f'}{2\kappa_4^2 z^2\sqrt{f}} + \frac{2\alpha_2 L^2\sqrt{f}}{\kappa_4^2 z^3} - \frac{2\alpha_2 L^2}{\kappa_4^2 z^3}\right) + \frac{\tilde{h}'_{tx}}{\kappa_4^2\sqrt{f}} - \frac{\tilde{h}_{tx}}{\kappa_4^2 z\sqrt{f}} + \frac{2\tilde{h}_{tx}}{\kappa_4^2 z f} . \tag{8.53}$$

Therefore the quantity $\frac{\sqrt{-g}}{\kappa_4^2}\nabla^z k^x$ (contained in $\bar{Q}$) computed at $z=0$ equals just the time-independent part of T^{tx} (i.e. the last three terms in (8.53)). Nevertheless, as discussed in [15] (see Appendix D for more details), in order to compute the DC response, only the time-independent part of T^{tx} is relevant. To the purpose of computing the DC thermal conductivity we can then assume that $\bar{Q}$ corresponds to the heat current. Then, evaluating it at the horizon, considering in this case the horizon conditions (8.51) and (8.52) and differentiating with respect to α_2 which, as anticipated, is the source for the thermal gradient $\nabla_x T/T$, we find

$$\bar{\kappa}_{DC} = \frac{1}{T}\frac{\bar{Q}}{\alpha_2} = \frac{\pi\left[\gamma^2\mu^2 z_h^2 - 2L^2\left(\beta z_h^2+3\right)\right]}{2\beta\kappa_4^2 z_h^3}\,, \tag{8.54}$$

which agrees with our previous numerical result reported in [35].

Eventually, relying on the boundary conditions (8.51) and (8.52) we evaluate the charge density current $\bar{J}^x$ (8.40) at $z=z_h$. We can then prove that the Onsager reciprocity relation holds, namely

$$\alpha_{DC} = \left.\frac{J_x}{-\nabla_x T}\right|_{E_x=0} = -\frac{2\pi\mu}{\beta q^2 z_h} = \frac{\Pi_{DC}}{T}\,, \tag{8.55}$$

where the last identity can be obtained by using (9.52) and dividing it by the temperature (8.8).
Said otherwise, the conductivity matrix is symmetrical and the Peltier coefficient Π_{DC} is equal to the thermal conductivity α_{DC} multiplied by T.

For completeness we still have to prove that α_2 is actually the source for the thermal gradient $\nabla_x T/T$. To do this let us consider the coordinate transformation on the boundary:

$$\begin{aligned} t &= \bar{t} - \alpha_2 \bar{t}\bar{x}\,, \\ x &= \bar{x}\,. \end{aligned} \tag{8.56}$$

At the linearised level we find that these coordinate transformation implies the following transformations for the stress-energy tensor:

$$\begin{aligned} &T^{\bar{t}\bar{t}} = (1+2\alpha_2\bar{x})T^{tt}\,, \\ &T^{\bar{x}\bar{x}} = T^{xx}\,, \qquad T^{\bar{t}\bar{x}} = T^{tx}\,, \qquad J^{\bar{t}} = (1+\alpha_2\bar{x})J^x\,, \qquad J^{\bar{x}} = J^x\,. \end{aligned} \tag{8.57}$$

In particular the time dependence has dropped out of the expectation values.

At the level of the bulk fields, the coordinates transformation (8.56) implies the following asymptotic behaviour at $z\to 0$:

$$\begin{aligned} ds^2 &= -\frac{L^2}{z^2}f(z)(1-2\alpha_2\bar{x})d\bar{t}^2 + \frac{L^2}{z^2}d\bar{x}^2 + \ldots\,, \\ A &= \phi(z)(1-\alpha_2\bar{x})d\bar{t} + \ldots\,. \end{aligned} \tag{8.58}$$

Finally, in order to identify α_2 with $\nabla_x T/T$ let us recall that the period of Euclidean time is $1/T$. In order to keep track of all the factors of the temperature, let us rescale the time so that there is no T dependence in the period: $t = \tilde{t}/T$. With the new dimensionless time coordinate, the metric has $g_{\tilde{t}\tilde{t}} = 1/T^2$. We are taking the original metric to be Minkowski space. It follows that a small constant thermal gradient, $T \to T + x\nabla_x T$, implies

$$\delta g_{tt} = -\frac{2x\nabla T}{T} \ . \tag{8.59}$$

where we have scaled back to the original time coordinate t. Comparing the previous expression with (8.58), we find that α_2 can be identified with $\nabla_x T/T$ as we have previously stated.

8.3.3 DC properties of the transport coefficients

The purpose of this section is to compare the temperature dependence of the transport coefficients of the simple massive gravity model analysed in the previous sections to those of the Fermi liquid and of the cuprates outlined in Part 1. Actually the simple massive gravity model (8.1), is a very simple toy model and we do not expect that it could reproduce phenomenological properties of the cuprates. However, the comparison of this section is useful in light of the analysis of more realistic models (see for example the following section) and especially for the analysis which we will perform in Chapter 9, where holography will be proposed as a machinery to generate effective field theory useful in the understanding phenomena which occurs in strongly coupled systems.

Coming back to the massive gravity model (8.1), the most serious problem in order to perform phenomenological comparison is probably the finite horizon area at zero temperature, which means, as in the Reinssner-Nordstr̈om case, that the system violates the third law o thermodynamics. The residual zero temperature entropy probably means that at some point an instability should occurs and the ground state of the system would change (see the following section for the analysis of a model which avoids this problem).

Regarding the thermo-electric transport coefficients, we have previously derived that the electric conductivity σ_{DC} is given by:

$$\sigma_{DC} = \frac{1}{q^2} - \frac{\gamma^2\mu^2}{L^2 q^2 \beta} \ . \tag{8.60}$$

As it is evident from the previous formula, the conductivity is completely consistent with the massless Raissner-Nordström case. In fact, in the massless limit $|\beta| \to 0$ σ_{DC} diverges as it should in a system where momentum is conserved. However, in the neutral limit $\mu = 0$ the conductivity remains finite even if β is zero. This is in agreement with the hydrodynamic prevision that in a neutral plasma the electric conductivity remains finite even if momentum is conserved.

Regarding the temperature dependence of σ_{DC}, we note from (8.60) that it does not depend on the horizon radius z_h and consequently it is constant in temperature as one can see from the thermodynamic expressions (8.8). The constant behaviour of the electric conductivity is recovered in the Fermi liquid in the (elastic) scattering dominate regime (see Part 1), but it is not realistic that this behaviour persist for al the temperature range. The constant behaviour disagrees also with the cuprates phenomenology where a stable linear in temperature resistivity is measured (see Part 1).

Regarding the thermo-electric conductivity, in the system at hand α_{DC} approaches a constant at $T = 0$ and then grows linearly with the temperature:

$$\alpha_{DC} = \frac{\sqrt{2}\pi\mu\left(2\beta L^2 - \gamma^2\mu^2\right)}{\beta q^2\sqrt{3\gamma^2\mu^2L^2 - 6\beta L^4}} - \frac{4\pi^2\mu}{3\beta q^2}T + O\left(T^2\right) \tag{8.61}$$

As we will explain better in Chapter 9, this is due to the fact that the entropy $\mathscr{S}$ is non-zero at $T = 0$ (see (8.8)).

(8.61) disagrees both with the cuprates phenomenology and with the Fermi liquid prediction. In fact, the Mott law describing the Fermi-liquid thermo-electric response for elastic scattering mechanisms

$$s_{\text{Mott}} = -\frac{\pi^2}{3q^2}\,T\,\frac{\partial\log\sigma_{DC}}{\partial\mu} \tag{8.62}$$

yields a Seebeck coefficient which goes linearly to zero as $T \to 0$.

Finally, the thermal conductivity $\bar{\kappa}_{DC}$ goes linearly to zero with the temperature and is proportional to the heat capacity $C = T\frac{\partial\mathscr{S}}{\partial T}$,

$$\bar{\kappa}_{DC} = -\frac{\sqrt{\frac{3}{2}\gamma^2\mu^2L^2 - 3\beta L^4}}{2\beta L^2 - 2\gamma^2\mu^2}C + \mathscr{O}\left(T^2\right)\ . \tag{8.63}$$

This is is agreement with the Reissner-Nordström limit, where we have seen that the coefficient of the delta function at $\omega = 0$ for the thermal conductivity is basically proportional to the entropy and consequently, since it is linear in temperature at low T, to the specific heat.

8.4 Adding the dilaton

As we have seen in the previous section, the simple massive gravity model (8.1) is not very interesting from the phenomenological point of view. We have just outlined that the temperature behaviour of the DC transport coefficients deviates from both the paradigmatic Fermi liquid and the phenomenology of the cuprates (see Part 1). Moreover, as in the Raissner-Nordström case, there is a residual non-zero entropy at $T = 0$. Consequently, the system violates the third law of thermodynamics, which

means that at sufficiently low T something has to happen which modify the ground state with respect to those described by (8.1). The core of the problem is that at zero temperature the horizon of the black hole, as in the Reissner-Nordström case, is located at some point which do not coincides with $z=\infty$. Then, to get rid of the zero temperature entropy this horizon has to be located at $z=\infty$. There are two common way to solve this issue. One can either introduce charged sources to discharge the horizon: an example of this case is the well known holographic superconductor [24] and the subsequent literature. The second way is to attempt to violate Gauss's law. This can be realized in a simple way by employing the so called Einstein-Maxwell Dilaton (EMD) gravity. Dilaton fields are quite unfamiliar to condensed matter physics but these turn out to be quite ubiquitous in string theory where they naturally appear in the low energy spectrum, and thereby also in top-down theories. A dilaton field ϕ is an object having its own potential while it typically shows up as well as determining dynamically the gauge coupling $Z(\phi)$ multiplying e.g. the Maxwell term.

In general the EMD model, including a mass term for the graviton, is described by the following action:

$$S=\int d^4x\sqrt{-g}\Big[R-V(\phi)-\frac{Z(\phi)}{4}F_{\mu\nu}F^{\mu\nu}-\frac{1}{2}\partial_\mu\phi\partial^\mu\phi+\mathscr{M}_\beta(g)\Big]+S_{\text{c.t.}}\ , \quad (8.64)$$

where $V(\phi)$ is the dilaton potential, which should tend to the cosmological constant $\Lambda/L^2=-6/L^2$ at $z\to 0$ in order for the space to be asymptotically AdS, $Z(\phi)$ is the coupling between the dilaton and the Maxwell field as stated above, and the mass term we consider is given by

$$\mathscr{M}_\beta(g)=\beta\left[\text{tr}(\mathscr{K})^2-\text{tr}(\mathscr{K}^2)\right]\ . \quad (8.65)$$

Holographic studies on the transport properties of this theory can be found e.g. in [18, 25, 26]. In particular in [18] the DC transport coefficient are computed analytically following the method illustrated in the previous sections for the massive gravity model (8.1). Even though the DC transport coefficient can be fully expressed in terms of the horizon data, to find a general analytical solution for the background which is well behaved at $z\to\infty$ and asymptotically AdS at $z\to 0$ (which is an essential ingredient to apply the holographic dictionary (see Part 2)) is not an easy task and, by now, very few solution of this kind are known analytically.

Here, in order to describe an holographic model which has several interesting properties from the phenomenological point of view, we will focus on the following EMD model:

$$S_d=\int d^4x\sqrt{-g}\Big[R+6\cosh\phi-\frac{e^\phi}{4}F_{\mu\nu}F^{\mu\nu}-\frac{3}{2}\partial_\mu\phi\partial^\mu\phi+\mathscr{M}_\beta(g)\Big]+S_{\text{c.t.}}\ . \quad (8.66)$$

This model is inspired by [22] which was considered in $3+1$ dimensions with a mass term for the graviton in [23].

The bulk solutions of (8.66) are

$$
\begin{aligned}
ds^2 &= \frac{g(z)}{z^2}\left(-h(z)dt^2+\frac{dz^2}{g(z)^2h(z)}+dx^2+dy^2\right)\,,\\
A_t &= \sqrt{\frac{3Q(Qz_h+1)}{z_h}\left(1+\frac{\beta z_h^2}{(Qz_h+1)^2}\right)}\frac{z_h-z}{z_h(Qz+1)}\,,\\
\phi(z) &= \frac{1}{3}\log g(z)\,, \qquad g(z)=(1+Qz)^{\frac{3}{2}}\,,\\
h(z) &= 1+\frac{\beta z^2}{(Qz+1)^2}-\frac{z^3(Qz_h+1)^3}{z_h^3(Qz+1)^3}\left(1+\frac{\beta z_h^2}{(Qz_h+1)^2}\right)\,.
\end{aligned}
\tag{8.67}
$$

The parameter Q controls the dilaton profile and is related to the chemical potential. In the asymptotical Minkowsky case, namely when $V(\phi)=0$ and the dilaton has no mass, the parameter Q is related to the conserved dilaton charge.

The thermodynamics of the model is holographically related to the bulk solution in the following way

$$
\begin{aligned}
T &= \frac{3(1+Qz_h)^2+\beta z_h^2}{4\pi(1+Qz_h)^{\frac{3}{2}}z_h}\,,\quad \mathscr{S}=\frac{4\pi}{z_h^2}(Qz_h+1)^{\frac{3}{2}}\,,\\
\mu &= \sqrt{\frac{3Q(Qz_h+1)}{z_h}\left[1+\frac{\beta z_h^2}{(Qz_h+1)^2}\right]}\,,\\
\rho &= \frac{\mu}{z_h}(Qz_h+1)\,,
\end{aligned}
\tag{8.68}
$$

As one can see from the previous solution in this case (asymptotically AdS) the parameter Q is no longer an independent parameter of the solution and is related to the chemical potential. Moreover, since the chemical potential μ must be real, the parameter Q and β are constrained in order for the radicand in (8.68) to be positive.

Following exactly the same method described in the previous section (see [15] for the details of the computation in the general EMD model) we have analytical control upon the entire set of thermo-electric transport coefficients and we obtain the following explicit expressions

$$
\begin{aligned}
\sigma_{DC} &= \frac{2\beta\,(Qz_h+1)-3Qz_h\left[\beta+\left(\frac{1}{z_h}+Q\right)^2\right]}{2\beta\sqrt{Qz_h+1}}\,,\\
\alpha_{DC} &= -\frac{2\sqrt{3}\pi}{\beta z_h}\sqrt{Q\,(Qz_h+1)\left[Q\,(Qz_h+2)+\beta z_h+\frac{1}{z_h}\right]}\,,\\
\bar{\kappa}_{DC} &= -\frac{2\pi\left(\frac{1}{z_h}\right)^{5/2}\sqrt{\frac{1}{z_h}+Q}\left(z_h^2\left(\beta+3Q^2\right)+6Qz_h+3\right)}{\beta\sqrt{Qz_h+1}}\,.
\end{aligned}
\tag{8.69}
$$

We remind the reader that, also in the present dilaton model, the positivity of the momentum dissipation rate requires $\beta<0$ so in the preceding formulæ β is always negative.

8.4.1 Properties of DC transport coefficients

We are now ready to briefly discuss the temperature dependence of both the thermodynamical quantities and the transport coefficients derived in the previous section. Actually the properties of the model at hand are very subtle and the temperature scalings strongly depends on the way in which one solve the relation between μ, Q, β and z_h in (8.68) (We will come back to this subtle point in Chapter 9). In this section we will suppose that Q is a non-zero real fixed number in line with what has been originally done in [23].

In this case the high temperature limit ($T/\mu \gg 1$) has exactly the same properties of the simple massive gravity model (8.1) discussed previously. This is in line with the fact that the dilaton introduced in the dual field theory an operator which is irrelevant in the UV while it modifies the near horizon geometry and consequently the low temperature properties of the model.

Stated this, we have only to discuss the low temperature ($T/\mu \ll 1$) properties of the various physical observables.

Let us start from the thermodynamics. In order to derive the relevant scalings it is useful to note that the relation (8.68) between the temperature T and the horizon radius z_h implies that, at low temperature (large horizon radius) the temperature scales as $T \simeq \sqrt{z_h}$. Consequently, we find that the entropy goes linearly to zero as the temperature decreases, namely:

$$\mathscr{S} \simeq 4\pi Q^{3/2} \frac{1}{\sqrt{z_h}} \simeq \frac{T}{\mu} \,. \tag{8.70}$$

Then as stated before there is no residual entropy density at $T = 0$ and the ground state of the system is stable. Regarding the charge density, it approaches a constant at $T = 0$ and grows quadratically at the increasing of the temperature:

$$\rho \simeq \sqrt{3} Q \sqrt{\beta + Q^2} + \frac{\sqrt{3}\left(\beta + 3Q^2\right)}{2 z_h \sqrt{\beta + Q^2}} \simeq A_1 + B_1 \frac{T^2}{\mu^2} \,, \tag{8.71}$$

where A_1 and B_1 are constants

Regarding the transport coefficients, the DC electric resistivity $\rho_{DC} = 1/\sigma_{DC}$ is linear in temperature

$$\rho_{DC} \simeq \frac{\left(-9Q^2\sqrt{Q\left(\beta+Q^2\right)} + 2\beta\sqrt{Q}\sqrt{\beta+Q^2} + 3\beta\sqrt{Q\left(\beta+Q^2\right)}\right)}{4\beta Q\sqrt{\beta+Q^2}} \frac{1}{\sqrt{\mathrm{zh}}} \propto \frac{T}{\mu} \,, \tag{8.72}$$

in agreement with the phenomenology of the cuprates. However, the thermo-electric conductivity, which in the cuprates is typically fitted with a power low of the kind $A - BT$,scales as follows:

$$\alpha_{DC} \simeq -\frac{2\sqrt{3}\pi Q\sqrt{\beta+Q^2}}{\beta} - \frac{\sqrt{3}\pi\left(\beta+3Q^2\right)}{\beta z_h\sqrt{\beta+Q^2}} \simeq A_2 - B_2\frac{T^2}{\mu^2} \,, \tag{8.73}$$

where A_2 and B_2 are constants.

Finally regarding the thermal conductivity, the experimental data are not conclusive and we can not make contact with the phenomenology. However, in this specific model $\bar{\kappa}_{DC}$ goes to zero quadratically:

$$\bar{\kappa}_{DC} \simeq \frac{-\frac{6\pi Q^2}{\beta} - 2\pi}{z_h} \propto \frac{T^2}{\mu^2} \,. \tag{8.74}$$

Note that from the previous relation we find that $|\beta| > 1/(3Q^2)$ in order for the thermal conductivity to be positive. This probably provides an additional constraints to the stability of the model even though a detailed study of the stability of the solution is still a work in progress.

As a final comment, we want to stress again that the temperature scalings depend on how you solve the constraints which relates the parameter Q to the chemical potential μ in (8.68). In Chapter 9 we will consider again this model analysing how different solutions of the constraint lead to different, phenomenologically relevant scalings.

8.5 Holographic magneto-transport

In Chapter 7 we have analysed the basic thermo-electric transport properties of a strongly correlated plasma which conserves momentum. Then we got rid that, in order to make contact with experiments some mechanisms of momentum dissipation must be considered since they are ubiquitous in condensed matter systems, and we consequently have analysed in some details a possible way to include momentum dissipation in holography in the previous sections of this chapter. Actually, as the reader should have noted in Part 1, most of the measurements for the cuprates are performed in systems immersed in an external magnetic field. This is due to the fact that, since the superconducting phase transition occurs at high critical temperature T_c, in order to analyse the transport properties in the normal phase, the critical temperature has to be suppressed in some way, and the external magnetic field do exactly this game. Eventually, in this section we want to include the effects of an external magnetic field in the effective holographic field theory discussed in the previous sections, namely, the massive gravity model (8.1).

Specifically, we want to discuss the effects due to the presence of an external magnetic field B orthogonal to the plane xy. In particular, its consequences on the thermoelectric transport coefficients in the holographic system (8.1) at non-zero chemical potential μ. To include the constant magnetic field B we adopt the following ansatz for the background metric $g_{\mu\nu}$ and the gauge field A_μ

$$\begin{aligned} ds^2 &= \frac{L^2}{z^2}\left[-f(z)dt^2 + dx^2 + dy^2 + \frac{1}{f(z)}dz^2\right] \,, \\ A &= \phi(z)\,dt + Bx\,dy \,. \end{aligned} \tag{8.75}$$

Substituting this ansatz within the equations of motion derived from (8.1), we obtain the following black brane solution

$$\begin{aligned}\phi(z) &= \mu - q^2\rho z = \mu\left(1-\frac{z}{z_h}\right), \qquad \rho \equiv \frac{\mu}{q^2 z_h}, \\ f(z) &= 1-\frac{z^3}{z_h^3}+\beta\left(z^2-\frac{z^3}{z_h}\right)-\frac{z^3}{z_h}\left(1-\frac{z}{z_h}\right)\frac{\gamma^2\left(B^2 z_h^2+\mu^2\right)}{2L^2},\end{aligned} \tag{8.76}$$

where we have denoted with z_h the horizon location defined by the vanishing of the emblackening factor, namely $f(z_h)=0$. The definition of ρ is actually substantiated by the explicit analysis of the thermodynamics that we perform in Section 8.5.1. For the sake of practical convenience, we introduced $\gamma \equiv \kappa_4/q$.

8.5.1 Thermodynamics

As discussed in the previous section, the black brane solution (8.76) corresponds to a planar demonic black hole having both electric and magnetic charges. From the boundary theory standpoint, B represents a magnetic field perpendicular to the spatial manifold xy which enters the boundary thermodynamical quantities; as usual in gauge/gravity, these are derived from the bulk on-shell action as we now show in detail.

The temperature T and the entropy density $\mathscr{S}$ are the easiest thermodynamical quantities to compute since they are determined from the horizon data, namely

$$T = -\frac{f'(z_h)}{4\pi} = -\frac{\kappa_4^2 z_h^2\left(B^2 z_h^2+\mu^2\right)-2L^2q^2\left(\beta z_h^2+3\right)}{8\pi L^2 q^2 z_h}, \qquad \mathscr{S} = \frac{2\pi L^2}{\kappa_4^2 z_h^2}. \tag{8.77}$$

In order to compute the energy density $\mathscr{E}$, the pressure P, the charge density ρ and the magnetization M, we need to evaluate explicitly the Landau potential Ω which, according to the holographic dictionary, is identified with the on-shell bulk action. Not surprisingly, the bulk action (8.1) when naively evaluated on the solution (8.76) is divergent and therefore needs to be renormalized. The standard renormalization process consists in regularizing the action by means of a UV cut-off $z_{\rm UV}$ and supplementing it with appropriate counter-terms. These could necessarily be written in terms of boundary fields but (proceeding as in [12]), once evaluated on the solution (8.76), can be explicitly expressed as follows

$$S_{\rm ct} = \frac{1}{2\kappa_4^2}\int_{z=z_{\rm UV}}\sqrt{-g_b}\left(\frac{4}{L}+\frac{2}{L}\beta z_{\rm UV}^2\right), \tag{8.78}$$

where g_b is the metric induced on the $z=z_{\rm UV}$ shell. With this counter-term in place, the Landau potential Ω assumes the following form

$$\Omega \equiv \lim_{z_{\rm UV}\to 0} (S+S_{\rm ct})_{\rm on\text{-}shell} = V\left(\frac{3B^2 z_h}{4q^2} - \frac{L^2}{2\kappa^2 z_h^3} + \frac{\beta L^2}{2\kappa^2 z_h} - \frac{\mu^2}{4q^2 z_h}\right) . \tag{8.79}$$

We have denoted with V the boundary spatial volume.

Once the Landau potential is known, the other thermodynamical quantities follow easily by means of standard thermodynamical relations. We explicitly obtain[4]

$$P = -\frac{\Omega}{V} = -\frac{3B^2 z_h}{4q^2} + \frac{L^2}{2\kappa_4^2 z_h^3} - \frac{\beta L^2}{2\kappa_4^2 z_h} + \frac{\mu^2}{4q^2 z_h} , \tag{8.80}$$

$$\mathscr{E} = -P + \mathscr{S}T + \mu\rho = \frac{B^2 z_h}{2q^2} + \frac{L^2}{\kappa_4^2 z_h^3} + \frac{\beta L^2}{\kappa_4^2 z_h} + \frac{\mu^2}{2q^2 z_h} , \tag{8.81}$$

$$\rho = \frac{\partial \mathscr{E}}{\partial \mu} = \frac{\mu}{q^2 z_h} , \qquad M = -\frac{\partial \mathscr{E}}{\partial B} = -\frac{B z_h}{q^2} . \tag{8.82}$$

For later purposes it is useful to define one additional and less common thermodynamical quantity, namely the magnetization energy M^E defined as

$$M^E \equiv -\frac{\delta \Omega}{\delta F^E_{xy}} , \tag{8.83}$$

where $F^E_{xy} = \partial_x \delta g_{ty} - \partial_y \delta g_{tx}$ and δg_{ta} represents a variation of the metric sourcing T^{ta}. Following [21], an operative method to evaluate the magnetization energy consists in computing the on-shell action on the following solution

$$\begin{gathered} A_t = \phi(z) , \qquad A_y = Bx - (\phi(z) - \mu) B^E x , \\ ds^2 = \frac{L^2}{z^2}\left[-f(z)\left(dt - B^E x dy\right)^2 + dx^2 + dy^2 + \frac{1}{f(z)} dz^2\right] , \end{gathered} \tag{8.84}$$

where $\phi(z)$ and $f(z)$ are the same as in (8.76); the magnetization energy M^E is then obtained by differentiating the on-shell action with respect to B^E and finally setting B^E to zero as one can understand comparing de definition of F^E_{xy} and the explicit form for the metric in (8.84). This computation proceeds exactly in the same way as in [21] and the mass term for the graviton does not affect the final result. Eventually we obtain

$$M^E = \frac{\mu M}{2} . \tag{8.85}$$

[4] In order to compute the thermodynamical derivatives with respect to T, μ and B one must recall that z_h is an implicit function of these quantities as given in (8.77).

8.5.2 Transport coefficients

We compute analytically the whole set of thermoelectric DC transport coefficients for the boundary theory corresponding to the bulk model (8.1). To this aim, we employ the method first illustrated in the previous sections. Since the application of the method presents some technical difficulties when the magnetic field is present, we will explain the computation in details in what follows.

8.5.2.1 Electric conductivity

We consider linearised fluctuations around the bulk background solution (8.76). Following [15], to the purpose of computing the linear response to a "pure" electric field (i.e. in the absence of a thermal gradient), one considers the following ansatz for the fluctuating fields

$$a_i(t,z) = -E_i\, t + \tilde{a}_i(z)\ , \tag{8.86}$$
$$h_{ti}(t,z) = \tilde{h}_{ti}(z)\ , \tag{8.87}$$
$$h_{zi}(t,z) = \tilde{h}_{zi}(z)\ , \tag{8.88}$$

where $i = x,y$; we henceforth adopt small Latin letters to refer to spatial boundary indices[5]. The vector E_i introduced in the ansatz corresponds to an external electric field perturbing the system.

The quantity

$$\bar{J}^\mu = -\frac{\sqrt{-g}}{q^2}\, F^{z\mu}\ , \tag{8.89}$$

(where $\mu = t,x,y$ is a boundary space-time index) is conserved along the holographic direction as a direct consequence of the Maxwell equation for the fluctuations. Indeed, recalling the ansatz (8.86), we obtain

$$\sqrt{-g}\nabla_M F^{MN} = 0 \quad \longrightarrow \quad \partial_z(\sqrt{-g}F^{zi}) = 0\ . \tag{8.90}$$

The capital indices refer to the bulk space-time and the arrow means that we consider just the spatial components. The quantities $\bar{J}^i$ are radially conserved and explicitly given by

$$\bar{J}_i = -\frac{f(z)}{q^2}\,\tilde{a}_i'(z) - \frac{Bz^2 f(z)}{L^2 q^2}\,\varepsilon_{ij}\,\tilde{h}_{zj}(z) + \frac{z^2\mu}{L^2 q^2 z_h}\,\tilde{h}_{ti}(z)\ , \tag{8.91}$$

where $\varepsilon_{ij} = -\varepsilon_{ji} = 1$. To obtain (8.91) we have again referred to the ansatz (8.86) and considered just up to the linear order in the fluctuating fields. We remind the reader that the boundary indices are raised and lowered with the flat boundary Minkowski metric.

[5] Note that the magnetic field mixes the x and y fluctuation sectors and therefore all the components along these directions in (8.86) must be switched on.

To study the near-horizon behaviour of the fluctuating fields and demand regular infra-red behaviour, it is convenient to adopt the Eddington-Finkelstein coordinates, namely

$$v = t - \frac{1}{4\pi T}\log\left[\frac{z_h - z}{L}\right] , \tag{8.92}$$

leaving all the other bulk coordinates untouched. Skipping the details (which are analogous to what illustrated for the $B = 0$ case in the previous sections), the infra-red regularity requirement amounts to having the following asymptotic behaviours

$$\tilde{h}_{ti}(z) = f'(z_h)\,\tilde{h}_{zi}(z_h)(z_h - z) + \mathcal{O}(z_h - z)^2 , \tag{8.93}$$

and

$$\tilde{a}_i(z) = \frac{E_i}{4\pi T}\log\left[\frac{z_h - z}{L}\right] + \mathcal{O}(z_h - z) . \tag{8.94}$$

To avoid clutter, we relegated the explicit expressions of the equations of motion for the linearised fluctuations in Appendix E.1. It is however important to recall that $\tilde{h}_{zi}(z)$ is governed by an algebraic equation and therefore expressible in terms of the other fluctuating fields (hence it does not demand further IR requirements). An explicit infra-red asymptotic analysis returns

$$\tilde{h}_{ti}(z_h) = -\frac{L^2\gamma^2\left[B\varepsilon_{ij}E_j z_h\left(\gamma^2 B^2 z_h^2 + \gamma^2\mu^2 - L^2\beta\right) + E_i L^2\beta\mu\right]}{z_h\left(L^2\beta - B^2 z_h^2\gamma^2\right)^2 + B^2 z_h^3\gamma^4\mu^2} , \tag{8.95}$$

which we report explicitly for the sake of completeness and to underline that its $B \to 0$ limit is consistent with previous results obtained directly at $B = 0$ in the previous sections.

It is essential to observe that, turning the attention to the near-boundary asymptotics, one actually identifies $\bar{J}(z = 0)$ with the electric current J_i of the boundary theory,

$$\bar{J}_i(z = 0) = J_i . \tag{8.96}$$

Moreover, being $\bar{J}$ radially conserved, it can be evaluated in the IR and then expressed exclusively in terms of the near-horizon asymptotic data, namely $\bar{J}(z = 0) = \bar{J}(z = z_h)$.

The electric conductivity matrix is

$$J_i = \sigma_{ij}E_j . \tag{8.97}$$

Hence its entries are directly read from the explicit expression of the electric current; this yields

$$\sigma_{xx} = \frac{\beta L^2\left[\beta L^2 q^2 - \kappa_4^2\left(B^2 z_h^2 + \mu^2\right)\right]}{-2\beta B^2\kappa_4^2 L^2 q^2 z_h^2 + B^2\kappa_4^4 z_h^2\left(B^2 z_h^2 + \mu^2\right) + \beta^2 L^4 q^4} , \tag{8.98}$$

and

$$\sigma_{xy} = \frac{B\mu z_h \left[\kappa_4^4 \left(B^2 z_h^2 + \mu^2\right) - 2\beta\kappa_4^2 L^2 q^2\right]}{q^2 \left[-2\beta B^2 \kappa_4^2 L^2 q^2 z_h^2 + B^2 \kappa_4^4 z_h^2 \left(B^2 z_h^2 + \mu^2\right) + \beta^2 L^4 q^4\right]} \,. \tag{8.99}$$

We have $\sigma_{xx} = \sigma_{yy}$ and $\sigma_{xy} = -\sigma_{yx}$.

8.5.2.2 Thermoelectric response

We want now to compute the thermoelectric conductivities α_{xx} and α_{xy}. Considering the system at non-zero electric field and zero thermal gradient, these two conductivities are defined by the following relation

$$Q_i = \alpha_{ij} T E^j \,, \tag{8.100}$$

where Q^i is the heat current in the i-direction, which can be related to the boundary stress-energy tensor $T^{\mu\nu}$ and to the electric current J^μ by the identity $Q^i = T^{ti} - \mu J^i$.

In order to apply the same procedure used for the electric conductivity in the previous section, we need to define in the gravitational system (8.1) a quantity $\bar{Q}_i$ which is radially conserved and that, choosing the appropriate UV boundary conditions for the functions appearing in the ansatz, can be identified at the boundary with the heat current Q_i. As illustrated in [15], the quantity which does the game in the absence of an external magnetic field is:

$$\bar{Q}_1^i = \frac{\sqrt{-g}}{\kappa_4^2} \nabla^z k^i - \phi(z) \vec{J}^i \,, \tag{8.101}$$

where $k = \partial_t$. The proof that this quantity is radially conserved relies on the fact that k is a Killing vector for the gravitational action (8.1) (see [15] for more details).

When one considers circumstances with a non-zero magnetic field B, the quantity (8.101) is no longer radially conserved. In fact, differentiating $\bar{Q}^i$ with respect to z and evaluating the result on the equations of motion (see Appendix E.1) we obtain

$$\partial_z \bar{Q}_1^i = \varepsilon^{ij} E_j \frac{B}{q^2} \,. \tag{8.102}$$

We can therefore define the following radially conserved quantity,

$$\bar{Q}^i = \frac{\sqrt{-g}}{\kappa_4^2} \nabla^z k^i - \phi(z) \vec{J}^i - \varepsilon^{ij} E_j \frac{B}{q^2} z \,. \tag{8.103}$$

Evaluating the expression (8.103) on the ansatz (8.86) at the linear order in the fluctuations we obtain

$$\bar{Q}_i = \frac{f(z)\phi(z)}{q^2}\,\tilde{a}_i'(z) - \frac{Bz}{q^2}\,\varepsilon_{ij}E_j + \frac{Bz^2 f(z)\phi(z)}{L^2 q^2}\,\varepsilon_{ij}\tilde{h}_{zj}(z) + \left(-\frac{f'(z)}{2\kappa_4^2} + \frac{f(z)}{z\kappa_4^2} - \frac{z^2\mu\,\phi(z)}{L^2 q^2 z_h}\right)\tilde{h}_{ti}(z) + \frac{f(z)}{2\kappa_4^2}\,\tilde{h}_{ti}'(z)\,. \tag{8.104}$$

The proof that $\bar{Q}$ corresponds to the heat current at the boundary is straightforward. In fact, the third term in (8.103) vanishes at $z=0$, the second term is equal[6] to $-\mu J^i$, and the first term coincides at the boundary with the ti component of the holographic stress-energy tensor,

$$T^{ti} = \frac{L^5}{\kappa_4^2 z^5}\left(-K^{ti} + K g_b^{ti} + \frac{2}{L}g_b^{ti}\right) = \frac{\tilde{h}_{ti}'(z)}{2\kappa_4^2\sqrt{f(z)}} - \frac{\tilde{h}_{ti}(z)}{z\kappa_4^2\sqrt{f(z)}} + \frac{2\tilde{h}_{ti}(z)}{z\kappa_4^2 f(z)}\,. \tag{8.105}$$

Exploiting its radial conservation, we can compute $\bar{Q}^i$ at $z=z_h$ and express the heat current only in terms of horizon data. Finally, using the definition of the thermoelectric conductivities (8.100), we obtain:

$$\alpha_{xx} = -\frac{2\pi\beta\mu L^4 q^2}{-2\beta B^2\kappa^2 L^2 q^2 z_h^3 + B^2\kappa^4 z_h^3\left(B^2 z_h^2+\mu^2\right) + \beta^2 L^4 q^4 z_h}\,, \tag{8.106}$$

and

$$\alpha_{xy} = \frac{2\pi B L^2\left(\kappa_4^2\left(B^2 z_h^2+\mu^2\right) - \beta L^2 q^2\right)}{-2\beta B^2\kappa_4^2 L^2 q^2 z_h^2 + B^2\kappa_4^4 z_h^2\left(B^2 z_h^2+\mu^2\right) + \beta^2 L^4 q^4} + \frac{8B\pi L^2 q^2 z_h^2}{\kappa_4^2 q^2 z_h^2\left(B^2 z_h^2+\mu^2\right) - 2L^2 q^4\left(\beta z_h^2+3\right)}\,. \tag{8.107}$$

However, as illustrated in [21, 27], in order to properly define the thermoelectric response in the presence of a magnetic field, one has to subtract to the heat current the contribution due to the magnetization current[7]. This implies that the off-diagonal components of the thermoelectric conductivity have to be defined as

$$\alpha_{xy}^{\rm sub} = \alpha_{xy} + \frac{M}{T}\,, \tag{8.108}$$

and, recalling the explicit expression of the temperature T and of the magnetization M derived in Section 8.5.1, we obtain

[6] We remind the reader that the quantity $\bar{J}^i$ is radially conserved and coincides with the boundary electric current, as illustrated in the previous section.

[7] We note that the radially conserved quantity (8.101) is defined up to an additive constant. Therefore it would be possible to add to $\bar{Q}_1^i$ the constant $\varepsilon_{ij}E_j\frac{Bz_h}{q^2}$ and the radially conserved quantity defined in such a way would coincide with the magnetization-subtracted heat current. This is in line with the analysis of [31].

$$\alpha_{xy}^{\text{sub}} = \frac{2\pi BL^2\left(\kappa_4^2\left(B^2 z_h^2+\mu^2\right)-\beta L^2 q^2\right)}{-2\beta B^2\kappa_4^2 L^2 q^2 z_h^2 + B^2\kappa_4^4 z_h^2\left(B^2 z_h^2+\mu^2\right)+\beta^2 L^4 q^4} \,. \tag{8.109}$$

From now on, we will refer to α_{xy}^{sub} as the off-diagonal component of the thermo-electric conductivity and we will indicate it with α_{xy}.

8.5.2.3 Thermal conductivity

The thermal conductivities $\bar{\kappa}_{xx}$ and $\bar{\kappa}_{xy}$ are defined in terms of the heat current generated by the presence of an external thermal gradient $\nabla_i T$ in the following way

$$Q_i = -\bar{\kappa}_{ij}\nabla_j T \tag{8.110}$$

As illustrated in [15], in order to study the holographic model (8.1) in the presence of an external thermal gradient and at zero electric field we have to consider the following ansatz for the fields of the theory

$$\begin{aligned} a_i(t,z) &= s_i\,\phi(z)\,t+\tilde{a}_i(z)\,, \\ h_{ti}(t,z) &= -s_i\frac{L^2}{z^2}f(z)\,t+\tilde{h}_{ti}(z)\,, \\ h_{zi}(t,z) &= \tilde{h}_{zi}(z)\,, \end{aligned} \tag{8.111}$$

where s_i can be proven to be equal to the quantity $-\frac{\nabla_i T}{T}$ in the boundary field theory (see [15]). The linearized equations of motion for this ansatz can be found in Appendix E.2.

As in the thermo-electric case, the quantity (8.101) evaluated on the ansatz (8.111) is not radially conserved. On the other hand, the quantity (already given in (8.103))

$$\bar{Q}^i = \frac{\sqrt{-g}}{\kappa_4^2}\nabla^z k^i - \phi(z)\,\vec{J}^i + \varepsilon^{ij}s_j\frac{B\mu}{q^2}z\,, \tag{8.112}$$

is radially conserved once evaluated on shell.

The computation of the thermal conductivities is now straightforward. As in the previous section, we evaluate the radially conserved quantity (8.112) on the ansatz (8.111) at the linear order in the fluctuations. Also in this case, as long as we consider the DC response, $\bar{Q}_i$ can be proven to coincide with the heat current in the boundary field theory (see Appendix E.3 for further details on this point)[8]. Finally, computing the quantity $\bar{Q}_i$ at the horizon $z = z_h$, and considering the definition of the thermal conductivities (8.110) we obtain

[8] Actually, considering the ansatz (8.111) there are some additional technical difficulties in proving this statement due to the fact that the quantity $\nabla^z k^i$ differs from the holographic stress-energy tensor T^{ti} by terms linear in the time coordinate t. However, as proven in [15], these terms do not contribute to DC transport properties.

$$\bar{\kappa}_{xx} = \frac{1}{T}\frac{\bar{Q}_x}{\alpha_x} = -\frac{\pi L^2\left(\beta L^2 q^2 - B^2\kappa^2 z_h^2\right)\left[2L^2q^2\left(\beta z_h^2+3\right)-\kappa^2 z_h^2\left(B^2 z_h^2+\mu^2\right)\right]}{2\kappa^2 z_h^3\left[-2\beta B^2\kappa^2 L^2 q^2 z_h^2 + B^2\kappa^4 z_h^2\left(B^2 z_h^2+\mu^2\right)+\beta^2 L^4 q^4\right]} \tag{8.113}$$

Also in this case we need to subtract the contribution due to the magnetization current [21, 27] from the off-diagonal conductivity $\bar{\kappa}_{xy}$, namely

$$\bar{\kappa}_{xy} = \frac{1}{T}\frac{\bar{Q}_x}{\alpha_y} + \frac{2\left(M^E-\mu M\right)}{T} = -\frac{\pi B\mu L^2\left[\kappa_4^2 z_h^2\left(B^2 z_h^2+\mu^2\right)-2L^2q^2\left(\beta z_h^2+3\right)\right]}{2z_h^2\left[-2\beta B^2\kappa_4^2 L^2 q^2 z_h^2 + B^2\kappa_4^4 z_h^2\left(B^2 z_h^2+\mu^2\right)+\beta^2 L^4 q^4\right]}\,, \tag{8.114}$$

where we have used equation (8.85) for M^E.

8.5.3 Structure of the thermoelectric transport coefficients

The behaviours of the transport coefficients found in the previous section depend on the specific form of the thermodynamical quantities obtained in the massive gravity model in Section 8.5.1. Nevertheless, as we will show, these transport coefficients can be cast in a form which may aspire to be universal, at least within the holographic framework. It is tempting, in fact, to argue that the formulæ obtained through holography with massive gravity could remain valid in a more general framework, namely as long as one considers strongly coupled systems with neutral mechanisms of momentum dissipation[9] (e.g. impurities). This statement is partially corroborated by [31, 32, 33], where formulæ for the thermo-electric transport coefficients in agreement with those obtained in this paper are computed in holographic Q-lattices [31] and, independently of holography, by means of the memory matrix approach [32].

In order to proceed, we write the full set of transport coefficients computed in massive gravity in terms of the thermodynamical quantities and two transport quantities $\tilde{\sigma}$ and h. Let us start defining the explicit expressions for these latter in the model at hand. As far as $\tilde{\sigma}$ is concerned, it appears manifestly from the expression of the transport coefficients that it represents the $\mu=\rho=B=0$ conductivity, then it takes the usual [12, 35, 36] form $\tilde{\sigma}=1/q^2$ and it is directly connected to the parameter q of the bulk model. Regarding h, we define it explicitly as follows

$$h = -\frac{\mathscr{S}\beta}{2\pi} = \frac{4\beta L^2 q^2 z_h}{\kappa_4^2 z_h^2\left(B^2 z_h^2-3\mu^2\right)-2L^2q^2\left(\beta z_h^2+3\right)}\,, \tag{8.115}$$

noticing its relation to the parameter β.

In order to gain physical intuition on the nature of h, we connect it to the characteristic time τ of momentum dissipation at $B=0$

[9] This statement might not be valid in cases when the momentum dissipation is obtained by adding an additional gauge field as in [39, 40].

$$\tau|_{B=0} = -\frac{2\pi\,(\mathscr{E}+P)}{\mathscr{S}\beta} = -\frac{2L^2q^2\left(\beta z_h^2+3\right)}{4\beta L^2 q^2 z_h}\ , \tag{8.116}$$

as found in [8] through an analysis at low momentum dissipation; combining (8.115) and (8.116), for h we have

$$h|_{B=0} = \frac{\mathscr{E}+P}{\tau}\ . \tag{8.117}$$

We also stress that, according to [29], the connection of τ to a momentum dissipation characteristic time is made up to order β^2 corrections; therefore τ can be, strictly speaking, interpreted as a dissipation characteristic time only when momentum is slowly dissipated [37] and at vanishing magnetic field. This said and still sticking to $B=0$, τ proved to be a formally very useful quantity to furnish explicit and exact expressions for the holographic transport coefficients in all dynamical regimes [12, 35, 36, 38]. In the present extended context, i.e. encompassing a non-trivial magnetic field, we prefer to express everything in terms of the quantity h (as defined in (8.115)) both inside and outside the regime of strong momentum dissipation and independently on the magnitude of the magnetic field B. Even reminding ourselves the connection of h to τ through (8.117), we adopt the former to prevent confusion and avoid a direct hint to a momentum dissipation characteristic time (whose explicit expression for $B\neq 0$ is yet unknown).

It amounts just to a matter of algebra to verify that the transport coefficients derived in Section 8.5.2 can be expressed in the following general form :

$$\sigma_{xx} = h\,\frac{\rho^2+\tilde{\sigma}\left(B^2\tilde{\sigma}+h\right)}{B^2\rho^2+\left(B^2\tilde{\sigma}+h\right)^2}\ , \qquad \sigma_{xy} = \rho B\,\frac{\rho^2+\tilde{\sigma}\left(B^2\tilde{\sigma}+2h\right)}{B^2\rho^2+\left(B^2\tilde{\sigma}+h\right)^2}\ , \tag{8.118}$$

$$\alpha_{xx} = \frac{\rho\,\mathscr{S}\,h}{B^2\rho^2+\left(B^2\tilde{\sigma}+h\right)^2}\ , \qquad \alpha_{xy} = \mathscr{S}B\,\frac{\rho^2+\tilde{\sigma}\left(B^2\tilde{\sigma}+h\right)}{B^2\rho^2+\left(B^2\tilde{\sigma}+h\right)^2}\ , \tag{8.119}$$

$$\bar{\kappa}_{xx} = \frac{\mathscr{S}^2T\left(B^2\tilde{\sigma}+h\right)}{B^2\rho^2+\left(B^2\tilde{\sigma}+h\right)^2}\ , \qquad \bar{\kappa}_{xy} = \frac{B\rho\,\mathscr{S}^2T}{B^2\rho^2+\left(B^2\tilde{\sigma}+h\right)^2}\ . \tag{8.120}$$

We highlight once more that the transport coefficients (8.118), (8.119), (8.120) are expressed as functions of the entropy density $\mathscr{S}$, the charge density ρ, the magnetic field B, the conductivity $\tilde{\sigma}$ and h only. They *formally* do not depend on any detail of the specific model that has been used to derive them. We therefore advance the proposal that they can have wider relevance. Within the holographic context, such a claim could be corroborated by the comparison of these formulæ with the corresponding results obtained in other holographic models [31]. More generally, a careful comparison with the phenomenology and real experiments must be pursued. In a later section we start addressing this wide question.

Finally we note that, even defining the incoherent conductivity $\sigma_Q \equiv [\mathscr{S}T/(\mathscr{E}+P)]^2$ as in [4], we find a mismatch between the holographic formulæ (8.118), (8.119), (8.120) and the hydrodynamic results of [21]. This is however expected, since (as recently pointed out in [29, 30]), in the zero magnetic field case the holographic DC formulæ for the thermo-electric transport agree with the modified hydrodynamic

result of [4] at order $1/\beta^2$ and there is a mismatch at order β^0. The discrepancy we have found here reflects most probably that an analogous situation arises also in the $B \neq 0$ case. To the purpose of identifying precisely the coherent and incoherent contributions to the thermo-electric conductivities for $B \neq 0$ a careful extension of the $B = 0$ analysis of [29] is in order. Complementary studies could also be pursued within the fluid/gravity approach as in [30].

8.5.4 Bulk electromagnetic duality and its consequences from the boundary perspective

The $3+1$ dimensional bulk Lagrangian (8.1) enjoys electromagnetic self-duality. From the boundary viewpoint this implies that the equilibrium states corresponding to two bulk solutions connected by the electromagnetic duality can be mapped into each other, which practically means that the information regarding the thermodynamics and the transport can be interpreted in two dual ways. Though, this does not correspond to a boundary electromagnetic duality; actually, from the holographic dictionary it emerges clearly that the bulk electromagnetic duality exchanges the boundary magnetic field with the charge density.

The physical relevance of these duality arguments is connected to the possible description of the theory in terms of dual degrees of freedom and is related to the ubiquitous particle/vortex dualities of critical or near-to-critical systems. Indeed, as noted in [21], in the limit $\rho,\, \tau^{-1}, B \ll T^2$, and $\rho \sim B$, the hydrodynamic transport coefficients enjoy the above mentioned duality (a priori of any gauge/gravity argument), namely, by exchanging the charge density with the magnetic field, $\rho \leftrightarrow B$ and the quantum critical conductivity with its inverse $\sigma_Q \leftrightarrow 1/\sigma_Q$, the hydrodynamical transport coefficient map into each other as follows

$$\begin{array}{c} \sigma_{xx},\ \sigma_{xy},\ \alpha_{xx},\ \alpha_{xy},\ \overline{\kappa}_{xx},\ \overline{\kappa}_{xy} \\ \updownarrow \\ \rho_{xx}, -\rho_{xy}, -\vartheta_{xy}, -\vartheta_{xx},\ \kappa_{xx}, -\kappa_{xy}\ , \end{array} \tag{8.121}$$

where $\hat{\rho} = \hat{\sigma}^{-1}$ is the resistivity matrix, $\hat{\theta} \equiv -\hat{\rho}\cdot\hat{\alpha}$ is the Nernst coefficient matrix and $\hat{\kappa} = \hat{\bar{\kappa}} - T\,\hat{\alpha}\cdot\hat{\rho}\cdot\hat{\alpha}$ is the thermal conductivity matrix at zero electric current[10].

As just argued, in a gauge/gravity context, the map (8.123) becomes particularly transparent as a direct consequence of the bulk electro-magnetic duality. So the transport coefficients (8.118), (8.119), (8.120) that we have obtained holographically naturally satisfy (8.123) in any dynamical regime; both within and outside the hydrodynamic approximation. The self-duality is naturally expressed in terms of the characteristic conductivity $\tilde{\sigma} = 1/q^2$ which is mapped into its inverse and

[10] Where

$$\hat{\rho} = \rho_{xx}\,1 + \rho_{xy}\,\hat{\varepsilon}\ , \tag{8.122}$$

and similarly for the other transport matrices.

not through the quantum critical conductivity σ_Q; we remind the reader that this latter is equal to $[\mathscr{S}T/(\mathscr{E}+P)]^2$ as described in [4]. The electro-magnetic duality formulated in terms of $\tilde{\sigma}$ is exactly valid in every dynamical regime, namely

$$\rho \leftrightarrow B\,, \qquad \tilde{\sigma} \leftrightarrow 1/\tilde{\sigma}\,,$$

$$\begin{array}{c} \sigma_{xx},\ \sigma_{xy},\ \alpha_{xx},\ \alpha_{xy},\ \overline{\kappa}_{xx},\ \overline{\kappa}_{xy} \\ \updownarrow \\ \rho_{xx}, -\rho_{xy}, -\vartheta_{xy}, -\vartheta_{xx},\ \kappa_{xx}, -\kappa_{xy}\,. \end{array} \tag{8.123}$$

The validity of (8.123) also far from the hydrodynamic approximation has interesting consequences. One can move away from hydrodynamical regime either lowering the temperature or increasing the magnetic field. This statements can be made precise referring to the charge density ρ; lowering the temperature means actually to consider a regime where the ratio $T/\sqrt{\rho}$ turns to be small. Then it is possible to appreciate that the two ways out of hydrodynamical regime just mentioned are dual in the sense of the map (8.123) and correspond roughly speaking to spoil criticality by means of a strong magnetic field or a strong charge density.

Chapter 9
Physical implications

Having described in Chapter 8 the technical details to obtain a holographic effective field theory which takes into account momentum dissipation effects, we are now ready to discuss the physical implication of the technical result previously obtained.

Specifically, in the present chapter we will discuss two physical implication in which holography takes a predominant role.

In section 9.1, we will discuss a recent conjecture, according to which in strongly correlated materials near criticality, such as the cuprates, some physical observables, namely the momentum, charge and heat diffusion constants, have to saturate certain bounds. At first we will analyse how these bounds can be conjectured starting from the principle of *Planckian dissipation*, namely the fact that in critical matter all the scales are setted by the indetermination principle. Secondly we will argue on the possible existence of such bounds in holography, which at the moment constitute almost the only way to analyse the diffusivities in strongly coupled field theories.

In section 9.2, we will discuss a different implication of the holographic result of Chapter 8, namely we will argue on how holography can be taken as an effective field theory to discuss the phenomenology of the cuprates. With the phenomenological intuition that massive gravity could have a more general validity if taken as an effective low energy field theory, we will promote the parameter of the model to temperature dependent quantities. Then, with some phenomenological input, we will discuss how some scalings of the thermo-electric transport coefficients of the normal phase of the cuprates can be reproduced in this way.

9.1 Criticality and diffusion bounds

9.1.1 The shear viscosity bound and the concept of Planckian dissipation

In order to understand how the bounds on the charge and heat diffusion have been conjectured, we now briefly review a very famous result of holography, namely the fact that in a holographic fluid the viscosity/entropy ratio $(\eta/\mathscr{S})$ is equal to [43]:

$$\frac{\eta}{\mathscr{S}} = \frac{1}{4\pi}\frac{\hbar}{k_B}\,, \tag{9.1}$$

where k_B is the Boltzman's constant. As we will see, this extremely small ratio, which does not depend on any thermodynamical quantity of the model, is directly related to the concept of *Planckian dissipation*, namely the fact that in the strongly interacting quantum critical state, Planck's constant sets, together with the temperature, the rate of the production of heat. This concept will be fundamental in order to formulate the possible existence of bounds in charge and heat diffusions in cuprates.

Let us start by illustrating how the result (9.1) was found in holography. The shear viscosity η is a kinetic transport coefficients which measures the resistance of a fluid to flow. It is well defined only in a system where momentum is strictly conserved. As all the kinetic transport coefficients of a fluid, the shear viscosity can be related to correlation functions via the Kubo's formulæ [44]. Specifically, η follows from the absorptive part of the spatially transversal stress-energy tensor (T_{xy}) propagator through,

$$\eta = \lim_{\omega\to 0}\frac{1}{2\omega}\int dtdx\langle[T_{xy}(t,x),T_{xy}(0,0)]\rangle\,. \tag{9.2}$$

To compute correlators such as that in (9.2) is actually the bread and butter of holography. To do this, we will follow the elegant method illustrated in [16].

Let us consider a theory of gravity coupled to matter

$$S = \int_{r>r_0} d^4x\sqrt{-g}\left[\frac{1}{16\pi G_N}(R-\Lambda)+\mathscr{L}_M\right]\,, \tag{9.3}$$

where G_N is the newton constant and $\mathscr{L}_M$ is a generic matter Lagrangian. We will assume that this theory has has a black-bran background of the following kind:

$$ds^2 = -g_{tt}dt^2 + g_{rr}dr^2 + g_{ij}dx^i dx^j\,, \tag{9.4}$$

where the indexes i,j run other the spatial boundary directions x and y. In order for the previous metric to be a black-brane, we assume that it has an event horizon at $r=r_0$, where g_{tt} has a first order zero and g_{rr} has a first order pole. Moreover, we will assume that all the metric components depend on r only, so that we have translational invariance in t and x^i directions, and that the system preserve the full

rotational symmetry, namely

$$g_{ij} = \delta_{ij} g_{xx} \ . \tag{9.5}$$

Finally we take the boundary at $r = \infty$ and assume that the metric asymptotes to a structure that supports gauge/gravity duality according to what have been explained in Part 2.

In order to compute the viscosity for the field theory dual to the gravitational system just introduced, we need to analyse the fluctuation of the metric $h^x_y = g^{xx} h_{xy}$ which, according to the holographic dictionary (see Part 2), is dual to the xy component of the stress-energy tensor T_{xy}. At this point an observation comes in help: for Einstein gravity coupled to matter fields, in the absence of a background off-diagonal component of the metric, as in (9.4), the effective action for h^x_y is simply that of a massless scalar field ϕ with coupling $1/(16\pi G_N)$:

$$S_{eff} = \int_{r>r_0} d^4x \sqrt{-g} \frac{1}{16\pi G_N} (\nabla\phi)^2 \ . \tag{9.6}$$

Consequently, using the standard prescription (see Part 2), the shear viscosity η is given by:

$$\eta = \lim_{\omega\to 0} \lim_{r\to\infty} \frac{\Pi(r,\omega)}{i\omega\tilde{\phi}(r,\omega)} \ , \tag{9.7}$$

where $\tilde{\phi}(r,\omega)$ is the Fourier transform in the time direction of the field ϕ, $\Pi(r,\omega) \equiv -\frac{\sqrt{-g}}{16\pi G_N} g^{rr} \partial_r \tilde{\phi}(r,\omega)$ is the subleading term for the scalar field in the $r\to\infty$ limit and we work in the zero momentum limit $k = 0$. As usual the field $\tilde{\phi}$ is evaluated on the equation of motion associated to (9.6),

$$\partial_r \Pi = \frac{\sqrt{-g}}{16\pi G_n} g^{rr} g^{tt} \omega^2 \tilde{\phi} \ , \tag{9.8}$$

imposing ingoing-wave boundary conditions at the horizon r_0. The relevant observation made in [16] is that in the low frequency limit the equations of motion become:

$$\partial_r \Pi = 0 + \mathscr{O}(\omega\phi) \ , \qquad \partial_r(\omega\phi) = 0 + \mathscr{O}(\omega\Pi) \ . \tag{9.9}$$

Thus, the evolution in r is completely trivial and we can evaluate (9.7) at any value of r. In particular it is convenient to compute it at the horizon r_0 where ingoing-wave boundary conditions fix everything. Consequently Π assumes the following form:

$$\Pi(r_0,\omega) = \frac{1}{16\pi G_N} \sqrt{\frac{-g}{g_{rr} g_{tt}}}\bigg|_{r=r_0} i\omega\tilde{\phi}(r_0,\omega) \ , \tag{9.10}$$

and eventually:

$$\eta = \frac{1}{16\pi G_N} \frac{A}{V} \ , \tag{9.11}$$

where A is the area of the horizon and V is the spatial volume of the boundary theory. Using the Beckenstein-Hawking formula for the entropy (see Part 1), $\mathscr{S} = A/(4G_N V)$ we recover the result anticipated in (9.1).

The proof here is extremely general, applying also to charged black-holes dual to theories with chemical potential.

It has been conjectured in [43] that the value of $\eta/\mathscr{S}$ in (9.1) is in fact a lower bound for all realistic critical matter. Restricting to the holographic framework we now know that in theory where the the effective gravitational coupling for h^x_y is stronger than the universal value (9.1) for Einstein gravity. An example of this kind is Gauss-Bonnet gravity (see [45] for a review on the topic).

Independently of the fact that the value $1/4\pi$ is effectively a bound or not, the important statement is that this number is actually always small and the order of magnitude of the ration $\eta/\mathscr{S}$ is basically dictated by the Planck's constant $\hbar$. Then, the notion that a bound of the form

$$\frac{\eta}{\mathscr{S}} \geq C\frac{\hbar}{k_B} \,, \tag{9.12}$$

where C is a constant of order one to be discovered has survived since now.

Let us now explain the physical relevance of this holographic result. We have anticipated that it is related to Planckian dissipation, namely the fact that in the strongly interacting quantum critical state, Planck's constant sets, together with the temperature, the rate of the production of heat. This can be made clear by recalling that the viscosity embodies the dissipative nature of the plasma under consideration. In particular, in the presence of a single intrinsic relaxation rate τ_E for the modes of the plasma, the viscosity of a relativistic liquids equals

$$\eta = (\mathscr{E} + P)\tau_E \,, \tag{9.13}$$

where $\mathscr{E}$ and P are the energy density and the pressure respectively (see e. g. [46]). Considering now a system at vanishing chemical potential we have $\mathscr{S} = (\mathscr{E} + P)/T$ and therefore the ration $\eta/\mathscr{S}$ assume the following form:

$$\frac{\eta}{\mathscr{S}} = T\tau_E \,. \tag{9.14}$$

But as we have anticipated, in a Planckian dissipator all the scales are setted by the Planck's constant and the temperature through the indetermination principle, namely $\tau_E \simeq C_1\hbar/(k_B T)$, where C_1 is a constant of order 1. Putting all together we find that in a system with Planckian dissipation we have a formulation of a bound on $\eta/\mathscr{S}$ as in (9.12).

This result acquires a great relevance since it is supported by measurements of $\eta/\mathscr{S}$ extremely near to the holographic prediction in in the quark gluon plasma created at the heavy ion colliders, as well as in the unitary fermionic cold atom gas [47]. Moreover, recent experimental ARPES measurements on an optimally doped cuprate show that, also in this case, the ratio η/s due to the intrinsic electronic contribution is close to saturate the afore mentioned bound [48].

It is worth mentioning that in the critical region of the phase diagram of a system with a quantum critical point all the scales are setted by the temperature and the Planck's constant (see Part 1). Then systems with a quantum critical point are always Planckian dissipator. Eventually, the measurements before mentioned partially corroborate the idea that the peculiar transport properties of the strange metals are caused by the existence of a quantum critical point in their phase diagram. Moreover the experimental observation of the holographic prediction (9.1) in these systems promote holography as a very interesting and powerful tools for analysing these peculiar materials.

As a final comment, in order to make contact with the conjecture of the bounds on the charge and heat diffusion constant [41] which we will outline in the next section, let us explain how the proposal of the conjectured bound on the ratio $\eta/\mathscr{S}$ in (9.12) can be translated in a bound for the momentum diffusion constant D. Actually, it is a well known result of relativistic hydrodynamics that, at zero chemical potential, $\eta/\mathscr{S} = DT/c^2$, where c is the speed of light. Then using the holographic prediction (9.12), we find for the momentum diffusion constant:

$$\frac{D}{c^2} \geq C\frac{\hbar}{k_B T} \ . \tag{9.15}$$

The measurements of [47, 48] corroborate the holographic intuition that quantum critical systems are close to saturate the bounds (9.15).

9.1.2 The diffusivity bounds conjecture in cuprates

We have seen in the previous section that the concept of Planckian dissipation and the consequent possibility to formulate a bound for the momentum diffusion constant is based on extremely general arguments and aspire to be a general feature of critical matter (this fact is also corroborated by measurements). Relying on a wider applicability of similar arguments, it is tempting to find whether other physical observables in strange metals and, more generally, in strongly correlated materials have to saturate a bound due to Planckian dissipation. However, the identification of the correct kinematic framework where one can formulate universal bounds is, in general, not easy. The reason being that in metallic materials the mechanisms for momentum relaxation, such as the lattice or scattering from disorder, which are necessary to make the conductivities finite, are *extrinsic* to the electron dynamics. Hence it is difficult to formulate *intrinsic* and universal bounds.

A recent proposal advanced in [41] suggested that, in analogy to the bound on η/s, the quantities that could be universally bounded in strange metals are the thermo-electric diffusion constants D_+ and D_-.

The idea beyond this proposal is that strongly correlated materials in general do not admit a description in terms of quasi-particles, and they typically do not manifest a well defined Drude peak in the low frequency spectrum of the thermo-electric transport coefficients (we have appreciated this fact explicitly for the cuprates in

Part 1). We will refer to this regime, where momentum is quickly dissipated and consequently there is no sharp Drude peak, as the *incoherent* regime, in contrast to the coherent regime where momentum is slowly dissipated. Due to this fact, the thermo-electric transport coefficients are not good quantities in order to formulate universal bounds since their form is extremely sensitive to the fact that the system under consideration is in the coherent or incoherent regime. On the contrary diffusion constants are typically setted by Einstein's relations (see below and Appendix F) and are not sensitive to the coherence or incoherence of the system.

Following this line of arguments, and conjecturing that the concept of Planckian dissipation should affect all the diffusion constants in the same way, the proposal of [41] is that the charge and heat diffusion constant $D_\pm$ (see below and Appendix F for a careful definition) have to saturate a bounds of the following kind:

$$D_\pm \geq C \frac{\hbar \bar{v}^2}{k_B T}, \tag{9.16}$$

where C is an undetermined constant and we have replaced the speed of light appearing in (9.12) with the characteristic speed in a metal $\bar{v}$ which might be identified with the Fermi velocity. This is a non-trivial sleight of hand. In particular, the bound on the ration $\eta/\mathscr{S}$ is only equivalent to (9.12) for relativistic systems with zero charge density. In some regards, however, $\bar{v}$ does play a role analogous to the speed of light for instance by mediating a linear dispersion relation for the low energy excitations of the Fermi surface. This velocity represents an extra scale of the relativistic low-energy effective description which may be naturally related to a UV cut-off (as described for instance in [42]). It is relevant to note that, in the holographic context, an extra scale of the effective description was for instance used in [38] in order to set two different temperature scalings for the resistivity and the Hall angle.

The diffusion constants D_+ and D_- are related to the transport coefficients via the Einstein relations, namely:

$$D_+ D_- = \frac{\sigma}{\chi}\frac{\kappa}{c_\rho}\,, \tag{9.17}$$

$$D_+ + D_- = \frac{\sigma}{\chi} + \frac{\kappa}{c_\rho} + \frac{T(\zeta\sigma - \chi\alpha)^2}{c_\rho \chi^2 \sigma}\,, \tag{9.18}$$

where σ, α and κ are respectively the electric, the thermo-electric and the thermal conductivities (see [41] for a derivation); c_ρ is the specific heat at fixed charge density ρ, ζ is the thermo-electric susceptibility and χ is the electric susceptibility.

In order to proceed, one has to note that typically the order of magnitude of the thermo-electric conductivity is smaller than that of the electric and thermal conductivity. Consequently the third term in (9.18) can be neglected and the universal bounds (9.16) translate directly in restrictions on the electric and thermal conductivity, namely

$$\frac{\sigma}{\chi},\ \frac{\kappa}{c_\rho} \geq \frac{\bar{v}\hbar}{k_B T}\,. \tag{9.19}$$

Let us now analyse the physical consequence of the conditions (9.19). In particular we will assume to be in a critical system in the incoherence regime, which, according to the previous arguments, has to saturate the bound (9.19). If the bound of the electric conductivity is saturated, then the resistivity $\rho = 1/\sigma$ behaves as follows:

$$\rho \sim \frac{1}{\vec{v}^2 \chi} \frac{k_B T}{\hbar} \ . \tag{9.20}$$

Assuming that the the susceptibility χ is almost independent of the temperature (in agreement with DMFT prediction) we find that once the bound on the diffusion constants (9.16) is saturated, the resistivity is linear in temperature, as experimentally observed in the cuprates (see Part 1). Moreover, if we (naively and incorrectly in a non-quasiparticle system) match the expression for the resistivity (9.20) to a Drude formula, we will extract the effective timescale

$$\tau_{ext} = \frac{\hbar}{k_B T} \ , \tag{9.21}$$

namely, in the incoherent regime also the scale of the extrinsic momentum dissipation rate τ_{ext} due to the extrinsic momentum dissipation mechanisms is basically setted by the temperature, in accordance with the principle of Planckian dissipation.

Soon after the analysis of [41], the author of [42], relying on hydrodynamical arguments, suggested that a bound on the sum of the thermoelectric diffusion constants is more natural than bounding the same diffusivities individually, namely

$$D_+ + D_- \geq C' \frac{\hbar \vec{v}^2}{k_B T} \ ; \tag{9.22}$$

still [42] (to which we refer for details) observes that the sum $D_+ + D_-$ is always a real quantity and argues on the basis of a perturbative approach.

We will see in the following sections that, in the holographic framework there are some hints that a bound on the sum of the diffusion constants could be formulated, in accordance with [42].

9.1.3 On the existence of diffusivity bounds in holography

We have understand in the previous sections that the possible existence of bounds on the diffusion constants is extremely interesting from the phenomenological point of view, especially in considering strongly coupled materials near the critical region, as the cuprates should be.

In the following two sections we will investigate the possibility of a formulation of bounds on the heat and charge diffusion constants in the context of holography.

In particular we will investigate two specific models. Firstly we will analyse the simple massive gravity model (8.1). Here we will find that the behaviour of the transport coefficients and of the susceptibilities does not fulfil all the requirements

illustrated in the previous sections in order to conjecture a bound. As a consequence we will find that in this simple model the diffusion constants are both unbounded and tend to zero in the full incoherent regime.

Secondly we will analyse the dilaton model (8.66). We have already explained in the previous chapter, how this model provides a linear in T resistivity, which is one of the basic requirements in order for the bounds to exist. Here we will analyse the model in a particular critical region, (we will be more clear later about this subtle point), showing that, in this case, all the phenomenological requirements for the formulation of the bounds are fulfilled and a bound *on the sum* of the charge and heat diffusion constants can be defined in accordance with [42].

9.1.3.1 Diffusion constants in simple massive gravity

Let us start from the simple massive gravity model (8.1). Having obtained the DC transport coefficients and the relevant thermodynamical quantities in the previous chapter, we are now ready to study the diffusion constants through the Einstein relations (9.17) and (9.18).

Eventually the diffusion constants take the following form

$$D_{\pm} = \frac{-12 + z_h^2\left(20\beta - 19\mu^2\right) \pm \sqrt{\Delta}}{32\beta z_h} \,, \tag{9.23}$$

where

$$\Delta = z_h^4\left(144\beta^2 - 696\beta\mu^2 + 361\mu^4\right) + z_h^2\left(288\beta + 456\mu^2\right) + 144 \,. \tag{9.24}$$

and we have set $\kappa_4 = L = q = 1$ since this parameters are not relevant in the present analysis.

We refer to Figure F.7 to have a qualitative idea of the generic behaviour of the diffusion constants with respect to the temperature. In the simple case of zero chemical potential $\mu = 0$ (see right panel of F.7) the electric and thermal sector decouple and the two diffusivities take the following form

$$D_c = \frac{\sigma}{\chi} = -\frac{\sqrt{4\pi^2T^2 - 3\beta} - 2\pi T}{\beta} \,, \tag{9.25}$$

$$D_h = \frac{\kappa}{c_\rho} = -\frac{\sqrt{4\pi^2T^2 - 3\beta}}{\beta} \,. \tag{9.26}$$

We observe that in the high temperature regime D_c has an $1/T$ behaviour.

Even though also for $\mu \neq 0$ the diffusivities are bounded from below by an $1/T$ power law in the high temperature region, the coefficient of such bounding behaviour can be apparently lowered at will acting on the mass parameter β. Nevertheless, to be precise on this point, one needs to consider whether the range of β is

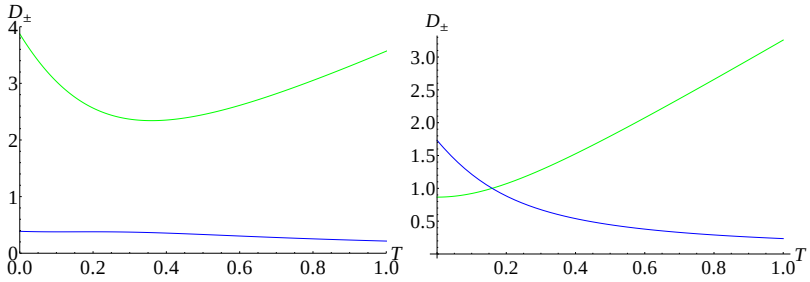

Fig. 9.1 Sample diagrams to illustrate the behaviour of thermo-electric diffusion constants at (left) finite chemical potential, namely $\mu = 1$ (blue line for D_- and green line for D_+), and (right) $\mu = 0$ (blue line for $D_- = D_c$ and green line for $D_+ = D_h$). The graviton mass parameter has been chosen to be $\beta = -1$.

possibly limited by consistency requirements of the model in such a way to produce a lower bound for the conductivities.

The first requirements comes from the stability of the models. We have mentioned in the previous chapter that in order for the momentum dissipation rate τ^{-1} to be positive we need:

$$\beta < 0 \,. \tag{9.27}$$

A further consistency requirement is provided by asking the positivity of the energy density. More specifically, we consider the holographic renormalization of the model (8.1) on the black brane solutions (7.3) and the assumption that finite counterterms do not affect the thermodynamics (namely that they do not depend on the thermodynamic variables) as discussed in [12]. It is then possible to refer the renormalized energy density to its value at zero T (keeping fixed all the other quantities) and ask that its value at finite T be never lower than that at $T = 0$, namely

$$\mathscr{E}(T,\mu;\beta) - \mathscr{E}(0,\mu;\beta) > 0 \,. \tag{9.28}$$

This energy requirement does not furnish any additional constraint on the parameter β, and the renormalized energy density appearing in (9.28) remains positive for every $\beta < 0$.

All in all, the consistency requirements, although restricting the possible choices of mass parameters, do not lead either to a diffusion bound nor to a minimal value for the diffusion constants below which the holographic model is not trustworthy. Indeed it is always possible to achieve a strongly incoherent regime (where momentum is quickly dissipated) by sending $|\beta|$ to infinity without any apparent consistency problem.

In line with these observations, one has that the infinite $|\beta|$ limit leads to vanishing diffusion constants, namely

$$\lim_{\beta\to-\infty} D_\pm(T,\beta) = 0 \,. \tag{9.29}$$

Despite this limit corresponds to a bulk model dominated just by the mass term of the graviton where the dynamics of the metric vector fluctuation of interest trivializes, such argument does not yield a quantitative ground to formulate a bound. Even observing that an infinite $|\beta|$ limit leads necessary to a regime where the graviton mass exceeds the Planck mass one could limit the value of the gravity model as an effective field theory rather than supporting the existence of a bound on diffusivity.

The outcome of the previous analyses is that the simple massive gravity model (8.1) does not allow to formulate consistent bounds on the thermo-electric diffusion constants even in the case where the mass of the graviton has non-trivial RG (i.e. radial) behaviour. In addition it is important to observe that the electric conductivity (8.5.2.1) is, in a regime of large $|\beta|$, dominated by the constant term, namely the charge conjugation symmetric piece $1/q^2$. This highlights a limitation in reproducing a linear in T resistivity in massive gravity in a regime where momentum dissipation exceeds the other scales of the system. In other words, the incoherent regime considered to formulate the conjecture on diffusion bounds (phenomenologically motivated by the consequent linear in T resistivity) does not lead to the desired phenomenology in the simple massive gravity model (8.1) and, as we will see in the next sections, an analysis of the diffusion constants in a model where these requirements are fulfilled is mandatory.

9.1.3.2 Diffusion constants in EMD

Let us now move to analyse the diffusion constants in the Einstein-Maxwell-Dilaton model which we have analysed in (8.66).

First of all, we note that the common structure of the cuprate phase diagram (see Part 1) shows that the strange metal phase is reached, in general, at high T. Given the scaling properties of the holographic model with respect to a rescaling of the boundary space-time[1], it is natural to compare the temperature to the chemical potential and consider the scaling invariant ratio T/μ. Hence we mean high temperatures in the sense $T/\mu \gg 1$ and, inverting the qualitative argument just given, it is natural to study the $\mu = 0$ case to describe the "criticality" condition which gives rise to the strange metal. On top of this, when the chemical potential is vanishing, the charge and heat transport of the model decouple.

Asking for $\mu = 0$ in (8.68) we face two possibilities. We can set $Q = 0$ and consequently trivialize the dilaton profile falling back to the solution (7.3) already found in simple massive gravity. Alternatively we can set

$$Qz_h + 1 = |\beta|^{1/2} z_h \, ; \tag{9.30}$$

we focus on this second case where the dilaton has non-trivial radial profile. For completeness, let us present explicitly the background solutions in this case,

[1] See for instance [35] for the analysis of the scaling properties of the pure massive gravity model.

$$
\begin{aligned}
&ds^2 = \frac{g(z)}{z^2}\left(-h(z)dt^2 + \frac{dz^2}{g(z)^2 h(z)} + dx^2 + dy^2\right) ,\\
&A_t = 0 , \qquad \phi(z) = \frac{1}{3}\log g(z) ,\\
&g(z) = \left(1 + |\beta|^{1/2} z - \frac{z}{z_h}\right)^{\frac{3}{2}} , \qquad h(z) = 1 + \frac{\beta z^2 z_h^2}{\left(z_h + |\beta|^{1/2} z z_h - z\right)^2} .
\end{aligned}
\tag{9.31}
$$

As we will see shortly, enforcing relation (9.30) is far more than a technicality; indeed it corresponds to considering non-trivial critical conditions which relate the parameter Q to the other scales of the model (the temperature, through z_h, and the graviton mass β) in a particular manner. Fixing $\mu = 0$ by imposing relation (9.30) defines a family of backgrounds whose phenomenology differs from that of simple massive gravity. As we are going to describe precisely, the new features of such a family present a linear in T resistivity and an overall physical behaviour in line with the that indicated in [41] as the basis for discussing diffusion bounds. Let us further underline that (9.30) and $Q = 0$ define two different branches of possible backgrounds that have different physical properties.

Studying the thermodynamics of the critical conditions associated to (9.30) leads to

$$
T = \frac{|\beta|^{1/4}}{2\pi z_h^{1/2}} , \quad \rho = 0 , \quad \mathscr{S} = 8\pi^2 |\beta|^{1/2} T , \tag{9.32}
$$

which feature linear in T entropy at all temperature. Moreover, regarding the susceptibilities, we obtain

$$
\zeta = 0 , \tag{9.33}
$$

$$
\chi = |\beta|^{1/2} , \tag{9.34}
$$

$$
c_\rho = 8\pi^2 |\beta|^{1/2} T . \tag{9.35}
$$

Particularly interesting to us is the electric susceptibility χ independent from the temperature. Continuing the analysis of the critical model resulting from the condition (9.30), we find the transport coefficients to be

$$
\sigma = |\beta|^{1/4} z_h^{1/2} \implies \sigma^{-1} = 2\pi |\beta|^{-1/2} T , \tag{9.36}
$$

$$
s = 0 , \tag{9.37}
$$

$$
\kappa = 16\pi^3 |\beta|^{-1/2} T^2 . \tag{9.38}
$$

We underline the fact that the resistivity is linear in T for the entire range of temperature.

The set of equilibrium and transport quantities just found fulfils precisely the phenomenological framework that was considered in formulating diffusion bounds in [41]. More specifically, a constant electric susceptibility was assumed as a hypothesis and a linear in T resistivity as the consequence of an electrical diffusivity saturating the bound. Moreover, in [41] it was conjectured that the charge diffusion

constant D_c obeys a bound which depends only on temperature; the arguments relying on the hypothesis that the momentum dissipation rate is fast with respect to the scale of T, a regime referred to as *incoherent* regime.

Analysing the dilaton model we find that, in the critical condition associated to (9.30), the charge diffusion constant takes a very simple form independent on the parameter β, namely

$$D_c^{(\text{crit})} = \frac{\sigma}{\chi} = \frac{1}{2\pi T} \,. \tag{9.39}$$

It is very important to note that (9.39) (emerging from (9.32)- (9.35) and (9.36)) does not refer to any specific regime for the momentum dissipation rate controlled by β; in this sense, it is not necessarily related to either an incoherent or a coherent regime. Such feature is very appealing because allows us to be "agnostic" about the hierarchy of T and the momentum dissipating scale $|\beta|$; the phenomenology of the critical model at hand is therefore robust also in this sense.

Let us now focus on the heat diffusion constant D_h. The assumptions of constant susceptibility χ and linear in T resistivity do not suggest a bound for D_h which, still following [41], can nevertheless be conjectured by analogy with D_c. For the critical dilaton model D_h takes the following explicit form

$$D_h^{(\text{crit})} = \frac{\kappa}{c_\rho} = \frac{2\pi T}{|\beta|} \,. \tag{9.40}$$

In order to discuss the possibility of formulating a bound, let us consider the incoherent regime where momentum is dissipated quickly. As for the simple massive gravity model considered in Section 9.1.3.1, the incoherent regime is achieved in the limit $T/|\beta| \to 0$. The heat diffusion constant (9.40) depends explicitly on β while instead the charge diffusion constant (9.39) does not. This crucial difference leads to the impossibility to rely on incoherence and formulate a lower bound which depends only on temperature for $D_h^{(\text{crit})}$.

Although one cannot formulate a bound for both the heat and charge diffusion constants separately, as a direct consequence of the bound on $D_c^{(\text{crit})}$, the sum of the two is naturally bounded once incoherence is considered, namely

$$D_h^{(\text{crit})} + D_c^{(\text{crit})} \geq \frac{1}{2\pi T} \,. \tag{9.41}$$

In [42] different arguments were proposed to motivate a bound on the sum of diffusion constants rather than on them individually relying on a hydrodynamical analysis. We refer to [42] for a detailed discussion on the topic but intuitively we note that the quantity $D_h + D_c$ is more natural to formulate a bound since in general the two diffusion constants separately could be a complex quantities while their sum is always real (see Appendix F).

The present analysis of the holographic dilaton model moves somehow oppositely with respect to [42]: we were able to compute the two diffusion constants

separately and we have found that a bound can be formulated only on the sum of the two once incoherence is considered.

The set of results obtained through the study of the critical massive gravity dilaton model, and specifically (9.41), appear to be intimately related to the detail of the model. Actually, as we have seen explicitly, simple massive gravity led to different results. At the best of our knowledge, the dilaton model under consideration studied at $\mu = 0$ according to (9.30) is the only holographic model were all the assumptions made in [41] are fulfilled. It is therefore particularly relevant that in such circumstances a bound on the sum of the diffusion constants can be naturally formulated. In other words it is possible to consider the present analysis as a support (at least in a specific and well defined case) of the physics conjectured in [41].

9.2 Holographic inspired phenomenology

In this section we discuss the possible general predictions based on the thermoelectric transport coefficients (8.118), (8.119), (8.120) explicitly computed with gauge/gravity techniques.

We want to express the behaviour of the holographic model (8.1) as independently as possible of its specific details. In line with this aim, the transport coefficients (8.118), (8.119), (8.120) were expressed in terms of the thermodynamical quantities (computed in Section 8.5.1) and in terms of the conductivity of the $\rho = 0$ system $\tilde{\sigma}$ and the quantity h defined in (8.115). These latter quantities can be thought of as "phenomenological parameters" whose value is not predicted within the model itself; as already observed, they are indeed directly related to parameters of the bulk model (q and β respectively). To clarify this idea of extending the results beyond the model used to obtain them, consider for example $\tilde{\sigma}$; for the model at hand it is related to the bulk coupling, namely $\tilde{\sigma} = 1/q$. However, expressing all the physical results directly in terms of $\tilde{\sigma}$, corresponds to a model-independent formulation where $\tilde{\sigma}$ is regarded as a parameter *per se* accounting for an a priori unspecified $\rho = 0$ conductivity.

We must also recall that, as usual in bottom-up holographic models (i.e. not derived as consistent low-energy effective theories of UV complete string setups), we have no direct control of the microscopic degrees of freedom. Hence, it is particularly natural to exploit the bottom-up holographic model as a simple example grasping essential features of a whole class of strongly coupled theories. On the technical level, we rely on promoting parameters to be temperature dependent functions to the purpose of performing a phenomenological analysis. As already stressed, such a logical leap constitutes a departure from the original holographic model and our current aim is to define how to test carefully this phenomenological approach against experimental data. When successful, it can inform us about universal characteristics and shed light on the mysterious behaviour of the transport properties in strongly correlated materials such as the cuprates (see [17] for a wide and precise exper-

imental report). Previous phenomenological analyses along these lines have been performed in [38, 41, 49, 50].

The purpose of this section is to generalize to the whole set of thermo-electric transport coefficients the proposal of [38] which instead considers phenomenological scalings only for the resistivity and the Hall angle. There it was noted that, at low-B[2], the electric conductivity follows an inverse Matthiessen's rule: the conductivity due to the zero density sector $\tilde{\sigma}$ and σ_D (this latter directly related to h and hence, in specific regimes, to a momentum relaxation scattering time) add up as follows

$$\sigma_{xx} = \tilde{\sigma} + \sigma_D \ , \quad \text{with} \quad \sigma_D = \frac{\rho^2}{h} \ , \tag{9.42}$$

while the Hall angle $\tan\theta_H$ does not depend on $\tilde{\sigma}$

$$\tan\theta_H = \frac{\sigma_{xy}}{\sigma_{xx}} \sim \frac{B}{\rho}\,\sigma_D \ . \tag{9.43}$$

In [38] it was also noted that, in order to fit the experimental scalings of the conductivity and Hall angle measured in the cuprates, namely $\rho_{xx} \sim \sigma_{xx}^{-1} \sim T$ and $\tan\theta_H \sim 1/T^2$, the two conductivities $\tilde{\sigma}$ and σ_D must have the following scalings in temperature[3]

$$\tilde{\sigma} \sim \tilde{\sigma}^0\,\frac{\sqrt{\rho}}{T} \ , \qquad \sigma_D \sim \sigma_D^0\left(\frac{\sqrt{\rho}}{T}\right)^2 \ , \tag{9.44}$$

where $\tilde{\sigma}^0$ and σ_D^0 are dimensionless parameter which do not depend on T. Inspired by phenomenological intuition, we have also supposed that the charge density ρ is constant in temperature. In addition, in the quantum critical region the DC conductivity must be dominated by $\tilde{\sigma}$, namely $\tilde{\sigma} \gg \sigma_D$.

To make contact with both the theoretical and experimental literature, we will determine the scalings for the same transport coefficients discussed in [49], namely the the resistivity ρ_{xx}, the Hall angle $\tan\theta_H$, the Hall Lorentz ratio L_{xy}, the magnetoresistance $\frac{\Delta\rho}{\rho} = \frac{\rho_{xx}(B)-\rho_{xx}(0)}{\rho_{xx}(0)}$, the Seebeck coefficient $s = \frac{\alpha_{xx}}{\sigma_{xx}}$, the Nernst coefficient $\nu = \frac{1}{B}\left[\frac{\alpha_{xy}}{\sigma_{xx}} - s\tan\theta_H\right]$, the thermal conductivity κ_{xx} and the thermal magnetoresistance $\frac{\Delta\kappa}{\kappa} = \frac{\kappa_{xx}(B)-\kappa_{xx}(0)}{\kappa_{xx}(0)}$.

As already argued before, we regard the transport coefficients (8.118), (8.119), (8.120) as (possibly) universal functions of the magnetic field B, the charge density ρ, the entropy $\mathscr{S}$, the $\rho = 0$ conductivity $\tilde{\sigma}$ and σ_D. Then, once the values of the charge density and the magnetic field are set, we need to fix the scalings of three quantities in order to determine the behaviour of all the transport coefficients[4].

---

[2] The values of external magnetic fields implemented in a typical experimental set up can generally be considered small with respect to the intrinsic scales of the materials.

[3] We have chosen to express the scalings in temperature as a function of the dimensionless quantity $T/\sqrt{\rho}$, considering the system at fixed charge density.

[4] Notice that this is exactly the same number of quantities which were needed to be fixed in the approach of [49].

Note that the same approach cannot be followed in the hydrodynamical analysis of [21] because the hydrodynamical expressions are not always writeable in terms of h which, in the small momentum dissipation and $B = 0$ regime, assumes the explicit form $\frac{\mathscr{E}+P}{\tau}$.

In order to discuss the consequences of the proposal of [38] extended to the whole set of thermoelectric transport coefficients, we consider the following phenomenologically inspired inputs

$$\begin{aligned} &\rho \sim \rho_0 = \text{const} \,, \qquad \tilde{\sigma} \sim \tilde{\sigma}^0 \, \frac{\sqrt{\rho_0}}{T} \,, \\ &\frac{1}{h} \sim R \, \frac{\tilde{\sigma}^0}{\rho_0^2} \left(\frac{\sqrt{\rho_0}}{T} \right)^2 \,, \qquad \mathscr{S} \sim \mathscr{S}_0 \left(\frac{T}{\sqrt{\rho_0}} \right)^{\delta} \,, \end{aligned} \tag{9.45}$$

where $R \equiv \frac{\sigma_D^0}{\tilde{\sigma}^0}$ and $\mathscr{S}_0$ are parameters independent of the temperature and δ is an exponent to be phenomenologically determined. Considering the scalings (9.45) within (8.118), (8.119) and (8.120), in order to analyse the consequences of the proposal of [38], we expand the transport coefficients at the first leading order in the dimensionless ratio R and at weak magnetic field, namely $B/\rho_0 \ll 1$.

In order to fix the scaling exponent of the entropy density δ, we compare the leading exponent of the thermal hall conductivity κ_{xy} (having imposed the scalings (9.45)) with the experimental predictions for optimally doped YBCO [52, 58]. We prefer to consider as a phenomenological input the scaling of this transport coefficient instead of the Hall Lorentz ratio L_H; the reason being that the experiments described in [52, 58] found unexplained discrepancies both in the order of magnitude and in the temperature scaling of L_H [51] while the same two experiments agree on κ_{xy}, which has to scale as T^{-1}. To reproduce this behaviour for the leading term of κ_{xy}, we have to set $\delta = 1$, namely the proposal of [38] combined with the input of experimental data forces the entropy to scale linearly in temperature in the quantum critical region

$$\mathscr{S} \sim \mathscr{S}_0 \, \frac{T}{\sqrt{\rho_0}} \,. \tag{9.46}$$

This behaviour is in agreement with the experimental measurements of the electronic specific heat in various series of cuprates near optimal doping [54, 55, 56] in a wide range of temperature and with the holographic analysis of [23].

With this assumptions, at the first sub-leading order in the dimensionless ratio R and at the first order in B/ρ_0, we find the following scalings

$$\rho_{xx} \sim \frac{1}{\tilde{\sigma}^0}\ \frac{T}{\sqrt{\rho_0}} - \frac{\sigma_D^0}{\tilde{\sigma}^{0\,2}}\ , \tag{9.47}$$

$$\frac{\Delta\rho}{\rho} \sim \tilde{\sigma}^0\,\sigma_D^0\ \left(\frac{B}{\rho_0}\right)^2\ \left(\frac{\sqrt{\rho_0}}{T}\right)^3 - 2\sigma_D^{0\,2}\ \left(\frac{B}{\rho_0}\right)^2\ \left(\frac{\sqrt{\rho_0}}{T}\right)^4\ , \tag{9.48}$$

$$L_{xy} \sim \frac{\mathscr{S}_0^2\,\sigma_D^0}{2\,\tilde{\sigma}^0\,\rho_0^2}\ \frac{T}{\sqrt{\rho_0}} - \frac{5\,\mathscr{S}_0^2\,\sigma_D^{0\,2}}{4\rho_0^2\,\tilde{\sigma}^{0\,2}}\ , \tag{9.49}$$

$$\tan\theta_H \sim 2\,\sigma_D^0\ \frac{B}{\rho_0}\ \left(\frac{\sqrt{\rho_0}}{T}\right)^2 - \frac{B\sigma_D^{0\,2}}{\tilde{\sigma}^0}\ \frac{B}{\rho_0}\ \left(\frac{\sqrt{\rho_0}}{T}\right)^3\ , \tag{9.50}$$

$$\nu \sim \frac{\tilde{\sigma}^0}{\rho}\ \frac{\sqrt{\rho_0}}{T} - \frac{\sigma_D^0}{\rho_0}\ \left(\frac{\sqrt{\rho_0}}{T}\right)^2\ , \tag{9.51}$$

$$s \sim \frac{\mathscr{S}_0\,\sigma_D^0}{\rho_0\,\tilde{\sigma}^0} - \frac{\mathscr{S}_0\sigma_D^{0\,2}}{\rho_0\tilde{\sigma}^{0\,2}}\ \frac{\sqrt{\rho_0}}{T}\ , \tag{9.52}$$

$$\kappa_{xx} \sim \frac{\mathscr{S}_0^2\,\sigma_D^0}{\rho_0^{3/2}}\ \frac{T}{\sqrt{\rho_0}} - \frac{\mathscr{S}_0^2\sigma_D^{0\,2}}{\tilde{\sigma}^0\rho_0^{3/2}}\ , \tag{9.53}$$

$$\frac{\Delta\kappa}{\kappa} \sim -(\sigma_D^0)^2\ \left(\frac{B}{\rho_0}\right)^2\ \left(\frac{\sqrt{\rho_0}}{T}\right)^4 + \frac{2\sigma_D^{0\,3}}{\tilde{\sigma}^0}\ \left(\frac{B}{\rho_0}\right)^2\ \left(\frac{\sqrt{\rho_0}}{T}\right)^5\ . \tag{9.54}$$

Some of the temperature scalings derived with this approach are in accordance with the analysis of [49]. There are however three discrepancies: the magneto-resistance for which we find a B^2T^{-3} scaling instead of B^2T^{-4} and the Nernst coefficients and the Seebeck coefficients for which the authors of [49] found behaviours of the type $T^{-3/2}$ and $-T^{1/2}$ respectively. This discrepancies are due to the fact that, as opposed to the assumptions made in [49], in the present analysis the charge density is non-zero and the entropy has to scale linearly in temperature (instead of T^2 as predicted in [49]).

Let us now make contact with the experimental literature on the cuprates. The Seebeck coefficient, in the normal phase of several families of cuprates, it is usually fitted with a law of the kind $A - BT$ [52] regardless of the doping concentration. In (9.52) we found (correctly) a constant leading term while the subleading term scales as T^{-1}, in contrast with the measurements of [52]. Actually, in [53] deviations from the linear behaviour were observed at high temperature ($T \geq 300$ K); due to these deviations, a power law of the kind $T^{-1/2}$ was proposed in [49] but also a term T^{-1} is compatible with the data. It is however not clear whether at this temperature the phonon-drag mechanism (which, at least in normal metals, has to be taken into account in the analysis of the thermopower) can be neglected [55, 56].

Concerning the magneto-resistance, in [54] the temperature dependence for YBCO and LSCO near optimal doping was studied. The result was that in YBCO $\frac{\Delta\rho}{\rho}$ follows a power law of the kind B^2/T^n with $n \simeq 3.5 - 3.9$ while in LSCO a behaviour of the kind $A/(B+CT)^2$ was found. It would be interesting to make a quantitative evaluation of the unknown coefficient in (9.48) to compute with our approach the correction to the T^{-3} behaviour due to the subleading T^{-4} term.

With regard to the other transport coefficients, namely ν, κ_{xx} and $\frac{\Delta\kappa}{\kappa}$, the experimental measurements in the normal phase are not conclusive. Specifically the Nernst coefficient in [57, 58] can be seen to go to zero at high temperature in accordance to (9.51) but the data are not sufficient to determine a proper scaling law. Finally

the thermal conductivity, and consequently also the thermal magneto-resistance, are extremely difficult to measure since typically in this materials the dominant contribution to these transport coefficients is given by phonons and not by electrons.

Except the most stable results, namely the resistivity and the Hall angle, the experiments do not seem in general conclusive on the other transport coefficients and we prefer to postpone any stringent comment on the possible connection between the present analysis and the experimental data to future discussions.

We want nonetheless to stress that, as it is evident from the universal formulæ (8.118), (8.119) and (8.120), the behaviour of the transport coefficients and that of the thermodynamical quantities are intimately related. If the universality of the transport formulæ is confirmed, any proposal on the mechanism which determines the transport properties of the cuprates (at finite charge density) has to keep into account also the correct behaviour for the thermodynamical quantities.

Appendices

Appendix D
Effect of linear source in time on DC transport

In this Appendix we will explain why the term linear in the time coordinate t in the expectation value for the stress energy tensor (8.53) does not contribute to the DC response of the system.

To do this, let us consider the set of source $\lambda(t)$ associated with a set of operator ϕ_A. As we have learned in Part 3,at the level of linear response theory the expectation value of phi_A is given by:

$$\langle \phi_A t) \rangle = \int dt' G_{AB}(t-t') \lambda_B(t') \ , \tag{D.1}$$

where G_{AB} is the associated Green's function. Expressing the latter in terms of its Fourier transform, we obtain:

$$\langle \phi_A(t) \rangle = \frac{1}{2\pi} \int dt' d\omega e^{-i(t-t')} t' \tilde{G}_{AB}(t-t') \lambda_B(t') \ . \tag{D.2}$$

We want to study the implication of a source linear in time on the DC transport properties. Then, we set $\lambda_A(t) = t c_A$:

$$\langle \phi_A(t) \rangle = \frac{1}{2\pi} \int dt' d\omega e^{-i(t-t')} t' \tilde{G}_{AB}(t-t') t' c_B \ . \tag{D.3}$$

Using the identity:

$$\int dt' e^{i\omega t'} t' = -2\pi \delta'(\omega) \ , \tag{D.4}$$

we find:

$$\langle \phi_A(t) \rangle = i \partial_\omega \left(e^{-i\omega t} \tilde{G}_{AB}(\omega) \right)_{\omega=0} c_B \ . \tag{D.5}$$

We next define the conductivity matrix σ_{AB} as the zero-frequency part of the spectral weight:

$$\sigma_{AB} = \lim_{\omega \to 0} \Im \frac{\tilde{G}_{AB}(\omega}{\omega} \ . \tag{D.6}$$

Then, using the fact that the real and imaginary parts of the Green's function are even and odd functions of ω respectively, we can express (D.5) in the following way:

$$\langle \phi_A(t) \rangle = \left(t\tilde{G}_{AB}(0) - \sigma_{AB} \right) c_B \ . \tag{D.7}$$

Then a source linear in the time coordinate t affects the expectation value of the associated operator with a term linear in t plus the DC conductivity matrix. We can therefore neglect the linear in t term when we are dealing with the DC response, as stated in the main text.

Appendix E
Technical aspects of holographic magneto-transport

In this Appendix we will explain some technical aspects of the computation of the holographic magneto-transport DC response.

E.1 Fluctuations equations with electric ansatz

$$\begin{aligned}\tilde{h}_{ti}''(z)+\frac{2}{z}\tilde{h}_{ti}'(z)+2\left[\frac{\beta L^2-B^2z^2\gamma^2}{L^2f(z)}-\frac{1}{z^2}\right]\tilde{h}_{ti}(z)\\ -\frac{2Bz^2\gamma^2\mu}{L^2z_h}\,\varepsilon_{ij}\tilde{h}_{zj}(z)-\frac{2\gamma^2\mu}{z_h}\,\tilde{a}_i'(z)-\frac{2B\gamma^2}{f(z)}\,\varepsilon_{ij}E_j=0\end{aligned} \tag{E.1}$$

$$B\,\varepsilon_{ij}\tilde{a}_j'(z)+\left(\frac{\beta}{\gamma^2}-\frac{B^2z^2}{L^2}\right)\tilde{h}_{zi}(z)-\frac{Bz^2\mu}{z_hf(z)L^2}\,\varepsilon_{ij}\tilde{h}_{tj}(z)+\frac{\mu}{z_hf(z)}\,E_i=0 \tag{E.2}$$

$$\begin{aligned}\tilde{a}_i''(z)+\frac{f'(z)}{f(z)}\,\tilde{a}_i'(z)+Bz\,\frac{zf'(z)+2f(z)}{L^2f(z)}\,\varepsilon_{ij}\tilde{h}_{zj}(z)+\frac{Bz^2}{L^2}\,\varepsilon_{ij}\tilde{h}_{zj}'(z)\\ -\frac{z^2\mu}{L^2z_hf(z)}\,\tilde{h}_{ti}'(z)-\frac{2z\mu}{L^2z_hf(z)}\,\tilde{h}_{ti}(z)=0\end{aligned} \tag{E.3}$$

E.2 Fluctuations equations with thermal ansatz

$$\tilde{h}_{ti}^{(\mathrm{th})}(z_h)=\tilde{h}_{ti}^{(\mathrm{el})}(z_h)+\frac{BL^2\varepsilon_{ij}s_j\gamma^2\mu\left[z_h^2\gamma^2\left(B^2z_h^2+\mu^2\right)-2L^2\left(z_h^2\beta+3\right)\right]}{4z_h^2\left[-2B^2L^2z_h^2\beta\gamma^2+B^2z_h^2\gamma^4\left(B^2z_h^2+\mu^2\right)+L^4\beta^2\right]}$$
$$-\frac{L^2s_i\left[-L^2z_h^2\gamma^2\left(3B^2\left(z_h^2\beta+2\right)+\beta\mu^2\right)\right]}{4z_h^3\left[-2B^2L^2z_h^2\beta\gamma^2+B^2z_h^2\gamma^4\left(B^2z_h^2+\mu^2\right)+L^4\beta^2\right]}$$
$$-\frac{L^2s_i\left[B^2z_h^4\gamma^4\left(B^2z_h^2+\mu^2\right)+2L^4\beta\left(z_h^2\beta+3\right)\right]}{4z_h^3\left[-2B^2L^2z_h^2\beta\gamma^2+B^2z_h^2\gamma^4\left(B^2z_h^2+\mu^2\right)+L^4\beta^2\right]} \tag{E.4}$$

$$\tilde{h}_{ti}''(z)+\frac{2}{z}\tilde{h}_{ti}'(z)+\left[\frac{-z^2\gamma^2\left(2B^2z_h^2+\mu^2\right)+2L^2z_h^2\beta+z^2z_h^2\gamma^2\phi'(z)^2}{L^2z_h^2f(z)}-\frac{2}{z^2}\right]\tilde{h}_{ti}(z)$$
$$+\frac{2Bz^2\gamma^2\phi'(z)}{L^2}\varepsilon_{ij}\tilde{h}_{zj}(z)+2\gamma^2\phi'(z)\,\tilde{a}_i'(z)$$
$$+\gamma^2\left[t\,s_i\left(\phi'(z)^2-\frac{\mu^2}{z_h^2}\right)-\frac{2B\varepsilon_{ij}(E_j-s_j\phi(z))}{f(z)}\right]=0 \tag{E.5}$$

$$4BL^2z^3z_h^2\gamma^2f(z)\,\varepsilon_{ij}\tilde{a}_j'(z)+4z_h^2f(z)\left(L^2z^3\beta-B^2z^5\gamma^2\right)\tilde{h}_{zi}(z)$$
$$-4Bz^5z_h\gamma^2\mu\,\varepsilon_{ij}\tilde{h}_{tj}(z)-6L^4z_h^2s_if(z)+2L^4z_h^2s_i\left(z^2\beta+3\right) \tag{E.6}$$
$$+L^2z^3\gamma^2\left[-B^2zz_h^2s_i+4E_iz_h\mu+s_i\mu^2(3z-4z_h)\right]=0$$

$$\tilde{a}_i''(z)+\frac{z^4\gamma^2\left(B^2z_h^2+\mu^2\right)+6L^2z_h^2f(z)-2L^2z_h^2\left(z^2\beta+3\right)}{2L^2zz_h^2f(z)}\tilde{a}_i'(z)$$
$$+Bz\frac{z^4\gamma^2\left(B^2z_h^2+\mu^2\right)+10L^2z_h^2f(z)-2L^2z_h^2\left(z^2\beta+3\right)}{2L^4z_h^2f(z)}\varepsilon_{ij}\tilde{h}_{zj}(z) \tag{E.7}$$
$$+\frac{B\varepsilon_{ij}s_j}{f(z)}+\frac{Bz^2}{L^2}\varepsilon_{ij}\tilde{h}_{zj}'(z)-\frac{z^2\mu}{L^2z_hf(z)}\tilde{h}_{ti}'(z)-\frac{2z\mu}{L^2z_hf(z)}\tilde{h}_{ti}(z)=0$$

E.3 Stress-energy tensor with thermal gradient

In this appendix we want to clarify a very subtle aspect of the computation of the DC transport coefficient illustrated in [15], namely the fact that the stress energy tensor T^{ti} (8.105) and the quantity $\frac{\sqrt{-g}}{\kappa_4^2}\nabla^z k^i$ coincide once evaluated on the boundary up to a term linear in the time coordinate t; this latter however does not contribute to the DC response as clearly explained in Appendix C of [15].

Once evaluated on the thermal ansatz (8.111), the two quantities previously mentioned take the following form

$$\frac{\sqrt{-g}}{\kappa_4^2}\nabla^z k^i = \frac{1}{\kappa_4^2}\left(\tilde{h}_{ti}\left(\frac{f(z)}{z}-\frac{f'(z)}{2}\right)+\frac{f(z)}{2}\tilde{h}'_{ti}\right)\,, \tag{E.8}$$

$$T^{ti} = \frac{L^5}{\kappa_4^2 z^5}\left(-K^{ti}+Kg_b^{ti}+\frac{2}{L}g_b^{ti}\right) = \frac{\tilde{h}'_{ti}(z)}{2\kappa_4^2\sqrt{f(z)}}-\frac{\tilde{h}_{ti}(z)}{z\kappa_4^2\sqrt{f(z)}}+\frac{2\tilde{h}_{ti}(z)}{z\kappa_4^2 f(z)} + t\alpha_i\left(-\frac{2L^2}{z^3\kappa_4^2}+\frac{2L^2\sqrt{f(z)}}{z^3\kappa_4^2}-\frac{L^2 f'(z)}{2z^2\kappa_4^2\sqrt{f(z)}}\right)\,. \tag{E.9}$$

In order to evaluate the previous quantities at the boundary $z=0$ we substitute the background solution (8.76) for $f(z)$ and we impose $\tilde{h}_{ti}\sim h_{ti}^{(0)}z$ near $z=0$. This latter condition is due to the fact that, as explained in [15], we need to switch off the term proportional to z^{-2} in the asymptotic expansion for $\tilde{h}_{ti}$ in order to avoid additional thermal deformation associated to this mode. Keeping into account these asymptotic behaviours it is easy to verify that the $z\to 0$ limit of (E.8) coincides with the time independent part of (E.9) evaluated in the same limit.

Appendix F
Einstein relations for charge and heat diffusion constants

In this Appendix we want to derive the Einstein relations (9.17) and (9.18) which relate the charge and heat diffusion constants to the transport coefficients and the thermodynamical susceptibilities.

From basics thermodynamics we find that the following relation holds between the spatial gradients of the the thermodynamical quantities ρ, ε, μ and T:

$$\begin{pmatrix} \nabla_i \rho \\ \nabla_i \varepsilon \end{pmatrix} = A \begin{pmatrix} \nabla_i \mu \\ \nabla_i T \ , \end{pmatrix} \tag{F.1}$$

where

$$A = \begin{pmatrix} \chi & \zeta \\ T\zeta + \mu\chi & \mu\zeta + c_\mu \ , \end{pmatrix} \tag{F.2}$$

and the susceptibilities χ, ζ and c_μ are given by:

$$\chi = \frac{d\rho}{dT}, \qquad \zeta = \frac{d\rho}{d\mu}, \qquad c_\mu = T\frac{dS}{dT} \ . \tag{F.3}$$

As explained in the main text, the transport coefficients relate the heat current J^Q and the charge current J to the gradients of the temperature and the chemical potential as follows:

$$\begin{pmatrix} J \\ J^Q \end{pmatrix} = - \begin{pmatrix} \hat{\sigma} & \hat{\alpha} \\ T\hat{\alpha} & \hat{\bar{\kappa}} \end{pmatrix} \begin{pmatrix} \nabla\mu \\ \nabla T \end{pmatrix} \ , \tag{F.4}$$

We recall that the heat current J^Q is related to the energy current J^E by the following relation:

$$J_i^E = J_i^Q + \mu J_i \ . \tag{F.5}$$

Since the energy density $\mathscr{E}$ and the charge density ρ are conserved in the system at hand, the following continuity relations hold:

$$\partial_t \rho = -\nabla \cdot J \ , \qquad \partial_t \mathscr{E} = -\nabla \cdot J^E \ . \tag{F.6}$$

Finally, using the previous relations, the following diffusion equation holds:

$$\partial_t \begin{pmatrix} \rho \\ \mathscr{E} \end{pmatrix} = \begin{pmatrix} \hat{\sigma} & \hat{\alpha} \\ T\hat{\alpha}+\mu\hat{\sigma} & \hat{\bar{\kappa}}+\mu\hat{\alpha} \end{pmatrix} A^{-1}\nabla^2 \begin{pmatrix} \rho \\ \mathscr{E} \end{pmatrix} . \tag{F.7}$$

The diffusivity matrix $\mathscr{D}$ is defined as:

$$\mathscr{D} \equiv \begin{pmatrix} \hat{\sigma} & \hat{\alpha} \\ T\hat{\alpha}+\mu\hat{\sigma} & \hat{\bar{\kappa}}+\mu\hat{\alpha} \end{pmatrix} A^{-1} . \tag{F.8}$$

The eigenvalues D_+ and D_- of $\mathscr{D}$ satisfy the following relations:

$$\begin{aligned} D_+ + D_- &= \frac{\hat{\sigma}}{\chi} + \frac{\hat{\kappa}}{\rho} + \frac{T(\zeta\hat{\sigma}-\chi\hat{\alpha})^2}{c_\rho \chi^2 \hat{\sigma}} , \\ D_+ D_- &= \frac{\hat{\sigma}\hat{\kappa}}{c_\rho \chi} , \end{aligned} \tag{F.9}$$

where $\hat{\kappa} = \hat{\bar{\kappa}} - T\hat{\alpha}\hat{\sigma}^{-1}\hat{\alpha}$ and $c_\rho = c_\mu - \frac{\zeta^2 T}{\chi}$. The relations (F.9) are called the Einstein's relation for the charge and heat diffusion constants.

References

1. Leo P. Kadanoff and Paul C. Martin, Annals of Physics, **24**, 419 (1963).
2. P. K. Kovtun and A. O. Starinets, Phys. Rev. D **72** (2005) 086009 [hep-th/0506184].
3. S. A. Hartnoll, Class. Quant. Grav. **26** (2009) 224002 [arXiv:0903.3246 [hep-th]].
4. S. A. Hartnoll and C. P. Herzog, Phys. Rev. D **76** (2007) 106012 [arXiv:0706.3228 [hep-th]].
5. C. P. Herzog, P. Kovtun, S. Sachdev and D. T. Son, Phys. Rev. D **75** (2007) 085020 [hep-th/0701036].
6. D. Vegh, arXiv:1301.0537 [hep-th].
7. S. F. Hassan and R. A. Rosen, JHEP **1107** (2011) 009 [arXiv:1103.6055 [hep-th]].
8. R. A. Davison, Phys. Rev. D **88** (2013) 086003 [arXiv:1306.5792 [hep-th]].
9. R. A. Davison and B. Goutraux, arXiv:1505.05092 [hep-th].
10. M. Blake, D. Tong and D. Vegh, Phys. Rev. Lett. **112** (2014) 7, 071602 [arXiv:1310.3832 [hep-th]].
11. G. T. Horowitz, J. E. Santos and D. Tong, JHEP **1207** (2012) 168 [arXiv:1204.0519 [hep-th]].
12. M. Blake and D. Tong, Phys. Rev. D **88** (2013) 106004 [arXiv:1308.4970 [hep-th]].
13. L. Alberte and A. Khmelnitsky, Phys. Rev. D **91** (2015) 4, 046006 [arXiv:1411.3027 [hep-th]].
14. A. Amoretti, A. Braggio, N. Maggiore, N. Magnoli and D. Musso, arXiv:1406.4134 [hep-th].
15. A. Donos and J. P. Gauntlett, arXiv:1406.4742 [hep-th].
16. N. Iqbal and H. Liu, Phys. Rev. D **79** (2009) 025023 [arXiv:0809.3808 [hep-th]].
17. A. Donos and S. A. Hartnoll, Nature Phys. **9** (2013) 649 [arXiv:1212.2998].
18. A. Donos and J. P. Gauntlett, JHEP **1404** (2014) 040 [arXiv:1311.3292 [hep-th]].
19. V. Balasubramanian and P. Kraus, Commun. Math. Phys. **208** (1999) 413 [hep-th/9902121].
20. C. P. Herzog, J. Phys. A **42** (2009) 343001 [arXiv:0904.1975 [hep-th]].
21. S. A. Hartnoll, P. K. Kovtun, M. Muller and S. Sachdev, Phys. Rev. B **76** (2007) 144502 [arXiv:0706.3215 [cond-mat.str-el]].
22. S. S. Gubser and F. D. Rocha, "Peculiar properties of a charged dilatonic black hole in AdS_5," Phys. Rev. D **81** (2010) 046001 [arXiv:0911.2898 [hep-th]].
23. R. A. Davison, K. Schalm and J. Zaanen, "Holographic duality and the resistivity of strange metals," Phys. Rev. B **89** (2014) 245116 [arXiv:1311.2451 [hep-th]].
24. S. A. Hartnoll, C. P. Herzog and G. T. Horowitz, Phys. Rev. Lett. **101** (2008) 031601 [arXiv:0803.3295 [hep-th]].
25. C. Charmousis, B. Gouteraux, B. S. Kim, E. Kiritsis and R. Meyer, JHEP **1011** (2010) 151 [arXiv:1005.4690 [hep-th]].
26. K. Goldstein, S. Kachru, S. Prakash and S. P. Trivedi, JHEP **1008** (2010) 078 [arXiv:0911.3586 [hep-th]].
27. N. R. Cooper, B. I. Halperin, and I. M. Ruzin, "Thermoelectric response of an interacting two-dimensional electron gas in a quantizing magnetic field," Phys. Rev. B **55**, 2344 (1997).
28. M. Blake, A. Donos and N. Lohitsiri, "Magnetothermoelectric Response from Holography," arXiv:1502.03789 [hep-th].

29. R. A. Davison and B. Goutraux, "Dissecting holographic conductivities," arXiv:1505.05092 [hep-th]. [29, 30]
30. M. Blake, arXiv:1505.06992 [hep-th].
31. M. Blake, A. Donos and N. Lohitsiri, "Magnetothermoelectric Response from Holography," arXiv:1502.03789 [hep-th].
32. A. Lucas and S. Sachdev, "Memory matrix theory of magnetotransport in strange metals," arXiv:1502.04704 [cond-mat.str-el].
33. K. Y. Kim, K. K. Kim, Y. Seo and S. J. Sin, "Thermoelectric Conductivities at Finite Magnetic Field and the Nernst Effect," arXiv:1502.05386 [hep-th].
34. A. Amoretti, A. Braggio, N. Magnoli and D. Musso, "Bounds on intrinsic diffusivities in momentum dissipating holography," arXiv:1411.6631 [hep-th].
35. A. Amoretti, A. Braggio, N. Maggiore, N. Magnoli and D. Musso, "Thermo-electric transport in gauge/gravity models with momentum dissipation," JHEP **1409** (2014) 160 [arXiv:1406.4134 [hep-th]].
36. A. Amoretti, A. Braggio, N. Maggiore, N. Magnoli and D. Musso, "Analytic dc thermoelectric conductivities in holography with massive gravitons," Phys. Rev. D **91** (2015) 2, 025002 [arXiv:1407.0306 [hep-th]].
37. R. A. Davison and B. Goutéraux, "Momentum dissipation and effective theories of coherent and incoherent transport," JHEP **1501** (2015) 039 [arXiv:1411.1062 [hep-th]].
38. M. Blake and A. Donos, "Quantum Critical Transport and the Hall Angle," Phys. Rev. Lett. **114** (2015) 021601 [arXiv:1406.1659 [hep-th]].
39. A. Donos, B. Goutéraux and E. Kiritsis, "Holographic Metals and Insulators with Helical Symmetry," JHEP **1409** (2014) 038 [arXiv:1406.6351 [hep-th]].
40. B. Goutéraux, "Charge transport in holography with momentum dissipation," JHEP **1404** (2014) 181 [arXiv:1401.5436 [hep-th]].
41. S. A. Hartnoll, "Theory of universal incoherent metallic transport," Nature Phys. **11** (2015) 54 [arXiv:1405.3651 [cond-mat.str-el]].
42. P. Kovtun, "Fluctuation bounds on charge and heat diffusion," arXiv:1407.0690 [cond-mat.stat-mech].
43. P. Kovtun, D. T. Son and A. O. Starinets, Phys. Rev. Lett. **94** (2005) 111601 [hep-th/0405231].
44. L. D. Landau and E. M. Lifschitz, "Theoretical physics Vol. 10: Statistical Mechanics,"
45. S. Cremonini, Mod. Phys. Lett. B **25** (2011) 1867 [arXiv:1108.0677 [hep-th]].
46. P. Kovtun, J. Phys. A **45** (2012) 473001 [arXiv:1205.5040 [hep-th]].
47. A. Adams, L. D. Carr, T. Schaefer, P. Steinberg and J. E. Thomas, "Strongly Correlated Quantum Fluids: Ultracold Quantum Gases, Quantum Chromodynamic Plasmas, and Holographic Duality," New J. Phys. **14**, 115009 (2012) [arXiv:1205.5180 [hep-th]].
48. J. D. Rameu, T. J. Reber, H. B. Yang, S. Akhanjee, G. D. Gu and P. D.Jonson, "Nearly perfect fluidity in High Temperature Superconductor [arXiv:1409.5820 [cond-mad.str-el]]
49. S. A. Hartnoll and A. Karch, "Scaling theory of the cuprate strange metals," arXiv:1501.03165 [cond-mat.str-el].
50. A. Karch, "Conductivities for Hyperscaling Violating Geometries," JHEP **1406** (2014) 140 [arXiv:1405.2926 [hep-th]].
51. D. V. Khveshchenko, "Constructing (un)successful phenomenologies of the normal state of cuprates," arXiv:1502.03375 [cond-mat.str-el].
52. S. D. Orbetelli, J. R. Cooper and J. L. Tallon, Phys. Rev. B **46**, (1992) 22.
53. J. S. Kim, B. H. Kim, D. C. Kim and Y. W. Park, Ann. Phys. (Leipzig) **13** (2004).
54. J. M. Harris, Y. F. Yan, P. Matl, N. P. Ong, P. W. Anderson, T. Kimura and K. Kitazawa, Phys. Rev. Lett. **75**, 7 (1995).
55. J. L. Cohn and S. A. Wolf, Phys. rev. Lett. **66**, (1991) 8.
56. Y. Zhao, Z. Xu, X. Zhang and Z.Jiao, Chinese Science Bulletin **47**, (2002) 7.
57. Y. Wang, L. Li, and N. Ong, "Nernst effect in high-Tc superconductors," Phys. Rev. B **73**, 024510 (2006).
58. M. Matusiak, S. H. Naqib, I. Kokanovi, and J. R. Cooper, "Influence of the pseudogap on the Nernst coefficient of $Y_{0.9}Ca_{0.1}$ Ba_2 Cu_3 O_y," EPL **86**, 17005 (2009).